

# Acetylenic Polymers: Syntheses, Structures, and Functions

Jianzhao Liu,<sup>†</sup> Jacky W. Y. Lam,<sup>†</sup> and Ben Zhong Tang<sup>\*,†,‡</sup>

Department of Chemistry, William Mong Institute of Nano Science and Technology, Bioengineering Graduate Program, The Hong Kong University of Science & Technology (HKUST), Clear Water Bay, Kowloon, Hong Kong, China, and Department of Polymer Science and Engineering, Key Laboratory of Macromolecular Synthesis and Functionalization of the Ministry of Education, Institute of Biomedical Macromolecules, Zhejiang University, Hangzhou 310027, China

Received April 10, 2009

## Contents

1. Introduction	5799
2. Syntheses	5801
2.1. Polymers from Monoynes	5802
2.1.1. Catalyst Systems	5802
2.1.2. Polymerization Behaviors	5803
2.1.3. Polymer Reactions	5805
2.2. Polymers from Diynes	5806
2.2.1. Monomer Structures	5806
2.2.2. Linear Polymerizations	5806
2.2.3. Nonlinear Polymerizations	5810
2.3. Polymers from Triynes	5813
2.3.1. Coupling Polymerizations	5813
2.3.2. Click Polymerizations	5813
2.3.3. Polymer Reactions	5815
3. Structures	5816
3.1. Linear Polymers	5816
3.1.1. Regiostructures	5816
3.1.2. Stereostructures	5817
3.1.3. Morphostructures	5820
3.2. Hyperbranched Polymers	5823
3.2.1. 1,2,4- and 1,3,5-Trisubstitutions	5823
3.2.2. 1,4- and 1,5-Disubstitutions	5824
3.2.3. Degree of Branching	5825
3.2.4. Structural Modulation	5827
4. Functions	5828
4.1. Electrical Conductivity	5829
4.2. Liquid Crystallinity	5832
4.3. Light Emission	5835
4.4. Fluorescence Sensing	5840
4.5. Optical Nonlinearity	5841
4.6. Chiral Recognition	5844
4.7. Light Refraction	5845
4.8. Thermal Chromism	5848
4.9. Patterning and Imaging	5849
4.10. Ceramization and Magnetization	5852
4.11. Microfabrication and Nanomechanics	5855
4.12. Biological Activity	5858
5. Summary and Perspective	5859
6. Acknowledgments	5860
7. References	5860

## 1. Introduction

The synthesis of polymers is of academic value and technological implication and has been developed as an important area of research over a long history.<sup>1</sup> The first reports about “polymerization” reactions can be traced back to as early as the 19th century: in 1839, Simon observed that styrene changed from liquid to solid upon heating, while in 1872, Bayer recorded that the reactions of phenols with aldehydes resulted in the formation of resinous substances,<sup>2,3</sup> although at that time people had no idea about what a “polymer” was. In the 1920s, Staudinger proposed the concept of “macromolecules”, and in the 1930s, Carothers succeeded in the syntheses of polyesters and worked out theoretical models for condensation polymerization.<sup>4,5</sup> These seminal works in the early 20th century laid a solid foundation for polymer chemistry and changed polymer syntheses from arts or skills to real science.<sup>1</sup>

In the modern textbook of polymer chemistry, polymerization reactions are generally categorized into two types: step and chain polymerizations, typical examples of which are condensation polymerization of difunctional monomers and addition polymerization of olefinic monomers, respectively.<sup>1,6–8</sup> We now know that Bayer’s phenol–aldehyde reaction is a step polymerization and that Simon’s styrene reaction is a chain polymerization. Generally speaking, when molecules of a difunctional monomer such as X–R–Y (where X and Y are mutually reactive functional groups) are polymerized via the elimination of small molecule byproducts of XY, a linear condensation polymer with a general formula of X–(–R–)<sub>n</sub>–Y is formed, while when molecules of an olefinic monomer such as H<sub>2</sub>C=CHR are polymerized, a vinyl polymer with a structure of –[–H<sub>2</sub>C–CH(R)–]<sub>n</sub>– is produced (Scheme 1). The difunctional and olefinic monomers have been the major monomer sources, and their step and chain polymerization reactions have been the main synthetic routes to the “conventional” polymers such as polyester and polystyrene (PS), respectively.

From the viewpoint of bond structure, the step polymerization of the difunctional monomer and the chain polymerization of the vinyl monomer sketched in Scheme 1 are single- and double-bond reactions, respectively. When the single and double bonds of the monomeric species are opened and reacted, new species with higher molecular weights are formed. The final destinies of these chemical reactions are the formation of polymeric products, whose monomer repeat units are connected by single bonds. Since the single bonds are electronically saturated, these polymers are generally electronically inactive. As a result, traditional polymers are

\* To whom correspondence should be addressed. Phone: +852-2358-7375. Fax: +852-2358-1594. E-mail: tangbenz@ust.hk.

<sup>†</sup> HKUST.

<sup>‡</sup> Zhejiang University.



Jianzhao Liu received his B.S. degree from Zhejiang University in 2006. He is now a Ph.D. student in Tang's group at HKUST. He is interested in the construction of linear and hyperbranched polymers from acetylenic building blocks, including exploration of efficient catalyst systems, development of new polymerization reactions, and discovery of advanced functional properties.



Jacky W. Y. Lam received his Ph.D. degree from HKUST in 2003 under the supervision of Prof. Tang. In 2003–2007, he conducted his postdoctoral work on the syntheses of acetylenic polymers with linear and hyperbranched structures and advanced materials properties in Tang's group. He has been a research assistant professor of chemistry at HKUST since August 2007.

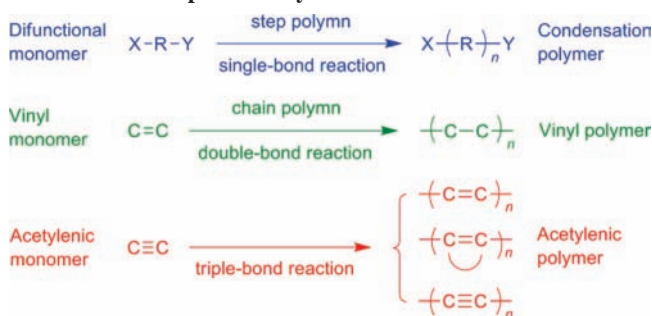
commonly used as commodity materials, such as plastics, fibers, rubbers, and elastomers.<sup>3</sup>

When a triple bond is opened, however, it yields a double bond. Multiple linkages of these double-bonded active species can furnish a polyene or polyarylene. The triple bonds can also be coupled in the unbroken or "intact" form, giving a polyene with multiple triple bonds. Thus, polymerizations of triple-bonded monomers can produce polymers with repeat units knitted together by electronically unsaturated double and triple bonds, as diagrammatically delineated in Scheme 1. Such polymers are expected to be electronically active. The triple-bonded molecules, however, had been much less explored as potential monomers in the formative years of polymer science, partially due to the fewer varieties of acetylenic compounds available in the early days and partially due to the higher tendency for acetylenic polymers to become insoluble, in comparison to the vast varieties of the difunctional and vinyl monomers and the excellent processability of their polymers. For example, Natta polymerized acetylene in 1958 but the obtained polyacetylene (PA) powder was completely intractable.<sup>9</sup> With the rapid advances in acetylene chemistry in the last century, much more acetylenic compounds have become synthetically accessible or even com-



Ben Zhong Tang received his Ph.D. degree from Kyoto University and conducted his postdoctoral work at University of Toronto. He joined HKUST in 1994 and was promoted to Chair Professor in 2008. His research interest lies in the creation of new molecules with novel structures and unique properties. He received the State Natural Science Award from the Chinese Government and the Senior Research Fellowship Award from the Croucher Foundation in 2007. He currently holds an adjunct position of Cao Guangbiao Chair Professor at Zhejiang University. He is serving as a science news contributor to *Noteworthy Chemistry* (ACS) and sitting in the editorial boards of a dozen journals, such as *Progress in Polymer Science* (Elsevier), *Macromolecules* (ACS), *Polymer* (Elsevier), *Journal of Polymer Science, Part A: Polymer Chemistry* (Wiley), and *Macromolecular Chemistry and Physics* (Wiley-VCH).

#### Scheme 1. Examples of Polymerization Reactions

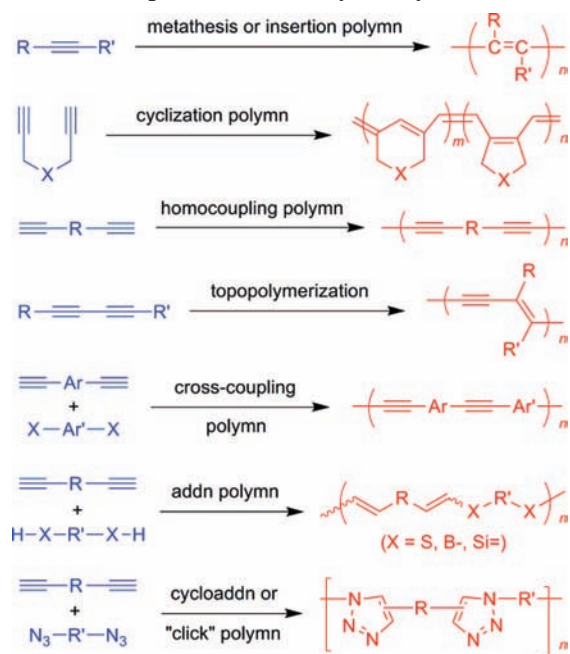


mercially available.<sup>10–12</sup> The pioneer work on the discovery of the metallic conductivity of the doped PA films by Shirakawa, MacDiarmid, and Heeger in the late 1970s verified the long-anticipated electronic activity of  $\pi$ -conjugated polymers and lent a strong impetus to the research on acetylenic polymers.<sup>13–16</sup>

As can be seen from Scheme 1, the backbones of the acetylenic polymers are  $\pi$ -conjugated due to the electronic communications between their electronically unsaturated repeat units. This unique electronic structure has the potential to endow the polymers with novel properties that are very difficult, if not impossible, to access by their congeners of condensation and vinyl polymers with electronic saturation. The prerequisite to realize this attractive potential is to establish versatile processes for synthesizing the polymers. This has motivated many research groups all over the world to work on the exploration of acetylene-based polymerization reactions.<sup>17–84</sup> As a result, a large variety of acetylenic polymerization reactions have been developed, especially after the ground-breaking work of Shirakawa, MacDiarmid, and Heeger in the 1970s.<sup>13</sup>

For example, effective polymerization processes of terminal and internal alkynes with one triple bond (monoynes) and two triple bonds (diynes) based on the reaction mechanisms of metathesis, insertion, cyclization, coupling, and

## Scheme 2. Examples of Linear Alkyne Polymerizations



addition have been well-established, affording acetylenic polymers with linear and cyclic molecular structures such as PA, polydiacetylene (PDA), poly(aryleneethynylene) (PAE), and poly(1,2,3-triazole) (PTA) as well as their substituted derivatives (Scheme 2). In the past decades, polymer scientists have been working on the expansion of their research territories from linear system to nonlinear, especially hyperbranched, system.<sup>85–91</sup> Along this line, a dozen research groups have embarked on the research programs on the development of effective polymerization processes for the syntheses of hyperbranched macromolecules from acetylenic monomers. As exemplified in Scheme 3, cyclotrimerizations of  $A_2$ -type diynes, cycloadditions of  $AB_2$ -type carbonyldiynes, and homocouplings of  $A_3$ -type triynes have been found useful for the syntheses of hyperbranched polyphenylene (*hb*-PP), polydiyne (*hb*-PDY), and their derivatives. Cross-couplings of  $A_2 + B_3$  monomers such as diynes and trihalides have been utilized to synthesize hyperbranched polyynes (*hb*-PY) and derivatives, while 1,3-dipolar cycloadditions or “click” reactions of  $A_3 + B_2$  monomers such as triynes and diazides have been developed into versatile polymerization techniques for the preparations of hyperbranched PTAs.

In the linear and nonlinear polymerization reactions discussed above, the acetylenic triple bonds are transformed into polyene chains in PAs, ene–yne chains in PDAs, benzene rings in PPs, triazole rings in PTAs, diyne rods in PDYs, etc. The structural issues unique to the linear and hyperbranched acetylenic polymers include steric conformation (e.g., *cis*- and *trans*-polyene chains) and topological pattern (e.g., 1,2,4- or 1,3,5-trisubstituted benzene and 1,4- or 1,5-disubstituted triazole rings), which determine the stereo- and regioregularities and the degrees of branching (DBs) of the polymers. Much work has been done to understand the structural issues, and various approaches have been taken to control or modulate the macromolecular structures, such as the design of molecular structures of alkyne monomers, the search for stereospecific or regioselective catalyst systems, and the optimization of polymerization conditions or parameters (Scheme 4). An appreciable

portion of these structural investigations has been carried out in combination with the studies of materials properties of the polymers, in an effort to collect information on and gain insights into the structure–property relationships involved in the acetylenic polymer systems.<sup>17–84</sup>

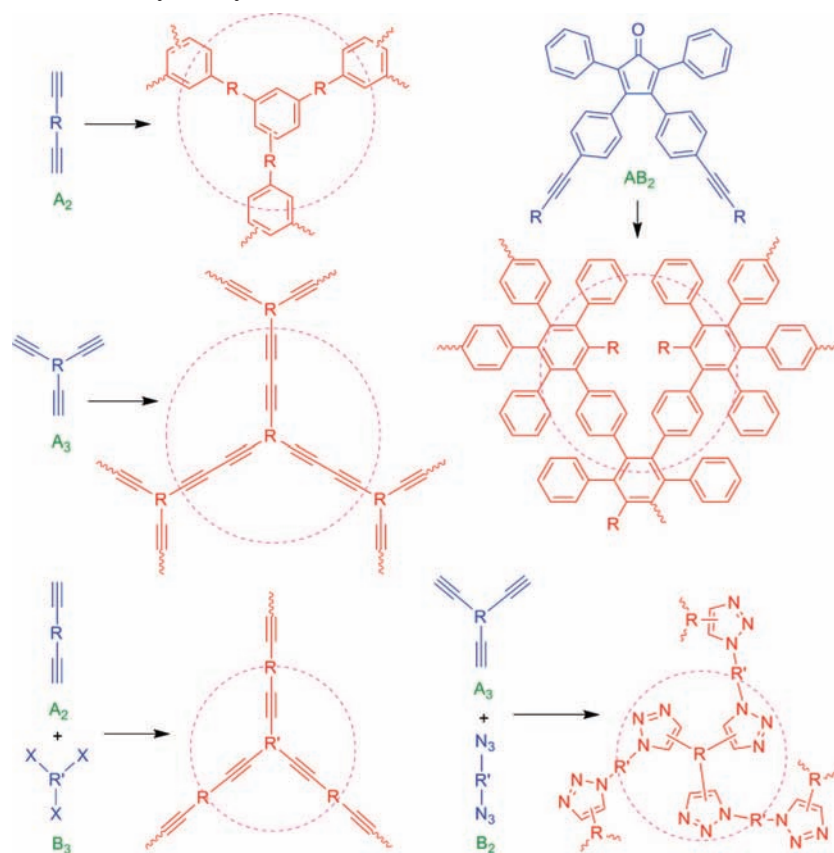
The property investigations have not only shed light on the structure–property relationships but also led to the development of specialty polymers with advanced functionalities.<sup>17–84</sup> Because the driving force for the acetylenic polymer research in the early days was to generate  $\pi$ -conjugated polymers with electronic activity, much of the early work had been devoted to the development of highly conductive materials. Since the ene, yne, enyne, diyne, phenyl, and triazole units in the acetylenic polymers are rich in  $\pi$ -electrons, the electronic communications between these units governed by the effective conjugation lengths in the polymer chains or spheres result in the formation of “dynamic” chromophores with varied optical and photonic responses. The recognition that the segments or branches of conjugated polymers are chromophoric units has triggered a surge of interest in the development of optically and photonic active polymers. As a result, a diversity of acetylenic polymers with photoconductivity, luminescence, chromatism, refractivity, optical nonlinearity, and photochemical patternability have been developed. Introductions of mesogens, chiral groups, metal ligands, and functional moieties of biological origin as pendants to the polymer chains or spheres have led to the generation of novel acetylenic polymers with liquid crystallinity, chiroptical activity, magnetic susceptibility, and biological compatibility.

Thus, thanks to the enthusiastic and fruitful efforts of polymer chemists and materials scientists in the past few decades, the acetylenic monomers have been nurtured into a group of versatile building blocks for the construction of  $\pi$ -conjugated polymers and the acetylenic polymerizations have emerged as useful techniques for the syntheses of advanced specialty polymers with novel molecular structures and unique functional properties. In this review, we will summarize the recent progress in this exciting area of research. Because a huge volume of work has been done by numerous research groups in the area, it is technically impossible for us to give an exhaustive coverage on the topic. Fortunately, a number of excellent review articles on the specific types of acetylenic polymers such as PAs, PPs, PAEs, and PDAs has already been published, examples of which are given in the reference section, to which interested readers are referred.<sup>92–122</sup> Therefore, instead of enumerating every detail with painstaking completeness or comprehensiveness in an encyclopedic fashion, we will use typical examples to tell an integrated story about the synthetic endeavors, structural insights, and function discoveries in the area of acetylenic polymer research, as outlined in Scheme 4, with an emphasis on the syntheses, structures, and functions that are unique to acetylenic polymers. It should be noted that the term “acetylenic polymers” used here does not refer to “acetylene polymer” or PA only but to all the polymers that are synthesized from acetylenic monomers containing single or multiple carbon–carbon triple bonds.

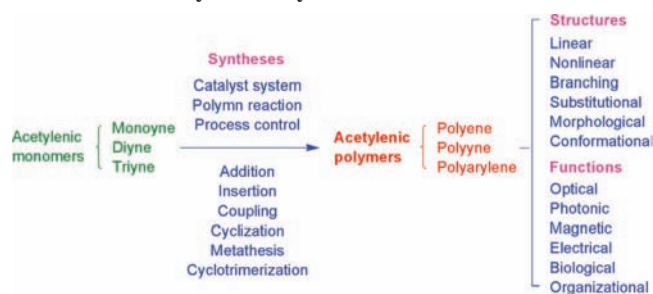
## 2. Syntheses

Although the polymer syntheses based on the triple-bonded acetylenic monomers had lagged behind those based on the double-bonded vinyl monomers in the early days, remarkable advances have been made in the area in recent decades. The

## Scheme 3. Examples of Nonlinear Alkyne Polymerizations



Scheme 4. Scope of This Review: Syntheses, Structures, and Functions of Acetylenic Polymers

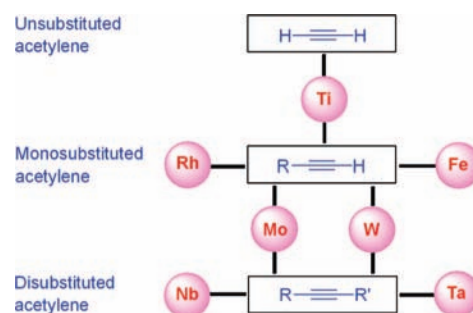


successes in the exploration of effective catalytic systems, the development of versatile polymerization reactions, and the control over the polymerization processes have resulted in the generation of a wide variety of acetylenic polymers. The acetylenic building blocks can now be readily connected together through various construction strategies to furnish linear and hyperbranched polymers. The combined use of the direct polymerizations of monomers and the postpolymerization reactions of polymers (or polymer reactions in short) offers a molecular engineering means for tuning the structures and modulating the functions of the polymers at a molecular level. In this section, we will give an account on the syntheses of various acetylenic polymers by the polymerization reactions of acetylenic monomers with one, two, and three triple bonds, that is, monoynes, diynes, and triynes, respectively.

## 2.1. Polymers from Monoynes

The monoyne polymerizations, especially the effectiveness of the catalyst systems based on various transition metals and the polymerizability of the acetylene monomers contain-

Scheme 5. Monomer–Catalyst Matching Map for Monoyne Polymerizations



ing different numbers and kinds of substituents, will be discussed in this part. The most noteworthy advancement in the area is the exploration of functionality-tolerant and living-polymerization catalysts, which have enabled the syntheses of highly functionalized substituted PAs with well-defined conformational structures and molecular weights. Furthermore, the successful development of effective postpolymerization reactions has allowed the preparations of functionalized PAs that are inaccessible by the direct polymerizations of their corresponding monomers.

## 2.1.1. Catalyst Systems

Typical examples of effective catalyst systems based on various transition-metal species for monoyne polymerizations are diagrammatically shown in Scheme 5. In 1958, Natta's group synthesized PA by using a Ti-based Ziegler catalyst.<sup>9</sup> Polymer scientists at that time envisioned that PA might exhibit semiconductivity. The theoretical calculations carried out in the late 1960s and early 1970s suggested that PA might show even high-temperature superconductivity.<sup>123,124</sup> These

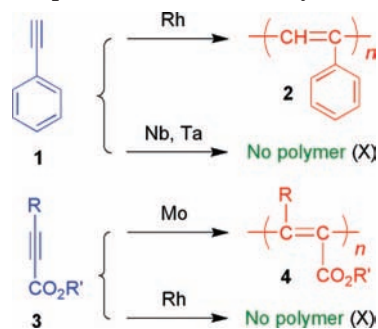
intriguing predictions had attracted several research groups to investigate acetylene polymerization by Ti- and Fe-based Ziegler–Natta catalysts.<sup>125,126</sup> The acetylene polymerization proceeded via an insertion mechanism, yielding a polymer with alternative single and double bonds. Unfortunately, however, the black powdery polymer was difficult to process into a sample suitable for the measurements of its physical properties due to its insolubility, infusibility, and instability. There was, thus, no significant progress in these early studies. In 1974, Shirakawa and co-workers reported that the PA films with metallic lusters could be prepared over a wide temperature range by using highly concentrated Ziegler–Natta catalyst of  $\text{Ti}(\text{OBU})_4\text{-AlEt}_3$ .<sup>127</sup> The PA films were later found by Heeger, MacDiarmid, and Shirakawa to exhibit very high electrical conductivity upon doping.<sup>13,128</sup>

In an effort to confer processability, stability, and functionality on PA, several research groups tried to polymerize substituted acetylenes. This task critically depended on the exploration of effective catalyst systems. In the early stage, the acetylene polymerizations were studied by using conventional Ziegler–Natta catalysts. However, the catalysts could only polymerize sterically unhindered monosubstituted acetylenes into insoluble polymers and/or soluble oligomers. Examples include the polymerizations of phenylacetylene (**1**) by Berlin,<sup>129</sup> Percec,<sup>130–133</sup> Kern,<sup>134</sup> and Ehrlich.<sup>135</sup> Efficient polymerization of **1** was achieved by Masuda and Higashimura in 1974:  $\text{WCl}_6$  and  $\text{MoCl}_5$  catalyzed the polymerization of **1** to give poly(phenylacetylene) (PPA) with molecular weights over 10 000.<sup>18</sup> Some cocatalysts such as  $\text{Ph}_4\text{Sn}$  and  $n\text{-Bu}_4\text{Sn}$  were found to accelerate the polymerization reactions of phenylacetylene.

The  $\text{WCl}_6$  and  $\text{MoCl}_5$  catalyst systems, however, are sensitive to air and moisture and intolerant of polar functional groups in the monomers, especially those monomers containing active hydrogen atoms, such as amino and amido groups.<sup>136</sup> Metal–carbonyl complexes are more stable than the metal halides but need to be preactivated by chlorine-containing additives and/or UV photoirradiation in halogenated solvents.<sup>137–139</sup> In 1989, Tang discovered that several stable metal–carbonyl complexes could catalyze polymerizations of 1-alkynes.<sup>21</sup> Tang's group extended their efforts in the area and prepared a series of transition metal–carbonyl complexes with a general formula of  $\text{M}(\text{CO})_x\text{L}_y$  with M being Mo and W.<sup>140</sup> Delightfully, these complexes were found to polymerize various functionalized acetylene monomers in normal, nonhalogenated solvents without UV irradiation. The metathesis mechanism of the Mo- and W-catalyzed polymerization was proposed by Masuda<sup>141</sup> and verified by Katz.<sup>142,143</sup> In addition to the commercially available metal-halide salts, well-defined Mo–carbene complexes have been developed by Schrock.<sup>144–146</sup> These salts and complexes have proven to be effective catalysts for the polymerizations of a variety of mono- and disubstituted acetylenes, including those sterically demanding monomers.

In parallel to the progressive developments of the metathesis catalysts, the Rh-based complexes were found to polymerize acetylenes to yield stereoregular PAs in an insertion mechanism. Although Kern found that **1** was polymerized in the presence of  $\text{RhCl}_3\text{-LiBH}_4$  and  $\text{Rh}(\text{PPh}_3)_3\text{Cl}$  in 1969,<sup>147</sup> the real interest in the Rh-based catalysts was stimulated by the work of Furlani in 1989 and Tabata in 1991, who found that a series of Rh complexes, such as  $[\text{Rh}(\text{diene})\text{Cl}]_2$  [diene = 2,5-norbornadiene (nbd), 1,5-cyclooctadiene (cod)], could effectively polymerize

### Scheme 6. Examples of Substrate–Catalyst Matching



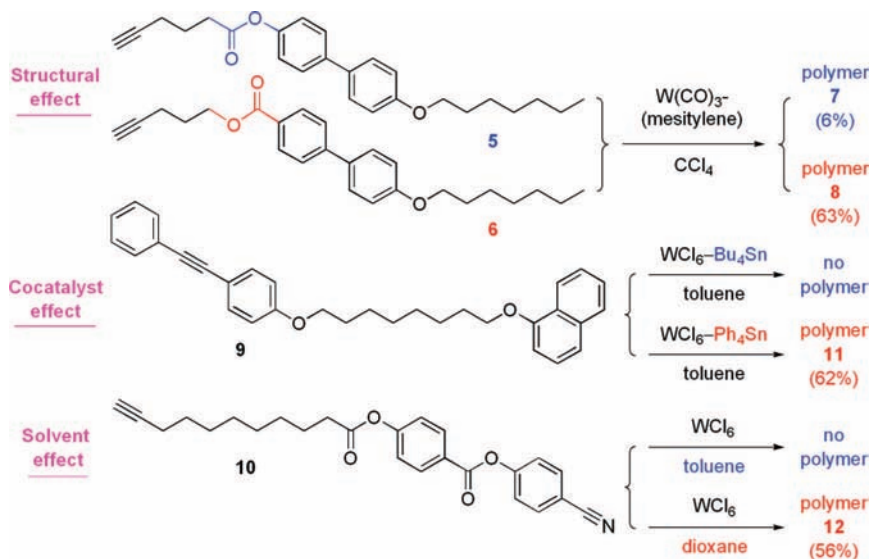
monosubstituted acetylenes such as **1**, especially in the presence of additives of inorganic and organic bases.<sup>148,149</sup> Masuda found that some organometallic additives such as  $\text{PhLi}$ ,  $\text{Et}_2\text{Zn}$ ,  $\text{Et}_3\text{B}$ , and  $\text{Et}_3\text{Al}$  served as effective cocatalysts.<sup>150</sup> Noroyi developed a zwitterionic Rh complex of  $\text{Rh}^+(\text{nbd})[\text{C}_6\text{H}_5\text{B}^-(\text{C}_6\text{H}_5)_3]$  that could polymerize acetylenes to polymers of moderate molecular weights in the absence of added cocatalysts.<sup>151</sup> Tang and co-workers developed water-soluble Rh-based catalysts such as  $\text{Rh}(\text{diene})(\text{tos})(\text{H}_2\text{O})$  ( $\text{tos} = p\text{-toluenesulfonate}$ ) that could catalyze acetylene polymerization even in tap water and open air, giving stereoregular polymers of high molecular weights in high yields.<sup>152</sup> All the Rh-based catalysts are tolerant to polar functional groups in the monomers and solvents and produce polymers with high *cis* contents but generally only work well for the polymerizations of monosubstituted acetylenes. For example, **3** cannot be polymerized by the Rh-based complexes, though it can be effectively polymerized by the Mo-based catalysts (Scheme 6).<sup>105</sup>

Halides of group 5 transition metals ( $\text{NbX}_5$ ,  $\text{TaX}_5$ ; X = Cl, Br, F) catalyzed the cyclotrimerization of **1**, giving no polymeric products (Scheme 6).<sup>153</sup> Cotton and co-workers synthesized dinuclear complexes of Nb and Ta with six chlorides and three tetrahydrothiophenes as ligands and demonstrated their catalytic activity in polymerizing 1-phenyl-1-propyne.<sup>154</sup> Stimulated by the work of Cotton, Masuda tried to polymerize 1-phenyl-1-alkynes in the presence of pentahalides of Nb and Ta.<sup>155</sup> Completely soluble polymers with very high weight-average molecular weights ( $M_w = 5 \times 10^5\text{--}1 \times 10^6$ ) were obtained from the polymerizations catalyzed by  $\text{TaCl}_5$  and  $\text{TaBr}_5$ . All the polymers are white-colored, air-stable, and electrically insulating solids because the steric crowdedness caused by the presence of two substituents in one repeat unit has significantly twisted the conformation of the polyene backbone. Generally, use of cocatalysts such as  $n\text{-Bu}_4\text{Sn}$  and  $\text{Et}_3\text{SiH}$  accelerates the polymerization and increases the molecular weights of resultant polymers.<sup>156</sup> Similar to the Mo- and W-based catalysts, the Ta and Nb halides and the Schrock's Ta–alkylidene complexes catalyze the polymerizations of disubstituted acetylenes in a metathesis mechanism. The catalysts are ineffective in polymerizing disubstituted functional acetylenes containing polar groups due to the poisoning effects of the functional groups on the metathesis catalysts.

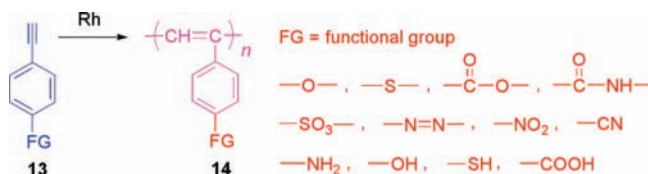
#### 2.1.2. Polymerization Behaviors

The molecular structures of the acetylenic monomers greatly affect their polymerization behaviors. For example, the substrate–catalyst matching discussed above is structurally susceptible: a seemingly subtle variation in the functional group can greatly influence the polymerizability of a

## Scheme 7. Effects of Substrate, Cocatalyst, and Solvent on Monoyne Polymerizations



## Scheme 8. Polymerizations of Functionalized Acetylene Monomers



monomer by a given catalyst. As can be seen from the examples shown in Scheme 7, monomers **5** and **6** differ only in the orientation of the ester unit but show distinct polymerization behaviors in the presence of metal carbonyl complex of  $W(CO)_3(\text{mesitylene})$ : **6** can be effectively polymerized but **5** cannot.<sup>140</sup> The polymerization conditions, such as cocatalyst and solvent, can affect the fate of a specific substrate–catalyst pair. For instance, **9**– $WCl_6$  can be a “bad” or “good” combination, depending on whether  $n\text{-Bu}_4\text{Sn}$  or  $\text{Ph}_4\text{Sn}$  is used as a cocatalyst.<sup>105</sup> Polymerization of **10** does not occur at all in toluene but proceeds well in dioxane.<sup>157</sup>

The syntheses of PAs carrying functional pendants have attracted much attention. The main obstacle to the polymerizations of functionalized acetylenes had been the incompatibility of the polar groups in the monomers with the early transition metals in the metathesis catalyst systems. Even by using the Rh-based catalysts, the polymerizations of highly polar monomers, especially those with acidic protons, had been a difficult proposition: for example, the direct polymerization of 4-ethynylbenzoic acid was very challenging.<sup>158–160</sup> As a result, its polymer was prepared indirectly by hydrolysis of preformed polymer of its protected monomer. Tang and co-workers tackled this difficult issue and succeeded in the direct polymerizations of a series of highly polar phenylacetylene derivatives.<sup>161–172</sup> Under optimized reaction conditions, the functionalized phenylacetylene derivatives (**13**) with various polar groups, such as oxy, carboxy, hydroxy, azo, cyano, thiol, amino, and nitro, have been directly polymerized in the presence of Rh complexes of  $[\text{Rh}(\text{cod})\text{Cl}]_2$ ,  $[\text{Rh}(\text{nbd})\text{Cl}]_2$ , and  $\text{Rh}^+(\text{nbd})[\text{C}_6\text{H}_5\text{B}^-(\text{C}_6\text{H}_5)_3]$  to afford corresponding polymers (**14**) with high molecular weights ( $M_w$  up to  $\sim 5 \times 10^5$ ) and low polydispersity indexes (PDI down to 1.03) in good yields (Scheme 8).

## Chart 1. Examples of Catalyst Systems for Living Acetylene Polymerizations

$\text{TaCl}_5$	<b>15</b>	$\text{Rh}(\text{C}\equiv\text{CPh})(\text{nbd})(\text{PPh}_3)_2\text{-DMAP}$	<b>23</b>
$\text{MoCl}_5$	<b>16</b>	$[\text{Rh}(\text{nbd})\text{OCH}_3]_2\text{-PPh}_3\text{-DMAP}$	<b>24</b>
$\text{MoCl}_5\text{-}n\text{-Bu}_4\text{Sn-EtOH}$	<b>17</b>	$[\text{Rh}(\text{nbd})\text{Cl}]_2\text{-NaOCH}_3\text{-PPh}_3\text{-DMAP}$	<b>25</b>
$\text{MoOCl}_4\text{-}n\text{-Bu}_4\text{Sn-EtOH}$	<b>18</b>	$[\text{Rh}(\text{nbd})\text{Cl}]_2\text{-Ph}_2\text{C=C(Ph)Li-PPh}_3$	<b>26</b>
$\text{MoOCl}_4\text{-}n\text{-BuLi}$	<b>19</b>	$\text{Rh}(\text{PhC}\equiv\text{CPh}_2)(\text{nbd})(\text{PAR}_3)\text{-PAR}_3$	<b>27</b>
$\text{WOCl}_4\text{-}n\text{-Bu}_4\text{Sn-}t\text{-BuOH}$	<b>20</b>	$\text{Rh}(\text{PhC}\equiv\text{CPh}_2)(\text{tfb})(\text{PPh}_3)\text{-PPh}_3$	<b>28</b>
$\text{Ta}(\text{Py})(\text{DIPP})_3$	<b>21</b>	Abbreviations:	
$\text{AdN}(\text{Mo})\text{CMe}_2\text{Ph}$	<b>22</b>	Py = pyridine, nbd = 2,5-norbornadiene	
		DMAP = 4-(dimethylamino)pyridine	
		Ad = 1-adamantyl, R' = $-\text{CH}(\text{CF}_3)_2$	
		DIPP = 2,6-diisopropylphenoxide	
		tfb = tetrafluorobenzobarrelene	
		$\text{PAR}_3 = \text{P}(4\text{-X-Ph})_3$ , X = F, Cl	

Living polymerizations have made a revolutionary impact on polymer science and have opened a new avenue for the syntheses of macromolecules with uniform molecular weights, precise architectures, and nanostructured morphologies.<sup>7,173–181</sup> In a living polymerization, the propagating chains undergo neither transfer nor termination. The number-average degree of polymerization ( $\text{DP}_n$ ) of a living polymer is thus determined by the ratio of the concentration of consumed monomer ( $[\text{M}]_0 - [\text{M}]_t$ ) to the initiator concentration ( $[\text{I}]_0$ ). The molecular weight distribution of a living polymer is normally very narrow (often close to unity). Most of the living polymerizations studied so far have been on vinyl monomers. Living polymerizations of acetylenic monomers may enable the syntheses of electronically conjugated polymers with well-defined structures and desired materials properties.<sup>182</sup> This intriguing possibility has prompted several research groups to explore the possibility of developing living polymerization systems of substituted acetylenes.

To date, transition-metal halides **15–20**,<sup>183–193</sup> transition-metal–alkylidene complexes **21** and **22**,<sup>144–146</sup> and rhodium complexes **23–28**<sup>194–199</sup> have been found capable of initiating the living polymerizations of acetylenes (Chart 1). In the late 1980s, Percec and Masuda reported on the living polymerizations of several substituted acetylenes catalyzed by  $\text{TaCl}_5$  (**15**)<sup>184,187</sup> and  $\text{MoCl}_5$ – and  $\text{MoOCl}_4$ – $n\text{-Bu}_4\text{Sn}$ – $\text{EtOH}$  mixtures (**17** and **18**).<sup>183,185,186</sup> It was hypothesized that the alkynes with bulky substituents would suppress the backbiting and interchain reactions due to the steric hindrance and thus promote living polymerizations. In the  $\text{MoCl}_5$ -initiated polymerization of  $t$ -butylacetylene, the

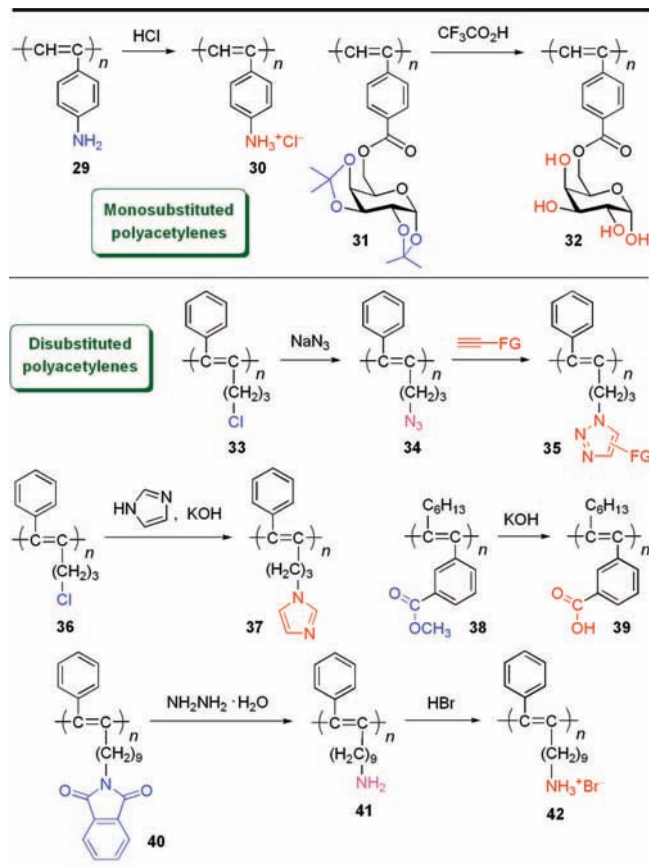
plots of molecular weight versus monomer conversion and  $\ln([M]_0/[M]_t)$  versus time ( $t$ ) gave linear lines, indicating the living nature of the acetylene polymerization, although the PDIs of the resulting polymers ( $>1.9$ ) were higher than those expected for a classical living polymer.<sup>182,187</sup> Masuda succeeded in the preparation of triblock PA copolymers of A–B–A and B–A–B types through the successive polymerizations of 1-chloro-1-hexane (A) and 1-chloro-1-hexadecyne (B) initiated by Mo-based ternary mixture **18**, although the initiation efficiency was very low ( $\sim 2.5\%$ ).<sup>186</sup>

In 1989, Schrock et al. reported the living polymerization of 2-butyne using a single-component, well-defined, Ta-based initiator (**21**).<sup>144</sup> The resultant poly(2-butyne) had  $DP_n$ 's up to 200 and PDIs down to 1.03. Remarkably, the initiation efficiency was virtually quantitative, and the living chain ends could be functionalized conveniently by an appropriate aldehyde via a Wittig-like capping reaction. However, **21** worked for living polymerization of 2-butyne only. Schrock's group further developed well-defined Mo-based alkylidene complexes, e.g., **22**, that were able to efficiently polymerize in a living manner a variety of acetylene monomers, such as *o*-substituted phenylacetylenes and metallocenyl-substituted 1-alkynes.<sup>145,146</sup> The activity and selectivity of the Mo-based alkylidene complexes could be tuned by the steric and electronic effects of the ligand peripheries surrounding the metal center.

The early transition metal-based living polymerization catalysts generally work for the disubstituted or sterically crowded monosubstituted acetylenes with no polar functional groups but are ineffective for the acetylenes with low steric effects such as **1**. Steric hindrance seems to have prevented the formation of *cis-cisoidal* backbone conformation and the occurrence of backbiting reaction. Furthermore, intra- and interchain reactions are presumably eliminated because of the protection of the polyene backbone by the bulky substituents. Different from these early transition-metal catalysts, the late transition-metal Rh-based catalysts can initiate the living polymerizations of sterically less demanding phenylacetylene derivatives. The living polymerization of **1** was first accomplished by Noyori and co-workers in 1994 by using mixture **23** as initiator, affording PPAs with PDI of  $\sim 1.1$  in quantitative yields.<sup>24</sup> The initiation efficiencies of the living polymerization reactions were  $\sim 33$ – $56\%$ . The living polymerization catalyst systems generated in situ, e.g., **24** and **25**, also enabled the controlled stereoregular polymerization of **1**.<sup>194,195</sup>

As the propagating species derived from the Rh catalysts was proposed to be vinylrhodium, Masuda designed a living polymerization system of **1** mediated by a ternary catalyst **26**.<sup>196</sup> In a typical run, the PDI of the resultant PPA was  $\sim 1.1$  and the initiation efficiency was virtually quantitative. A successive addition polymerization experiment revealed that the  $DP_n$  value of the polymer increased in proportion to the polymer yield, while its PDI remained to be as small as  $\sim 1.1$ . This indicates that the propagating species remained active even after the consumptions of the early added batches of monomers. Soluble star polymers and star block copolymers were synthesized from the living linear PPA and poly(*p*-methylphenylacetylene) by employing 1,4-diethynylbenzene and 1,4-diethynyl-2,5-dimethylbenzene as linking agents. Furthermore, use of the (triphenylvinyl)lithium reagents containing functional groups led to the formation of functionalized PPA with the functional groups located at the initiating chain end. Thereafter, well-defined Rh com-

**Scheme 9. Syntheses of Highly Functionalized Polyacetylenes through Polymer Reactions**

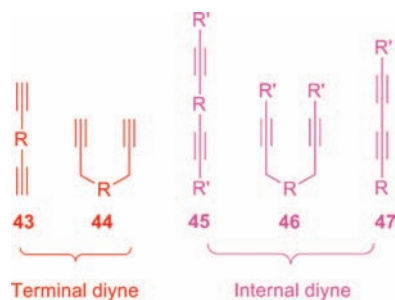


plexes **27** and **28** were developed for the living polymerizations of **1**, yielding PPAs with PDIs as low as 1.04 in virtually quantitative initiation efficiency.<sup>197,198</sup>

### 2.1.3. Polymer Reactions

Postpolymerization reactions can be used to further functionalize the preformed acetylenic polymers, to prepare the functional polymers that are inaccessible by direct polymerizations of their corresponding monomers, and to modulate the properties of the acetylenic polymers by structural modifications.<sup>199–207</sup> Tang and co-workers have developed a series of facile polymer reactions for the functionalizations of acetylenic polymers. For example, **29** consists of hydrophobic PPA skeleton and hydrophilic amine pendant (Scheme 9). Because of this unique structural feature, the polymer is insoluble in either organic solvents or aqueous media. Ionization of **29** by hydrochloric acid gives rise to polyelectrolyte salt **30** and makes the polymer readily soluble in water.<sup>161</sup> Although macromolecular reactions normally do not proceed to 100%, remarkably the deprotection reaction of **31** beautifully proceeds to completion: the cleavage of its ether protection groups by acid-catalyzed hydrolysis furnishes **32** with cytocompatible sugar pendants that do not contain any ether residues.<sup>208</sup>

While the studies on the polymerizations of acetylenic monomers have made impressive progress in the past decades, it is still very difficult to access functionalized disubstituted PAs through the direct polymerizations of their corresponding monomers, owing to the thorny problems associated with the intrinsic intolerance of the early transition-metal-based metathesis catalyst systems to the polar

**Chart 2. General Structures of Terminal and Internal Diyne Monomers**

functional groups. Polymer-reaction approaches can help solve this problem. For example, using the azide–alkyne click reactions, Tang and co-workers succeeded in attaching a number of polar functional groups (FGs) to the pendants of disubstituted PA **34**.<sup>204</sup> Nucleophilic substitutions<sup>205–208</sup> and hydrolysis reactions<sup>199</sup> of polymers **36** and **38** resulted in the formation of imidazole- and carboxy-functionalized disubstituted PAs **37** and **39**, respectively. Hydrazine-catalyzed deprotection of polyimide **40** brought about polyamine **41**, which could be further ionized by hydrobromic acid to give polyelectrolyte salt **42**.<sup>168,169,200</sup>

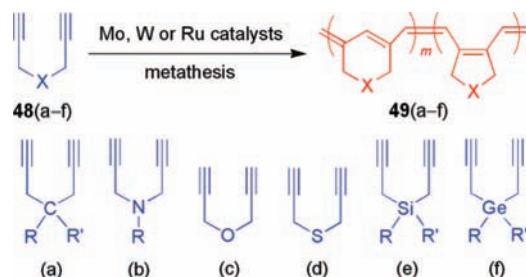
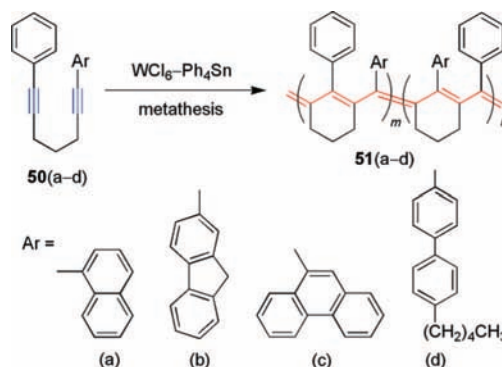
## 2.2. Polymers from Dienes

### 2.2.1. Monomer Structures

Dienes are a group of acetylene derivatives with two triple bonds in a single molecule that have been extensively studied as potential monomers for acetylenic polymerizations. Terminal and internal diyne monomers **43–47** (Chart 2) have been utilized as building blocks to construct polymers with different molecular conformations and topological structures. Different from the monoynes discussed above, the diyne monomers can be polymerized by not only linear but also nonlinear polymerization reactions. Typical examples of the linear polymerization reactions include cyclopolymerization of 1,6-heptadiynes, metathesis polymerization of internal diynes, cross-coupling polymerization of diynes with dihalides, photoinduced solid-state topopolymerization of diacetylenes, polyhydrosilylation of diynes with (di)silanes, polyhydroboration of diynes with boranes, polyhydrothiolation of diynes with dithiols, Diels–Alder polycycloaddition of diynes with dicyclopentadienones, and click polymerization of diynes with diazides. The nonlinear polymerization reactions include polycoupling of diynes with triiodides, polyhydrosilylation of diethynylsilanes, polybisthiolation of diethynyl disulfides, polycycloaddition of cyclopentadienonyldiynes, polycyclotrimerizations of diynes, and click polymerization of azidodiynes.

### 2.2.2. Linear Polymerizations

It is already known that monoynes undergo metathesis polymerization in the presence of Mo- and W-based catalysts. Theoretically, polymerization of diyne monomers generally gives highly cross-linking polymers. However, owing to their special geometrical arrangements, 1,6-heptadiynes **44** and **46** can be polymerized into linear polyenes with cyclic structures recurring along the backbone.<sup>93,209</sup> The advances in the area of research on poly(1,6-heptadiyne)s have been thoroughly reviewed by Kim et al.<sup>93</sup> and recently by Buchmeiser,<sup>209</sup> and we thus will not repeat what has been summarized in those reviews. Typical examples of 1,6-

**Scheme 10. Cyclopolymerization of 1,6-Heptadiyne Derivatives****Scheme 11. Cyclopolymerization of Internal Dienes**

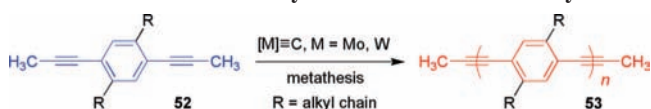
heptadiyne monomers are given in Scheme 10 [**48(a–f)**]. A mixture of five- and six-membered alkenyl rings are usually formed in the cyclopolymerizations of 1,6-heptadiynes. Schrock-type metathesis complexes, however, can cyclopolymerize diethyl dipropargylmalonate (**48a**,  $R = R' = -CO_2C_2H_5$ ) in a regioselective manner, giving polymers with either five- or six-membered repeat units.<sup>210–215</sup> A series of trifluoroacetate- and pentafluorobenzoate-modified Grubbs–Hoveyda catalysts were found to polymerize sterically demanding 1,6-heptadiyne esters, dipropargylamines, dipropargylammonium salts, and an alkyl-substituted dipropargyl ether into cyclic polyenes (**49**) with repeat units of predominantly (>95%) five-membered rings.<sup>216</sup>

In sharp contrast to the active research on the polymerizations of terminal 1,6-heptadiynes, little work has been done on internal 1,6-heptadiynes, mainly due to the involved synthetic difficulty. Tang and co-workers designed and synthesized a group of  $\alpha,\omega$ -disubstituted alkadiynes containing different aryl rings.<sup>217</sup> The terminally disubstituted 1,6-heptadiynes [**50(a–d)**], whose structures are given in Scheme 11, show polymerization behaviors distinctly different from those of their unsubstituted parents: the former cannot be effectively polymerized by the binary  $MoCl_5-Ph_4Sn$  mixture, which is a good catalyst for the polymerization of the latter. Delightfully, however, Tang and co-workers found that the binary  $WCl_6-Ph_4Sn$  mixture could effectively transform the aryl-disubstituted 1,6-heptadiyne derivatives into high-molecular-weight cyclic polyenes (**51**) consisting of exclusively six-membered rings. The polyenes with their labile olefinic hydrogen atoms replaced by the stable aromatic rings are, as anticipated, very stable and readily processable.

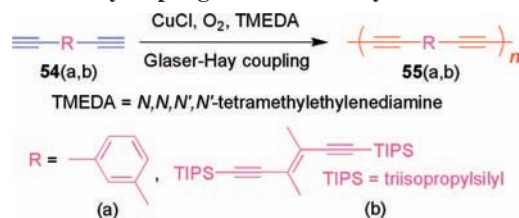
Schrock tungsten–carbyne complex ( $t-BuO)_3W\equiv C-t-Bu$  can catalyze alkyne metathesis.<sup>218,219</sup> Schrock and Bazan have shown that the complex is capable of initiating ring-opening metathesis polymerization of cyclic alkynes.<sup>220,221</sup> In 1997, Bunz and Müllen reported the synthesis of poly(phenyleneethynylene)s (PPEs) by alkyne metathesis: ( $t-BuO)_3W\equiv C-t-Bu$  was used to initiate acyclic metathesis polymerization



## Scheme 12. Metathesis Polymerization of Internal Diynes



## Scheme 13. Polycoupling of Terminal Diynes



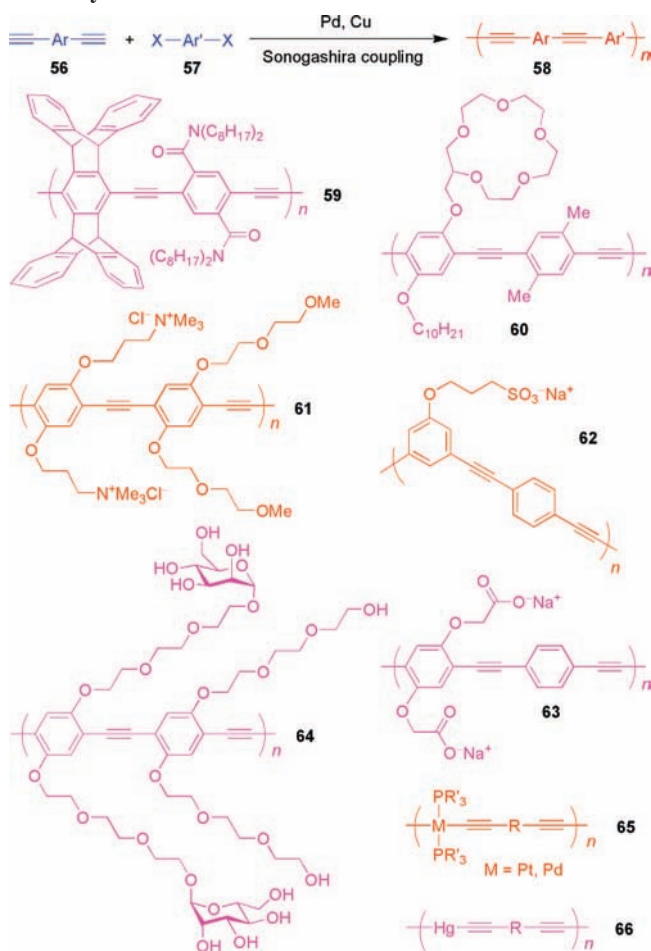
of 2,5-dihexyl-1,4-dipropynylbenzene, producing defect-free polymers with  $DP_n \approx 100$  in high yields.<sup>222</sup> The Schrock catalyst, however, is difficult to prepare and sensitive to air and moisture and must be used in carefully dried solvents in a glovebox or Schlenk line. On the other hand, the Mortreux–Mori–Bunz catalyst generated in situ from commercially available reagents of  $Mo(CO)_6$  and phenols could work in unpurified solvents.<sup>223</sup> A series of dipropynylated benzenes (52) was metathesis polymerized to furnish PPEs 53 in quantitative yields and high purity (Scheme 12). The  $DP_n$ 's of the PPEs can reach very high values (up to 2 000) when long side chains (R) are used as solubilizing groups in 53. The metathesis polymerizations carried out at elevated temperatures produced high-molecular-weight polymers.

One of the characteristic reactions of alkynes is the coupling reaction: under appropriate conditions, alkynes can undergo homo- and cross-coupling reactions to yield molecules with newly formed carbon–carbon bonds.<sup>10–12</sup> The first oxidative polycoupling of terminal diynes was investigated by Hay,<sup>224–226</sup> from which a new class of PDYs was generated, which could be solution cast into films or spun into fibers. Polymer 55a from *m*-diethynylbenzene 54a has exceptionally high carbon content ( $\sim 97\%$ ) and forms transparent, flexible films (Scheme 13). Carbon fibers with high mechanical strengths and moduli were fabricated from these carbon-rich polymers. The conversions from the polymers to the graphite fibers were fast and could be completed in a few minutes. The polymers containing the diyne moieties were photosensitive and could be cross-linked by photoirradiation.<sup>227,228</sup>

Diederich et al. have designed and synthesized a large variety of acetylenic all-carbon or carbon-rich polymers, using Glaser–Hay coupling reactions between the carbon–carbon triple bonds. Diederich has comprehensively reviewed the progress in this area, and interested readers are referred to the review articles.<sup>104,121,229,230</sup> The constructions of these carbon-rich acetylenic scaffolds and nanometer-sized structures have opened up new avenues for basic research and technological innovation at the interface between chemistry and material sciences. For example, stable and soluble conjugated molecular wires with persilylethynylated poly(triacetylene) 55b and its derivatives modified by different peripheral groups have been found to exhibit useful electronic and optical properties.<sup>231</sup>

In addition to the alkyne metathesis approach, Sonogashira coupling between diynes and dihalides<sup>232</sup> is another powerful tool for the syntheses of conjugated PAEs (Scheme 14). It should be noted that, in this  $A_2 + B_2$ -construction strategy, stoichiometric balance of the mutually reactive A and B groups must be ensured in order to obtain high-molecular-

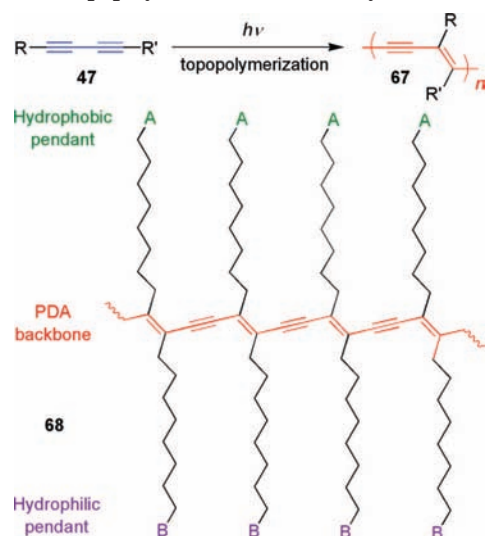
## Scheme 14. Cross-Coupling Polymerization of Arylenediynes with Arylenediiodides



weight PAEs. Bunz has reviewed the synthesis of PAEs including the influence of substrate structures and reaction conditions.<sup>94,223</sup> This Pd-catalyzed cross-coupling polymerization is highly tolerant of substrate variations. Through direct polymerizations and polymer reactions, a wide variety of functionalized PAEs have been prepared. Selected examples include the PAEs containing bulky pentiptycene group (59),<sup>233</sup> crown ether chelator (60),<sup>234</sup> electrolyte ions (61–63),<sup>235–237</sup> hydrophilic sugar moiety (64),<sup>238</sup> and transition metals (65 and 66).<sup>103,239</sup> A number of research groups, including those led by Swager,<sup>240,241</sup> Müllen,<sup>242</sup> Weder,<sup>243,244</sup> Bunz,<sup>94,223</sup> Schanze,<sup>245</sup> Whitten,<sup>235,246</sup> Huang,<sup>247</sup> and Wong,<sup>103,239</sup> have demonstrated that the functionalized PAEs can find practical applications in explosive detectors, biological sensors, organic light-emitting diodes (OLEDs), liquid crystal displays (LCDs), photovoltaic cells (PVCs), etc. Typical examples of the applications will be discussed in section 4 of this review.

Wegner discovered a unique diyne polymerization reaction, namely, solid-state polymerization of 1,4-diacetylenes (Scheme 15).<sup>248–251</sup> When the reactive diyne monomers are preorganized at a distance commensurate with the distance between the repeat units in the final PDAs, application of thermal or photochemical energy can initiate the topopolymerization reaction. This preorganization is satisfied in some diacetylene crystals and some diacetylene amphiphiles in monolayers, LB-multilayers, bilayer vesicles, and tubules.<sup>252–260</sup> For example, closely packed and properly ordered diacetylene lipids readily undergo polymerization through 1,4-addition to give alternative ene–yne polymer chains, e.g.,

## Scheme 15. Topopolymerization of Diacetylenes

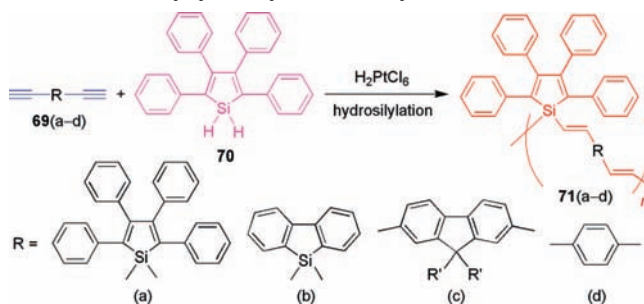


**68**, upon irradiation with UV light (in the case of thin films and vesicle solutions) or with  $\gamma$ -ray irradiation (in the case of solid powders). Since no chemical initiators or catalysts are used in the polymerization process, the PDAs are not contaminated with impurities and, consequently, the purification steps are not required. The PDAs possess novel structures and exhibit unique properties, such as large quasi-one-dimensional structure of their single crystals, large optical nonlinearity (especially high third-order susceptibility), and high photoconductivity.<sup>261,262</sup> The most characteristic and attractive property of the PDAs is their dramatic chromic transitions. Normally, the PDAs generated by photoinduced topopolymerization have a blue color. The PDAs undergo a blue-to-red color change in response to thermal agitation, solvent fumigation, mechanical stress, or ligand–receptor interactive perturbation.<sup>258,260,263,265</sup>

Acetylene derivatives readily undergo addition reactions with heteroatom-containing compounds, such as silane (hydrosilylation), borane (hydroboration), and thiol (hydrothiolation).<sup>10–12</sup> Many research groups have worked on the utilization of these reactions for the syntheses of heteroatom-containing acetylenic polymers. Polyhydrosilylation of diynes leads to the formation of poly(silylenevinylene)s, which possess excellent processability and stability and have found applications as ceramic precursors, cross-linkable prepolymers, electron-transport media, and luminescent materials,<sup>109,119,266–270</sup> thanks to the unique  $\sigma^*-\pi^*$  conjugation along the polymer backbone.<sup>119,271</sup> The alkyne hydrosilylation is realized by the oxidative addition of the Si–H bond across the C $\equiv$ C bond, which yields the silylenevinylene unit. The reaction is tolerant of various functional groups, such as ester, nitrile, amine, amide, nitro, ketone, ether, phosphate, sulfide, and sulfone. Structurally, alkyne hydrosilylation can produce several isomers, including *trans* (*E*), *cis* (*Z*), and geminal products that result from the  $\beta$ -1,2 (*syn* and *anti*) and  $\alpha$ -2,1 additions. The regio- and stereoselectivities depend on the steric effect, kinetic control, and the catalyst used. Over the past decades, many metal complexes have been investigated as potential hydrosilylation catalysts. Among the most popular are platinum, palladium, rhodium, and ruthenium complexes. The Speier hexachloroplatinic acid has become the catalyst of choice for most hydrosilylation reactions.<sup>272</sup>

By increasing the steric hindrance of substrates and exercising kinetic control (e.g., high temperature), Keller,<sup>273</sup>

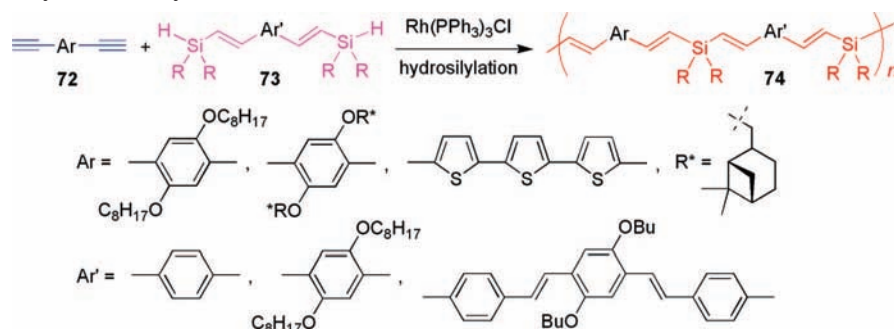
## Scheme 16. Polyhydrosilylation of Diynes with Silanes



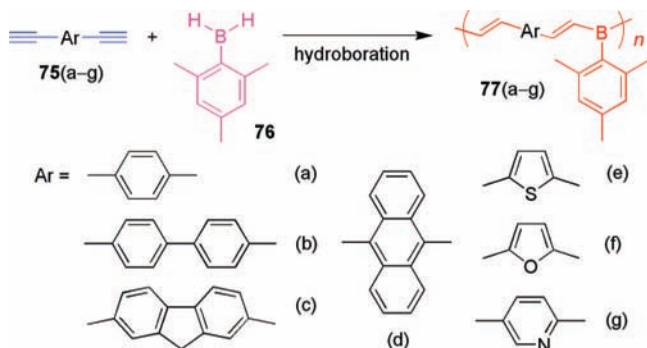
Luneva,<sup>274</sup> Shim,<sup>275</sup> and Troglor<sup>270,276</sup> have prepared various poly(silylenevinylene)s with *trans*-rich stereoregularity by using the Speier's catalyst (e.g., Scheme 16). In some cases, geminal linkage and chain branching have occurred as a result of further hydrosilylation of the Si–H bond to the vinylene unit formed during the polymerization process.<sup>277</sup> The palladium complexes are not as reactive as their platinum counterparts. The rhodium catalysts can control the ratio of the regio- and stereoisomers formed. Using Wilkinson's catalyst  $\text{Rh}(\text{PPh}_3)_3\text{Cl}$ , Luh and co-workers have developed very useful hydrosilylation protocols for the synthesis of polymers carrying more than two different chromophores in a regio- and stereoregular manner (Scheme 17).<sup>109,278</sup> The optical properties of the polymers with all *trans*-vinylene structures have been actively investigated (vide post). Mori found that  $\text{Rh}(\text{PPh}_3)_3\text{I}$  could be used to prepare polymers with *trans*- or *cis*-rich conformation, depending on the sequence of monomer addition and the polymerization temperature.<sup>279</sup> Using the bis(silyl)arylene and bisethynylarylene monomer pairs, high-molecular-weight polymers with *trans*- or *cis*-rich structures were prepared. The fluorescence quantum yield ( $\Phi_F$ ) of the *trans*-polymer is much higher than that of its *cis* counterpart. This is because the *trans*-isomer is electronically more delocalized, which enables more extensive orbital overlapping between the monomer units as compared to the *cis*-isomer. Upon UV irradiation, *cis* structure is isomerized to all-*trans* structure, which shows the expected increase in  $\Phi_F$  as well as the high stability of the Si–C bond.<sup>280</sup>

Although alkyne hydroboration is well-known in organic chemistry, examples of using this reaction to synthesize polymers are rare. Chujo et al. synthesized organoboron polymers **77** with moderate molecular weights by polyhydroboration of aromatic diynes **75** with mesitylborane **76** in tetrahydrofuran (THF) at room temperature, utilizing the highly regioselective nature of the reaction of borane with alkyne (Scheme 18).<sup>65</sup> The polymers showed high solubility but relatively low stability to air and heat. Corriu, Douglas, and Siebert found that 2,5-dialkynylthiophenes ( $\text{RC}\equiv\text{C})_2\text{C}_4\text{H}_2\text{S}$  ( $\text{R} = \text{Ph}, \text{Me}_3\text{Si}, t\text{-Bu}$ ) treated with  $\text{HBCl}_2$  and  $\text{Et}_3\text{SiH}$  in dichloromethane (DCM) underwent hydroboration polymerization to give highly colored polymers, which were extremely sensitive to oxygen and water.<sup>281</sup> In the polymers prepared by Chujo, the extension of  $\pi$ -conjugation through the boron atom was observed.<sup>282</sup> Further studies revealed that the polymers belonged to typical electron-deficient n-type conjugated polymer. Incorporation of donor (D) chromophores is expected to modulate the optical properties of the polymers. Indeed, while polymers **77(a-d)** emit blue light, the polymers containing electron-donating units of thiophene, furan, and pyridine, i.e., **77(e,f)** and **77g**, emit green and white lights, respectively, due to the donor–acceptor (D–A) interactions in the polymers.

## Scheme 17. Polyhydrosilylation of Diynes with Disilanes



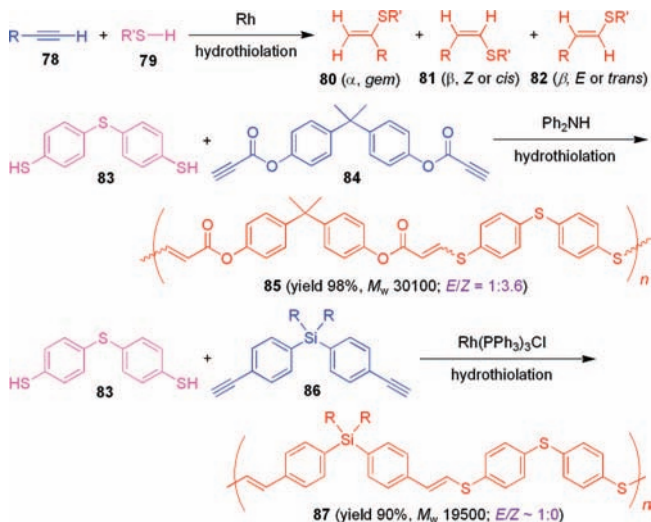
## Scheme 18. Polyhydroboration of Diynes with Boranes



Similar to hydrosilylation and hydroboration, hydrothiolation is a potentially useful reaction for the syntheses of heteroatom-containing acetylenic polymers. The reaction was first reported by Truce and Simms in the 1950s: when aryl- or alkylacetylenes were admixed with sodium thiolates, nucleophilic reactions occurred and vinyl sulfides were formed.<sup>283</sup> Newton tried to use a molybdenum complex to catalyze the reaction, but the product was obtained in a low yield.<sup>284</sup> Ogawa<sup>285</sup> and Shimada<sup>286</sup> found that rhodium and palladium complexes could effectively catalyze alkyne hydrothiolation, giving vinyl sulfides with linear and branched structures. Love and co-workers developed Rh-based catalysts for the synthesis of vinyl sulfides.<sup>287,288</sup> Although alkyne hydrothiolation can proceed via radical, nucleophilic, and coordination mechanisms with excellent atom economy, the products are often mixtures of regio- and stereoisomers.<sup>289</sup> For example, thiol **79** can undergo Markovnikov addition with alkyne **78** to give a branched vinyl sulfide **80**; the reaction can also proceed in an anti-Markovnikov fashion to yield linear adducts with *Z* (**81**) and *E* (**82**) conformations (Scheme 19). Clearly, the regio- and stereochemistries are the important issues to be solved for the development of more useful reactions. Synthesis of sulfur-rich polymers by alkyne hydrothiolation has been virtually unexplored, although such polymers are expected to show intriguing photonic properties such as high refractive indexes (RIs). The development of processable polymeric materials with high RI values is a fascinating area of research because of their promising applications in photonic devices such as optical waveguides and holographic image-recording systems.

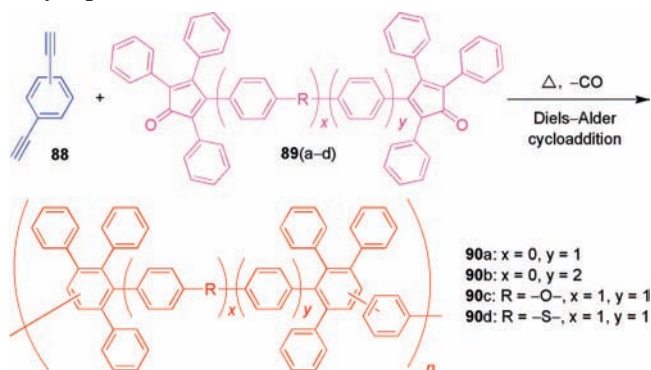
Recently, Tang and co-workers succeeded in developing alkyne hydrothiolation reaction into a useful polymerization technique.<sup>290</sup> Dithiol **83** was admixed with bipropiolate **84** in dimethylformamide (DMF) in the presence of a secondary amine such as diphenylamine (Scheme 19). After stirring at room temperature for 24 h, polymer **85** with a high molecular weight ( $M_w \approx 30 \times 10^3$ ) was obtained in a nearly quantitative yield. Spectroscopic analysis revealed that the polymer was

## Scheme 19. Polyhydrothiolation of Diynes with Dithiols



a linear anti-Markovnikov reaction product with a predominant *Z* conformation ( $Z/E = 3.6:1$ ). No branched isomer was obtained at all, indicating that the polyhydrothiolation reaction proceeded in a regioselective fashion. Rhodium complex  $\text{Rh}(\text{PPh}_3)_3\text{Cl}$  was found to effectively catalyze polyhydrothiolation of **83** and **86**, giving polymer **87** with a high molecular weight and an exclusive *E*-conformation in a high yield. This is very exciting, because it proves that the stereochemistry of the alkyne polyhydrothiolation can be controlled by the choice of catalyst system and that the Rh-catalyzed polymerization is both regio- and stereoselective.

Oligaruso,<sup>291</sup> Ried,<sup>292</sup> and Müllen<sup>293</sup> have utilized intermolecular Diels–Alder [4 + 2]-cycloadditions of tetraphenylcyclopentadienone with monoynes, diynes, or triynes derivatives to establish effective synthetic routes to large, mono-disperse oligophenylenes with potential applications as electronic materials. The preparation of linear PPs was achieved by Stille and co-workers.<sup>294,295</sup> The polycycloaddition reactions of *p*- or *m*-diethynylbenzene **88** with bis(tetraphenylcyclopentadienone) **89** at high temperatures (up to 250 °C) proceeded with spontaneous extrusion of carbon monoxide, leading to the formation of **90** in high yields (Scheme 20). The polymers were almost colorless and amorphous and had high molecular weights (number-average molecular weight  $M_n \sim 20\,000$ – $100\,000$ ). The polymers, however, had poor solubility, with only 15% being soluble in common organic solvents. The polycycloaddition reaction is regiorandom: even when *p*-diethynylbenzene **88**(*p*) was used in the reaction, a structurally unambiguous poly(*p*-phenylene) **90**(*p*) could not be obtained. In principle, two

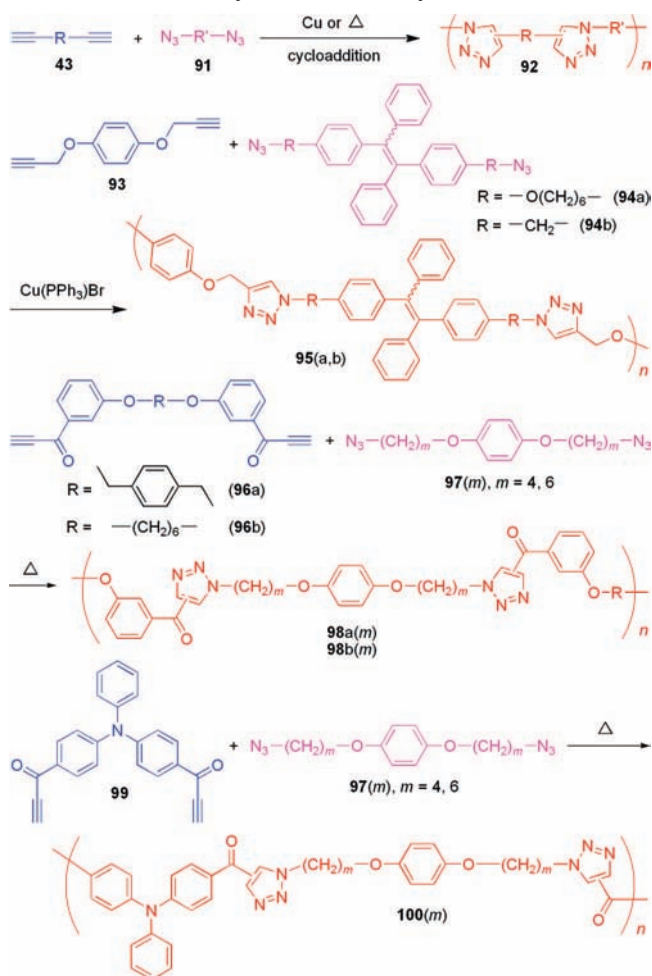
**Scheme 20. Polycycloaddition of Diynes with Dicyclopentadienones**


regioisomers are possible in each  $[4 + 2]$ -cycloaddition. This is why the polymer chains contain both *p*- and *m*-isomeric units.

Alkyne–azide 1,3-dipolar cycloaddition was systematically studied by Huisgen in the 1980s.<sup>296</sup> The area had remained silent until Sharpless and co-workers reported that Cu(I) species efficiently catalyzed the cycloaddition reaction to give regioselective 1,4-disubstituted triazoles. This reaction was coined “click reaction” by Sharpless and co-workers, which enjoys a number of remarkable features, such as wide substrate applicability, high efficiency, excellent regioselectivity, mild reaction conditions, and simple purification procedures.<sup>297–299</sup> The click reaction has become a versatile synthetic tool and has been widely used in a diverse area of research, such as bioconjugation, surface functionalization, and materials modification.<sup>300–307</sup> The click reaction has also been utilized in polymer science, but the emphasis has been on the modification of preformed polymers via postpolymerization approaches.<sup>2,308–318</sup> The efforts of developing the click reaction into a polymerization technique have met with only limited success. In the early studies, polymer chemists had used click chemistry to construct dendritic and linear polymers. The preparations of dendritic polymers, however, require multistep reactions and tedious product isolations, while long reaction time and poor product solubility have been the obstacles to the syntheses of linear polymers via the click reaction route.<sup>48,59,319</sup>

In the attempted click polymerizations, diynes and diazides have often been copolymerized by using  $\text{CuSO}_4$ /sodium ascorbate in the THF/water mixtures (Scheme 21).<sup>46,48,59</sup> The Cu(I)-catalyzed click polymerizations of aryldiazides and aryldiynes (aryl = phenyl, pyridyl, fluorenyl, etc.) were sluggish, taking as long as 7–10 days to finish. The products often precipitated from the reaction mixtures even at the oligomeric stage or became insoluble in common organic solvents after purifications, unless very long alkyl chains (e.g., dodecyl groups) were attached to the aryl rings of the polymers. The insolubility is most likely caused by the low solvating power of the aqueous mixtures to the resultant PTAs. This drawback may be overcome if the click polymerization is performed in organic media using a catalyst that is soluble in the organic solvents. Indeed, by using organosoluble catalyst  $\text{Cu}(\text{PPh}_3)_3\text{Br}$ , Tang and co-workers succeeded in polymerizing diyne **93** with diazides **94** to obtain soluble, linear PTAs **95** with high molecular weights and 1,4-regioregularity.<sup>82</sup>

Experimental and theoretical studies indicate that the reactions are largely affected by the substrate: the alkyne monomers with electron-withdrawing groups adjacent to the

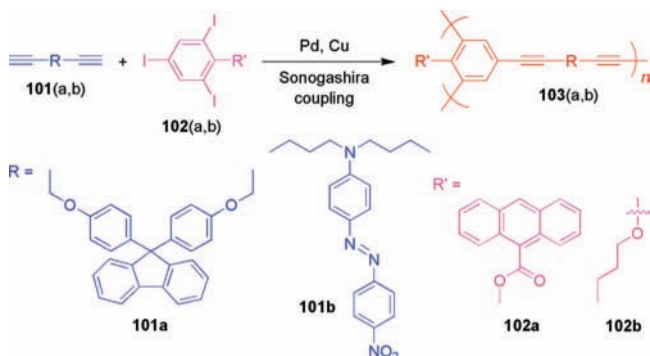
**Scheme 21. Click Polymerization of Diynes with Diazides**


carbon–carbon triple bonds readily undergo the polycycloaddition reaction even in the absence of a metallic catalyst. Tang and co-workers have recently developed a thermally activated, metal-free, click polymerization process for electron-deficient alkyne monomers. Linear poly(aryltriazole)s (**98** and **100**) with high regioselectivity (1,4-content or  $F_{1,4}$  up to ~92%) and excellent solubility in common organic solvents are obtained in high yields by simply refluxing the reaction mixtures of bis(arylacetylene)s (**96** and **99**) and diazides (**97**) in polar solvents such as DNF/toluene at a moderate temperature (100 °C) for a short period of time (6 h) in an open atmosphere.<sup>63,81</sup>

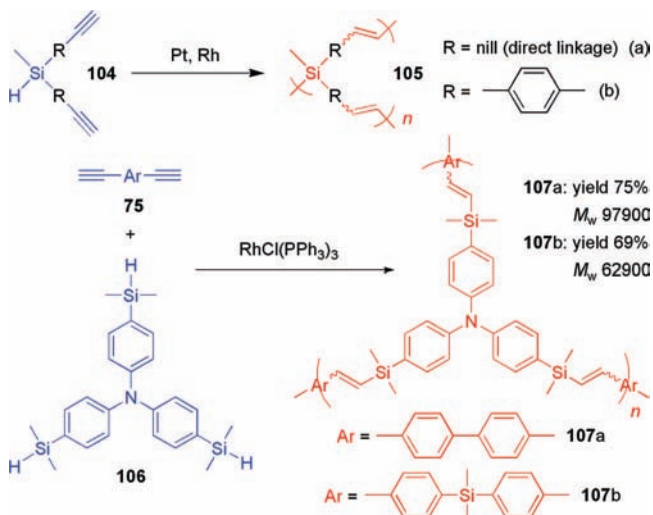
**2.2.3. Nonlinear Polymerizations**

Nonlinear alkyne polymerizations enable the syntheses of acetylenic polymers with three-dimensional molecular architectures. Polycoupling of aryldiynes with aryltriazides is an effective way to construct hyperbranched poly(aryleneethynylene)s (*hb*-PAEs). The polymers can also be prepared from  $\text{AB}_2$ -type monomers, but such an approach suffers from the difficulty in the monomer syntheses because of the self-oligomerization between the mutually reactive A and B functional groups.<sup>320–322</sup> The  $\text{A}_2 + \text{B}_3$  strategy offers the choices of a wider variety of monomers but has the risk of forming cross-linked networks or gels. Control of the polycoupling conditions is thus a necessity for the syntheses of processable *hb*-PAEs with desired structures and properties. Through optimization of the polymerization conditions such as reaction time, monomer and catalyst concentrations,

## Scheme 22. Polycoupling of Diynes with Triiodides



## Scheme 23. Examples of Alkyne–Silane Polyhydrosilylation

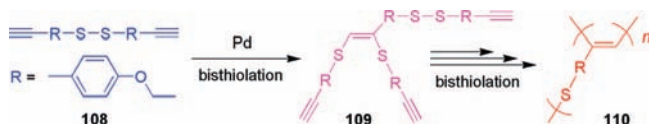


and addition mode of comonomers, Tang and co-workers successfully synthesized *hb*-PAEs **103** containing luminophoric groups such as fluorene and anthracene and azo-cored push–pull nonlinear optical (NLO) chromophores (Scheme 22).<sup>323,324</sup>

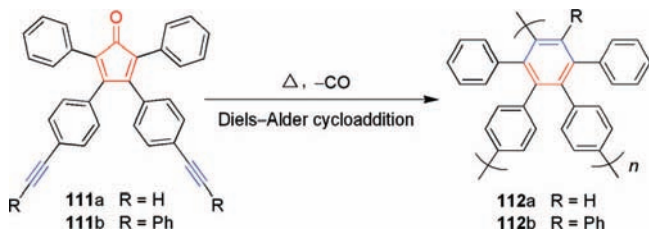
Hyperbranched poly(vinylenesilane) **105a** was prepared by Son et al. through palladium-catalyzed polyhydrosilylation of diethynylmethylsilane **104a** (Scheme 23).<sup>266</sup> The peripheral ethynyl groups of the tacky, soluble, and stable polymer underwent thermo- and photoinduced cross-linking reactions. A hyperbranched polymer with  $\sigma$ – $\pi$  conjugation (**105b**) was prepared by Kwak and Masuda through Rh-catalyzed polyhydrosilylation of AB<sub>2</sub>-type silane monomer **104b**.<sup>267</sup> The resultant polymer contained 95% *trans*-vinylene units and lost merely 9% of its weight when heated under nitrogen to a temperature as high as 900 °C. Tang and co-workers synthesized hyperbranched poly(arylenevinylenesilane)s **107** in high yields through the RhCl(PPh<sub>3</sub>)<sub>3</sub>-catalyzed A<sub>2</sub> + B<sub>3</sub> polyhydrosilylation of arylenediynes **75** with arylenetrisilane **106**. Gel-permeation chromatography (GPC) measurements of the polymers gave *M<sub>w</sub>* values in the range of ~63 000–98 000, although the GPC analysis calibrated by the standards of linear polymers (e.g., polystyrene) often greatly underestimates molecular weights of nonlinear hyperbranched polymers. The polymers were film-forming and showed remarkable photonic properties, which will be discussed in section 4 of this review.

In a unique self-addition polymerization, diethynyl disulfide **108**, an A<sub>2</sub>B<sub>2</sub>-type monomer, underwent self-bisthiolation reaction in the presence of Pd catalyst.<sup>61</sup> Through the formation of oligomeric species (e.g., **109**), hyperbranched

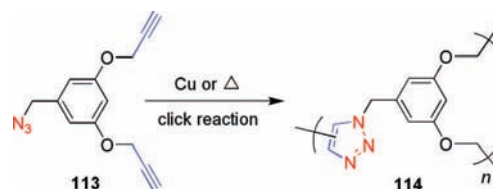
## Scheme 24. Polybisthiolation of Diethynyl Disulfide



## Scheme 25. Polycycloaddition of Cyclopentadienyndiynes



## Scheme 26. Click Polymerization of Azidodiynes



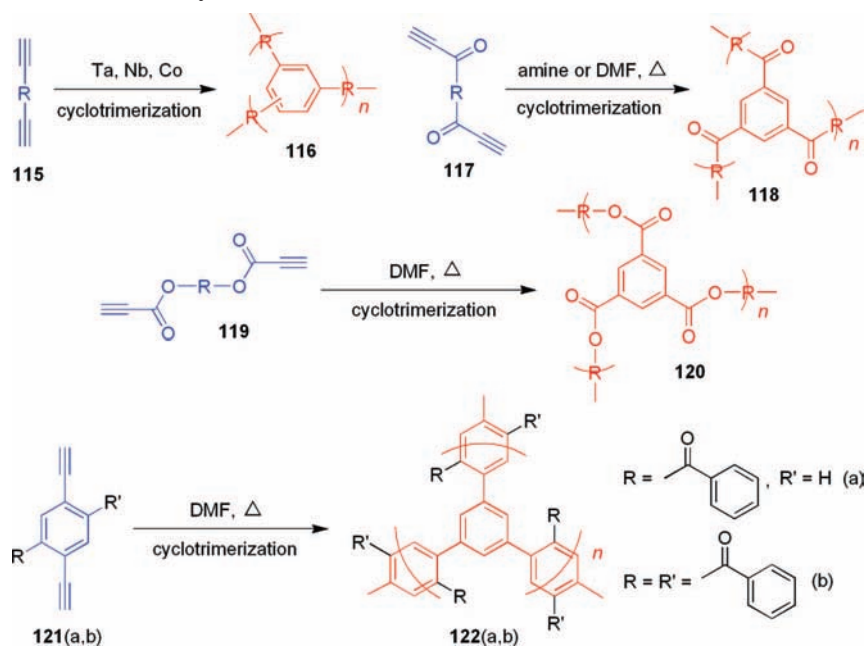
polymer **110** with Z-substituted dithioalkene units were generated (Scheme 24). The *M<sub>n</sub>* and *M<sub>w</sub>* values of polymer **110** were up to 8 100 and 57 000, respectively. The stereoregular conformation of **110** was confirmed by <sup>1</sup>H and <sup>13</sup>C NMR spectral analyses. The polymer was soluble in common organic solvents, such as benzene, acetone, and chloroform. Insoluble gels were formed when the polymerization reactions were carried out for a prolonged period of time.

Müllen reported the syntheses of three-dimensional hyperbranched polyphenylenes (*hb*-PPs) **112** by self-condensation of AB<sub>2</sub> monomers of 3,4-bis(4-ethynylphenyl)-2,5-diphenylcyclopentadienones **111** (Scheme 25).<sup>325</sup> The *hb*-PPs are composed of exclusively pentaphenylbenzene units and possess high DBs. Polymer **112a** is light-brown colored and poorly soluble in common solvents. The poor solubility is probably due to the dense packing of the phenyl rings or the rigid core structure of the polymer. From a synthetic point of view, the polymer still contains a multitude of reactive terminal ethynyl groups, due to the steric effect and statistical rule. Polymer **112b** was characterized by dynamic light scattering (DLS) technique and was found to have an average diameter of about 15 nm. Polymers **112** thus can be considered as polydisperse *hb*-PP nanoparticles.

Voit and co-workers found that *hb*-PTAs could be synthesized from AB<sub>2</sub> monomers by 1,3-dipolar cycloaddition reaction. The polymerization of **113** was either initiated by heating or catalyzed by Cu(I) species (Scheme 26).<sup>43</sup> The thermal approach resulted in the formation of fully soluble 1,4- and 1,5-disubstituted PTAs, while the copper-catalyzed system gave insoluble 1,4-disubstituted PTAs. The AB<sub>2</sub> monomers of internal alkynes could be thermally polymerized to soluble *hb*-PTAs with high molecular weights. The AB<sub>2</sub> approach, however, suffers from the complexity in monomer synthesis and the risk of self-oligomerization during the monomer preparation and storage.<sup>63,81,82,326</sup>

Acetylene cyclotrimerization is a century-old reaction for the effective transformation of monoyne molecules to benzene rings.<sup>10</sup> Polycyclotrimerizations of diyne molecules can yield *hb*-PPs with repeat units knitted together by robust benzene rings. The diyne polycycloaddition, however, can

## Scheme 27. Polycyclotrimerizations of Diynes



easily run out of control to give cross-linked insoluble gels,<sup>327</sup> and the challenge is thus how to manage to put the reaction under control. Tang and co-workers have taken this challenge and worked on the syntheses of hyperbranched polymers by  $A_2$ -type diyne polycyclotrimerizations.<sup>112,113,118,328–332</sup> Through elaborate efforts, especially those in the catalyst exploration and process optimization, Tang's group succeeded in the establishment of controlled polymerization systems and the syntheses of a wide variety of functional hyperbranched polymers by diyne polycyclotrimerizations.<sup>333–355</sup>

The diyne polycyclotrimerization is unique in that it uses only a single type of  $A_2$  monomer (Scheme 27). The commonly taken synthetic approaches to hyperbranched polymers have been the utilization of polycondensation reactions of  $AB_n$ - ( $n \geq 2$ ) and  $(A_2 + B_3)$ -type monomers, where A and B denote the mutually reactive functional groups, e.g., carboxy ( $-\text{CO}_2\text{H}$ ) and hydroxy ( $-\text{OH}$ ) groups, respectively. The  $AB_n$  approach, however, suffers from the synthetic difficulty in monomer preparation and the self-oligomerization during the monomer storage due to the existence of multiple mutually reactive groups in a single molecule. The  $A_2 + B_3$  approach, on the other hand, requires stoichiometric balance of the two monomers in order to obtain polymers with high molecular weights and DB values. In contrast, the  $A_2$ -type diyne monomers are stable at room temperature in the absence of a catalytic species and their polycyclotrimerization reactions are basically a unimolecular event. In other words, there are no complication of self-oligomerization and requirement of stoichiometric balance in the diyne systems, whose polymerizations can thus potentially produce hyperbranched polymers with very high molecular weights and DB values. Moreover, the linkage of the branches by the robust benzene rings in the three-dimensional space enables the synthesis of hyperbranched polymers with high stability and excellent processability, whereas the hyperbranched polymers prepared from polycondensation are often unstable (e.g., undergoing hydrolysis degradation), and the linear (unsubstituted) PPs usually become insoluble when their molecular weights reach merely a few thousands, due to the regular packing of their linear chains.

Tang and co-workers have encountered the cross-linking problems during the course of developing the alkyne cyclotrimerization into a useful protocol for the syntheses of hyperbranched polymers. Initially, they used terminal diynes **115** bridged with alkyl chain or aromatic rings as monomers. Cross-linking or gelation was involved in the reactions, but through the molecular engineering of monomer structures and the optimization of polymerization conditions, they succeeded in the syntheses of hyperbranched poly(alkylene-phenylene)s or polyarylenes with excellent solubility.<sup>333–343,345–350,452,354</sup> The polymers have been found to show an array of novel properties, such as high thermal stability (up to  $\sim 600$  °C), ready photocurability, efficient light emission ( $\Phi_{\text{F}}$  up to 98%), large optical nonlinearity, and low optical dispersion. The Ta- and Nb-catalyzed diyne polycyclotrimerizations can produce polymers with high molecular weights but have little intolerance to polar functional groups. Although the Co catalysts can polymerize diynes carrying certain polar groups, the resultant polymers generally have lower molecular weights and inferior optical and photonic properties than those prepared by the Ta and Nb catalysts due to the presence of hard-to-remove catalyst residues in the polymers.

Through further investigations, Tang and co-workers have found that the polycyclotrimerizations of bis(arylacetylene)s **117** initiated by nonmetallic catalysts or organocatalysts such as piperidine proceed smoothly in an ionic mechanism and produce hyperbranched poly(arylarylene)s (*hb*-PAAs) **118** with high DBs in high yields.<sup>344,351</sup> The polymerization is tolerant of polar functional groups and is strictly regioselective, giving polymers with sole 1,3,5-regiostructure. The bis(arylacetylene) monomers are, however, difficult to prepare. It takes many steps of reactions to prepare the monomers, and the reactions involve the use of toxic heavy metals such as  $\text{MnO}_2$  and  $\text{CrO}_3$ . Analysis of the structure of monomer **117** reveals that this polymerization reaction works for diynes whose triple bonds are linked to electron-withdrawing groups. If the carbonyl linkage in the arylacetylene can be replaced by an ester group, it will make the monomer synthesis much easier, because acetylenecarboxylic acid (or propiolic acid) is a commercially available

compound and can be readily esterified with a diol to form a bipropiolate. If the bipropiolate monomer can be readily polymerized, it will pave the synthetic path to facile and economic syntheses of hyperbranched polymers. Tang's group has explored the possibility and demonstrated that polycyclotrimerizations of bipropiolate **119** in refluxed DMF can produce processable hyperbranched polymer **120** with perfectly branched structure and 1,3,5-regioregularity in high yields.<sup>355</sup>

Along this line of research endeavor, it is envisioned that this polycyclotrimerization may also work for the monomers with electron-deficient groups linked to the acetylene triple bond via electronically communicable or transmissible units. Tang and co-workers designed a group of new aromatic diynes **121**, in which the carbonyl group is linked to the acetylene triple bond through a benzene ring to make the system electron-deficient. Indeed, polycyclotrimerizations of **121** in refluxed DMF worked well to afford 1,3,5-regioselective, processable, hyperbranched polymers **122** in high yields. This success helps us further understand the polymerization mechanism and shows that there is vast room for extending the applicability of this polymerization route to other monomer systems.<sup>355</sup>

## 2.3. Polymers from Triynes

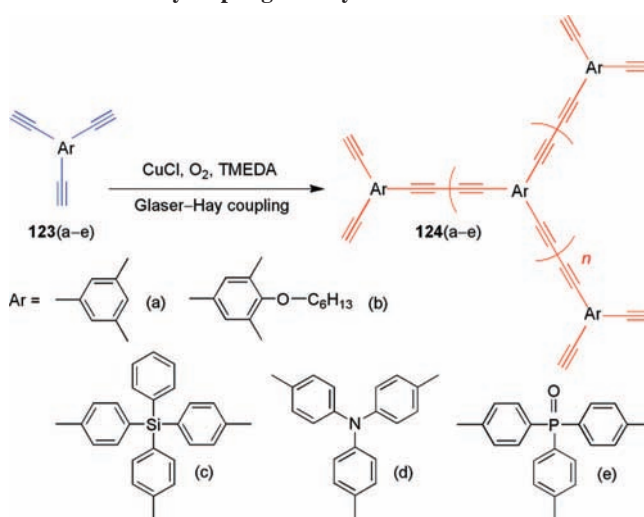
### 2.3.1. Coupling Polymerizations

The utility of Glaser–Hay oxidative coupling reaction in the construction of carbon-rich polymers has been actively explored. The challenge has been how to enhance the processability of such polymers, for their linear chains often become insoluble even at the oligomer stage. Synthesis of hyperbranched polymers may help circumvent the processability problem because of the unique globular topology of the polymers, which contain numerous intramolecular voids or large free volumes that facilitate ready solvation. Tang and co-workers have been interested in the design and synthesis of carbon-rich *hb*-PDYs. Such polymers are expected to exhibit novel properties associated with their high density of diyne rods. The rich reactivity of the diyne functional group, for example, may endow the polymers with photosusceptibility, thermal curability, and metal-coordinating capability. To synthesize the *hb*-PDYs, Tang's group took an  $A_3$ -coupling approach: the triyne monomers are knitted together by using Glaser–Hay oxidative coupling reaction. *hb*-PDYs **124** containing various functional groups such as ether, amine, and phosphorus oxide were synthesized by the homopolymerization of the corresponding triyne monomers **123** (Scheme 28).<sup>45</sup> To prevent the network from being formed, the polymerizations were stopped by pouring the reaction mixtures into acidified methanol before gel points.

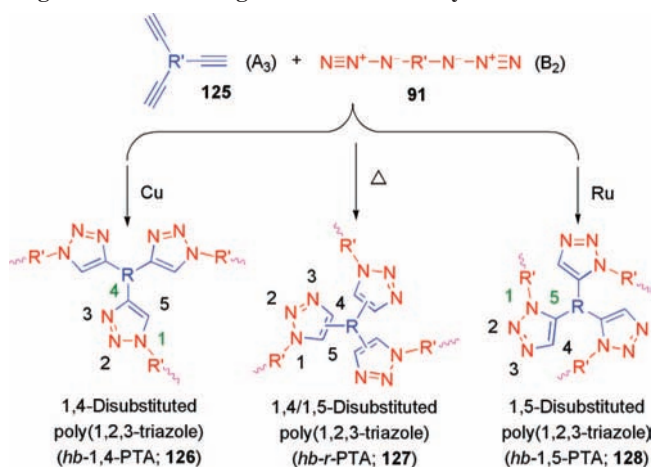
### 2.3.2. Click Polymerizations

In their studies on the linear click polymerizations, Tang et al. developed a metal-free, thermally initiated, regioselective polycycloaddition process: simply heating a mixture of bis(arylacetylene) (e.g., **96**) and diazide (e.g., **97**) in a polar solvent such as a DMF/toluene mixture readily furnished linear PTAs with high regioregularities ( $F_{1,4}$  up to ~92%) in high yields (up to ~98%).<sup>63</sup> Tang's group went one step further and tried to apply this process to the synthesis of *hb*-PTAs. An  $A_3 + B_2$  approach was taken: easy-

Scheme 28. Polycoupling of Triynes



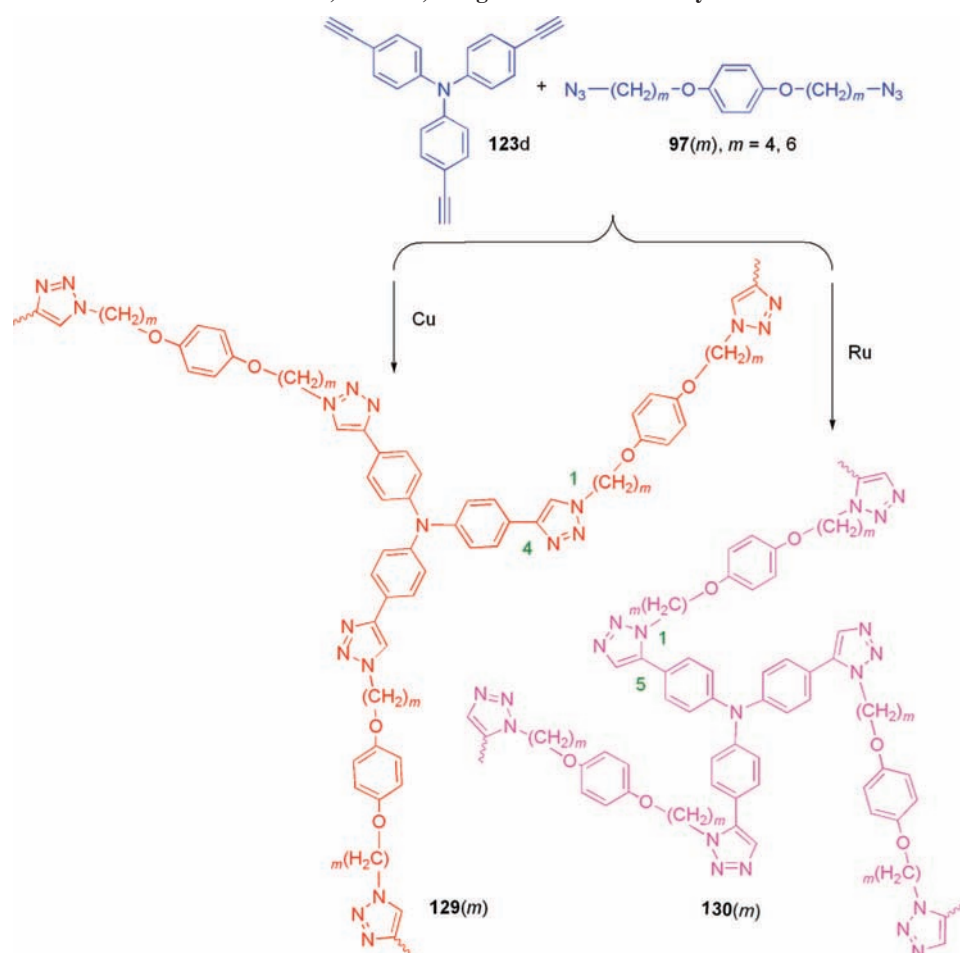
Scheme 29. Metal-Mediated and Thermally Activated Regioselective and Regiorandom Click Polymerizations



to-make and stable-to-keep triyne ( $A_3$ ) and diazide ( $B_2$ ) were used as monomers (Scheme 29), in order to avoid the self-oligomerization problem encountered in the  $AB_2$  systems. The  $A_2/B_3$  monomers (**91/125**) were readily polymerized by the metal-mediated click reactions and the thermally activated cycloaddition reaction.<sup>71</sup> The copper- and ruthenium-catalyzed click polymerizations afforded hyperbranched polymers with regular 1,4- and 1,5-linkages, i.e., *hb*-1,4-PTA (**126**) and *hb*-1,5-PTA (**128**), respectively, while the thermally initiated polymerization system yielded regiorandom polymer *hb*-*r*-PTA **127**. All the polymers are readily soluble in common organic solvents, such as DCM, THF, and dimethyl sulfoxide (DMSO), representing the first examples of *hb*-PTAs with regioregular structures and macroscopic processability.

The thermal polymerization of **97(6)** and **123d** transformed the azide-alkyne monomers to *hb*-*r*-PTA **127(6)** in a high yield, whose  $M_w$  and PDI were estimated by GPC to be 11 400 and 2.7, respectively. As mentioned above, it is well-known that the GPC system often underestimates the molecular weights of hyperbranched polymers. Tang and co-workers employed laser light-scattering technique to measure the absolute  $M_w$  of the polymer, which was found to be 177 500, about 14-fold higher than the value estimated by GPC. In an attempt to synthesize regioregular polymers, Tang and co-workers mixed **123d** and **97** with  $\text{CuSO}_4/\text{sodium ascorbate}$  under "standard" click reaction conditions. In-

## Scheme 30. Copper- and Ruthenium-Mediated 1,4- and 1,5-Regioselective Click Polymerizations



soluble precipitates were immediately formed, which could not be dissolved in any common organic solvents. The standard recipe for the click reaction, therefore, is not suitable for the synthesis of processable *hb*-PTAs.

In the standard click system, the  $\text{CuSO}_4$ /sodium ascorbate catalyst is used in a THF/water mixture. The incompatibility between the growing *hb*-PTA species and the aqueous medium may have induced the polymers to agglomerate and hence precipitate. To avoid the use of aqueous medium, Tang's group used a nonaqueous click catalyst of  $\text{Cu}(\text{PPh}_3)_3\text{Br}$  to initiate the click polymerization of triyne **123d** with diazides **97** (Scheme 30). The  $\text{Cu}(\text{PPh}_3)_3\text{Br}$ -catalyzed polymerization of **123d** with **97(4)** produced *hb*-1,4-PTA **129(4)** in ~46% yield, which was soluble in common organic solvents, including DCM, THF, DMF, and DMSO. Similarly, the polymerization of **123d** with **97(6)** carried out in the nonaqueous medium gave a soluble *hb*-1,4-PTA **129(6)** in ~52% yield. The Cu(I) catalyst has greatly accelerated the polycycloaddition process (e.g., 80 min at 60 °C), in comparison to the thermally activated system (e.g., 72 h at 100 °C).<sup>71</sup>

The 1,5-regioselective click polymerization of **123d** with **97** catalyzed by  $\text{Cp}^*\text{Ru}(\text{PPh}_3)_2\text{Cl}$  proceeded even faster: for example, the polymerization of **123d** and **97(6)** produced soluble *hb*-1,5-PTA **130(6)** in ~75% yield in as short as 30 min. The preparation of the Ru(II) complex, however, is a nontrivial job that requires high synthetic skills.<sup>356</sup> Dichloro(pentamethylcyclopentadienyl)ruthenium(III) oligomer ( $\text{Cp}^*\text{RuCl}_2$ )<sub>n</sub> is a precursor to  $\text{Cp}^*\text{Ru}(\text{PPh}_3)_2\text{Cl}$  and can be readily prepared in high yield by refluxing  $\text{RuCl}_3 \cdot n\text{H}_2\text{O}$  and

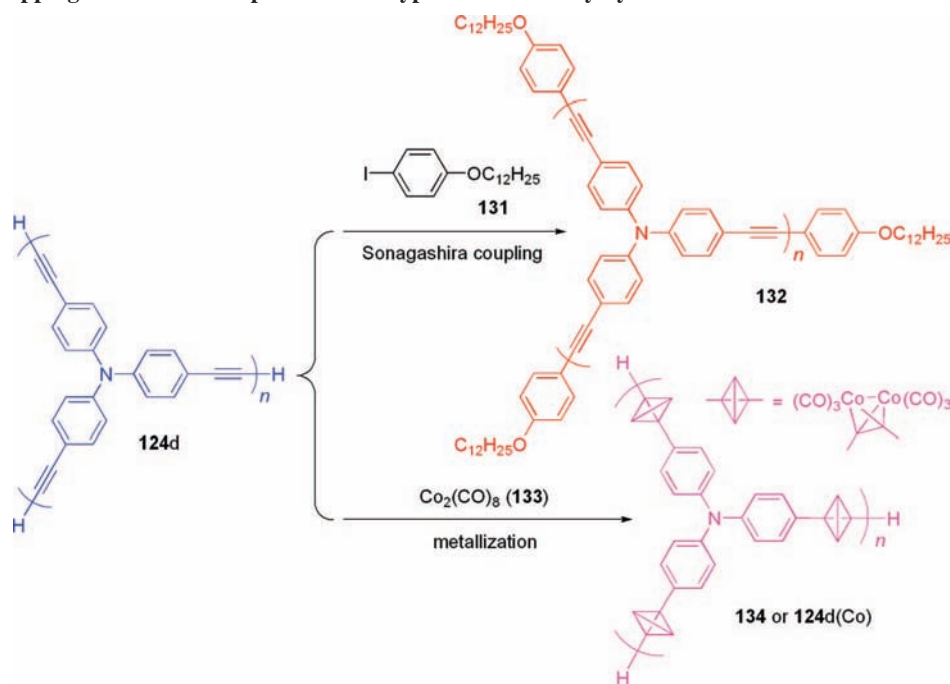
pentamethylcyclopentadiene in ethanol for a few hours. Although there was a concern that the stable Ru(III) precursor might not work well as a click catalyst, ( $\text{Cp}^*\text{RuCl}_2$ )<sub>n</sub> smoothly catalyzed the polycycloaddition of **123d** and **97** at a moderate temperature (40 °C), giving soluble *hb*-1,5-PTAs in high yields (>83%).<sup>71</sup>

All the freshly prepared samples of hyperbranched polymers, including the regiorandom *hb-r*-PTA and regioregular *hb*-1,4- and *hb*-1,5-PTAs, are processable: thin solid films can be readily prepared by static casting or spin coating of their 1,2-dichloroethane solutions onto solid substrates, such as silicon wafers, glass slides, and mica plates. All the polymers are stable, irrespective of the polymerization processes by which they were prepared. For example, the *hb*-PTAs lose 10% of their original weights in the temperature region of 374–407 °C, indicative of their strong resistance to thermolysis. No glass transition temperatures were detected by differential scanning calorimetry (DSC) measurements when the polymers were heated up to 200 °C.

The *hb*-1,4-PTA prepared by the  $\text{Cu}(\text{PPh}_3)_3\text{Br}$  catalyst, however, gradually became partially insoluble upon storage under ambient conditions. One possible reason for this solubility change is the postpolymerization reactions of the polymers catalyzed by the metallic residues trapped in the *hb*-1,4-PTA samples. The Cu species may have coordinated with the “old” amino functional groups in the monomer repeat units and/or the “new” triazole rings formed during the polycycloaddition reaction. In a control experiment, a small amount of  $\text{CuSO}_4$ /sodium ascorbate was mixed with



## Scheme 31. End-Capping and Metal Complexation of Hyperbranched Polydiynes



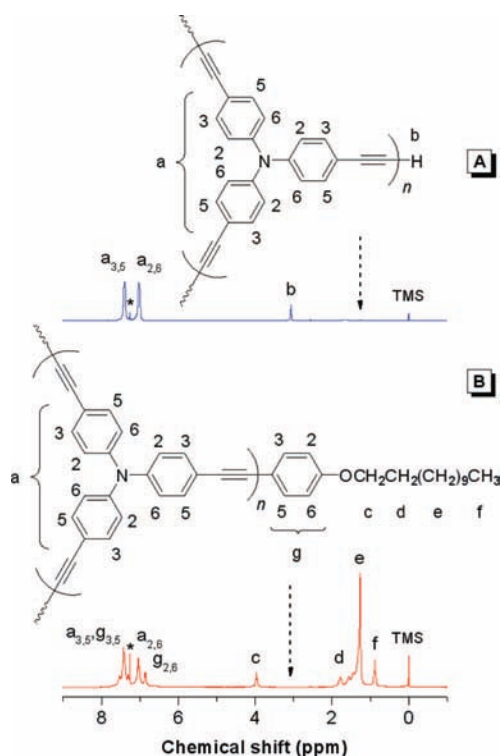
the *hb*-1,5-PTA prepared from the Ru-catalyzed click polymerization. The polymer became insoluble within a few minutes, although it remained soluble after storage for several months in the absence of the externally added Cu catalyst. The Cu species may have catalyzed the cycloaddition reaction of the azido and ethynyl terminal groups in the periphery of the polymer, making it cross-linked and hence insoluble. Much effort has been devoted to removing the catalyst residues by washing the *hb*-1,4-PTA with amine solvents, but the result was unsatisfactory because of the poor solubility of the polymer in the hydrophilic solvents.

Another possible reason for the solubility change of the *hb*-1,4-PTA with storage is the aggregate formation in the solid state. Theoretic simulation shows that, in the optimized conformation, the phenyl and triazole rings of the 1,4-isomer experience little steric interaction and can locate almost in the same plane. During storage, the cyclic plates of the *hb*-1,4-PTA may gradually pack, with the aid of the  $\pi$ - $\pi$  stacking attractions between their aromatic units. This “physical cross-linking” process progressively knits more polymer molecules together and widens the three-dimensional networks, hence gradually decreasing the polymer solubility. On the contrary, there exists steric repulsion between the phenyl and triazole rings in the 1,5-isomer. The rings are thus twisted out of planarity to alleviate the involved steric effect. This twisted, nonplanar structure makes the cyclic units of *hb*-1,5-PTA difficult to pack in the solid state. The 1,5-regioregular polymers thus can maintain their good solubility for a long period of time. The *hb-r*-PTA prepared by the thermal polymerizations possesses a regiorandom structure and would be difficult to pack in the solid state. In addition, no transition metal catalyst was used in the thermal polymerization process; in other words, no metallic residues were left in the polymer. The *hb-r*-PTA thus should have good solubility: indeed, the polymer remained soluble after it had been stored in the solid state under ambient conditions for several months.

## 2.3.3. Polymer Reactions

Compared to the reactions of linear polymers, hyperbranched polymer reactions are more interesting. Because of the high density of reactive groups in their peripheries, hyperbranched polymers can be postmodified by many functional groups to furnish a variety of polymers with new functional properties. For example, many hydrophilic brushes may be grafted onto the surface of hydrophobic hyperbranched polymers to give individual amphiphilic nanoparticles that can be dispersed in water as macromolecular micelles. Spectroscopic analyses reveal that *hb*-PDYs contain terminal monoyne triple bonds, which allow the peripheries to be decorated by end-capping reactions. This is demonstrated by the coupling of **124d** with aryl iodide **131** (Scheme 31).<sup>113</sup> Thanks to the long *n*-dodecyloxy group of the end-capping agent **131**, the end-capped polymer **132** shows much higher solubility than its parent form **124d**. No signal of resonance of the terminal acetylene proton is observed in the <sup>1</sup>H NMR spectrum (Figure 1), indicating that the end-capping reaction has proceeded to completion.<sup>45</sup>

Since alkynes are well-known and widely used ligands in organometallic chemistry,<sup>10</sup> metallization of *hb*-PDYs can therefore be realized through the coordination interactions of their alkyne triple bonds with metallic species. Polymer **124d** contains numerous acetylenic triple bonds, which enable it to be readily metallized by the complexation with, for example, cobalt carbonyls **133**, to give organometallic polymer **134** (Scheme 31).<sup>45,113</sup> Upon mixing **124d** with **133** in THF at room temperature, the solution color changed from yellow to brown, accompanied with carbon monoxide gas evolution. The mixtures remained homogeneous toward the end of the reaction, and the product was purified by pouring the THF solution into hexane. The resultant polymer complex is stable in air, and the incorporation of the cobalt metal into the polymer structure is verified by spectroscopic analyses.<sup>45</sup> The polymer-metal complex proves to be a good precursor for magnetic ceramics (vide post). This example



**Figure 1.**  $^1\text{H}$  NMR spectra of (A) **124d** and (B) its end-capped product **132** taken in chloroform-*d*. The solvent peaks are marked with asterisks. Reproduced with permission from ref 45. Copyright 2004 American Chemical Society.

also serves as an excellent demonstration of the utility of polymer reaction in the preparation of highly functionalized materials.

### 3. Structures

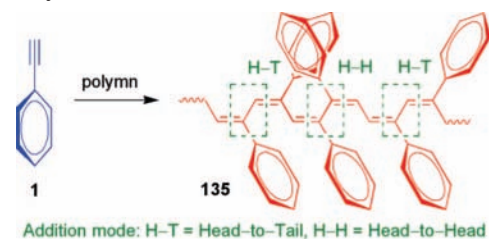
Different from the conventional nonconjugated condensation and vinyl polymers, the  $\pi$ -conjugated acetylenic polymers have their unique structural issues, understanding of which is of scientific value in its own right. Because structure determines properties, it is thus essentially important to find out proper answers to such structural questions as how to generate a desired structure and how to modulate the structure through structural tailoring or by external stimuli. Understanding the exact mechanisms for the processes of structure formation and variation will help establish structure–property relationships, which will in turn guide the molecular engineering or structural design endeavors in polymer synthesis. The investigations carried out, the information gathered, and the insights gained by different research groups on the hierarchical structures of the acetylenic polymers, including their primary configurations, secondary conformations, and higher-order morphologies, will be elaborated in this section.

#### 3.1. Linear Polymers

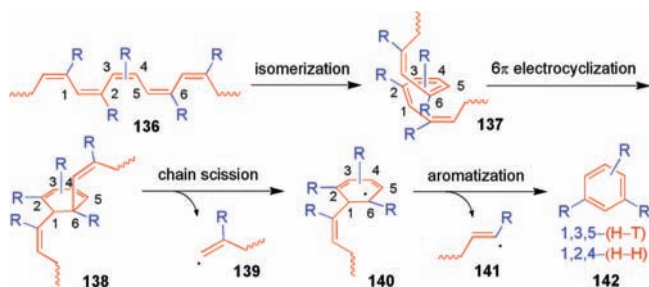
##### 3.1.1. Regiostructures

The primary structure of a polymer includes chemical composition (e.g., elements in the repeat unit), connection mode [e.g., head-to-tail (H–T) or head-to-head (H–H) addition], and various isomerisms (e.g., *cis* or *trans* conformation and *R* or *S* stereoisomer). An outstanding mechanistic issue in the acetylene polymerization had been the addition mode. The polymerization of **1** is shown in Scheme 32 as an example, in which the active species may be propagating

#### Scheme 32. Addition Modes in Polymerization of Phenylacetylene



#### Scheme 33. Mechanism for Thermal Decomposition of PPA

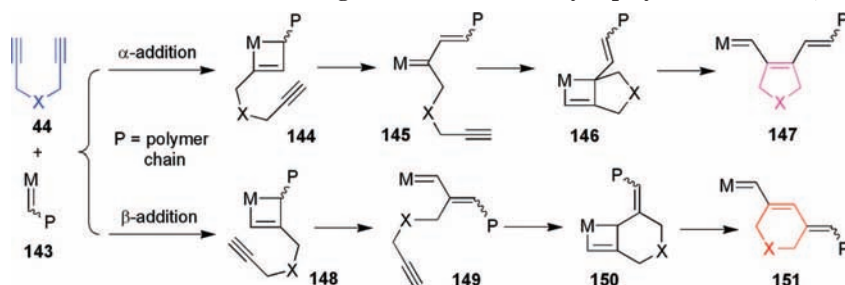


or the monomer repeat unit may be incorporated into the polymer chain through an H–T or H–H addition mode. Understanding how the monomer is added to the propagating chain is of fundamental importance, but collecting experimental information on this dynamic growth step of reaction in the fast chain polymerization process is very difficult, if not impossible. Spectroscopic techniques cannot be employed to discriminate between the resonance peaks of the H–T and H–H units because of the subtle difference between the signals.

Simionescu and Percec found that the thermal degradation of PPA was accompanied with cyclization and release of triphenylbenzenes as thermolysis products.<sup>357–362</sup> As shown in Scheme 33, upon heating, a segment of **136** chain isomerizes to **137** through conformational isomerization. The hexatriene moiety of **137** undergoes thermally allowed pericyclic reaction of  $6\pi$  electrocyclic ring closure, giving cyclohexadiene species **138**. Chain scission of the sterically crowded **138** generates two radicals **139** and **140**, and subsequent aromatization of the cyclohexadiene moiety in **140** produces trisubstituted benzene **142**. By analyzing aromatization products of a PPA derivative, Tang and co-workers gained insights into the addition modes in the polymerization reaction.<sup>163</sup> The rationale behind their approach is that: (i) If the aromatization yields only 1,3,5-trisubstituted benzene, the monomer repeat units must be linked or the polymerization reaction must have propagated in an H–T mode. (ii) If the trisubstitution is at the 1,2,4-position, the chain growth must be via an H–H addition mode. (iii) If a mixture of 1,3,5- and 1,2,4-trisubstituted benzenes is produced, the polymerization would have proceeded in a nonregiospecific manner. Spectroscopic analyses revealed that the 1,3,5-trisubstituted benzene was the sole product of the thermal aromatization reaction,<sup>63</sup> which offered the first unambiguous experimental evidence for the H–T linkage of the monomer repeat units in the PPA chain. This presents a nice example of using the “static” or “dead” degradation products to collect mechanistic information on a “dynamic” or “living” chain-polymerization process.

The cyclopolymerizations of 1,6-heptadiyne monomers initiated by the metathesis catalysts produce cyclic polyenes.

## Scheme 34. Formation of Five- and Six-Membered Rings in the Metathesis Cyclopolymerization of 1,6-Heptadiyne



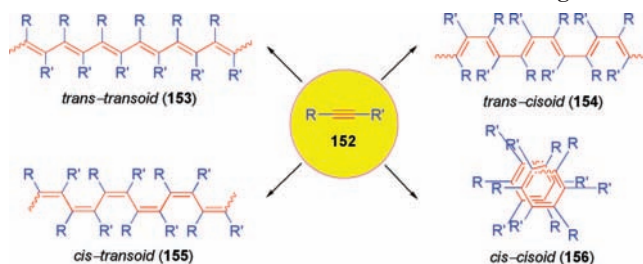
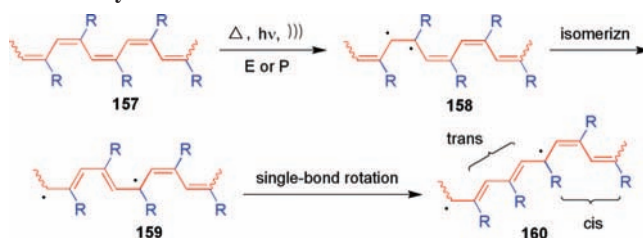
The repeat units in the cyclopolymerization products may consist of five- and/or six-membered rings, depending on the addition mode of the monomer units in the propagation reaction. Schrock et al. have proposed an addition mechanism for cyclopolymerization of 1,6-heptadiynes (Scheme 34).<sup>210,211</sup> In the propagation reaction, one of the acetylene triple bond in monomer **43** reacts with the metal-carbene ( $M=C$ ;  $M = Mo, W$ ) bond in **143** with  $\alpha$ - and  $\beta$ -addition modes to give metallacyclobutene intermediates **144** or **148**, followed by the ring-opening reactions to give vinyl alkylidene complexes **145** and **149**, respectively. Another acetylene triple bond of the monomer reacts with the newly formed  $M=C$  bond to generate metallacyclobutene intermediates **146** and **150**, followed by the ring-opening reactions again to yield five- and six-membered alkenyl rings in **147** or **151**, respectively. Thus, the  $\alpha$ - and  $\beta$ -addition modes give rise to five- and six-membered rings, respectively. Although the polymers composed of five- and six-membered rings are both electronically conjugated,<sup>363</sup> it has been shown that the polymers consisting of five-membered repeat units possess longer effective conjugation lengths and higher electrical conductivities.<sup>364</sup>

The ring size is controlled by the extent of  $\alpha$ - versus  $\beta$ -addition of the first acetylene triple bond to the alkylidene species. As discussed in the polymer synthesis section, the variations in the catalyst system and substrate structure determine the contents of five- and six-membered repeat units in the cyclic polyene. So far, polymers comprising of sole five- or six-membered repeat units have been successfully prepared by using Schrock and Grubbs-Hoveyda metathesis catalysts.<sup>209</sup> In addition to modulating the regioselectivity, another issue worth noting is that the “dangling” acetylene triple bonds in **145** and **149** may serve as cross-link points to make the polymers insoluble if the intramolecular cyclization reaction is not fast enough relative to the ordinary intermolecular polymerization reaction.

## 3.1.2. Stereostructures

The backbone of a PA consists of alternative single and double bonds, which is more rigid than the single-bond backbone of a vinyl polymer. Theoretically, there exist four stereoconformations in a PA chain: *trans-transoid* (**153**), *trans-cisoid* (**154**), *cis-transoid* (**155**), and *cis-cisoid* (**156**), as shown in Scheme 35.<sup>365</sup> The polymers prepared by the rhodium-catalyzed polymerizations commonly take a *cis-transoid* chain conformation. The polymers with *cis-cisoid* conformation are normally crystalline and thus insoluble. The conformation interchange between **153** and **154** or **155** and **156** occurs via single-bond rotation, which involves little amount of energy and is therefore sensitive to the changes in the environmental surroundings. This offers a nice opportunity to tune the chain conformation by external stimuli such as solvent, temperature, pH, and additives.<sup>105</sup>

## Scheme 35. Stereochemical Conformations of PA Segments

Scheme 36. *Cis-Trans* Isomerizations of PA Chain Segments Induced by External Stimuli

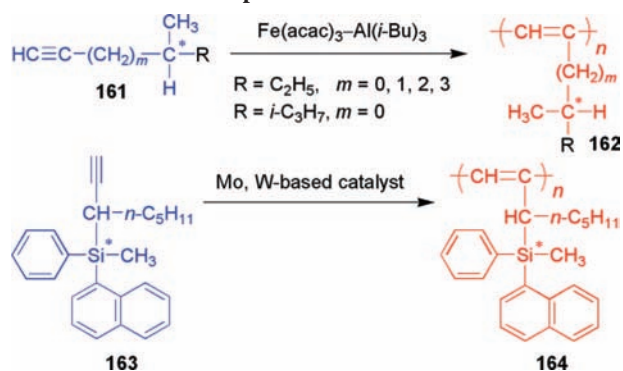
In the late 1970s, Percec and co-workers developed a simple method for determining *cis* content of PPA by deriving the following equation on the basis of  $^1H$  NMR spectroscopy analysis:

$$cis (\%) = \frac{A_{5.82} \times 10^4}{A_t \times 16.66} \quad (1)$$

where  $A_{5.82}$  and  $A_t$  are the integrated peak areas of the resonance of the *cis* olefinic proton of PPA at  $\delta$  5.82 and those of the total resonance of its aromatic and olefinic protons, respectively.<sup>357</sup> Tang and co-workers have modified eq 1 to make it useful for the estimation of *cis* contents of PPA derivatives and other substituted PAs.<sup>99,105</sup> In addition to modulating stereoregularity of PA chains by controlling polymerization processes through changing catalyst, ligand, additive, reaction conditions, and so forth, external stimuli have also been used to induce changes in the chain conformations. Percec, Tabata, and Tang's groups have reported various *cis-trans* isomerization processes activated by heating,<sup>357-363</sup> pressurization,<sup>366,367</sup> electric field,<sup>368</sup> photonic,<sup>369</sup> and ultrasonic irradiations.<sup>370</sup> These isomerization processes have been proposed to proceed through a radical mechanism (Scheme 36), which has been supported by the electron spin resonance measurement. As a result of these research efforts, a wide platform has been established for manipulating the conformations of PA chains in the solution and solid states.

While the unsubstituted PA is a symmetric macromolecule, its chain symmetry can be broken by attaching pendant groups to the polyene backbone (internal perturbation) and

## Scheme 37. First Examples of Helical PAs



its chain conformation can be tuned by changing environmental conditions (external perturbation). Theoretical simulations suggest that the segments in a substituted PA chain carrying bulky pendants can take a helical conformation.<sup>371</sup> When the appendages are chiral species, a majority of the chain segments with long persistence lengths will rotate in one predominant screw sense. Besides fusing the chiral species into the polymer structure at the molecular level through covalent bonding, the PA chains can also be induced to spirally rotate in asymmetric force fields when the  $\pi$  electrons of the conjugated polyene backbone and/or the functional groups of achiral substituents experience molecular interactions with external chiral species.

Artificial generation of chiral PAs with chain helicity is particularly intriguing. The helical chirality coupled with  $\pi$ -electron conjugation may confer a range of unique materials properties on the polymers, which may find high-tech applications as optical polarizing films, chiral stationary phases, asymmetric electrodes, anisotropic molecular wires, and so forth. These captivating potentials have sparked great interest on the development of optically active PAs. Over the past few decades, polymer scientists have developed versatile processes for internally and externally perturbing the conformations of PA chains and have created a large variety of optically active PAs with microscopic helicity and macroscopic handedness.

The synthesis of the first optically active PAs can trace back to the late 1960s and early 1970s, when Ciardelli and co-workers used a Ziegler–Natta catalyst of  $\text{Fe}(\text{acac})_3-\text{Al}(\text{i-Bu})_3$  to polymerize a group of acetylene derivatives with chiral alkyl chains (**161**) to poly(1-alkyne)s **162** of a helical conformation (Scheme 37).<sup>372–374</sup> Ciardelli's work, however, was not followed by other groups, and the area remained silent for about two decades. Part of the reasons for this is probably due to the poor solubility (partially soluble) and instability of the polymers. The polymers are sensitive to oxygen, light, and heat and must be stored in a refrigerator under nitrogen and in the dark.<sup>372–374</sup>

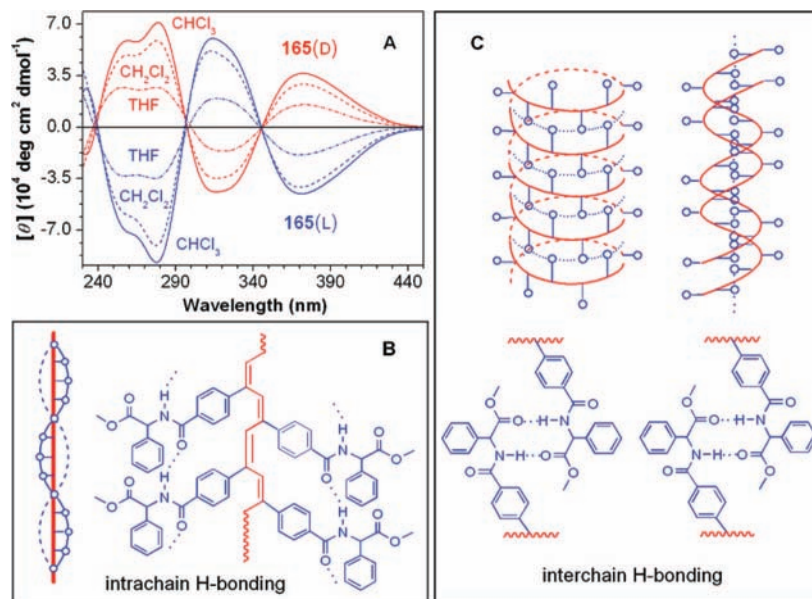
In the late 1980s, Tang et al. designed and synthesized a chiral alkyne monomer **163** by introducing a bulky pendant containing a stereogenic silicon center to the 3 position of 1-octyne and developed a group of environmentally stable transition-metal carbonyl catalysts of general formula  $\text{M}(\text{CO})_x\text{-L}_y$  ( $\text{M} = \text{Mo}, \text{W}$ ) to convert **163** to optically active polymer **164**.<sup>21</sup> This is a first example of a PA derivative, whose chain chirality is induced by an enantiopure heteroatom ( $\text{Si}^*$ ). Unlike polymers **162** discussed above, polymer **164** is thermally stable and completely soluble in common organic solvents. In 1991, Moore, Gorman, and Grubbs synthesized a group of monosubstituted chiral cyclooctatetraenes and

used a tungsten alkylidene catalyst to initiate their ring-opening metathesis polymerizations.<sup>375</sup> The resultant polymers are conjugated PAs, in whose repeat units there exists one branched chiral substituent of  $\text{R}^*$  in every eight backbone carbon atoms, i.e.,  $-\left[\text{HC}=\text{CH}\right]_8\left(\text{HC}=\text{CR}^*\right)_n-$ . The polymers showed substantial circular dichroism (CD), indicating that the chiral pendants have asymmetrically perturbed the chain conformations of the polymers, effectively twisting them in a predominant screw sense.

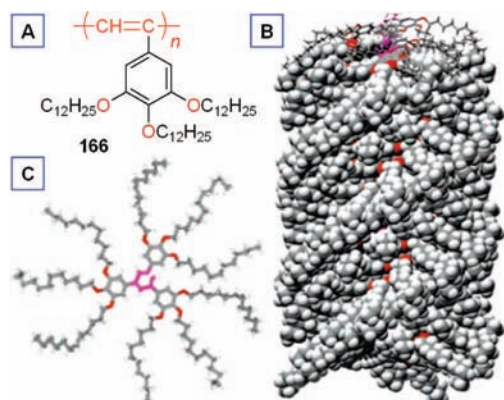
Since the reports of these early studies on the generation of optically active PAs by internal chiral perturbations, many research groups have worked on the design and synthesis of helical PA derivatives. Attachment of stereogenic groups ( $\text{R}^*$ ) to the benzene rings of PPA results in the formation of a variety of optically active PPA derivatives with a general formula of  $-\left[\text{HC}=\text{C}(\text{C}_6\text{H}_4\text{R}^*)\right]_n-$ , as reported by the research groups of Tang,<sup>36,40,41,66,376–384</sup> Aoki,<sup>385</sup> Yashima and Okamoto,<sup>386,387</sup> and Masuda.<sup>388</sup> Helical poly(1-alkyne)s with chiral pendants have been synthesized by the groups of Noyori<sup>151</sup> and Tang.<sup>389–392</sup> Masuda and Tabata's groups prepared helical poly(propionic ester)s  $-\left[\text{HC}=\text{C}(\text{COOR}^*)\right]_n-$  containing asymmetric alkyl groups of different chain lengths and branching points and cyclic hydrocarbons with different numbers and sizes of rings.<sup>392–394</sup> Compared with the monosubstituted PAs, disubstituted PAs with helical chain chirality have been rarely prepared, due to the involved synthetic difficulty. Tang and Aoki's groups have successfully synthesized optically active disubstituted PAs.<sup>395–398</sup> For example, Tang and co-workers have developed a facile polymerization system for the syntheses of a number of poly(phenylpropionate) derivatives with a general structure of  $-\left[(\text{C}_6\text{H}_5)\text{C}=\text{C}(\text{CO}_2\text{R}^*)\right]_n-$ .<sup>395,396</sup>

Tang's group has extensively studied the effects of the chiral pendants on the chain helicity of the optically active PPAs containing naturally occurring building blocks such as amino acids, saccharides, nucleosides, and sterols.<sup>105</sup> Figure 2A shows the examples of the CD spectra of a pair of PPAs carrying  $\alpha$ -phenylglycine pendants with D [**165(D)**] and L [**165(L)**] configurations. The positively and negatively signed Cotton effects in the long wavelength region corroborate that the segments of the PPA chains bearing the pendant groups with opposite chirality form spirals of opposite helicity, which are stabilized by the intra- and interstrand hydrogen bonds. Evidently, the backbone helicity is determined by the pendant chirality under the same environmental conditions.

Attaching bulky achiral pendants to the polyene backbones can also induce the formation of helical conformation. Percec and co-workers synthesized a series of self-organizable PPA derivatives carrying achiral dendritic pendants.<sup>110,116,399,400</sup> The steric effects due to the branching in the dendrons resulted in the distortion in the polymer backbone conformation. On the basis of X-ray diffraction analysis data of the oriented films or fibers of the polymers, their helical structures were proposed. For example, the PPA derivative **166** shown in Figure 3 was analyzed to possess a helical conformation with a cylinder shape.<sup>400</sup> This polymer, however, did not show an optical activity because it is a dynamically helical polymer with no screw-sense preference. It has an equal probability for the formation of left- and right-handed helices that are separated by the helical reversal junctions along the polymer chain. However, by introducing a chiral center to the



**Figure 2.** (A) Chain helicity of **165** determined by pendant chirality and manipulated by solvent change. Diagrammatic sketch of (B) single and (C) double helical strands of PA chains stabilized by intra- and interchain hydrogen bonds. Reproduced with permission from ref 105. Copyright 2005 American Chemical Society.



**Figure 3.** (A) Chemical structure of dendronized PPA derivative **166** and (B) side and (C) top views of its self-organizable cylinder structure with (B) space- and (C) stick-filling models. Reproduced with permission from ref 400. Copyright 2006 American Chemical Society.

dendritic pendant, self-organizable dendronized polymers with a preferred helical handedness were successfully developed.<sup>401</sup>

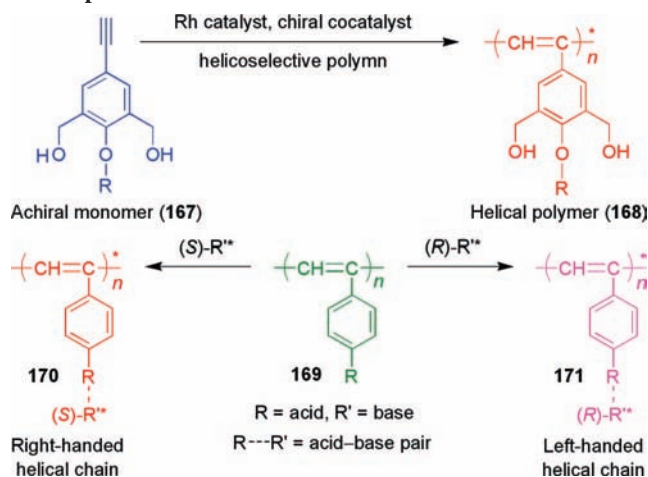
Besides the internal approach through the molecular engineering endeavors, the external perturbation strategy has also been utilized to generate helical PA chains. For example, the helicity of the PA chain with chiral pendants has been tuned by external stimuli, the achiral acetylenic monomers have been polymerized into helical polymers by helix-sense-selective (or helicoselective) polymerizations under asymmetric reaction fields or in the presence of chiral catalyst systems, and the chain helicity has been induced by noncovalent association of achiral pendants with chiral dopants.

As discussed above, the chain conformation of a PA derivative carrying chiral pendants is sensitive to the variations in the environment (e.g., solvent, temperature, pH, and additives) and its helical chirality is tunable by external stimuli. This is clearly demonstrated by the data shown in Figure 2A: when the solvent of the solution of polymer **165** is changed from chloroform to THF, the Cotton effect of the polymer is dramatically decreased.<sup>402</sup> The helical chain

segments are believed to be stabilized by the intra- and interstrand hydrogen bonds between the chiral pendants (Figure 2, panels B and C). The noncovalent stabilization can be broken by external perturbation and the system will reach a new equilibrium. This dynamic process enables the optically active PAs to cope with the variations in their environmental surrounding, as do the helical biopolymers such as proteins.

The research groups led by Akagi and Shirakawa fabricated (unsubstituted) PAs with macroscopic helicities of left- and right-handed screw senses by the acetylene polymerizations initiated by Ziegler–Natta catalyst of  $\text{Ti}(\text{O}i\text{Bu})_4\text{–AlEt}_3$  under the asymmetric reaction fields generated by chiral binaphthyl nematic liquid crystals.<sup>403</sup> The asymmetric cavities and channels created by the chiral mesogenic molecules may have guided the propagating chains to grow in one preferred addition mode, and the force fields generated by the  $\pi\text{–}\pi$  electronic interaction between the resultant conjugated PA chains and the chiral binaphthyl rings of the liquid crystals may have stabilized the helical conformations of the formed polymer chains. The preferred one-handed helical conformations of the PA chains were proved by their CD spectral analysis.<sup>403</sup> While Akagi and Shirakawa's helicoselective polymerization is on unsubstituted PA, Aoki and co-workers developed a rhodium-catalyzed polymerization system for the synthesis of chiral-substituted PA **168** from an achiral monomer **167** by using a chiral amine cocatalyst (Scheme 38).<sup>404</sup> The resultant polymer possessed a one-handed helical chain. This system is the first example of helicoselective polymerization of substituted acetylenes, in which the helical conformation of the formed polymer chains is stabilized by the intramolecular hydrogen bonding in the solution.

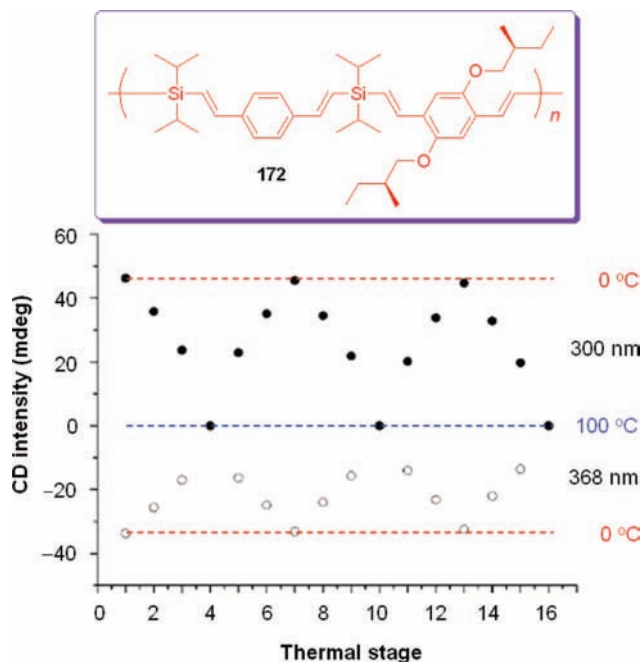
Formation of polymer complexes between functional groups of chiral molecules ( $\text{R}^*$ ) and achiral pendants (R) of substituted PAs has been found to spirally twist the PA chains. Yashima and co-workers have developed a facile method for the construction of dynamic helical PAs with an excess in helical sense through noncovalent bonding interactions with specific chiral guests after polymerization. PPA derivative **169** carrying achiral carboxy pendants is optically

**Scheme 38. Chain Helicity Induced by Chiral Cocatalysts and Dopants**


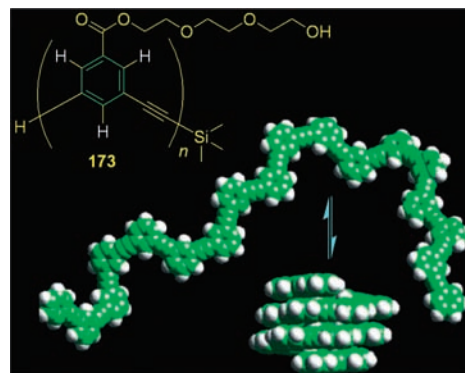
inactive (Scheme 38). However, upon its complexation with chiral bases, the PA chains are induced to take dynamically preferred one-handed helical conformations (170 or 171). The macromolecule complexes exhibit induced CD signals in the wavelength region typical of the polyene backbone absorption.<sup>117,405,406</sup> This CD induction is attributed to an unbalanced distribution in the population of the interconvertible left- and right-handed helices, which is realized by the noncovalent bonding interactions between the achiral pendants and the chiral ligands. Remarkably, the helical chain chirality induced by the complexation with chiral amines can be “memorized” by the polymer even after the ligand is removed or the polymer is decomplexed.

Besides the PA system, other acetylenic polymers with double bonds in the backbones have also been found to take helical conformations. Luh and co-workers have used the concept of Thorpe–Ingold effect to rationalize the chain helicity of poly(silylenevinylene)s containing chiral substituents.<sup>73</sup> For example, in a poly(silylenevinylene) prepared by alkyne hydrosilylation (172), the bulky isopropyl substituents on the silicon atom forces the monomer repeat units to take a *syn-syn* conformation. The polymer chain is folded into a helical structure, as revealed by its CD activity. The reversible temperature-dependent CD profiles shown in Figure 4 verify the helical conformation of the polymer chain. The CD signals of 172 in dodecane were monitored at 300 and 368 nm in multiple thermal stages at 0, 30, 60, and 100 °C. The signals disappeared at 100 °C as a result of dynamic conformation changes, gradually reappeared at 60 and 30 °C, and completely recovered at 0 °C. These CD profiles are reproducible in several cycles of thermal treatments, as can be seen from the data shown in Figure 4.<sup>73</sup>

“Foldamers” based on *m*-phenyleneethynylene oligomers have aroused much interest because of their capability of folding into helical conformation under appropriate conditions.<sup>96</sup> Much research effort has been devoted to the control or modulation of the secondary structure of the nonbiological or unnatural oligomers through the use of solvophobic interactions, because such studies are expected to help deepen our understanding on the natural folding or self-organization behaviors of biomacromolecules. Moore and co-workers have synthesized and investigated the oligomer systems that can fold into helical chain conformation (e.g., 173; Figure 5).<sup>96,407</sup> In these systems, the helical preference is controlled by several factors, including the *meta*-connectivity of the monomer repeat units, which allows the oligomer chain to



**Figure 4.** Changes of CD intensities of polymer 172 in dodecane in multiple thermal treatment stages and monitored at 300 nm (●) and 368 nm (○). Stages 1, 7, and 13: 0 °C; stages 2, 6, 8, 12, and 14: 30 °C; stages 3, 5, 9, 11, and 15: 60 °C; stages 4, 10, and 16: 100 °C. Reproduced with permission from ref 73. Copyright 2008 Wiley-VCH.

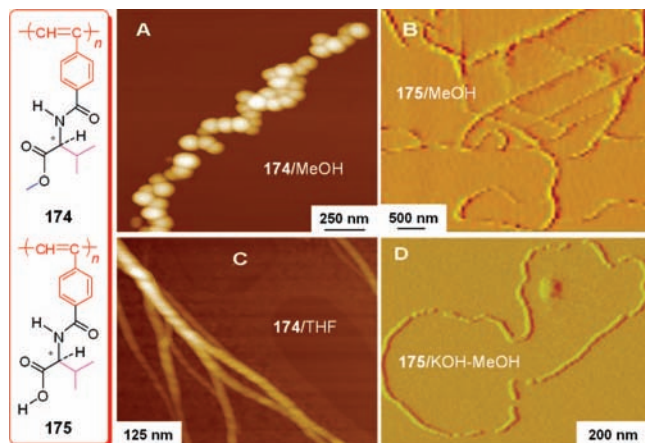


**Figure 5.** Space-filling model for the chain folding–defolding process in oligo(*m*-phenyleneethynylene) 173 ( $n = 18$ ) in response to a change in the environmental conditions. Side chains and end groups have been omitted for clarity. Reproduced with permission from ref 96. Copyright 2001 American Chemical Society.

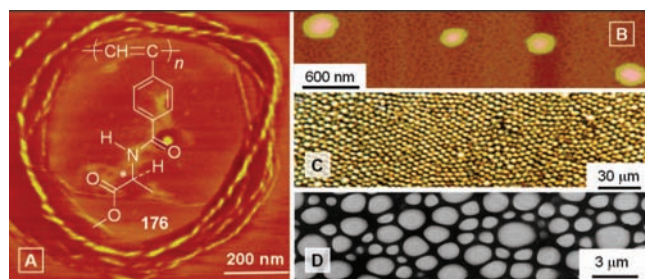
fold back upon itself, and the use of polar pendants and nonpolar backbone. When such amphiphilic oligomers with sufficient lengths are dissolved in a polar solvent, a helical conformation would be formed, because such a conformation maximizes the favorable interactions of the polar solvent with the polar pendants as well as the aromatic  $\pi$ – $\pi$  stacking interactions but minimizes the unfavorable contacts between the hydrocarbon backbone and the polar solvent.<sup>407</sup>

### 3.1.3. Morphostructures

The fabrication of biomimetic hierarchical structures by synthetic polymers is of great current interest. Inspired by the structural hierarchy of biopolymers such as proteins, several research groups have been investigating the organizational morphostructures of acetylenic polymers. Tang and co-workers have designed and synthesized a series of helical PAs carrying naturally occurring amino-acid pendants.



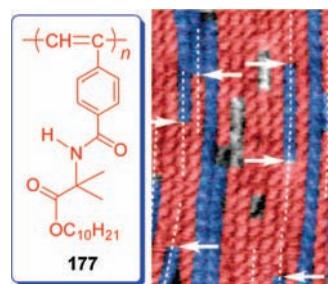
**Figure 6.** AFM images of supramolecular assembling structures formed by natural evaporation of the solutions of amino acid-containing PA derivatives **174** and **175**. The assembly images for **174** and **175** are reproduced with permission from refs 105 and 36. Copyright 2005 and 2001 American Chemical Society, respectively.



**Figure 7.** AFM images of (A) superhelical ribbons with left-handed twists and (B) nanospheres formed upon natural evaporation of dilute (A) THF and (B) chloroform solutions of polymer **176** on newly cleaved mica surfaces. (C) POM and (D) TEM images of porous films formed by natural evaporation of a "concentrated" chloroform solution of **176** on (C) glass slide and (D) carbon-coated copper grid. Reproduced with permission from ref 66. Copyright 2008 American Chemical Society.

Noticing the unique amphiphilicity of these polymers originating from their hydrophobic backbones and hydrophilic pendants, Tang's group studied their supramolecular assembly behaviors. The amphiphilic PAs are found to self-organize into various morphostructures reminiscent of natural structural motifs such as vesicles, tubules, helices, and honeycombs.<sup>36,97,98,105,408</sup> For example, natural evaporation of a methanol solution of **174** gives a string of nanopearls (Figure 6A). Helical ropes are formed when the solvent is changed to THF. Addition of KOH into the methanol solution of **175** changes helical cables (Figure 6B) to random threads (Figure 6D). The association of  $K^+$  ions with the carboxyl ( $CO_2^-$ ) groups breaks the hydrogen bonds. The charged polyelectrolyte chains repulse each other, making it difficult for the polymer chains to associate into multistranded helical cables. This is why the thin random coils are formed under the alkaline conditions.<sup>36</sup> These morphology data clearly manifest that the assembling structures of the polymers can be manipulated by changing their molecular structures and environmental conditions.

Similarly, polymer films with helical ribbons are formed upon natural evaporation of a dilute THF solution of **176** (Figure 7A).<sup>66</sup> Unlike those obtained from the evaporation of the methanol solution, the helical ribbons observed here are left-handed and twisting spirally. Some of them are coiling around to form ring-shaped or cagelike morphologies.

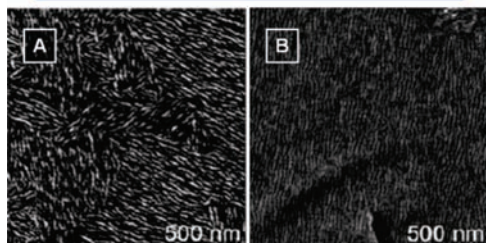
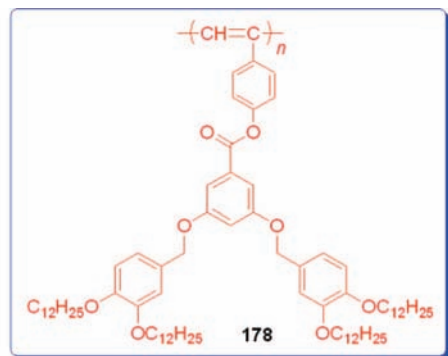


**Figure 8.** AFM height images of 2D self-assembled right- (red) and left-handed (blue) chains of **177** with achiral pendant on highly oriented pyrolytic graphite. Reproduced with permission from ref 409. Copyright 2007 Wiley-VCH.

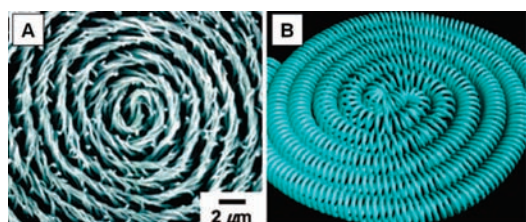
Polymer **176** exhibits stronger Cotton effect in THF than in methanol; as a result, better-ordered hierarchical structures of superhelical ribbons are formed via the evaporation-induced supramolecular self-assembling processes of the THF solution. The morphology obtained from the natural evaporation of a chloroform solution of **176** with a similar concentration is distinctly different. Instead of helical cables, oval eggs or spherical vesicles are formed (Figure 7B). This difference, however, is not totally unexpected. Unlike methanol and THF, chloroform is a poor solvent of the amino acid pendants. The amphiphilic polymer chains may form micelle-like structures with the L-alanine methyl ester pendants located in the cores and the polyene backbones positioned outward on the shells. During the solvent evaporation process, the micelles may grow in size and stick together via intermicellar hydrogen bonding to form large micelles to minimize the interfacial surface areas. The large micelles can further merge into pearl-like nanospheres, again with the aid of intershell hydrogen bonding. When a chloroform solution with a relatively high concentration (6.5  $\mu M$ ) is used, a piece of nice mesoporous film is formed (Figure 7C), thanks to the excellent film-forming ability of this high molecular weight polymer. Spreading a tiny drop of the polymer solution on a carbon-coated copper grid affords a thin film with many concentric rings of varying diameters (Figure 7D).<sup>66</sup>

Two-dimensional self-assembly behaviors of PA derivatives have also been investigated. Yashima and co-workers reported that, upon exposure to specific solvent vapor, polymer chains of a dynamic helical PPA derivative (**177**) deposited on highly oriented pyrolytic graphite (HOPG) can self-assemble into two-dimensional helix bundles.<sup>409</sup> In the solution state, **177** comprises an equal mixture of interconvertible right- and left-handed helical segments separated by helical reversals and, hence, shows no optical activity. The high-resolution atomic force microscopy (AFM) image of **177** on HOPG reveals that, in individual polymer chains, right- and left-handed helical segments are separated by helical reversal junctures (marked by arrows in Figure 8). The AFM images of **177** together with its X-ray diffraction (XRD) data give an 11/5 helix with a helical pitch of 2.3 nm. On the basis of statistical analysis of a series of high-resolution AFM images, helical reversals in **177** are found to appear only once in about every 300 monomer units on average.

Self-organizable dendronized polymers exhibit interesting single-molecule assembly behaviors. For example, the polymers themselves can self-assemble into discrete cylindrical and spherical structures with well-defined dimensions. Percec and co-workers have been actively exploring this area.



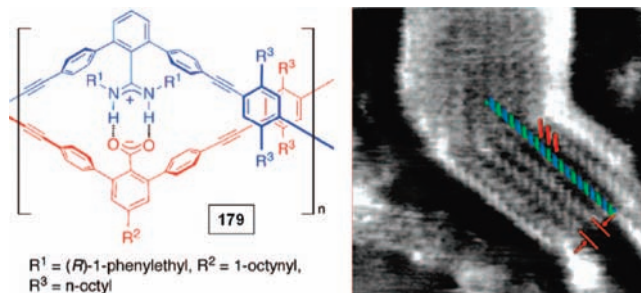
**Figure 9.** AFM phase image of a single layer of self-organizable dendronized PPA derivative **178** spin-cast on HOPG after annealing for 1 h at (A) 50 °C and (B) 100 °C. Reproduced with permission from ref 410. Copyright 2006 American Chemical Society.



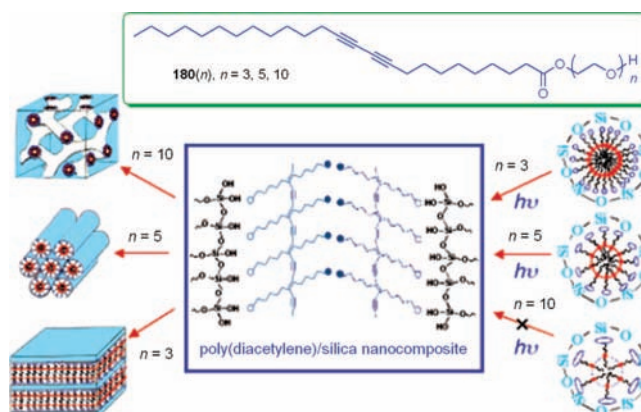
**Figure 10.** (A) SEM image of helical PA microfiber and (B) diagrammatic representation of the helical morphology consisting of twisted bundles of the PA nanofibrils. Reproduced with permission from ref 411. Copyright 2008 American Chemical Society.

Recently, Percec's group has reported that a PPA derivative carrying self-assembling dendron pendants (**178**) shows epitaxial adsorption on HOPG due to the interaction with the peripheral alkyl tails.<sup>410</sup> Individual polymer chains are visualized by AFM as oblate cylindrical objects. After annealing at 50 °C for 1 h, the single layer of **178** undergoes distinctive structural changes, accompanying the formation of submicrometer domains with different orientations of elongated linear structures, which are composed of small rods (Figure 9A). Further annealing at 100 °C brings about an increase in the domain size and an improvement in the order along the cylindrical axis within the domains (Figure 9B).

Whereas the self-assembly capability of the above-discussed substituted PAs is mainly endowed by their amphiphilic structures and interactive pendants, the unsubstituted PA chains self-organize into higher-order morphostructures by virtue of external control. Akagi and co-workers have found that the PA chains assemble into microfibers under the asymmetric reaction field, which exhibit clear spiral morphologies with structural hierarchy (Figure 10).<sup>411</sup> In the PA microfibers, the helical bundles comprise nanofibrils with diameters smaller than 100 nm, which are twisted and concentrically curled. Through careful microscopic examinations, Akagi has concluded that, in this system, the left- and right-handed helical PA chains are formed in the presence of the (*R*)- and (*S*)-chiral nematogens, respectively, and that these helical chains are further bundled through van der



**Figure 11.** AFM image of complementary double-helical chains of polymer **179** on HOPG. Reproduced with permission from ref 412. Copyright 2008 American Chemical Society.



**Figure 12.** Increasing the number ( $n$ ) of the subunits of the hydrophilic surfactant headgroup in **180** resulted in the formation of higher-curvature mesophases: lamellar ( $n = 3$ ), hexagonal ( $n = 5$ ), and cubic ( $n = 10$ ). Large headgroup ( $n = 10$ ) served as spacers and prevented the polymerization of pure **180**(10) surfactant from occurring. Reproduced with permission from ref 414. Copyright 2003 American Chemical Society.

Waals interactions to give helical nanofibrils with the opposite screw directions to those of the chiral nematogens.

While the morphostructures of the acetylenic polymers with single helical conformations have been well-studied, double helical polymers have been rarely investigated. Yashima and co-workers reported a double-stranded helical polymer consisting of complementary homopolymers.<sup>412</sup> The homopolymers bearing chiral amidines and achiral carboxylic acids with *m*-terphenyl backbones were prepared by the Sonogashira polycondensation of the corresponding monomers. Upon mixing in an appropriate solvent, the complementary homopolymers self-assembled into a double-stranded helical polymer with a twist-sense bias through the interstrand salt bridges (**179**; Figure 11). The supramolecular assembly structure of **179** was characterized by high-resolution AFM combined with XRD analysis, which gave a helical pitch of 1.47 nm with an excess in right-handed screw sense.

Morphostructure has been found to critically affect the functions of organic–inorganic nanohybrids. Acetylenic polymers have been hybridized with many inorganic materials. Lu and Brinker have used a series of oligo(ethylene glycol)-functionalized diacetylenic surfactants **180**( $n$ ) both as amphiphiles to direct the self-assembly of thin-film silica mesophases and as monomeric precursors to conjugated PDAs (Figure 12).<sup>413,414</sup> Beginning with a homogeneous solution of silicic acid and the surfactant in a THF/water mixture with an initial surfactant concentration much less than critical micelle concentration, Lu and Brinker used



evaporative dip-coating, spin-coating, or static casting procedure to prepare thin films on silicon (100) or fused silica substrates. During the deposition, preferential evaporation of the THF solvent concentrates the depositing solution. The progressively increased surfactant concentration induces the formation of diacetylene/silica surfactant micelles and drives their assembly into ordered, three-dimensional LC mesophases. The UV irradiation-initiated polymerization of the diacetylene units and the catalyst-promoted siloxane polycondensation topochemically converts the colorless mesophase into a blue PDA/silica nanocomposite with preserved highly ordered self-assembled architecture.

The choice of surfactant greatly influences the mesostructure of the resultant nanohybrid. Increasing the value of  $n$  increases the surfactant headgroup area. This in turn reduces the surfactant packing parameter and promotes the formation of progressively higher-curvature mesophases: lamellar for  $n = 3 \rightarrow$  hexagonal for  $n = 5 \rightarrow$  cubic for  $n = 10$ . From the highly ordered nanocomposite mesostructures observed by transmission electron microscopy (TEM), it is inferred that the surfactant monomers/structure-directing agents are uniformly organized into precise spatial arrangements before polymerization.<sup>413,414</sup> These arrangements establish the proximity of the reactive diacetylene units in the surfactant monomers, thereby facilitating the acetylene polymerization process.

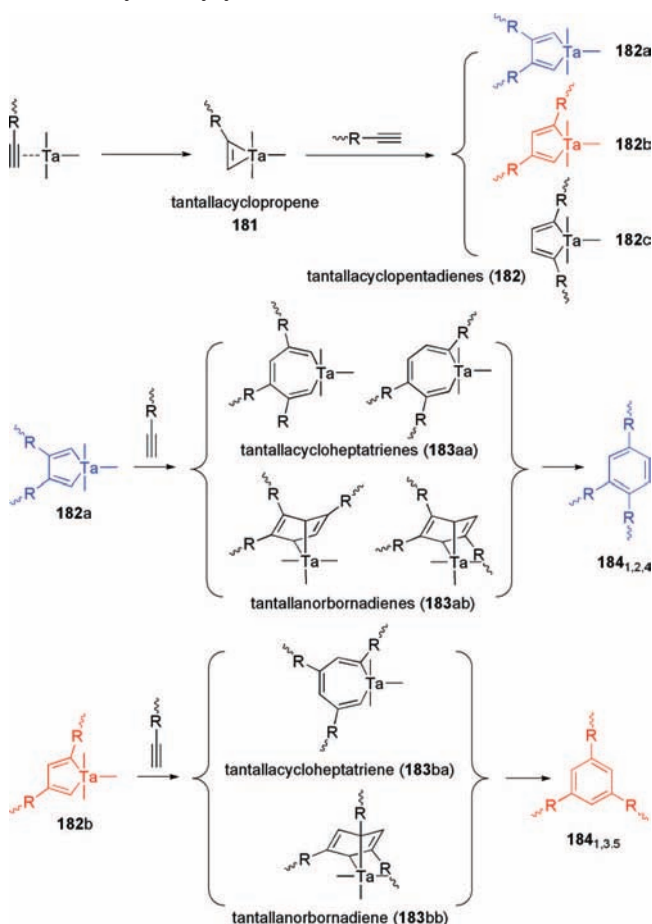
## 3.2. Hyperbranched Polymers

### 3.2.1. 1,2,4- and 1,3,5-Trisubstitutions

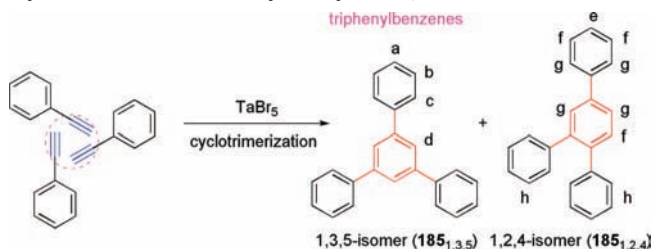
How the monomers repeat units are knitted together in the polymerization reaction determines the topological structures of the resultant polymers and eventual their solubility and functionality. There is a regiostructural issue in the transition-metal-catalyzed polycyclotrimerization reaction of  $A_2$ -type diyne monomers: three acetylenic triple bonds are cyclized to form benzene rings with symmetric 1,3,5- and/or asymmetric 1,2,4-trisubstitution patterns.<sup>328–343,345–350,352–354</sup> According to the Ta-catalyzed polycyclotrimerization mechanism proposed by Tang and co-workers (Scheme 39), the active Ta species oxidatively adds to an acetylene triple bond to produce a tantallacyclopentadiene regioisomers (**182**), among which, the likelihood to form **182c** is the lowest because of the involved stereochemical effect. Addition of a third triple bond to **182a** may yield two tantallacycloheptatriene species (**183aa**) and two Diels–Alder adducts of tantallanorbornadienes (**183ab**), each experiencing different steric hindrances but all giving the same product **184**<sub>1,2,4</sub>, a 1,2,4-trisubstituted benzene isomer. On the other hand, addition of an acetylene triple bond to **182b** furnishes a tantallacycloheptatriene (**183ba**) and a tantallanorbornadiene (**183bb**), whose reductive elimination furnishes **184**<sub>1,3,5</sub>, a 1,3,5-trisubstituted benzene isomer.

To collect experimental information on the regiochemistry involved in the polycyclotrimerization reaction, Tang and co-workers designed and conducted two model reactions. The first model reaction is the cyclotrimerization of **1** catalyzed by  $TaBr_5$  (Scheme 40).<sup>353</sup> No polymeric products are formed in the model reaction, which unambiguously rules out the possibility that the diynes are polymerized into polyenes via a metathesis polymerization mechanism by  $TaBr_5$ .  $^1H$  NMR spectrum of the raw products reveals that they are a mixture

**Scheme 39. Formation of 1,2,4- and 1,3,5-Regioisomeric Units in Diyne Polycyclotrimerization**



**Scheme 40. Model Reaction of Phenylacetylene Cyclotrimerization Catalyzed by  $TaBr_5$**

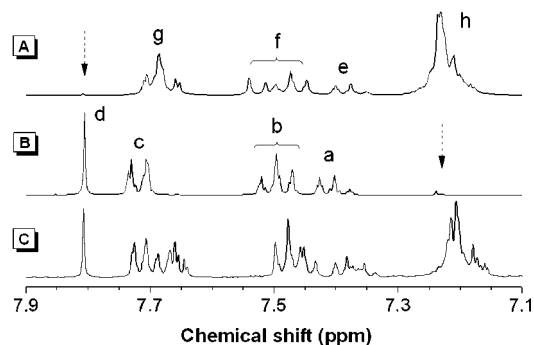


of 1,2,4- and 1,3,5-triphenylbenzenes, i.e., **185**<sub>1,2,4</sub> and **185**<sub>1,3,5</sub>. The raw products are separated and purified by recrystallization, and the  $^1H$  NMR spectra of pure isomers **185**<sub>1,2,4</sub> and **185**<sub>1,3,5</sub> are given in panels A and B of Figure 13. These experimental results attest that the  $TaBr_5$ -catalyzed reaction has transformed three triple bonds into one benzene ring via the cyclotrimerization mechanism. From the  $^1H$  NMR spectra of the reaction mixture, the molar ratio of **185**<sub>1,2,4</sub> to **185**<sub>1,3,5</sub> is calculated to be 2.0:1.0 according to eq 2,

$$\frac{N_{1,2,4}}{N_{1,3,5}} = \frac{A_h/10}{A_d/3} = \frac{3A_h}{10A_d} \quad (2)$$

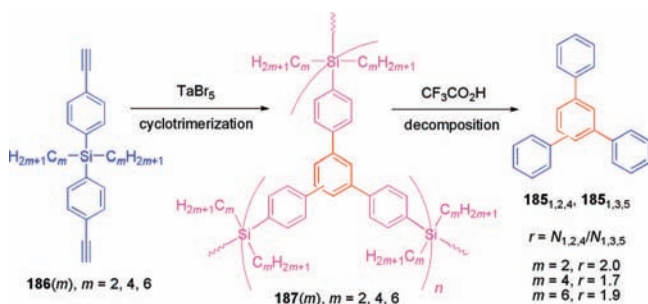
where  $N_{1,2,4}$  and  $N_{1,3,5}$  are the numbers of isomers **185**<sub>1,2,4</sub> and **185**<sub>1,3,5</sub> and  $A_h$  and  $A_d$  are the integrated areas of resonance peaks h and d, respectively (Scheme 40 and Figure 13).

The second model reaction is the acid-catalyzed decomposition of polymer **187**( $m$ ) (Scheme 41).<sup>353</sup> It is well-known



**Figure 13.**  $^1\text{H}$  NMR spectra of triphenylbenzenes (A)  $185_{1,2,4}$ , (B)  $185_{1,3,5}$ , and (C) desilylated products of  $187(2)$ . Reproduced with permission from ref 353. Copyright 2007 American Chemical Society.

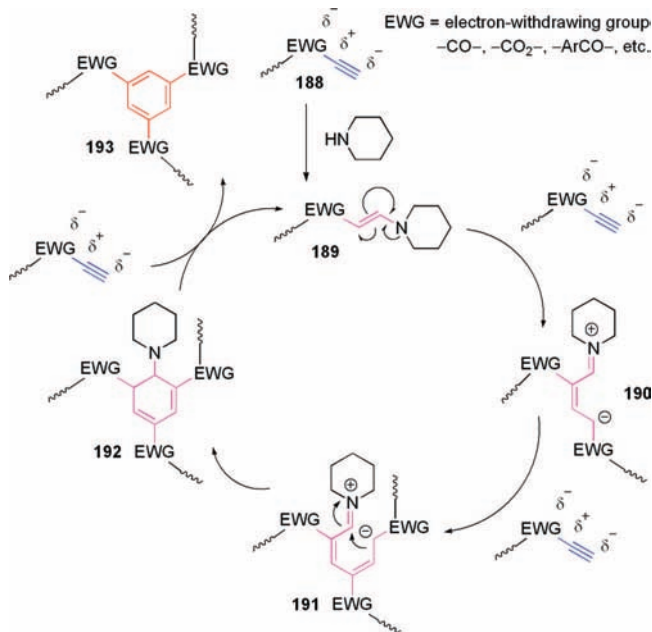
**Scheme 41. Evaluation of the Regioisomeric Ratio ( $r$ ) of 1,2,4- and 1,3,5-Trisubstituted Benzene Units in Polymer  $187$  by Acid-Catalyzed Desilylation**



that strong protonic acids, such as  $\text{CF}_3\text{CO}_2\text{H}$ ,  $\text{HClO}_4$ , and  $\text{H}_2\text{SO}_4$ , can cleave the Si–C bond. When a mixture of  $187(2)$  and  $\text{CF}_3\text{CO}_2\text{H}$  is refluxed in DCM for 96 h under nitrogen, the polymer is decomposed to  $185_{1,2,4}$  and  $185_{1,3,5}$ , as confirmed by the IR, NMR, and MS analyses. The spectroscopic results further confirm that new benzene rings have been formed in the  $\text{TaBr}_5$ -catalyzed polymerization of  $186(2)$ . An example of its  $^1\text{H}$  NMR is given in Figure 13C. Calculation of the isomeric contents of  $185_{1,2,4}$  and  $185_{1,3,5}$  gives a molar ratio of 2.0:1.0. The structures of  $187(4)$  and  $187(6)$  are analyzed under the same experimental conditions. The calculated molar ratios of  $185_{1,2,4}$  to  $185_{1,3,5}$  for  $187(4)$  and  $187(6)$  are 1.7:1.0 and 1.9:1.0, respectively. The ratios derived from the decomposition products agree well with that obtained from the first model reaction, i.e., phenylacetylene cyclotrimerization.

The transition-metal-catalyzed  $\text{A}_2$ -type diyne polycyclotrimerization gives hyperbranched polymers composed of regio-random mixtures of 1,2,4- and 1,3,5-trisubstituted benzenes, often in the ratio of  $\sim 2:1$ , that make the polymer structures irregular. Tang and co-workers have further developed a new synthetic route to hyperbranched polyarylenes with perfect 1,3,5-regioregularity.<sup>344,351</sup> The monomers here are different from those used in the transition-metal-catalyzed coordination polymerizations discussed above and contain electron-withdrawing groups (EWGs). The diyne polycyclotrimerization is catalyzed by simple organic amines such as piperidine, which proceeds in an ionic mechanism and furnishes hyperbranched polymers with 1,3,5-regioregular structure. The proposed polymerization mechanism is shown in Scheme 42.<sup>344</sup> The regioselectivity stems from the ionic, instead of coordination, mechanism of the base-catalyzed reaction. In the diyne polycyclotrimerization, piperidine reacts with an acetylene triple bond ( $188$ ) in a Michael addition mode to give a

**Scheme 42. Mechanism of Amine-Catalyzed 1,3,5-Regioselective Polycyclotrimerization of Electron-Deficient Diyne**

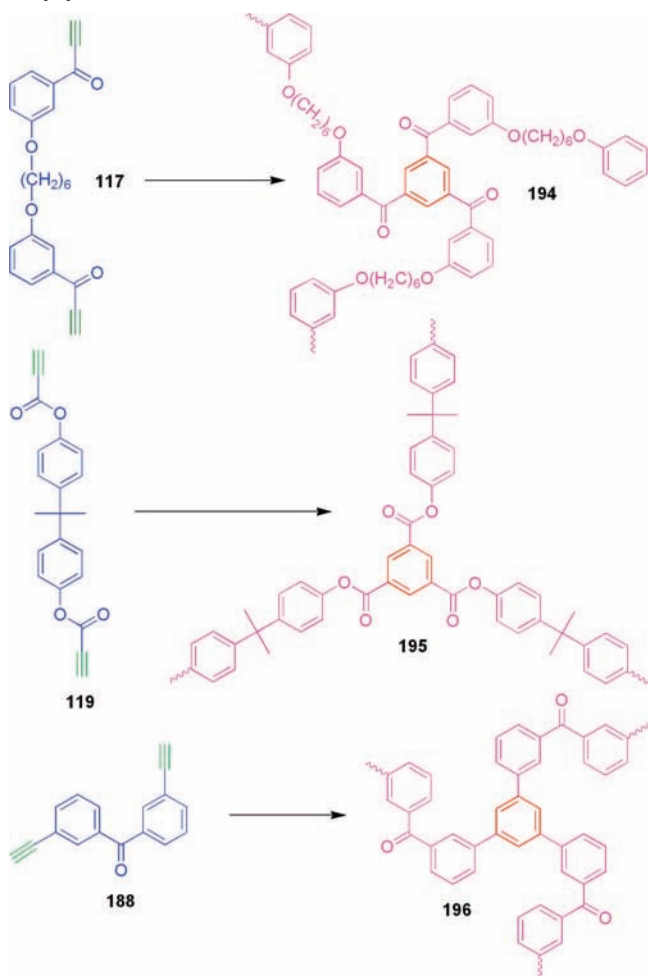


ketoenamine ( $189$ ), which further reacts with two more acetylene triple bonds to yield a dihydrobenzene ( $192$ ). The amine moiety in  $192$  is cleaved by its reaction with another triple bond, and aromatization furnishes a 1,3,5-trisubstituted benzene ring ( $193$ ). Repetition of this reaction cycle results in the formation of a hyperbranched polymer with a high molecular weight. This polycyclotrimerization mechanism applies to several types of diyne monomers containing electron-withdrawing groups (EWGs), such as aryl ethynyl ketones, propiolic esters, and ethynylaryl ketones. Typical examples of the base-catalyzed diyne polycyclotrimerization systems are shown in Scheme 43.<sup>344,351,355</sup>

**3.2.2. 1,4- and 1,5-Disubstitutions**

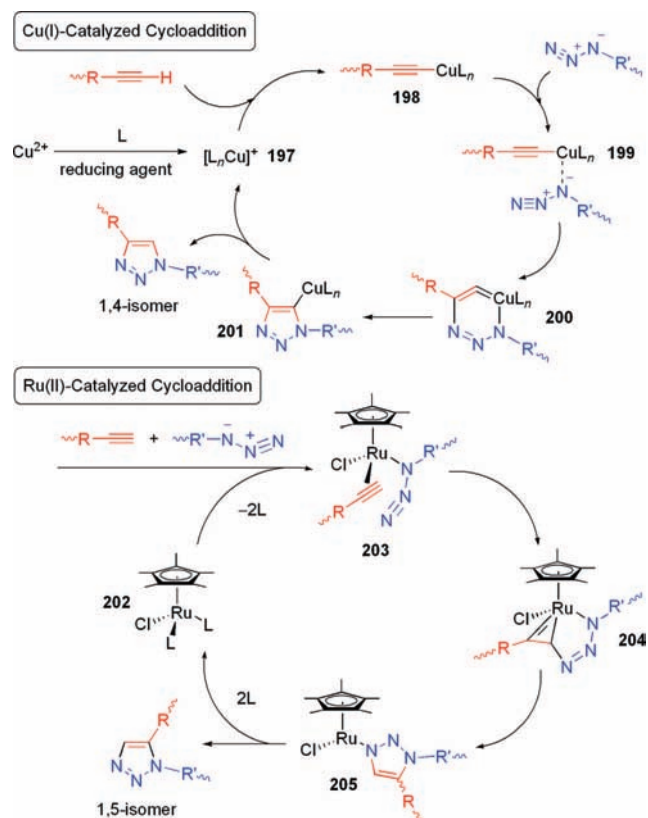
The regioselective syntheses of *hb*-1,4-PTAs and *hb*-1,5-PTAs have been accomplished by the Cu(I)- and Ru(II)-mediated click polymerizations, respectively. Particularly intriguing is that the variation in the regioregularity greatly affects the solubility and functionality of the polymers. For example, *hb*-1,5-PTAs  $130$  (Scheme 30) show better solubility, bluer emission, and milder aggregation, in comparison to their 1,4-counterparts  $129$ .<sup>71</sup> Understanding the polymerization mechanism thus may help guide further endeavors in designing and generating new PTA-based functional materials.

Scheme 44 shows the proposed catalytic processes of the Cu(I)- and Ru(II)-mediated 1,4- and 1,5-regioselective click polymerizations.<sup>71,113,415,416</sup> The active catalytic species  $197$  is usually generated from a Cu(II) salt in the presence of a reducing agent such as sodium ascorbate. The catalytic cycle commences from the generation of Cu(I) acetylide ( $198$ ). The azide replaces one of the ligands in  $198$  and binds to the Cu(I) center via the nitrogen proximal to carbon, forming intermediate  $199$ . The distal nitrogen of the azide in  $199$  attacks the C-2 carbon of the Cu(I) acetylide, forming an unusual six-membered Cu(III) metallacycle  $200$ . The barrier for ring contraction that yields triazolyl–Cu derivative  $201$  is very low. Proteolysis of  $201$  releases the triazole product, thereby completing the catalytic cycle.

**Scheme 43. Examples of 1,3,5-Regioselective Diyne Polycyclotrimerizations**

In the Ru(II)-catalyzed click reaction, the displacement of the spectator ligands from  $\text{Cp}^*\text{Ru}(\text{PPh}_3)_2\text{Cl}$  (**202**) gives activated complex **203**, which is converted, via the oxidative coupling of an alkyne and an azide, to ruthenacycle **204** (Scheme 44). This step controls the regioselectivity of the overall process. The new C–N bond is formed between the more electronegative and less sterically demanding carbon of the alkyne and the terminal nitrogen of the azide. The metallacycle intermediate undergoes reductive elimination, releasing the aromatic triazole product and regenerating the catalyst or activated complex **203**. Repetition of the catalytic cycle leads to the formation of 1,5-regioregular PTA.

Tang and co-workers carried out model reactions in an effort to analyze regiostructures of their PTAs and to collect information on the mechanisms of the click polymerizations.<sup>71</sup> Triyne **123d** was reacted with monoazide **206** in the presence of Cu(I) and Ru(II) catalysts, which furnished the expected reaction products of 1,4- and 1,5-disubstituted 1,2,3-triazoles **207** and **208**, respectively (Scheme 45). The pure isomers were characterized by standard spectroscopic methods. Examples of their <sup>1</sup>H NMR spectra are given in Figure 14. Whereas **207** shows a strong resonance peak at  $\delta \approx 8.64$ , **208** does not resonate in this chemical shift region. By comparison of the NMR spectra between these model compounds and the hyperbranched polymers, *hb*-PTAs **129(6)** and **130(6)** were confirmed to be 1,4- and 1,5-regioregular, respectively (Figure 14). This is the first systematic study of *hb*-PTAs with their regiostructures duly verified by spectroscopic analyses.

**Scheme 44. Proposed Mechanisms for Cu(I)- and Ru(II)-Mediated 1,4- and 1,5-Regioselective Click Polymerizations**

### 3.2.3. Degree of Branching

Since the first intentional synthesis of hyperbranched polymers was reported in the late 1980s, many research groups have worked on this new class of polymers.<sup>91,417</sup> With a globular molecular architecture, hyperbranched polymers exhibit higher solubility and lower viscosity, in comparison to their linear analogues. An important structural parameter for a hyperbranched polymer is its DB, which affects many of its chemical and physical properties, especially the two solution properties mentioned above. A hyperbranched polymer contains three basic legos, that is, dendritic (*D*), linear (*L*), and terminal (*T*) units. DB is defined by the following equations:

$$f_D = \frac{N_D}{N_D + N_T + N_L} \quad (3)$$

$$f_T = \frac{N_T}{N_D + N_T + N_L} \quad (4)$$

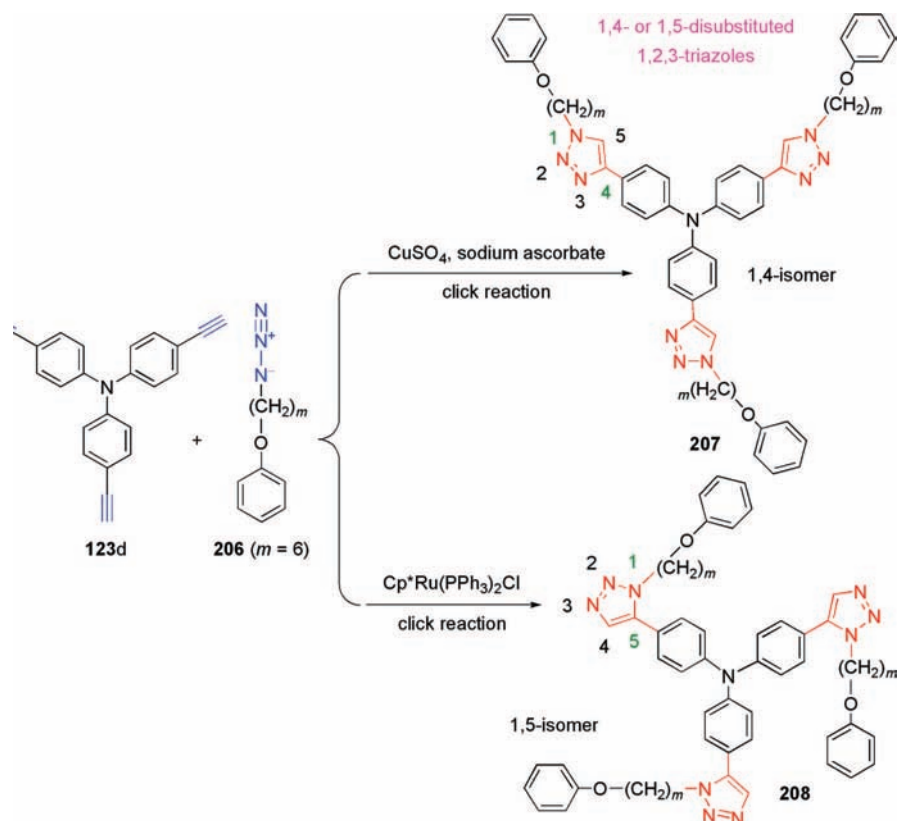
$$f_L = \frac{N_L}{N_D + N_T + N_L} \quad (5)$$

$$f_T + f_D + f_L = 1 \quad (6)$$

$$\text{DB} = \frac{N_D + N_T}{N_D + N_T + N_L} = f_D + f_T \quad (7)$$

where  $N_D$ ,  $N_L$ , and  $N_T$  are the numbers of *D*, *L*, and *T* units and  $f_D$ ,  $f_T$ , and  $f_L$  are the fractions of *D*, *T*, and *L* units, respectively. By definition, DB is 100% for a dendrimer and less than 100% for a hyperbranched polymer.

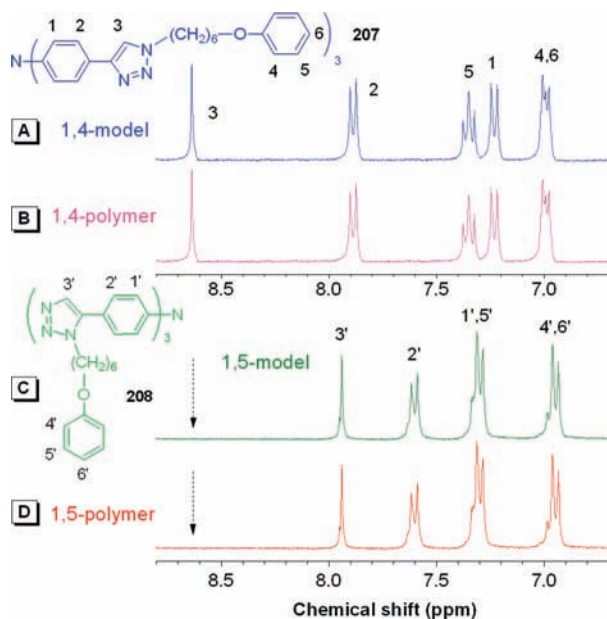
## Scheme 45. Model Reactions of Cu(I)- and Ru(II)-Mediated Click Reactions



The determination of DB values for hyperbranched acetylenic polymers has not been an easy job. For example, the hyperbranched polymers prepared from the newly developed polycyclotrimerization of  $A_2$ -type monomers have the general structures of  $D$ ,  $L$ , and  $T$  units shown in Chart 3. Unfortunately, the NMR signals of the newly formed benzene rings in the  $D$ ,  $T$ , and  $L$  units and the unreacted acetylene triple bonds in the  $T$  and  $L$  units of the polymers cannot be easily

distinguished from each other. It has been difficult to calculate the ratio of  $D$ ,  $T$ , and  $L$  units in the polymers, which in turn makes it difficult to directly determine their DB values.<sup>328–354</sup> However, some relationships between the DB value and other characterizable parameters, e.g.,  $DP_n$  and fraction of reacted triple bonds ( $p$ ), can be established. With the aid of theoretical simulations, DBs of the polymers have been estimated. Whereas the DB values for the conventional hyperbranched polymers prepared from  $AB_2$ -type monomers are generally about 0.5, those for the hyperbranched acetylenic polymers are often much higher than 0.5.

Although the DBs have been estimated to be very high for the hyperbranched polymers synthesized from the  $A_2$ -type diene monomers, the determination of their absolute DB values remains a challenging task. Recently, Tang and co-workers have succeeded in the determination of absolute DB values for the hyperbranched acetylenic polymers with 1,3,5-regioregularity.<sup>355</sup> The deduction of the DB value of **195** is illustrated below as an example. Polymer **195** is synthesized from the diene polycyclotrimerization of monomer **212**. Because this polycyclotrimerization proceeds in an ionic mechanism (cf., Scheme 42), it generates  $L$  and  $T$  units with enamine groups, but not acetylene triple bonds, at the branch ends (Chart 4). It is this unique structural feature that has enabled the determination of its absolute DB value.



**Figure 14.**  $^1\text{H}$  NMR spectra of model compounds (A) **207** and (C) **208** and hyperbranched polymers (B) **129(6)** and (D) **130(6)** with (A and B) 1,4- and (C and D) 1,5-regioregularities measured in  $\text{DMSO}-d_6$ . Reproduced with permission from ref 71. Copyright 2008 American Chemical Society.

**Chart 3.** General Structures of Dendritic, Linear, and Terminal Units Formed in Diene Polycyclotrimerization

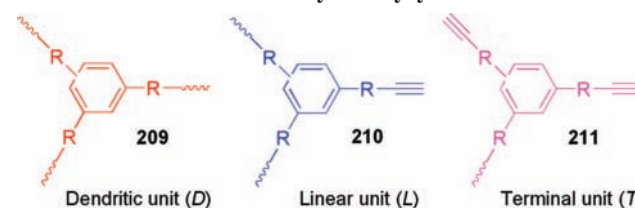
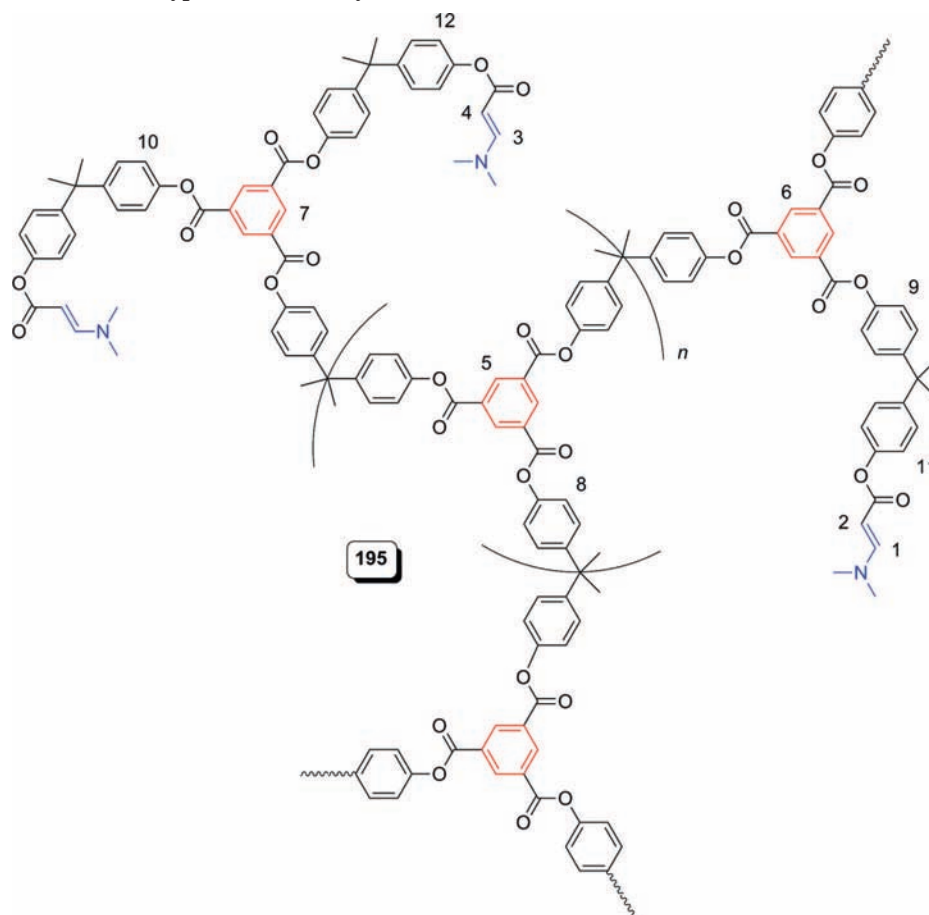


Chart 4. Chemical Structure of Hyperbranched Polymer **195**

The *D* (**214**), *L* (**215**), and *T* (**216**) units in polymer **195** are shown in Chart 5. By comparison of the  $^1\text{H}$  NMR spectrum of **195** with those of monomer **212** and model compound **213** (Figure 15), it is found that the following relationship among the fractions of the three structural units ( $f_D$ ,  $f_L$ , and  $f_T$ ) holds

$$\frac{3f_L + 3f_T + 3f_D}{f_L + 2f_T} = \frac{A_{5-7}}{A_{1,3}} \quad (8)$$

where  $A_{5-7}$  and  $A_{1,3}$  are the integrals of the areas of the resonance peaks (5–7) and (1,3), as labeled in Chart 4 and Figure 15.

From the  $^1\text{H}$  NMR spectra, the following equation is obtained:

$$\frac{3f_L + 3f_T + 3f_D}{f_L + 2f_T} = \frac{1}{0.362} \quad (9)$$

The combination of eqs 6 and 9 gives eq 10:

$$f_L + 2f_T = 1.086 \quad (10)$$

Enlarging the resonance peak at  $\delta$  7.91 reveals that it is actually a doublet. The amount of the olefinic protons in the linear unit is 8 times lower than that in the terminal unit. Equation 11 is thus established:

$$\frac{f_L}{2f_T} = \frac{1}{8} \quad (11)$$

From eqs 10 and 11,  $f_L$  is calculated to be

$$f_L = 0.121 \quad (12)$$

The combination of eqs 6 and 12 gives the DB value of **195**:

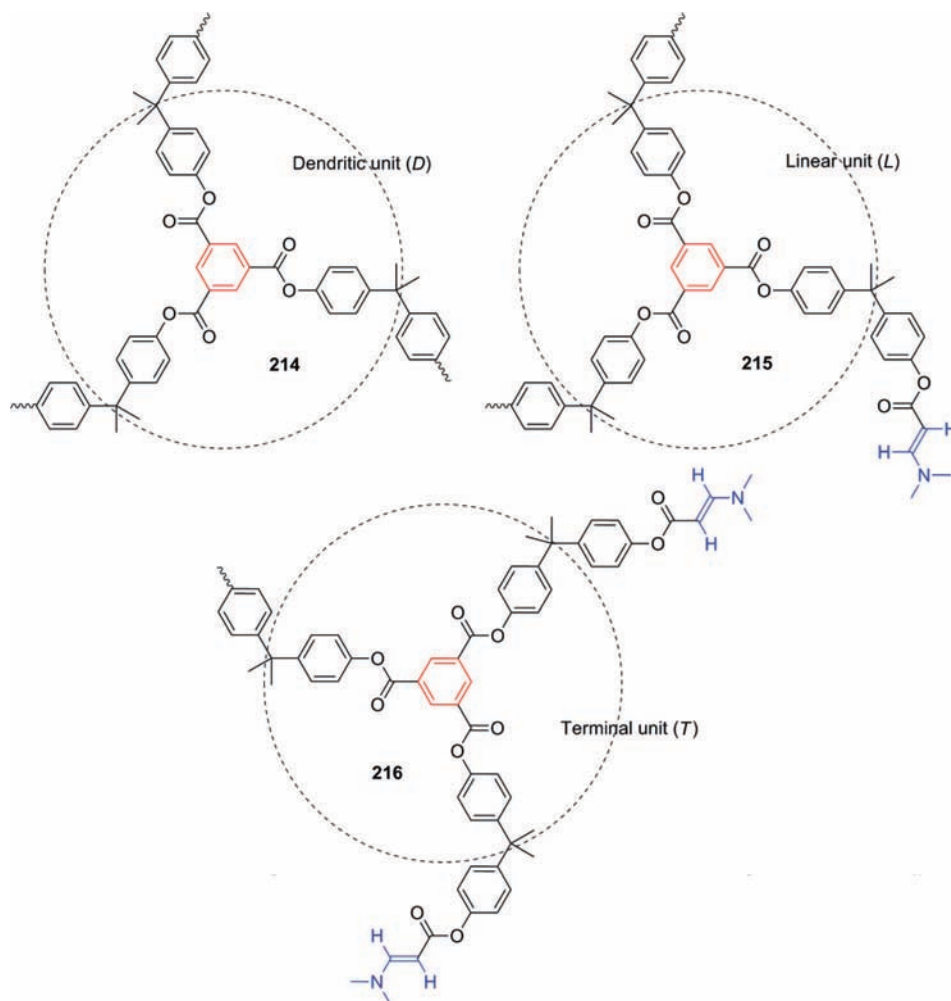
$$\text{DB} = f_D + f_T = 1 - f_L = 0.879 \quad (13)$$

This value is much higher than those of the traditional hyperbranched polymers. This example clearly demonstrates that the simple  $A_2$ -type construction strategy is a versatile tool for the synthesis of highly branched polymers.

The determinations of the DB values for the *hb*-PTAs synthesized from the click polymerizations of ( $A_2 + B_3$ )-type monomers are somewhat more complicated in procedure. In the *hb*-PTAs, there are six basic structural units as shown in Chart 6, that is, one *D* (**217**), two *L* [ $L_c$  (**218**) and  $L_a$  (**219**)], and three *T* [ $T_{cc}$  (**220**),  $T_{aa}$  (**221**), and  $T_{ea}$  (**222**)] units. Through careful mathematic derivatizations, the DB values of the PTAs were calculated to be  $\sim 90\%$  (details not given here for the purpose of space saving; interested readers are referred to the original paper cited in the reference section).<sup>71</sup> This once again proves that the acetylenic monomers are excellent building blocks for the construction of hyperbranched polymers with very high DB values.

### 3.2.4. Structural Modulation

The diyne homopolycyclotrimerizations have enjoyed a great success and have readily transformed a large variety of diyne monomers into hyperbranched PPs. The molecular structures of the polymers have been tuned by Tang and co-

Chart 5. *D*, *L*, and *T* Units in Hyperbranched Polymer 195

workers through the design of monomer structures, choice of catalyst systems, variation of polymerization conditions, etc.<sup>112,113</sup> Tang's group has further manipulated the polymer structures by the copolycyclotrimerizations of diynes with monoynes, in which the monoyne comonomers serve as reactivity-adjusting agents and help put the often fast-proceeding polymerization reactions under control. The gel formation can thus be completely circumvented in the polymerization systems through the judicious use of diyne–monomer combinations. The cocyclotrimerization of one triple bond from a monoyne with two triple bonds from an active center generates an *L* unit, while that of two triple bonds from a monoyne with one triple bond from an active center yields a *T* unit. The cocyclotrimerization thus produces *L* and *T* units but not *D* unit, resulting in a change in the ratio of the structural units. The topological structures of the polymers can therefore be varied by simply changing the amounts of the monoyne comonomers in the copolycyclotrimerization systems. Also because of the generation of *L* and *T* units by the diyne–monoyne cocyclotrimerization, the cores of the hyperbranched polymers can be decorated by the functional groups embedded in the monoyne comonomers.

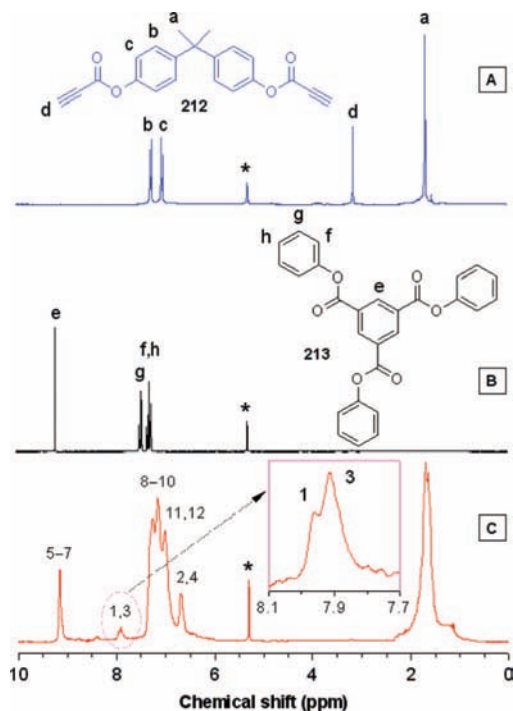
Several examples are given below to demonstrate the utility of the copolycyclotrimerization approach. The homopolycyclotrimerization of 1,4-diethynylbenzene (**69d**) initiated by Ta-based catalyst resulted in an all-aromatic hyperbranched PP with very poor solubility, because the diyne polycyclotrimerization reaction proceeded very fast and the extremely high density of benzene rings made the polymer

difficult to be solvated. Tang and co-workers copolycyclotrimerized diyne **69d** with monoyne **1** and obtained hyperbranched PP **223** that was soluble in common organic solvents (Scheme 46). It is still a carbon-rich, all-aromatic polymer but has a reduced density of benzene rings. The increased free volume within the polymer and the enlarged spatial radius of the three-dimensional sphere have enabled the polymer to be readily solvated by solvent molecules.<sup>113,419,420</sup>

Tang's group has further extended this strategy to ferrocene-containing acetylenic monomers with an aim of tuning the density and distribution of the ferrocenyl units in the hyperbranched polymers. As can be seen from Scheme 47, the copolymerizations of diynes **43** with ferrocenylalkynes **224** result in the formation of organometallic hyperbranched polymers with the ferrocenyl units mainly located in the peripheries,<sup>348,352</sup> while the copolymerizations of ferrocene-containing diynes **226** and monoynes **224** afford polymers **227** with the ferrocenyl units distributed in both cores and peripheries.<sup>354</sup> A typical example for the latter case is shown in Scheme 48. The copolymerization of **228** and **229** gives polymer **230**, which is electroactive and serves as an excellent precursor to magnetic ceramics (vide post).<sup>354</sup>

#### 4. Functions

With the inherent nature of electronic unsaturation or  $\pi$ -conjugation and the great structural diversity and hierarchy discussed above, the acetylenic polymers are anticipated to exhibit an array of functional properties that are difficult to



**Figure 15.**  $^1\text{H}$  NMR spectra of (A) monomer **212**, (B) model compound **213**, and (C) polymer **195** measured in  $\text{DCM-}d_2$ . Reproduced with permission from ref 355. Copyright 2009 American Chemical Society.

realize by conventional condensation and vinyl polymers. Many research groups have been working on the development of advanced functional materials based on the acetylenic polymers. As a result, a variety of novel electrical, optical, photonic, magnetic, and biological properties has been reported for this class of polymeric materials. In this section, a library of advanced functional properties of the

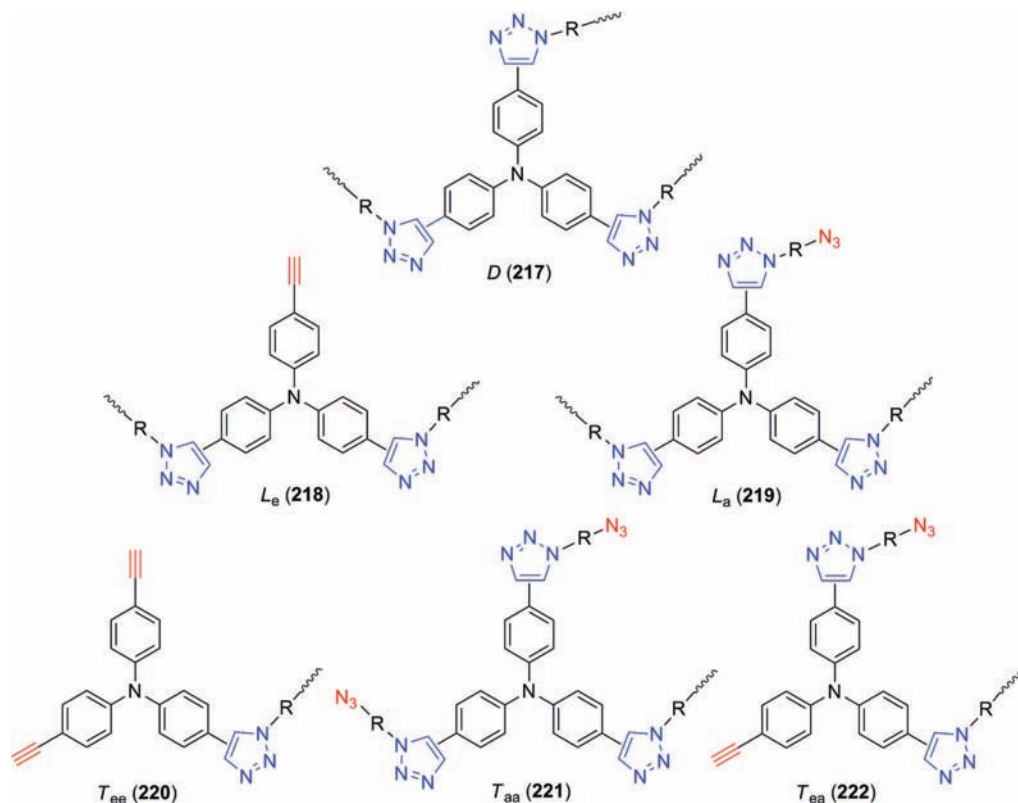
acetylenic polymers will be presented and discussed. Note that not all the acetylenic polymers will be discussed in each property category in an exclusive manner. Emphasis will be given to representative examples of the functional properties that are unique or characteristic to the acetylenic polymers.

#### 4.1. Electrical Conductivity

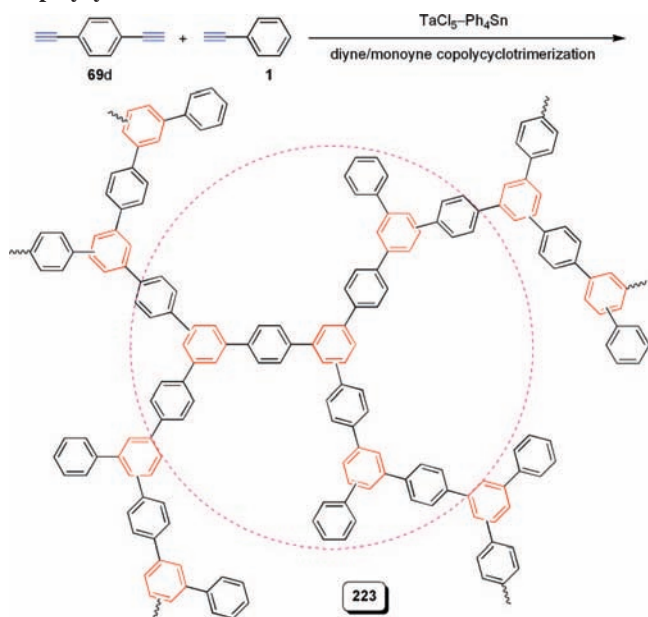
The seminal discovery of the metallic conductivity of doped PA made by the Nobel laureates, Heeger, MacDiarmid, and Shirakawa, has stimulated a huge surge of interest in synthetic metals and spawned an active area of research on electronically conjugated polymers. The remarkable progress in the area has brought us to the threshold of a “plastic-electronics era” that previously could only be imagined in science fiction. PA itself, however, is notoriously intractable (insoluble and infusible) and extremely sensitive to air, which has greatly detracted from its potential for real-world technological applications. The introduction of substituents onto the PA backbone has proved to be an excellent solution to solve the processability and stability problems. The electrical conductivities of the doped forms of these substituted PAs, however, are often in the semiconductor region and much lower than that of the doped form of their PA parent, due to the backbone twisting induced by the substituent groups and, hence, the decreased overlap of the  $\pi$ -orbitals of the monomer repeat units.

Although the substituted PAs show low absolute electrical conductivities, their relative conductivities are still higher than those of the conventional single-bonded polymers and may be further enhanced by external stimuli. Of particular interest and technological implication is the enhancement in the electrical conductivity by photoirradiation, commonly known as photoconductivity (PC). Much work has been done on the PCs of the substituted PAs.<sup>421–427</sup> Through systematic

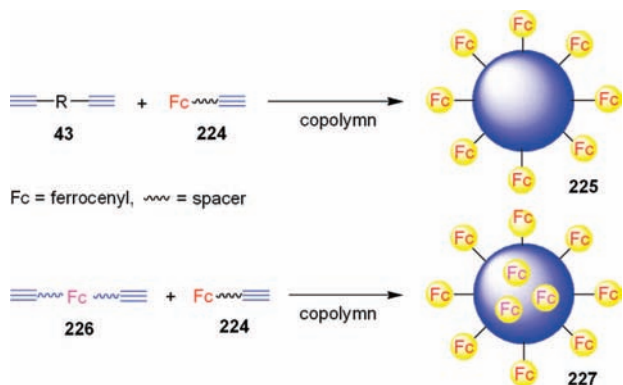
**Chart 6.** *D*, *L*, and *T* Units in a Hyperbranched Polytriazole Prepared by Click Polymerization



**Scheme 46. Synthesis of Soluble, Pure, Hyperbranched Polyphenylene without Substituents by Alkyne Copolycyclotrimerization**



**Scheme 47. Diagrammatic Illustration for Modulation of Density and Distribution of Ferrocenyl Units in Hyperbranched Polymers by Alkyne Copolycyclotrimerization**



studies, Tang's group has observed the following structure–property relationships in the photoconductions in the substituted PAs: (i) The substituted PAs containing electron-donating substituents exhibit higher PCs than those with electron-accepting ones. (ii) The PCs are further improved when the electron donors are simultaneously hole-transporters. (iii) The photoconduction becomes even more efficient when the donor substituents are mesogenic and can be packed in an ordered fashion.<sup>421</sup>

Some examples of photoconductive PAs are shown in Figure 16. Polymers **232** and **233** contain donor substituents and show higher PCs than PPA (**2**), which carries no donor pendants, and **231**, whose pendants contain antagonistic donor (ether) and acceptor (ester) units.<sup>421</sup> The PC value of **233** is higher than that of **232** because the former is simultaneously a good hole-transporter. A liquid crystalline PA (LCPA) is expected to exhibit a high PC because of the high charge mobility in its orderly packed mesogenic phase. The interfaces between the amorphous and mesogenic domains also favor photoconduction, as excitons dissociate efficiently at, and carriers move rapidly along, the interfaces. Indeed, LCPA **231** shows higher PC than PPA (**2**), a well-

known non-LC photoconductor. LCPA **234** shows even higher PC, because of its better-ordered LC aggregates formed in the photoreceptor fabrication process (Figure 16).<sup>421</sup>

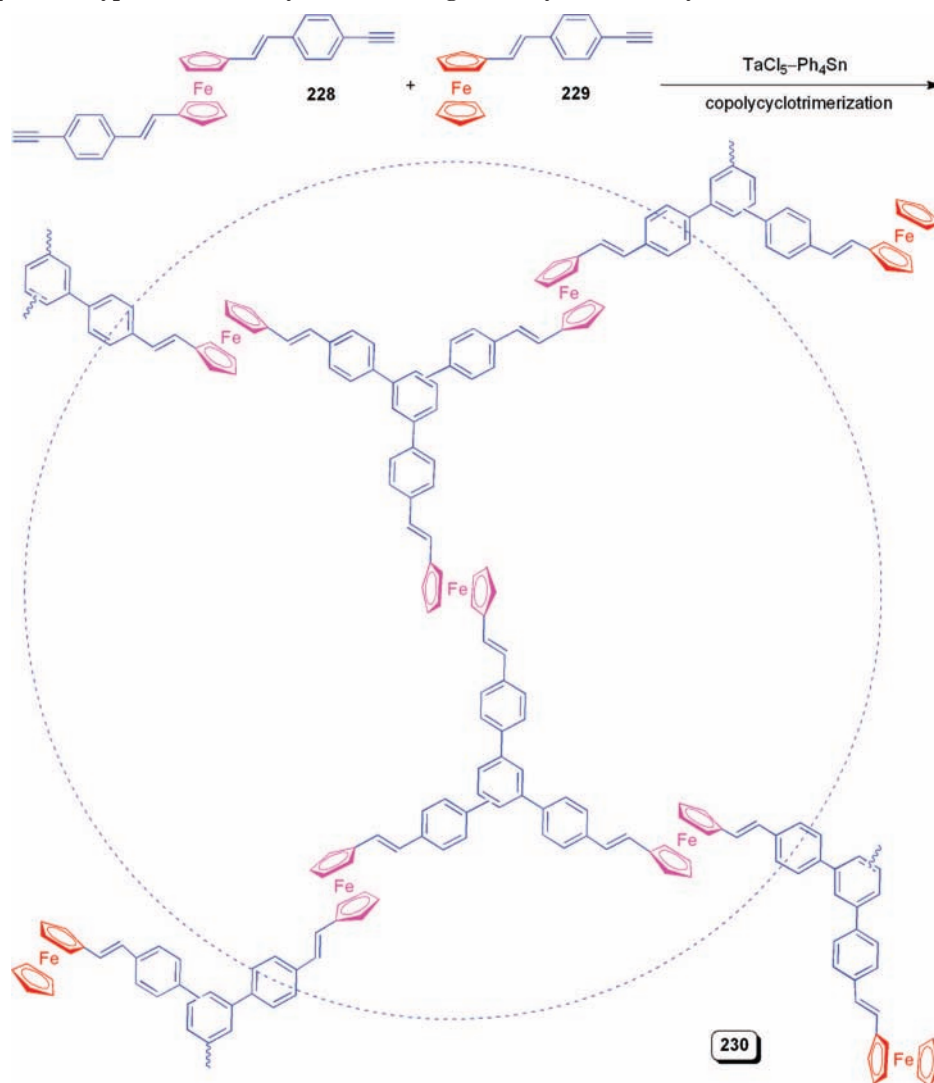
Triphenylamine (TPA) is a typical electron donor and a famous building block for constructing hole-transporting materials. With an anticipation of obtaining PAs with good photoconduction performances, Tang and co-workers incorporated TPA into PAs (Chart 7) and fabricated photoreceptor devices using the TPA-containing PAs as charge-generation materials (CGMs). The device performance investigations revealed that the half-discharge time ( $T_{1/2}$ ) of **235** was as short as 0.09 s and its photosensitivity ( $S$ ) was as high as  $1010.1 \text{ mm}^2/(\text{mW s})$ .<sup>428</sup> The photoreceptor device using **236** as CGM gave a lower  $S$  value than the device based on **235**. This is easy to understand because the formyl group attached to the TPA moiety in **236** is an electron-acceptor, which decreases the hole-transport efficiency. The photoreceptor with **237** as CGM displayed the lowest  $S$  value among the three TPA-containing PAs. This result can be explained in terms of charge-generation efficiency. This polymer exhibited the highest fluorescence quantum efficiency among the three polymers, indicating that the photogenerated geminate pairs in **237** have a high probability to recombine. Consequently, the number of the photogenerated free charges in the photoreceptor based on **237** becomes smaller, hence its observed low PC value.<sup>428</sup>

Like other conjugated polymers, substituted PAs can be regarded as  $p$ -type semiconductors. It is thus envisioned that their hybridizations with  $n$ -type carbon nanotubes (CNTs) and inorganic semiconductors may generate nanohybrid materials with enhanced PC performances due to the ease in heterojunction formation.<sup>428</sup> Tang and co-workers found that the substituted PAs carrying aromatic pendants could efficiently wrap around CNTs, which dramatically enhance the solubility and, hence, the processability of the nanotubes.<sup>161,166,167,428–432</sup> The solubilization mechanism of CNTs is summarized as sketched in Figure 17.<sup>428</sup> The polymer chains attach onto and/or wrap around the CNT shells due to strong  $\pi$ – $\pi$  stacking and D–A interactions of their aromatic pendants and conjugated backbones with the CNT wall surfaces. The polymer coating is thickened by the deposition of polymer chains through the pendant–pendant electronic interactions and the physical chain entanglements. The high affinity of the polymer chains with the molecules of solvent brings the polymer-coated or -wrapped CNTs into the solvent media, leading to the dissolution of the CNTs.

Employing the  $p$ – $n$  junction strategy and the CNT-solubilization method discussed above, Tang and co-workers fabricated photoreceptor devices using the PA/CNT nanohybrids as CGMs.<sup>346</sup> As expected, the photoreceptor devices displayed improved PCs, in comparison to those of the devices based on the parent polymers. Amazingly, the **236**/multiwalled CNT (MWNT)-based device shows a  $T_{1/2}$  value as low as 0.01 s. Its corresponding  $S$  value is as high as  $\sim 9091 \text{ mm}^2/(\text{mW s})$ , about 40 times that of the device based on the pure **236**. This dramatically enhanced PC is due to the MWNT component in the device. As discussed above, the MWNTs behave as an electron acceptor. The existence of the MWNTs in the charge-generation layer improves charge-generation efficiency via a mechanism of photoinduced charge transfer from **236** to MWNTs (Figure 17). Meanwhile, the MWNTs work as one-dimensional electron-transport channels. Their conductive networks quickly



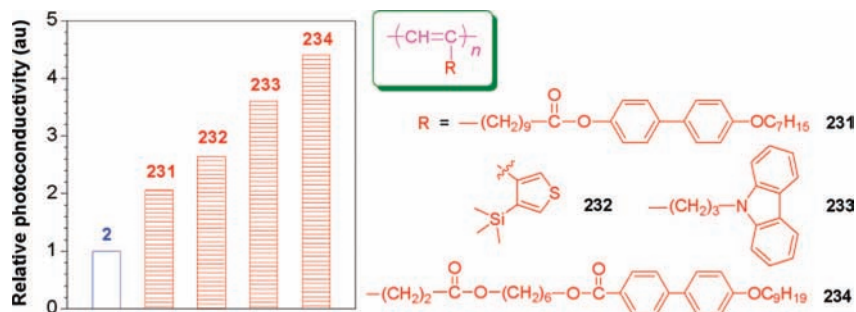
## Scheme 48. Example of a Hyperbranched Polymer with a High Density of Ferrocenyl Units in Its Core and Periphery



transport the photogenerated electrons to the surface of the photoreceptor to neutralize the surface charge, thus resulting in steeply decreased surface potential and transiently short  $T_{1/2}$  value.<sup>346</sup>

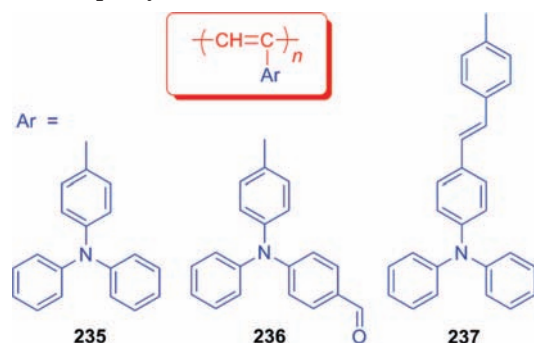
Nanohybridization of inorganic semiconductors with organic conjugated PAs offers the possibility to create new hybrids with combined advantages of the two components, that is, the high charge mobility of the inorganics and the ready processability of the organics, which may serve as active materials in the fabrication of photoreceptors. Tang's group developed a facile strategy for the nanohybridization of CdS nanorods with PPA chains. Taking an approach of

“pre-assembly plus copolymerization”, CdS–PPA nanohybrid **240** was successfully prepared (Figure 18).<sup>170</sup> This nanohybrid was completely soluble in common organic solvents and could form homogeneous thin films when its solutions were cast on solid substrates. Taking advantage of its high solubility and excellent film-forming capability, a series of photoreceptors based on **240** was prepared by solution-casting technique and their PCs were evaluated. One of the devices showed a  $T_{1/2}$  value of 2.63 s and an  $S$  value of 34.3 mm<sup>2</sup>/(mW s), which were better than those for all the devices using its parent forms of PPA ( $T_{1/2}$  = 3.67 s and  $S$  = 24.5 mm<sup>2</sup>/(mW s)) and CdS ( $T_{1/2}$  = 4.74 s and  $S$  =



**Figure 16.** Comparison of photoconductivities of substituted PAs. Reproduced with permission from ref 421. Copyright 2000 American Chemical Society.

## Chart 7. Triphenylamine-Functionalized PAs

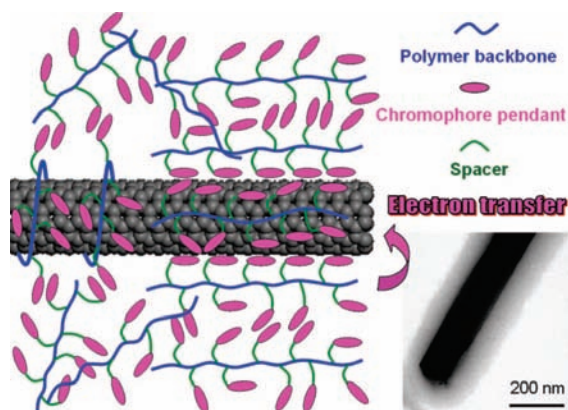


19.0 mm<sup>2</sup>/(mW s)) as well as their physical blend of PPA/CdS ( $T_{1/2} = 4.30$  s and  $S = 21.0$  mm<sup>2</sup>/(mW s)) as CGMs. The better performance of the nanohybrid was due to the intimate mixing of its two components and the ready formation of nanoscopic heterojunctions in the device.

Similarly, functional perovskite nanohybrid **241** generated from PA–ammonium **42** and PbBr<sub>2</sub> shows a higher PC than its parent polymer **42** (Scheme 49).<sup>169</sup> The PC performance of the photoreceptor of **42** is poor, as evidenced by its high  $T_{1/2}$  (10 s) and low  $S$  (9.1 mm<sup>2</sup>/(mW s)) values. In the solid film, the ammonium cations and the bromide anions of the polysalt form a network of randomly distributed electrostatic centers. The photogenerated charges are readily attracted to, and detained by, the network of the ions, which reduces their likelihoods of contributing to photoconduction. When **42** is hybridized with lead bromide, its once-free ammonium cations now become confined in an ordered fashion through their coordination with the sheets of the corner-sharing metal-halide octahedrons. The interactions between the fixed ions anchored to the inorganic frameworks and the mobile charges photogenerated on the conjugated PA backbones are weaker than those in the polysalt film. Some of the charges may find their pathways to the electrodes to discharge the surface potential. As a result, nanohybrid **241** displays an enhanced PC performance ( $T_{1/2} = 3.96$  s and  $S = 23.0$  mm<sup>2</sup>/(mW s)), in comparison to its polysalt precursor.<sup>169</sup>

## 4.2. Liquid Crystallinity

There are two major types of liquid crystals: thermotropic and lyotropic. LC polymers can be further divided into main- and side-chain categories. Liquid crystals and PAs are optically and electronically active, respectively. Melding of



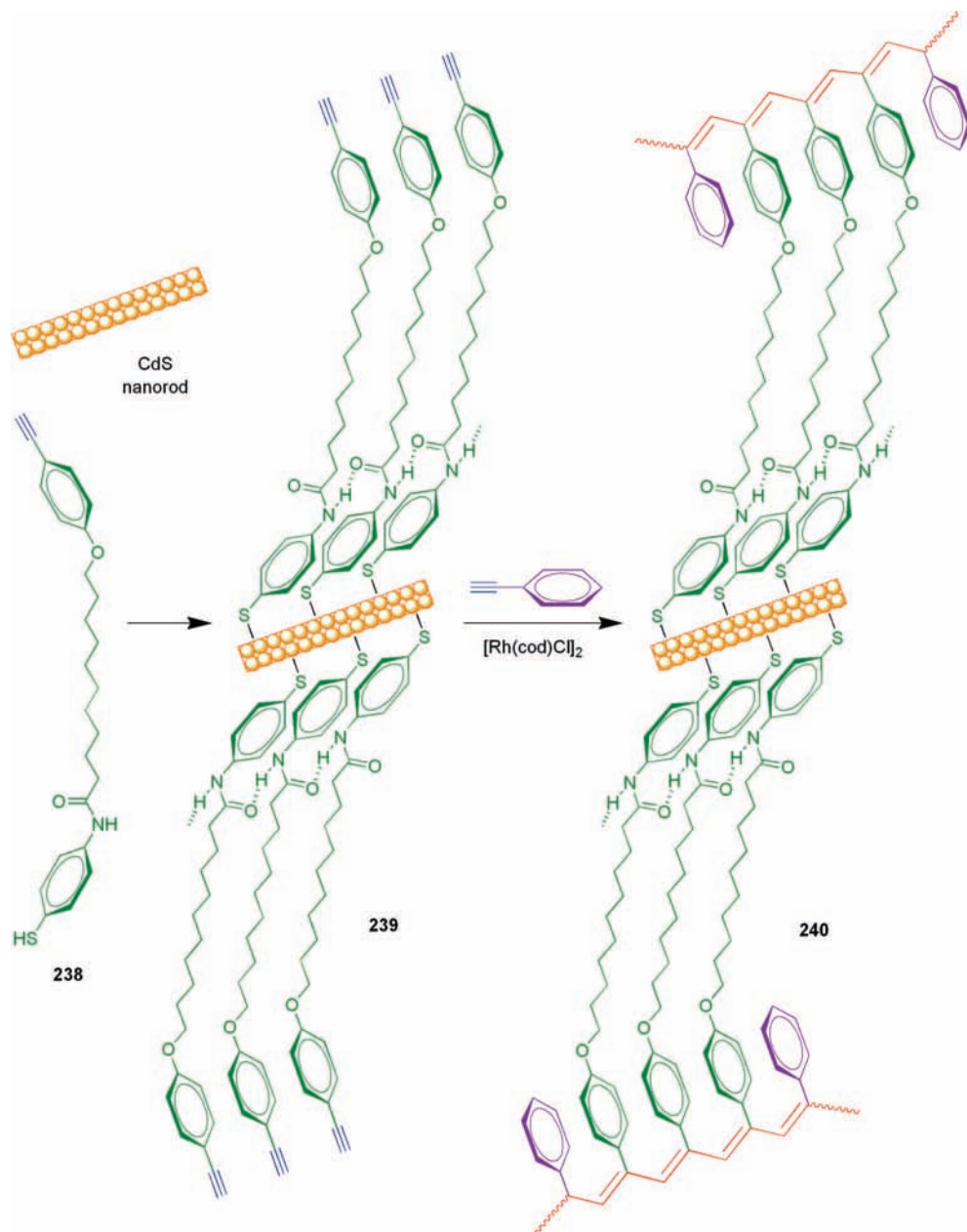
**Figure 17.** Schematic illustration of hybridization of CNT with PAs. Inset: TEM image of nanohybrid of **235** and MWNT. Reproduced with permission from ref 428. Copyright 2008 American Chemical Society.

the two at molecular level may generate LCPAs with both optical and electronic activities. The LCPAs may also be third- and second-order nonlinear optically susceptible, as conjugated polymer chains and polarized mesogenic groups can be  $\chi^{(3)}$ - and  $\chi^{(2)}$ -active, respectively. The common recipe for the structural design of side-chain LC polymers has been “mesogenic pendant + flexible backbone”. Rigid polymer backbones have generally been believed to be detrimental to the packing arrangements of the mesogens in the side chains. As a result of this common belief, LC polymers with rigid backbones have seldom been developed. The study of LCPAs with rigid polyene backbones is of interest, and successful development of such polymers may open a new avenue for the exploration of new types of LC polymers and help deepen our understanding on liquid crystals. Since stiff-chain polymers can be oriented by external forces, the LCPAs may show anisotropic mechanical properties, which may contribute to the search for high-performance engineering materials.

Inspired by these attractive prospects, many research groups have worked on the development of LCPAs.<sup>93,99,105,433–468</sup> Through careful design of flexible spacers, functional bridges, mesogenic cores, and functional tails, Tang’s group has synthesized a series of highly soluble and thermally stable mono- and disubstituted thermotropic LCPAs,<sup>64,99,105,165,451–466</sup> typical examples of which are shown in Chart 8. Tang and co-workers have systematically studied their LC behaviors, especially the structure–property relationships in the LCPA systems. The packing arrangements in the mesophases of the LCPAs and their mesomorphic transitions have been found to vary with the molecular structures of their mesogenic pendants.<sup>99</sup> Some examples of the structure–property relationships are given in Table 1.

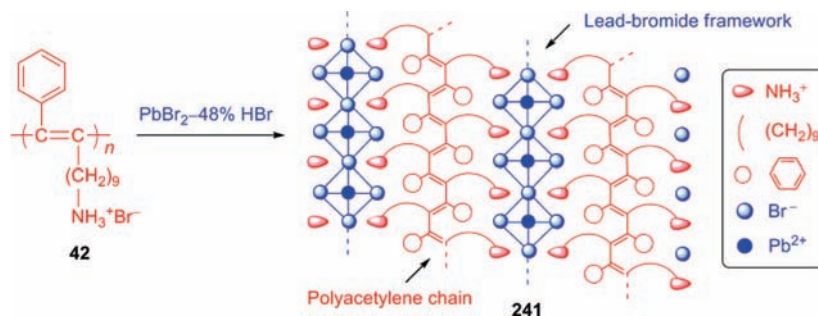
Polymer **247** is a poly(1-phenyl-1-alkyne) derivative containing a mesogenic pendant with a biphenyl core. It displays a smectic A ( $S_A$ ) mesophase in the temperature range of 172–158 °C when cooled from its isotropic melt (Table 1, no. 1). Its cousin with a phenylcyclohexyl core (**248**) exhibits a nematic (N) mesophase at much lower temperatures (108–90 °C), although it differs from **247** by only one ring in the mesogenic core (cyclohexyl in **248** versus phenyl in **247**). The molecular structures for polymers **243** and **244** are almost identical, except for that the former and latter have ester and ether bridges, respectively. This seemingly subtle structural difference greatly affects the arrangements of mesogenic packing, with the former ordered in a bilayer structure in an interdigitated fashion, namely, interdigitated smectic A phase ( $S_{Ad}$ ), while the latter packs in a monolayer structure ( $S_A$ ; cf., Table 1, nos. 3 and 4).

The elemental composition or molecular formula for **7** and **8** is exactly the same; the two polymers differ only in the orientation of their ester bridge (Chart 8). This small structural difference also causes a big change in the mesogenic packing: the mesostructure of **8** involves mixed monolayer and bilayer packing arrangements, while the mesophase of **7** is associated with a pure bilayer mesogenic alignment (Table, 1, nos. 5 and 6). An increase in the length of flexible spacer ( $m$ ) encourages better mesogenic order and induces a transition from nematicity to smecticity in the poly(1-alkyne) LC system **242**( $m$ ) (Table 1, nos. 7 and 8). The increase in the spacer length also widens the LC temperature range ( $\Delta T$ ): in the case of **242**( $m$ ),  $\Delta T$  for **242**(8) is approximately 3-fold wider than that for **242**(3). The polymer with polar cyano tails (**245**) undergoes an enantio-



**Figure 18.** Self-assembly of molecules of monomer **238** on the surface of CdS nanorod gives composite **239**, whose copolymerization with phenylacetylene (**1**) yields CdS-PPA nanohybrid **240**. Reproduced with permission from ref 170. Copyright 2007 The Royal Society of Chemistry.

#### Scheme 49. Preparation of PA-Perovskite Hybrid

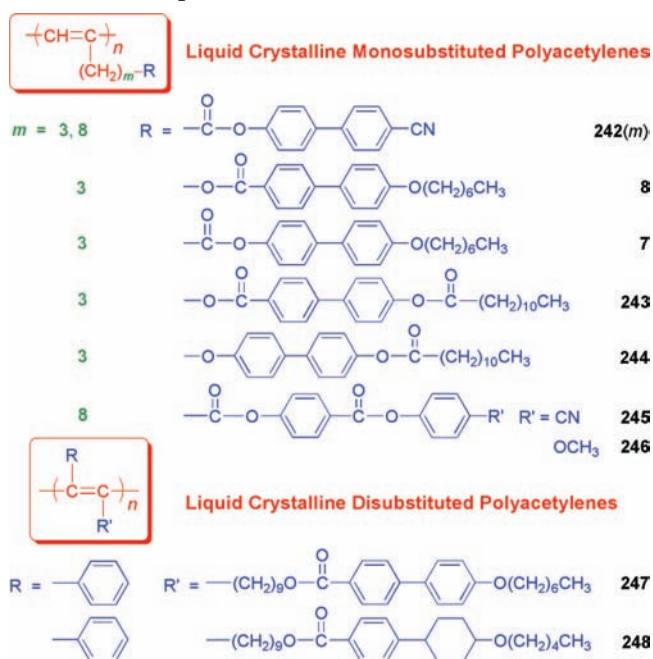


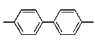
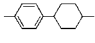
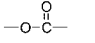
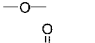
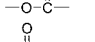
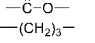
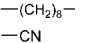
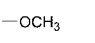


tropic  $S_A$  transition over a wide temperature range (115 °C), but its counterpart with less polar methoxy tails (**246**) goes through enantiotropic  $S_A$  and N transitions in a much narrower temperature range (Table 1, nos. 9 and 10).

The most distinct structural feature of the LCPAs is the rigidity of their double-bond backbones, in comparison to

the flexibility of the single-bond backbones of conventional nonconjugated polymers. As mentioned above, in the research community of LC polymers, a stiff backbone is normally regarded as a structural defect that distorts the packing arrangements of mesogens. This is why flexible backbones of polysiloxane, polyethylene, and polyacrylate

Chart 8. Examples of Mono- and Disubstituted LCPAs

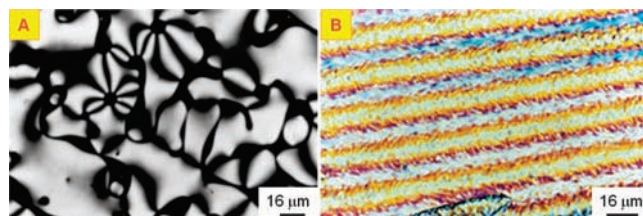
Table 1. Effects of Molecular Structures on the Mesogenic Properties of LCPAs<sup>a</sup>

no.	structural variation	mesophase	$T_c - T_m$ (°C)	$\Delta T$ (°C)	
1	mesogenic core	 <b>247</b>	$S_A$	172–158	14
2		 <b>248</b>	$N$	108–90	18
3	functional bridge	 <b>243</b>	$S_{Ad}$	199–162	37
4		 <b>244</b>	$S_A$	180–122	58
5	bridge orientation	 <b>8</b>	$S_A + S_{Ad}^b$	174–100	74
6		 <b>7</b>	$S_{Ad}$	206–127	79
7	flexible spacer <sup>c</sup>	 <b>242(3)</b>	$N$	189–152	37
8		 <b>242(8)</b>	$S_{Ad}$	190–81	109
9	functional tail	 <b>245</b>	$S_A$	195–80	115
10		 <b>246</b>	$S_A - N^d$	141–114–96	45

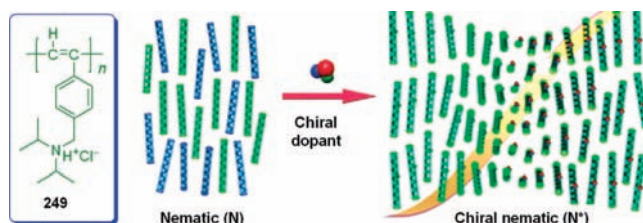
<sup>a</sup> Data taken from the DSC thermograms recorded under nitrogen in the first cooling scan. Abbreviations:  $S_A$  = Smectic A phase,  $N$  = nematic phase,  $S_{Ad}$  = interdigitated smectic A phase,  $T_c$  = clearing point,  $T_m$  = melting point, and  $\Delta T = T_c - T_m$  (temperature range of the LC phase). Data reproduced with permission from ref 99. Copyright 2003 Wiley-VCH. <sup>b</sup> Coexistent mono- ( $S_A$ ) and bilayer ( $S_{Ad}$ ) mesophases. <sup>c</sup> For mesogenic poly(1-alkyne)s. <sup>d</sup> Consecutive  $S_A$  and  $N$  mesophase transitions.

have often been used in the development of traditional LC polymers. Is a rigid backbone only destructive or can it play a constructive role? Tang and co-workers envisioned that an oriented rigid main chain might induce unique alignments of its mesogenic side chains. The stiff polyene backbone of an LCPA has a long relaxation time,<sup>469,470</sup> and a mechanically oriented LCPA system might not quickly return to the preperturbed state, thus offering the opportunity to generate macroscopic anisotropy by the application of a mechanical force.

To examine its response to mechanical perturbation, Tang and co-workers applied a rotational force to **246** when it was cooled from the isotropic state to the  $N$  phase. As shown in Figure 19A, unusual high-strength disclinations of 3/2 and 2 are observed in the LC texture of the polymer.<sup>451</sup> Such high-strength disclinations have been observed in a few systems of main-chain LC polymers with rigid backbones



**Figure 19.** (A) Schlieren textures with disclination strengths of 3/2 and 2 observed after a rotationally agitated **246** has been annealed at 136 °C for 5 min. (B) Induced alignments of **246** by mechanical shearing. Reproduced with permission from ref 451. Copyright 1998 American Chemical Society.

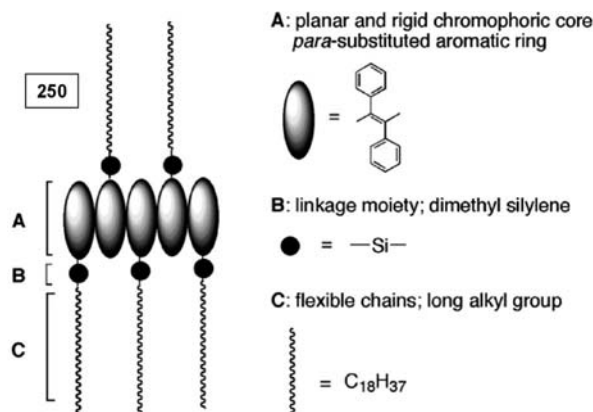


**Figure 20.** Proposed mechanism of formation of lyotropic  $N^*$  mesophase of **249** mediated by a chiral dopant in a concentrated water solution. Reproduced with permission from ref 467. Copyright 2006 American Chemical Society.

but never in any systems of side-chain LC polymers with flexible backbones. The high disclination values are demonstrative of the backbone rigidity of the LCPA because only a stiff backbone can survive the severe director field distortions involved in the formation of the high-strength disclinations. When a shear force is applied to the  $N$  phase of **246** at  $\sim 140$  °C, inversion walls are generated. Natural cooling of the system to room temperature results in the formation of well-ordered parallel microbands (Figure 19B).<sup>451</sup> Generally, a main-chain LC polymer with a rigid backbone can be easily aligned by a shear force, while a side-chain LC polymer with a flexible backbone can be readily processed by solution processes. Evidently, **246** possesses the combined advantages of main- and side-chain LC polymers: it can be readily aligned by a shear force and can meanwhile be easily processed because of its excellent solubility in common organic solvents.

In addition to the aforementioned thermotropic LCPAs, lyotropic LCPAs have also been reported. Yashima and co-workers found that polysalt **249** formed  $N$  mesophase at a high concentration in water, which was further converted into chiral nematic ( $N^*$ ) mesophase upon adding a small amount of chiral dopant.<sup>467</sup> The proposed mechanism of mesophase formation is shown in Figure 20. The theoretical calculation revealed that **249** possessed a long persistence length, indicative of its stiff backbone. In addition, **249** was a dynamic helical polymer with interconvertible right- and left-handed helical chain segments separated by rarely occurring helix reversals in the dilute aqueous solution. Thus, when the concentration of **249** was increased, an  $N$  phase was formed but it exhibited no optical activity. Upon complexation with a small amount of chiral acid, a great excess in one helical sense was induced in the polymer due to the “sergeant and soldier” rule coined by Green.<sup>471,472</sup> Accompanying the transcription of the chiral information to the polymer backbone, the  $N$  phase was converted to an  $N^*$  phase.<sup>467</sup>

Kwak and Fujiki found that poly(diphenylacetylene) derivative **250** with  $n$ -octadecylsilane moiety in the side chain exhibited smectic liquid crystallinity in highly concentrated



**Figure 21.** Schematic molecular structure of lyotropic LCPA **250**. Reproduced with permission from ref 468. Copyright 2007 American Chemical Society.

solutions in aromatic solvents such as toluene, despite its very high molecular weight of  $4.18 \times 10^6$  (Figure 21).<sup>468</sup> The formation of the lyotropic LC phase has been rationalized by Kwak and Fujiki as follows: the polymer backbone of **250** is sufficiently stiff to serve as a mesogenic unit, as expected from its high viscosity index of  $\alpha \approx 1.03$ , and a high degree of intermolecular packing of the long *n*-octadecyl chains through hydrophobic interactions has hampered the  $\pi-\pi^*$  stacking of the main chains. Polymer **250** showed highly polarized absorption and fluorescence bands in its sheared film, because the axes of the polyene main-chain of **250** and its stilbene-like side-chain were aligned parallel and perpendicular to the shearing direction, respectively.

### 4.3. Light Emission

The study of luminescence properties of  $\pi$ -conjugated polymers is a hot topic of great current interest. Whereas PA is an archetypal  $\pi$ -conjugated polymer, little work had been done on the development of light-emitting PAs (LEPAs) in the early days, because PA itself is a very poor lumino-phore. Following their successful work on the development of novel LCPAs, Tang and co-workers extended their efforts to explore the possibility of developing efficient LEPA systems.<sup>64,99,105,165,457,461,473–489</sup> Modifications of molecular structure of PA, such as attachments of the pendant groups with different electronic and steric effects, have been used to tune the conjugation length along the polyene backbone and the electronic interaction between the polymer chains. These approaches have worked well and led to the generation of a large variety of LEPAs with high photoluminescence (PL) yields and good electroluminescence (EL) efficiencies. In the LEPAs, the emitting center can be pendant or backbone, the energy transfer can be from pendant to backbone or from backbone to pendant, and the emission color can be violet, blue, green, or red—all tunable by changing the backbone and pendant structures.<sup>111,473–491</sup>

The PL properties of the LEPAs bearing biphenyl (BP) pendants are shown in Table 2 as an example to demonstrate how the light emissions of LCPAs are tuned by changing their molecular structures.<sup>99</sup> The data for their parent form of (unsubstituted) PA is also given in the table for the purpose of comparison, which emits very weakly in the infrared spectral region due to the existence of exciton traps in the polyene chain. Similarly, PPA itself is a poor light emitter owing to the photogenerated radical defects in the conjugated skeleton. The PPA derivatives with BP pendant emit UV

**Table 2. Photoluminescence of the LEPAs Bearing Biphenyl (BP) Pendants<sup>a</sup>**

no.	polymer	skeleton <sup>b</sup>	emitting center	emission color	quantum yield
(1)	PA	$-(\text{CH}=\text{CH})_n-$	backbone	IR	low <sup>c</sup>
2	PPAs	$-(\text{HC}=\text{C})_n-$ 	pendant	UV	low
3	poly(1-alkyne)s	$-(\text{HC}=\text{C})_n-$ 	pendant	UV	medium
4	poly(propiolate)s	$-(\text{C}=\text{C})_n-$ 	pendant	UV	high
5	poly(1-phenyl-1-alkyne)s	$-(\text{C}=\text{C})_n-$ 	skeleton	blue	high
6	poly(diphenylacetylene)s	$-(\text{C}=\text{C})_n-$ 	skeleton	green	high

<sup>a</sup> Data reproduced with permission from ref 99. Copyright 2003 Wiley-VCH. <sup>b</sup> The wavy line ( $\sim\sim\sim$ ) in the structure denotes a linkage unit, which is normally an alkyl or alkoxy group (cf., Chart 8). <sup>c</sup> Data for pure PA is shown for comparison.

light in low efficiency because the light emitted from the BP pendant is partially quenched by the defects in the PPA skeleton (Table 2, no. 2). BP-containing poly(1-alkyne) derivatives display higher  $\Phi_F$  values due to the alleviated quenching by the poly(1-alkyne) skeleton. Disubstituted poly(propiolate)s emit efficiently (Table 2, no. 4), thanks to their photochemically stable, defect-free skeleton structure.

From the result of disubstituted poly(propiolate)s, it is envisioned that, if the hydrogen atom in the repeat unit of a poly(1-alkyne) is replaced by a bulky aromatic substituent, the backbone would become twisted and more stable. The involved steric effect would shorten the effective conjugation length of the resultant disubstituted PA, hence widening its band gap and shifting its skeleton emission from IR to visible. Indeed, poly(1-phenyl-1-alkyne)s emit strongly in the blue region (Table 2, no. 5). Meanwhile, the polymer skeleton absorbs the UV light emitted from the BP pendant, which helps enhance the light emission efficiency. Following this strategy, BP-containing poly(diphenylacetylene) derivatives have been synthesized whose luminescence efficiencies are comparably high but their emission colors are red-shifted from blue to green.

The molecular engineering endeavors change not only the location of emitting center, as discussed above (Table 2), but also the direction of energy transfer, as exemplified in Chart 9.<sup>99</sup> In polymer **251**, an efficient fluorescence resonance energy transfer (FRET) process occurs from the green light-emitting silole pendant to the red light-emitting polyene backbone, due to the direct electronic communication between the pendant and the backbone. The PA backbone of **251** emits faintly in the long-wavelength region, in agreement with the early observation that pure PA is a weak IR emitter. In polymer **252**, however, the FRET is from the poly(1-phenyl-1-alkyne) skeleton to the silole pendant. The blue light emitted from the skeleton excites the pendant, resulting in a green light emission. Polymer **253** emits a green

## Chart 9. Energy Transfers in LEPAs



light efficiently, because the excited states of the silole pendant and the poly(diphenylacetylene) skeleton both undergo radiative transitions in the similar spectral region.

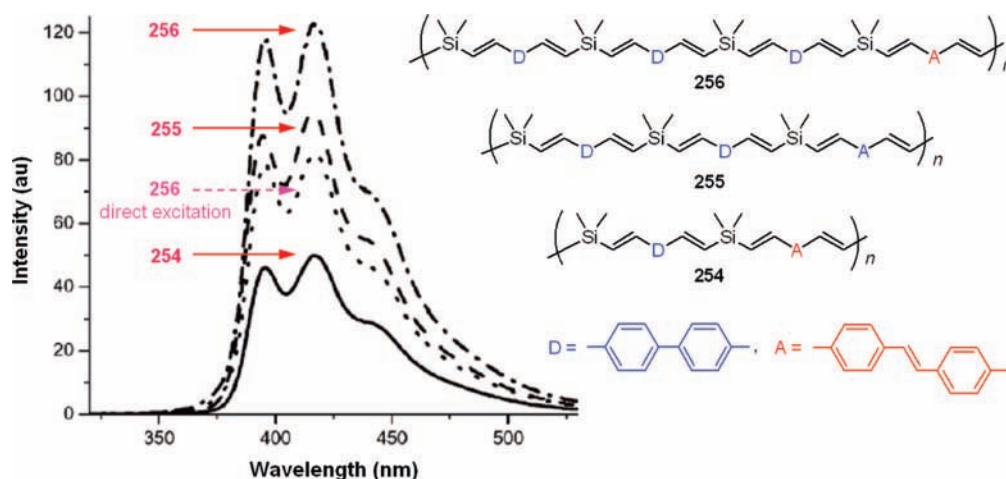
Interesting FRET processes were observed by Luh's group in the poly(silylenevinylene)s prepared by alkyne hydrosilylation polymerization.<sup>492</sup> The D and A chromophores shown in Figure 22 are paired on the basis of their absorption and emission spectral profiles. Polymers **256**, **255**, and **254** possess the same A chromophore but emit in a descending order when their D chromophores are excited at 300 nm, although the density of their A chromophores is increased in the same order. This is a reflection of the difference in the light-harvesting capability of the polymers. In other words, the data indicate that the more D units in the polymer, the higher is its light-harvesting ability. For comparison, the A chromophore in **256** was directly excited at 360 nm. The intensity of the emission generated by this direct excitation is much lower than that generated by the indirect excitation at 300 nm or via the D-to-A energy transfer. Evidently, the FRET process induces more efficient light emission.

Aggregation of conjugated polymer chains in the solid state often results in the formation of less-emissive or nonemissive species such as excimers and exciplexes, which partially or completely quench the luminescence of the polymers. This aggregation-caused quenching effect has been a thorny problem in the development of efficient polymer light-emitting diodes (PLEDs) because the conjugated polymers are commonly used as thin solid films in the EL devices. During their search for efficient light-emitting materials, Tang

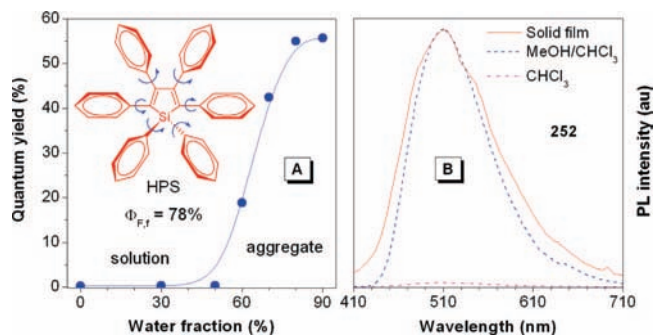
and co-workers found a group of highly luminescent molecules called siloles in the solid state.<sup>493,494</sup> The silole molecules exhibit an invaluable effect of aggregation-induced emission (AIE): they are virtually nonluminescent when molecularly dissolved in good solvents but become strongly emissive when aggregated in poor solvents or fabricated into solid films.

1,1,2,3,4,5-Hexaphenylsilole (HPS) is a typical paradigm of AIE luminogen (Figure 23A). Its  $\Phi_F$  value in pure acetonitrile is as low as 0.2%. The  $\Phi_F$  value keeps almost unchanged when up to ~50 vol % of water is added into its acetonitrile solution but starts to swiftly increase afterward due to the formation of nanoaggregates in the aqueous mixtures with high water contents. When the water content in the acetonitrile/water mixture is 90 vol %, the  $\Phi_F$  value of HPS rises to ~56%, which is ~280 times higher than that in the acetonitrile solution. In the film state, the  $\Phi_F$  value is even higher and goes to ~78%.<sup>496</sup> Through experimental and theoretical investigations, the AIE mechanism is understood as follows.<sup>494–497</sup> In the dilute solution at room temperature, the active intramolecular rotations of the peripheral phenyl rings of HPS around the axes of the single bonds linked to the central silole core nonradiatively annihilate the excitons, thereby making the silole molecules practically nonluminescent. In the aggregates, the propeller shape of the silole molecules prevents them from forming excimeric species but the physical constraint in the solid state restricts their intramolecular rotations, which blocks the nonradiative relaxation channels and populates the radiative decay, thus making the silole molecules highly emissive.

Siloles are, therefore, a group of excellent molecules for OLED applications.<sup>498–501</sup> The low molecular weight compounds, however, have to be fabricated into thin solid films by such expensive techniques as vacuum vapor deposition, which are not well-suited to the manufacture of large area devices. One way to overcome this processing disadvantage is to prepare high molecular weight polymers, which can be readily processed from their solutions into thin solid films over large areas by a simple spin-coating technique. Motivated by these considerations, Tang and co-workers incorporated the silole moieties into the PA structure with the aim of generating AIE-active polymers.<sup>482</sup> HPS-containing poly(1-phenyl-1-alkyne) **252** is an example of such polymers (cf., Chart 9). The solution of **252** is nonemissive (Figure



**Figure 22.** Emission spectra of polymers **254** (solid line), **255** (dashed line), and **256** (dash-dotted line) measured at  $\lambda_{\text{ex}} = 300$  nm. Data for the emission from **256** with direct excitation of its acceptor at 360 nm is given in dotted line for comparison. Reproduced with permission from ref 492. Copyright 2004 Wiley-VCH.



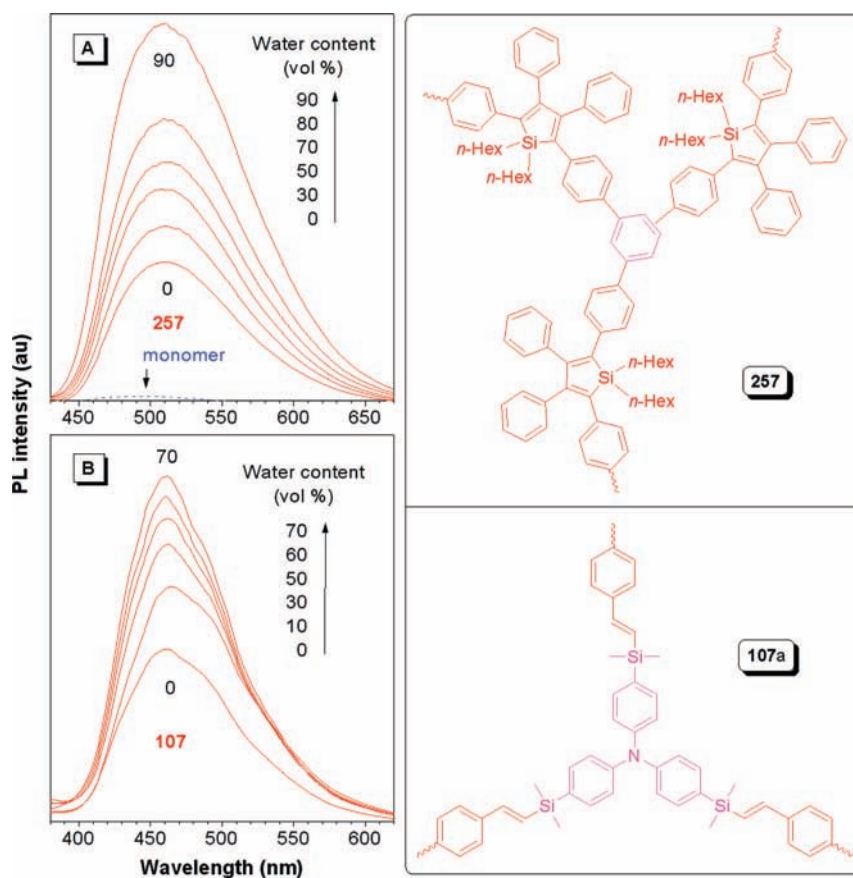
**Figure 23.** (A) Plot of fluorescence quantum yield of HPS vs solvent composition of acetonitrile/water mixture. The quantum yield of its film ( $\Phi_{F,f}$ ) is given for comparison. (B) Emission spectra of polymer **252** in chloroform (molecularly dissolved solution), a 9:1 methanol/chloroform mixture (nanoaggregate suspension), and solid state (thin film). Panels A and B are reproduced with permission from refs 494 and 482. Copyrights 2003 American Chemical Society, respectively.

23B), because in the FRET process of this polymer, the PL from the emissive poly(1-phenyl-1-alkyne) skeleton is quenched by the nonemissive HPS pendant. Thanks to its AIE attribute, the  $\Phi_F$  value of its nanoaggregates in the methanol/chloroform mixture with 90% methanol is  $\sim$ 46-fold higher than that in the chloroform solution. Recently, Chujo and co-workers have observed the similar AIE effect in the polymers with *p*-phenyleneethynylene and *o*-carborane sequences.<sup>83</sup>

Tang and co-workers have further observed an aggregation-induced emission enhancement (AIEE) phenomenon in the hyperbranched poly(2,5-silole)s prepared from the poly-

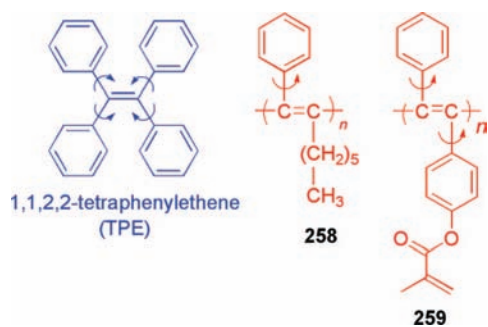
cyclotrimerization of HPS-based diyne monomers.<sup>113</sup> Whereas the diyne monomers are nonemissive in the solution state, their polymers are somewhat luminescent even when they are molecularly dissolved in good solvents, as can be seen from the example shown in Figure 24A. The silole units in the hyperbranched polymer are knitted together by the rigid benzene rings and located within a stiffened polymer sphere, which restricts the intramolecular rotations of the peripheral benzene rings around the central silole core to some extent and thus makes the polymer somewhat luminescent in the solution state. Gradual addition of water into the THF solution of **257** causes progressive formation of polymer aggregates. In the aggregates, the intramolecular rotations are further restricted and the light emission of the polymer is thus enhanced. The AIEE system is thus operating in a mechanism similar to that in the AIE system discussed above. Similar AIEE is observed in the hyperbranched poly(arylenevinylsilane) system. As exemplified by the data shown in Figure 24B, the weak emission of **107a** in pure THF is enhanced by the aggregate formation of the polymer in the aqueous media.

Retrostructural analysis of another AIE-active luminogen 1,1,2-tetraphenylethene (TPE) discovered by Tang and co-workers<sup>502–505</sup> reveals that there is structural similarity between TPE and disubstituted PAs such as poly(1-phenyl-1-alkyne) **258** and poly(diphenylacetylene) **259**: one or more aromatic rings are connected to an olefinic core (Chart 10).<sup>487,489</sup> In a dilute solution of TPE, intramolecular rotations of the peripheral aromatic rings against the olefinic core effectively and nonradiatively deactivate the excited states, which makes TPE nonemissive (“off”). In the aggregates,



**Figure 24.** Emission spectra of (A) **257** and (B) **107a** in the THF/water mixtures with different water contents. Data for 1,1-dihexyl-2,5-bis(4-ethynylphenyl)-3,4-diphenylsilole (monomer of **257**) in THF is shown in panel A for comparison. Reproduced with permission from ref 113. Copyright 2007 Elsevier.

Chart 10. Intramolecular Rotations in TPE and LEPAs

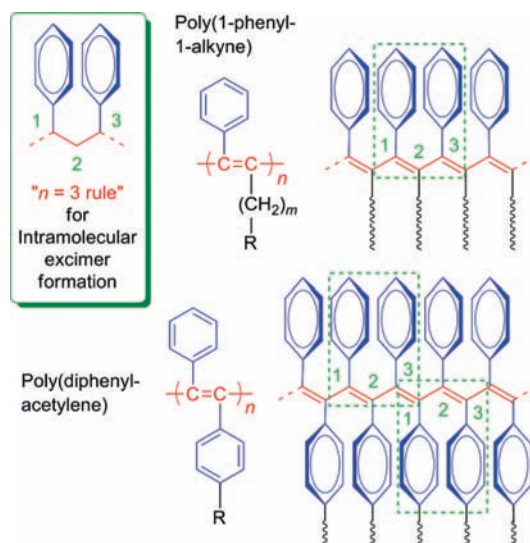


such rotations are restricted. The blockage of the nonradiative relaxation pathway turns the light emission of TPE “on”. Because of the structural similarity, it is expected that polymers **258** and **259** may be enhanced by aggregate formation or show AIEE effect, since the polymers themselves are already luminescent in the solution state (vide supra). As anticipated, **258**<sup>489</sup> and **259**<sup>487</sup> are AIEE-active, with their emission intensities progressively increased with increasing water fraction in the THF/water mixture (Figure 25). The spectral profile of **258** remains almost unchanged, while the emission spectrum of **259** is slightly red-shifted.

Further studies of the light-emitting behaviors of these disubstituted PAs reveal that their PL spectra are commonly very broad and lack fine structures, characteristic of excimer emissions. According to the “ $n = 3$  rule” shown in Chart 11, molecules with phenyl rings spatially separated by 3 carbon atoms (e.g., 1,3-diphenylpropane and PS) can form intramolecular excimers that emit in the redder spectral regions, in comparison to their “monomer” emissions. Both the poly(diphenylacetylene) and poly(1-phenyl-1-alkyne)s derivatives meet this “ $n = 3$  rule”.<sup>166,487</sup> While this rule has frequently been used to explain why light emissions of organic luminophores are quenched in the aggregate state, Tang’s group has found that the emissions from the poly(diphenylacetylene) and poly(1-phenyl-1-alkyne) derivatives are enhanced by aggregate formation or show the AIEE effect, as discussed above.

Through systematic investigations assisted by theoretical simulations, Tang’s group has gained some insights into the relationship between the AIEE effect and the intramolecular excimer formation.<sup>487,489</sup> In the poly(diphenylacetylene) and poly(1-phenyl-1-alkyne) skeletons, some “ $n = 3$ ” intramolecular or intrachain excimer pairs have already formed in

Chart 11. Formation of Intramolecular Excimers in Disubstituted LEPAs



the solution state, as indicated by the broad and structureless spectra of the polymer solutions, although due to the polyene backbone twisting, the phenyl ring pairing is disrupted from place to place, leaving some phenyl rings unpaired and stood alone as monomers. Upon aggregate formation, the volume shrinkage of the poly(diphenylacetylene) chains in the solvent mixture with poor solvating power draws the phenyl rings to closer vicinities. This enhances the  $\pi$ - $\pi$  stacking interactions of the phenyl rings and restricts their intramolecular rotations: the former effect populates the excimer species, hence red-shifting the emission spectrum, while the latter effect boosts its emission intensity, hence resulting in the observed AIEE phenomenon. In the poly(1-phenyl-1-alkyne) system, however, the population of the excimers does not change too much with aggregate formation; hence, there is no apparent red-shift in the PL spectrum. A unique feature to be noted in this system is that the twisted polyene backbone and long side chains weaken the interactions between the polymer strands, which helps prevent the light emission of polymer from being quenched by the formation of interchain excimers.<sup>487,489</sup>

The LEPAs have been found to enjoy excellent spectral stability: for example, **260** emits a blue light, whose PL profile does not change after the polymer has been heated

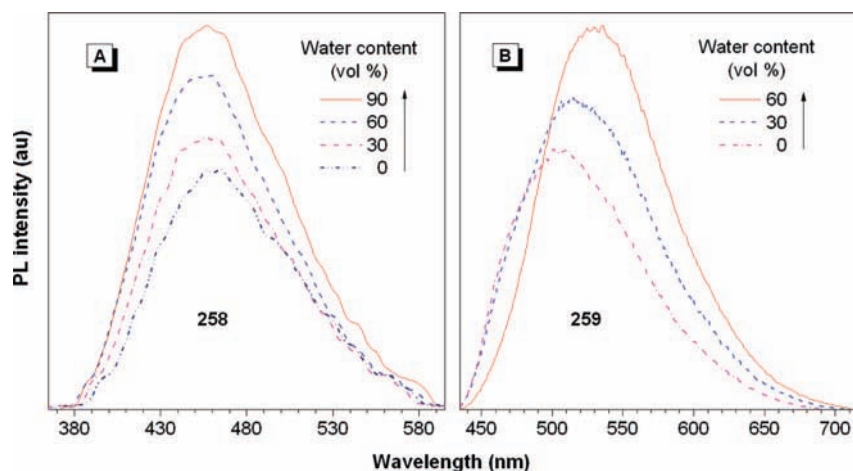
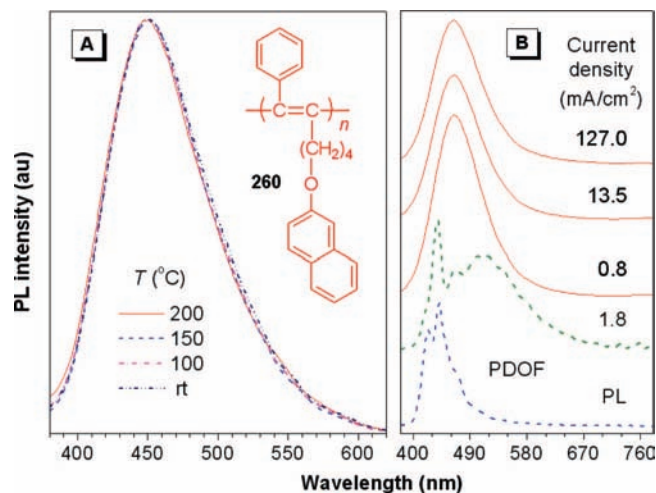


Figure 25. Emission spectra of (A) **258** and (B) **259** in THF/water mixtures with different contents of water. Data in panels A and B are reproduced with permission from refs 489 and 487. Copyright 2008 and 2007 American Chemical Society, respectively.

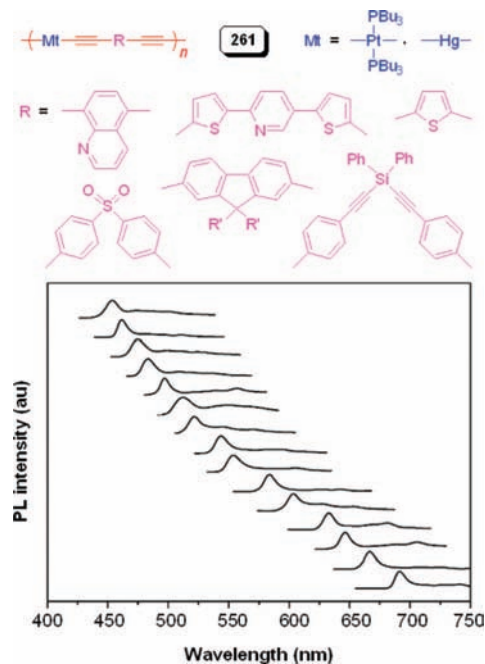




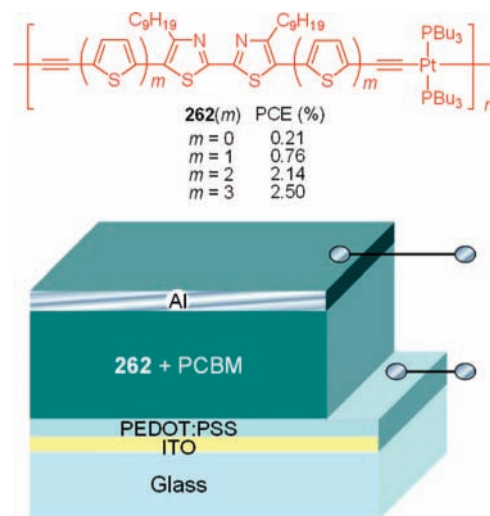
**Figure 26.** (A) PL spectral stability of **260** against thermolysis and (B) comparison of its EL spectral stability with that of poly(9,9-dioctylfluorene) (PDOF). Reproduced with permission from ref 488. Copyright 2008 American Chemical Society.

to 200 °C in air or exposed to UV irradiation in nitrogen or under vacuum (Figure 26A).<sup>488</sup> The efficient PL has encouraged researchers in the area to examine the EL performances of the LEPAs. The research groups of Tang, Masuda, Hsu, Kobayashi, and Yoshino<sup>80,506,507</sup> have contributed to this area of research. The PLED of **260** fabricated by Tang and co-workers, for example, emits a blue light of 460 nm, whose EL peak is symmetrically shaped with no sidebands (Figure 26B). Its external quantum efficiency ( $\eta_{\text{EL}}$ ) reaches 0.85%, which is comparable to those of some of the best blue light-emitting polymers.<sup>122</sup> Although the device configurations of the PLEDs based on the functionalized LEPAs developed by Tang's group have not been optimized, many of them already display  $\eta_{\text{EL}}$  of 0.5–0.86%, much higher than that (0.01%) based on nonfunctionalized poly(1-phenyl-1-octyne). The chromophoric pendants attached to the polyene skeleton may have helped boost the EL performance of the LEPAs. Recently, Hsu's group reported that a disubstituted PA copolymer-based PLED showed impressive device performances, with a maximum luminescence of 4230 cd/m<sup>2</sup> at 14 V and a maximum current efficiency of 3.37 cd/A at 7 V.<sup>80</sup> Polyfluorenes are the best-known blue light-emitting polymers, but their spectral stabilities are low. For example, a broad peak centered at ~520 nm appears when a current density as low as 1.8 mA/cm<sup>2</sup> passes through the PLED based on poly(9,9-dioctylfluorene) (Figure 26B). The EL spectrum of **260** does not change when a current density as high as 127 mA/cm<sup>2</sup> is applied to its device, indicative of the very high spectral stability of the disubstituted PA-based PLED.<sup>99</sup>

In addition to the studies on the fluorescence of the acetylenic polymers, their phosphorescence has also been investigated. Through molecular structure design, Wong and co-workers have developed a series of metallopolynes **261**, e.g., poly(platinayne)s, with phosphorescence emission covering the full visible spectral region from 462 to 832 nm (Figure 27).<sup>239</sup> Systematic studies show that the molecular orbitals and energy gaps of the metallopolynes can be easily tuned by using various central aryl cores that include carbocyclic, heterocyclic, and inorganic main-group elements with various extents of electronic conjugations. The triplet emission wavelengths of the polymers can be modulated from blue to red by changing the structures of the spacers, although the light emissions are only observable at low temperatures in most cases.

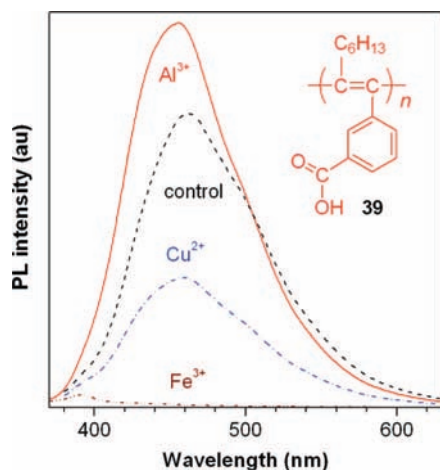


**Figure 27.** Phosphorescence of poly(platinayne)s **261** covering the full visible spectral region. Data reproduced with permission from ref 239. Copyright 2007 The Royal Society of Chemistry.



**Figure 28.** Power conversion efficiencies (PCEs) of poly(platinayne)-based heterojunction solar cells. Reproduced with permission from ref 509. Copyright 2007 American Chemical Society.

Apart from the applications as phosphorescence emitters, the metallopolynes have also been studied as potential PVC materials.<sup>508,509</sup> Wong's group developed a series of solution-processable polymers containing bithiazole–oligothiophene rings (**262**) with strong visible-light absorption (Figure 28). They fabricated the PVCs with a device configuration of Al/**262(m)**:PCBM/PEDOT:PSS/ITO, where PCBM = [6,6]-phenyl-C<sub>61</sub>-butyric acid methyl ester, PEDOT = poly(3,4-ethylenedioxythiophene), PSS = polystyrenesulfonate, and ITO = indium tin oxide.<sup>509</sup> The power conversion efficiency (PCE) as well as optical and charge-transport properties of the polymers have been found to be tunable by the number of thiophene rings (*m*) in **262**. PCE of the polymer is increased as its oligothiophene chain is lengthened. This work provides an attractive approach to the development of conjugated metallopolymers with broad solar absorption and



**Figure 29.** Fluorescence reponses of THF solutions of **39** to different metal ions. Reproduced with permission from ref 105. Copyright 2005 American Chemical Society.

tunable light-harvesting ability and demonstrates the potential of utilizing metalated conjugated polymers for efficient power generation.

#### 4.4. Fluorescence Sensing

Luminescent acetylenic polymers have been actively utilized for fluorescence-sensing applications by virtue of their rapid, specific, and sensitive PL responses to a variety of analytes.<sup>105,240,241</sup> The attractive attribute that has sparked great interest in the exploration of fluorescent polymers as potential sensors is their extraordinary signal amplification effect. For analyte-induced PL quenching, the large quenching constant in a polymer reflects the fact that the quencher can be bound to any of the repeating units, while in a small molecule there is only one individual chromophoric unit to bind. The luminescence of some LEPA has been found to show different responses to different metal ions. For example, Tang and co-workers have found that, when  $\text{Cu}^{2+}$  ion is added to a solution of **39**, the PL of the polymer drops to half of its original intensity (Figure 29).<sup>105,199</sup> The effect of  $\text{Fe}^{3+}$  is striking: it almost completely quenches the emission of **39**. In contrast, the PL of **39** becomes stronger in the presence of  $\text{Al}^{3+}$ . These distinct PL responses associated with specific polymer–metal interactions enable the LEPA to function as a selective chemosensor for ion discrimination.

Li, Tang, and co-workers have developed a sequential chemosensor based on imidazole-containing LEPA **263** (Scheme 50).<sup>205</sup> Among many different kinds of metal ions, only  $\text{Cu}^{2+}$  ion can completely and efficiently quench or turn

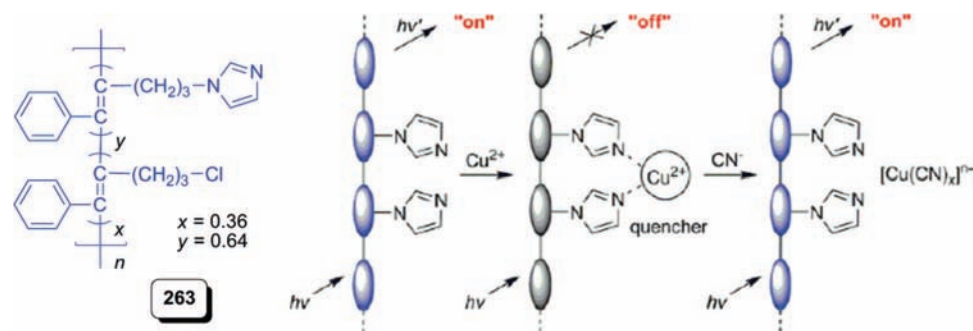
off the strong fluorescence of **263**, with a detection limit as low as 1.48 ppm. The associated Stern–Volmer quenching constant ( $K_{\text{SV}}$ ) is as high as  $3.7 \times 10^5 \text{ M}^{-1}$ , due to the high affinity of  $\text{Cu}^{2+}$  ion with the imidazole group, which enables the polymer to differentiate  $\text{Cu}^{2+}$  from other metal ions. The  $\text{Cu}^{2+}$ -quenched light emission of **263** can be turned on by the addition of  $\text{CN}^-$  ion, thus allowing the polymer to work as a unique dual-response sequential chemosensor for the detection of copper and cyanide ions.<sup>205</sup>

Bunz's group has synthesized a PAE with sugar moiety as pendant (**264**), which can be used to detect  $\text{Hg}^{2+}$  ion in a very high sensitivity.<sup>510</sup> When  $\text{Hg}^{2+}$  ion is added into **264** solution, the polymer emission is swiftly decreased. The  $K_{\text{SV}}$  value of **264** is >1000-fold higher than that of its small-molecule model compound with only one glucose unit. The enhanced emission quenching is due to not only molecular-wire amplifying but also cooperative binding. In the cooperative binding process (Scheme 51), two or more neighboring glucoses along the PAE backbone partake in the complexation with a single mercury ion to give a high  $K_{\text{SV}}$  value, which accounts for the much higher sensitivity of the polymer in detecting the  $\text{Hg}^{2+}$  ion, in comparison to its small-molecule counterpart.

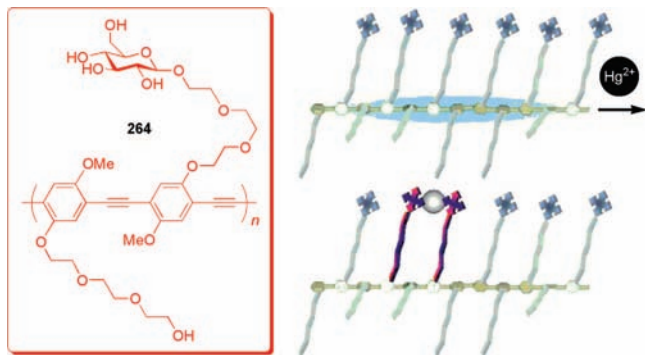
Many research groups have explored the potential of using acetylenic polymers as explosive sensors. Swager and co-workers have developed a variety of rigid, shape-persistent pentyptycene-derived PAEs with microporous structures, such as **265** (Scheme 52), into a platform for the sensitive detection of explosives. Swager's group has found that a series of strongly electron-accepting nitroaromatic analytes, including 2,4,6-trinitrotoluene (TNT) and 2,4-dinitrotoluene (DNT), dramatically quenches the fluorescence of **265** through an electron-transfer mechanism.<sup>233</sup> A thin solid film of **265** displays a sizable quenching within seconds of exposure to a trace amount (10 ppb) of TNT vapor, demonstrative of its extraordinary sensitivity to explosives.

Silole and silafluorene fluorophores have recently emerged as a new class of sensing materials for explosive detections.<sup>119,511,512</sup> Trogler and co-workers have employed alkyne hydrosilylation to prepare poly(silafluorene)s as potential fluorescence sensor materials.<sup>276</sup> Inclusion of the silole ring into the polymer structure offers a new method of analyte binding, while maintaining delocalization for an amplified sensor response. The light emissions of the polymers are extremely sensitive to explosives, with detection limit on the order of  $\text{pg}/\text{cm}^2$ . The fluorescence of the silolyl polymers responds to many different classes of warfare explosives. Polymer **266**, for example, can detect “common” explosives such as TNT and DNT as well as those less common explosives with low

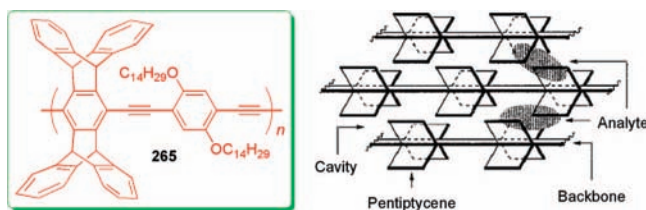
**Scheme 50.** Sequential Dual Chemosensor for  $\text{Cu}^{2+}$  and  $\text{CN}^-$  Ions Based on an Imidazole-Functionalized LEPA (**263**)<sup>a</sup>



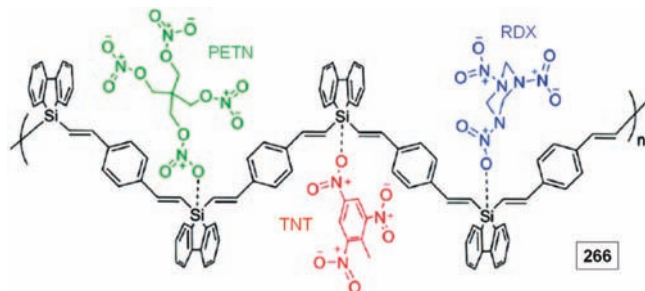
<sup>a</sup> Reproduced with permission from ref 205. Copyright 2008 The Royal Society of Chemistry

**Scheme 51. Detection of  $\text{Hg}^{2+}$  Ion by a Sugar-Functionalized PAE (**264**)<sup>a</sup>**

<sup>a</sup> Reproduced with permission from ref 510. Copyright 2004 Wiley-VCH.

**Scheme 52. Chemosensor Based on a Pentiptycene-Containing PAE<sup>a</sup>**

<sup>a</sup> Reproduced with permission from ref 233. Copyright 1998 American Chemical Society.

**Scheme 53. Poly(silafluorene)-Based Explosive Sensor<sup>a</sup>**

<sup>a</sup> Reproduced with permission from ref 276. Copyright 2008 American Chemical Society.

vapor pressures, such as cyclotetramethylene-tetranitramine and pentaerythritol tetranitrate (PETN), and with low reduction potentials, such as cyclotrimethylenetrinitramine (RDX) and trinitroglycerin (Scheme 53).

Whitten and co-workers have used fluorescent PAE polyelectrolytes as biosensors to assay kinase and phosphatase activity.<sup>246</sup> In their fluorescence bioassay systems, quaternary ammonium-functionalized latex microspheres are coated with anionic polymer **267** through electrostatic attraction (Scheme 54). The polymer-coated microspheres are then exposed to  $\text{GaCl}_3$ . The carboxylate groups in the polymer form chelate complexes with the  $\text{Ga}^{3+}$  ions, affording  $\text{Ga}^{3+}$ -functionalized microspheres that can bind with phosphorylated peptides. The assay process utilizes a peptide substrate labeled with a rhodamine dye at its *N*-terminus. In the absence of kinase, the dye-labeled peptide does not bind to the fluorescent microspheres. Upon kinase-mediated phosphorylation, the peptide binds to the  $\text{Ga}^{3+}$ -coated microspheres through  $\text{Ga}^{3+}$ -phosphate interaction, which quenches the fluorescence of the **267**-coated microsphere via a FRET process. The modulation of fluorescence signal is

proportional to the activity of kinase or phosphatase. This assay is homogeneous and simple and can be run either as an end-point measurement or in a kinetic mode.

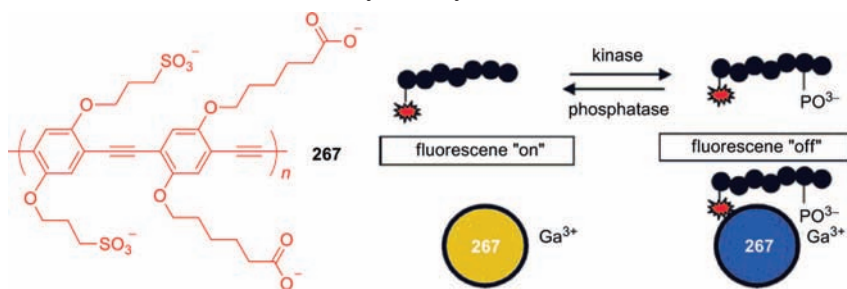
**4.5. Optical Nonlinearity**

Conjugated organic materials exhibiting strong NLO properties and fast response time have attracted considerable interest because of their potential high-tech applications in various optical and photonic devices.<sup>513–518</sup> Of particular interest is optical limiter, which is a novel optical material that transmits light of normal intensity but attenuates light of high power.<sup>519,520</sup> In other words, it allows mild light to pass through but prevents harsh light from being transmitted. The rapid advancements in the laser-based technologies and the growing enthusiasm in the space exploration have motivated intensive research efforts in the development of new optical power-limiting materials with novel structures and improved performances.

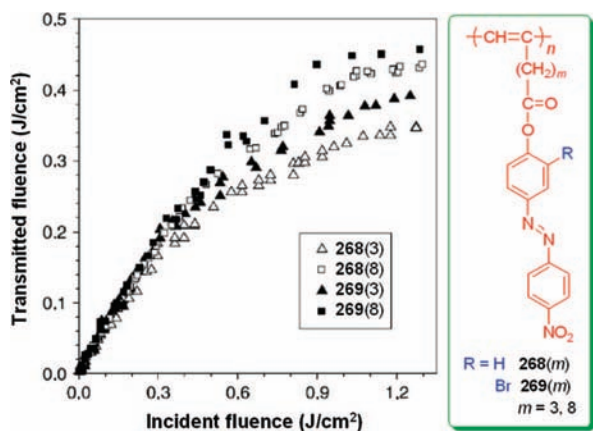
Many research groups have investigated the NLO properties, especially optical limiting performances, of substituted PAs containing various functional groups.<sup>172,521–527</sup> Azobenzene is a well-known, second-order NLO-active chromophore. Incorporation of such a chromophore into the PA structure is expected to endow the polymer with novel optical properties. Xu, Tang, and co-workers synthesized a series of PA derivatives with azobenzene as pendants (e.g., **268** and **269**) and studied their NLO properties.<sup>526</sup> Figure 30 shows the optical limiting properties of **268** and **269** at the same linear transmittance ( $T = 75\%$ ). All the polymers are good optical limiters, especially those with shorter spacer lengths. For example, the limiting threshold and saturation fluence of **268**(3) are 0.245 and 0.349  $\text{J}/\text{cm}^2$ , which are 1.3- and 1.2-times better than those of **268**(8), respectively. The optical limiting properties are also affected by the ring substituent: the polymer containing bromo substituent shows inferior performance, as can be understood from the comparison of the limiting threshold (0.295  $\text{J}/\text{cm}^2$ ) and saturation fluence (0.393  $\text{J}/\text{cm}^2$ ) of **269**(3) with those of **268**(3).

Fullerenes are known to limit intense optical pulses via a reverse saturable absorption mechanism.<sup>518</sup> The fullerene tips and the graphene sheets of the CNTs also undergo NLO absorption processes, while their cylindrical bodies, although with high aspect ratios, are light-scattering centers. Both the NLO absorption and the light scattering make the CNTs promising for optical limiting applications.  $\text{C}_{60}$  and CNTs, however, have notoriously poor solubility and processability. Hybridization of  $\text{C}_{60}$  and CNTs with processable  $\pi$ -conjugated polymers is a promising way to enhance the solubility of the carbon allotropes, with the possibility of generating new materials with novel properties. Tang and co-workers have done pioneer work in wrapping CNTs by  $\pi$ -conjugated polymers. In 1999, Tang's research group successfully prepared 2/CNT hybrid by the in situ polymerization of **1** in the presence of CNTs,<sup>429</sup> and thereafter they have established a platform for fabricating nanohybrids of PA/CNTs<sup>161,166,167,201,428–432</sup> and PA/ $\text{C}_{60}$ s<sup>528–531</sup> by physical and chemical methods, as exemplified in Scheme 55.

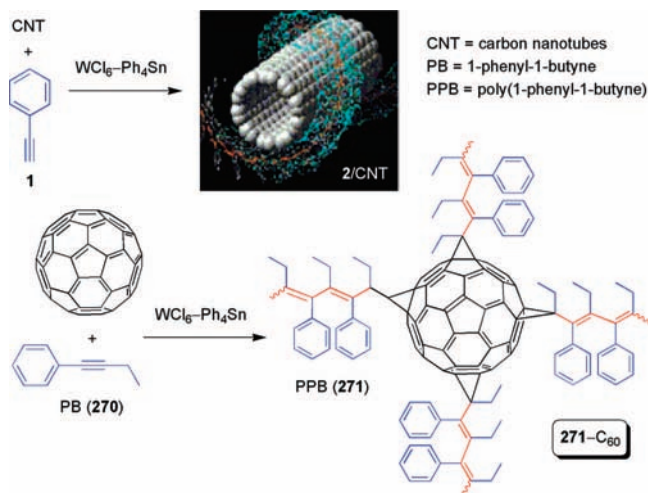
The optical limiting performances of 2/CNT<sup>429</sup> and **271**- $\text{C}_{60}$ <sup>529</sup> nanohybrids are shown in Figure 31. The data for the parent forms, i.e., **2** and  $\text{C}_{60}$ , are given in the same figure for comparison. When a THF solution of polymer **2** is shot by the 8 ns, 532 nm laser pulses, the transmitted fluence linearly increases in the region of low incident fluence (Figure 31A). The output starts and continues to deviate from

Scheme 54. Biosensor Based on a Water-Soluble PAE Polyelectrolyte<sup>a</sup>

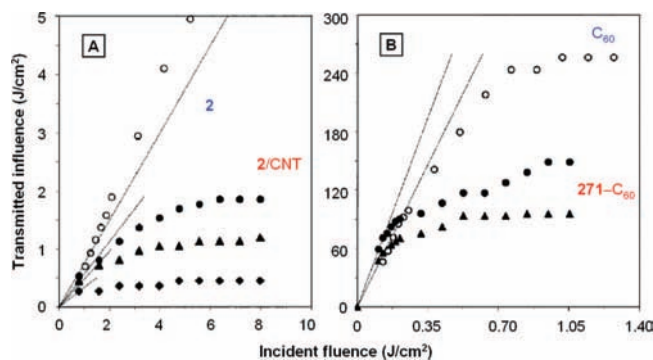
<sup>a</sup> Reproduced with permission from ref 246. Copyright 2004 National Academy of Sciences, U.S.A.



**Figure 30.** Optical power-limiting responses to 8 ns, 532 nm laser light, of THF solutions of **268**(*m*) and **269**(*m*) with a linear transmission of 75%. Reproduced with permission from ref 526. Copyright 2005 Elsevier.

Scheme 55. Functionalizations of CNT and  $\text{C}_{60}$  by Substituted PAs

the linear-transmission line from the input of about 1.7  $\text{J}/\text{cm}^2$ , suggesting that the intense illumination has gradually bleached polymer **2** to transparency, probably by the laser-induced photolysis of the polyene backbone. The solutions of the **2/CNT** hybrids, however, respond to the optical pulses in a strikingly different way. The linear transmittance of a dilute **2/CNT** solution (0.4 mg/mL) is only 57% (Figure 31A), although its concentration is only one-tenth of that of polymer **2** (4 mg/mL), due to the optical losses caused by the nanotube absorption and scattering. As the incident fluence is increased, the **2/CNT** solution becomes opaque, instead of transparent, with its transmitted fluence eventually leveling

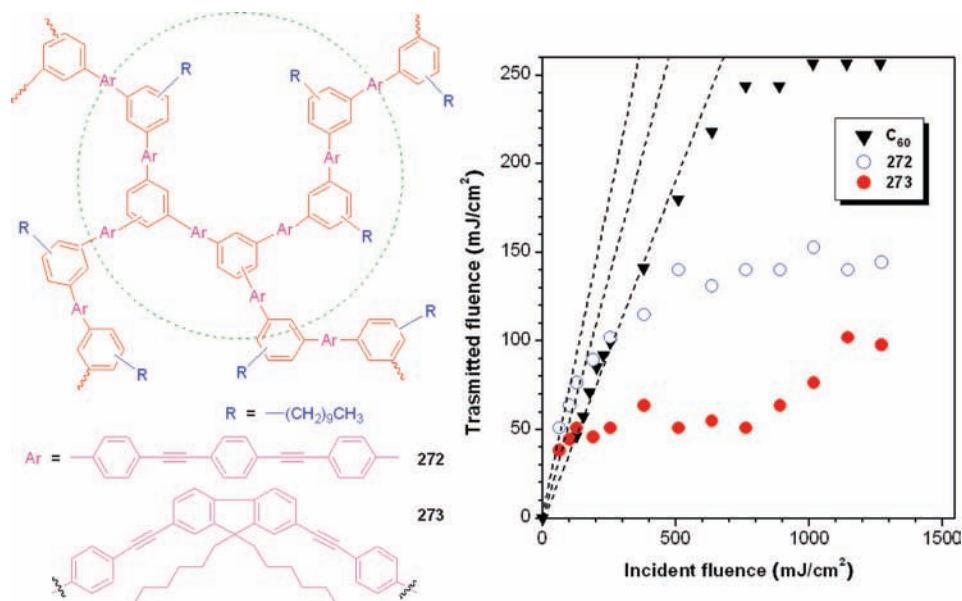


**Figure 31.** (A) Optical limiting responses to 8 ns, 532 nm laser light, of THF solutions of **2/CNT** hybrid. Concentration (*c*; mg/mL)/linear transmittance (*T*; %): 0.4/57 (●), 0.5/48 (▲), 0.6/34 (◆). A THF solution of **2** is shown for comparison [*c* (mg/mL)/*T* (%): 4.0/75 (○)]. (B) Optical limiting responses of a toluene solution of  $\text{C}_{60}$  (○) and THF solutions of **271-C<sub>60</sub>** (● and ▲); *c* (mg/mL)/*T* (%): 0.16/43 (○), 1.50/56 (●), 3.00/43 (▲). Data in panels A and B reproduced with permission from refs 429 and 529. Copyright 1999 and 2000 American Chemical Society, respectively.

off or saturating at 1.85  $\text{J}/\text{cm}^2$ . Clearly, the CNTs have endowed **2/CNT** with the optical limiting power.

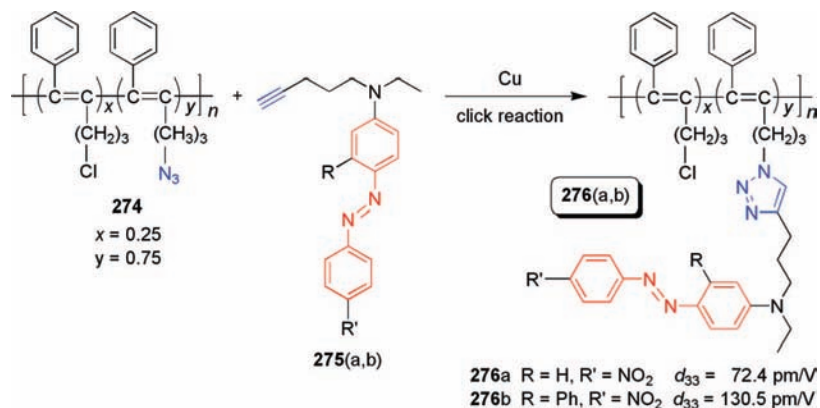
While polymer **2** is liable to photolysis, its nanohybrids with CNTs are stable at very high incident fluence.<sup>429</sup> The energy-sinking and radical-trapping functions of aromatic rings often protect polymers from photodegradation,<sup>532,533</sup> and the extensively conjugated graphitic aromatic system of the CNTs may have enhanced the resistance of the polyene backbone of **2** against the harsh laser irradiation. As the concentration of the **2/CNT** solution is increased, its saturation fluence is decreased. Increasing the concentration to 0.6 mg/mL readily decreases the saturation fluence to as low as 0.45  $\text{J}/\text{cm}^2$ . Similarly, the **271-C<sub>60</sub>** also effectively limits the strong laser pulses. Compared to the solution of the parent  $\text{C}_{60}$ , the **271-C<sub>60</sub>** solutions show higher or the same linear transmittance but much lower saturation fluence.<sup>529</sup>

Not only the linear acetylenic polymers and their nanohybrids but also the hyperbranched acetylenic polymers show excellent optical power-limiting performances. Tang's research group has found that hyperbranched poly(arylenephenylene)s are NLO-active and strongly attenuate the optical power of harsh laser pulses. As shown in Figure 32, in the low-energy region, the fluence transmitted from a solution of **272** is linearly increased with an increase in the incident fluence.<sup>534</sup> The transmitted fluence, however, begins to deviate from the linearity at an incident fluence of  $\sim 250$   $\text{mJ}/\text{cm}^2$  and reaches a saturation plateau of  $\sim 140$   $\text{mJ}/\text{cm}^2$ . The optical limiting performance of **272** is superior to that of  $\text{C}_{60}$ . Taking into account that  $\text{C}_{60}$  is a three-dimensionally  $\pi$ -conjugated buckyball, it may be concluded that the three-



**Figure 32.** Optical limiting responses to 8 ns, 532 nm optical pulses, of DCM solutions (0.86 mg/mL) of **272** and **273**. Data for a toluene solution of  $C_{60}$  (0.16 mg/mL) is shown for comparison. Reproduced with permission from ref 534. Copyright 2002 American Chemical Society.

#### Scheme 56. Preparation of NLO-Active PAs by Polymer Reaction



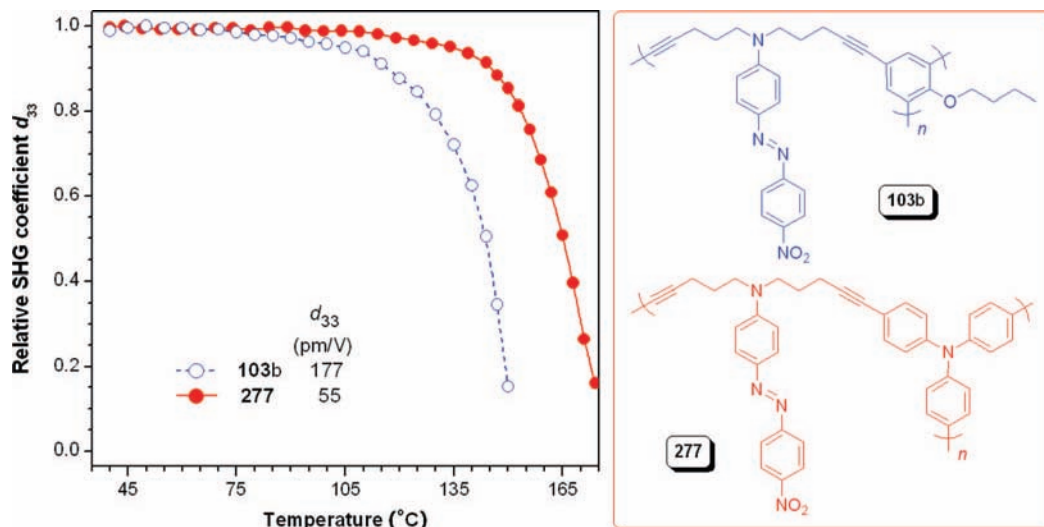
dimensionally  $\pi$ -conjugated electronic structure of the hyperbranched polymer is responsible for its optical limiting properties. Compared with **272**, **273** is a better optical limiter (with a saturation plateau as low as  $\sim 50$  mJ/cm<sup>2</sup>). Evidently, the optical limiting effect of the polymer is sensitive to a change in its molecular structure, which offers the opportunity to manipulate its performance through molecular engineering endeavors.

Much effort has been devoted to the development of second-order NLO materials, particularly to the efficient translation of large molecular first hyperpolarizability to high second harmonic generation (SHG) coefficient ( $d_{33}$ ). The greatest obstacle in the area has been the chromophoric aggregation in the solid films. The NLO chromophores are usually highly polarized by the D–A push–pull interactions. During the film formation, the chromophores with large dipole moments tend to compactly pack owing to the strong intermolecular electrostatic interactions, leading to the diminishment or cancellation of the NLO effects in the solid state. Researchers have been working on the development of effective means to overcome this thorny aggregation problem.

Attachment of azobenzene pendants to part of the chain segments of a disubstituted PA may help to alleviate the

problem because, in addition to the twisted polyene backbone, the chain segments without the azobenzene pendants may serve as isolation buffers to hamper the NLO chromophores from being aggregated. It is, however, difficult to synthesize disubstituted PAs with polar azobenzene pendants because of the lack of efficient catalyst systems. Li, Tang, et al. have taken a polymer-reaction approach to prepare the polymers inaccessible by the direct polymerizations of their corresponding monomers. For example, utilizing click reaction, they have successfully synthesized disubstituted PA derivatives with varying contents of functional azobenzene groups, examples of which are shown in Scheme 56.<sup>204</sup> As expected, the resultant PAs (**276**) exhibited high  $d_{33}$  values (up to  $\sim 131$  pm/V).

Structurally, hyperbranched macromolecules should be ideal matrix materials because they provide three-dimensional spatial separation of the NLO chromophores in the spherical architecture and their void-rich topological structure should help minimize optical losses in the NLO process. The *hb*-PAEs containing the NLO-active azobenzene chromophores are film-forming and morphologically stable ( $T_g > 180$  °C). Tang and co-workers examined their NLO performances and found that their poled thin films exhibited high SHG coefficients ( $d_{33}$  up to 177 pm/V), thanks to the chromophore-



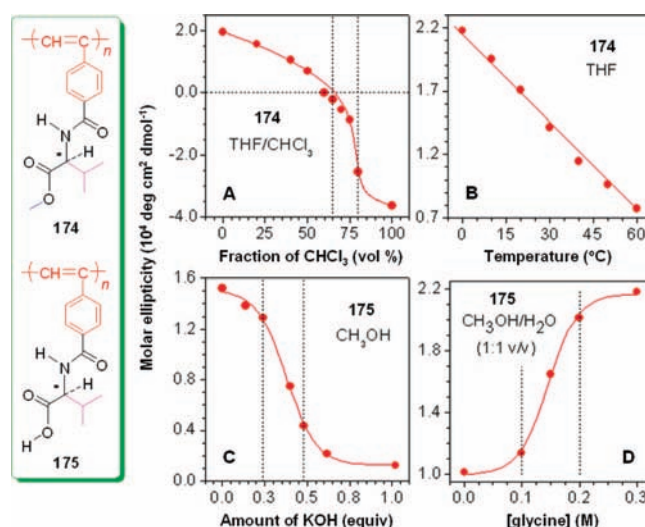
**Figure 33.** Decays of SHG coefficients of **103b** and **277** as a function of temperature. Reproduced with permission from ref 324. Copyright 2006 American Chemical Society.

separation and site-isolation effects of the hyperbranched structures of the polymers in the three-dimensional space (Figure 33).<sup>324</sup> The optical nonlinearity of the poled thin film of polymer **277** is thermally stable with no drop in  $d_{33}$  observable when heated to a temperature as high as 152 °C, due to the facile cross-linking of the multiple triple bonds in the polymer at a moderate temperature of ~88 °C.

#### 4.6. Chiral Recognition

Biological systems are in essence molecular machines built upon chiral biopolymers, which smartly respond to temperature change, pH variation, foreign entrant, light stimulus, mechanical force, electric and magnetic fields, etc. It is of great interest to develop stimuli-responsive smart biomimetic materials based on chiral synthetic polymers, especially those capable of chiral discrimination or enantiomeric recognition. Several research groups have investigated chiral polymers that respond to environmental changes and that detect achiral analytes, while other groups have studied achiral polymers that sense chiral analytes and form complexes with enantiopure guests.<sup>105,406</sup>

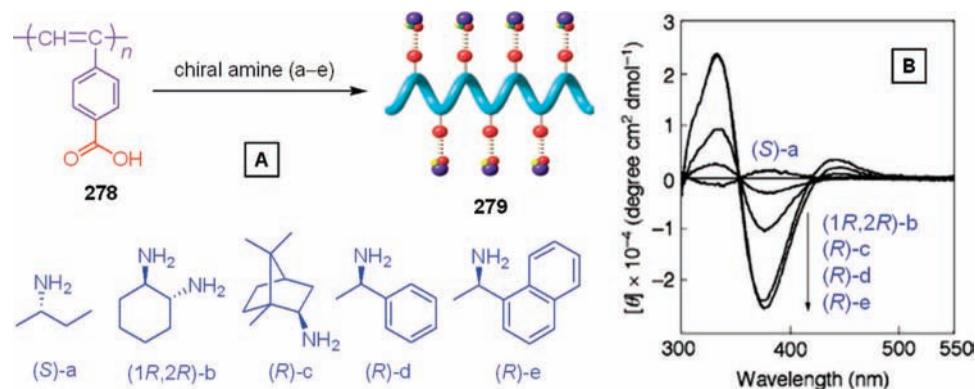
Tang and co-workers have found that helical PPA derivatives respond to external changes, such as the variations in solvent, temperature, pH, and additives, as indicated by the changes in their characteristic molar ellipticities ( $[\theta]$ ).<sup>402</sup> For example, the  $[\theta]$  values of polymer **174** are positive and negative in THF and  $\text{CHCl}_3$ , respectively; that is, the majority of its chain segments form coils of opposite helicity in these two solvents. The helical preference can be reversed by simply changing the solvent; in other words, the polymer can be used to differentiate the two solvents by the change in its CD signal. The helicity change is continuous and reversible, as revealed by the  $[\theta]$ –solvent plot shown in Figure 34A. The ellipticity displays a rapid change when the chloroform content is increased from ~65% to ~80%. This is indicative of a cooperative process: once some chain segments are associated via noncovalent interactions (e.g., hydrogen bonding), their neighboring segments will be zipped up quickly along the preferred direction. The molar ellipticity of **174** is monotonically decreased with increasing temperature because the thermally activated chain randomization induces the segments to unwind (Figure 34B).



**Figure 34.** Modulations of the molar ellipticities of helical PPA derivatives of (A, B) **174** and (C, D) **175** at ~375 nm by (A) solvent, (B) temperature, (C) pH, and (D) additive. Reproduced with permission from ref 402. Copyright 2003 American Chemical Society.

Addition of KOH into a solution of **175** progressively weakens its  $[\theta]$  because the ionic interaction of  $\text{K}^+$  with  $\text{CO}_2^-$  breaks the intra- and interchain hydrogen bonds (Figure 34C). The original  $[\theta]$  value can be regained when the KOH solution is neutralized by HCl. This reversibility makes **175** an excellent indicator for sensing the pH variation in external environment. Intriguingly,  $[\theta]$  of **175** can also be tuned by achiral additives. With continuous addition of glycine (an achiral essential amino acid) into the solution of **175**, its  $[\theta]$  value is continuously increased (Figure 34D). The glycine molecules may have bound to the L-valine pendants, causing an increase in the pendant bulkiness and thereby inducing further twists in the chain segments.<sup>105</sup>

Yashima and Okamoto have developed a series of novel chirality-responsive polymers that fold into helical chain conformations of preferred handedness upon complexation with nonracemic molecules. Poly[(4-carboxyphenyl)acetylene] (**278**) is such a polymer,<sup>535</sup> whose complexes with chiral amines (**279**) exhibit induced CD signals in the long-wavelength regions where the  $\pi$ -conjugated polyene backbone absorbs. The induced Cotton-effect signs corresponding

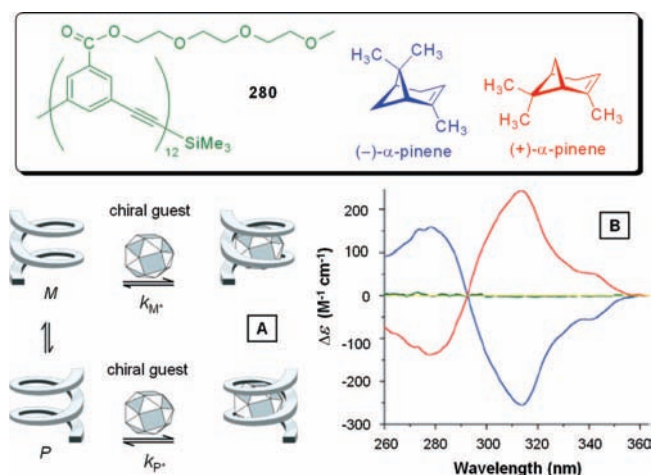


**Figure 35.** (A) Schematic representation of helicity induction and (B) CD spectra of polymer **278** upon complexation with chiral amines **279**(a–e) in DMSO. Reproduced with permission from ref 535. Copyright 1997 American Chemical Society.

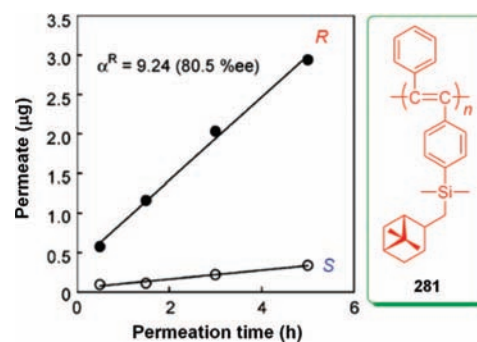
to the helical senses of **279** can be utilized to predict the absolute configurations of the chiral amines, because all the primary amines with the same configurations give the same Cotton-effect signs. Polymer **278** is a dynamic helical macromolecule, the conformations of whose chain segments with right- and left-handedness are interconvertibly separated by helical reversals. As a result, the polymer shows no optical activity. Upon addition of chiral amines, a drastic change in the population of right- or left-handed segments leads to the formation of chiral complex **279** with a dominant one-handedness, hence producing the observed induced CD activity (Figure 35).

Moore's foldamer system generates a tubular hydrophobic cavity under appropriate conditions. The induced tubular cavity in *m*-phenyleneethynylene oligomers (e.g., **280**) can accommodate specific size and shape of chiral guest molecules.<sup>536</sup> These foldamers have been used to determine the chirality of guest molecules encapsulated within the molecular cavity. Oligomer **280** is an achiral chain, which takes a random conformation in chloroform but folds into right- and left-handed helical conformations in polar solvents, e.g., acetonitrile, driven by the solvophobic force. The foldamer exists as a dynamic racemate with *M* and *P* helical conformations. In the presence of an optically active hydrophobic guest that can be encapsulated into the cavity of **280**, one of the helices is favorably formed and the resultant complex displays an induced CD signal. Chiral guest molecules with different chirality can induce the formation of helix with different handedness. A typical example is shown in Figure 36. In the absence of  $\alpha$ -pinene, **280** shows no CD signal as expected for an achiral oligomer. Addition of enantiomerically pure (–)- $\alpha$ -pinene induces a strong Cotton effect in the wavelength range where oligomer **280** absorbs. A mirror image spectrum is obtained when (+)- $\alpha$ -pinene is used as chiral guest.

If a chiral polymer is environmentally stable, macroscopically processable, and mechanically strong, it has the potential to be used as a chiral membrane for selective permeation and as a stationary phase for high-performance liquid chromatography (HPLC) enantioseparation. The racemates with different configurations may pass through the molecular voids in the chiral membranes in different permeation rates, resulting in separation of racemic mixtures. Teraguchi et al. explored this possibility and fabricated a chiral membrane of polymer **281** with a one-handed helical conformation.<sup>537</sup> 2-Butanol is a small, not-so-polar molecule and the direct separation of its racemates by chiral HPLC column has been difficult. Teraguchi et al. examined the



**Figure 36.** (A) Association models of oligomer **280** with chiral guest of  $\alpha$ -pinene. (B) CD spectra of **280** in the absence (green line) and presence of 100 equiv of (–)- (blue line) and (+)- $\alpha$ -pinenes (red line). Reproduced with permission from ref 536. Copyright 2000 American Chemical Society.



**Figure 37.** Time course of enantiopermeation of (R)-(+)- (●) and (S)-(-)-2-BuOH (○) through a chiral membrane of polymer **281**. Reproduced with permission from ref 537. Copyright 2003 American Chemical Society.

enantioselective permeation of racemic 2-BuOH through the chiral membrane of **281**. Figure 37 shows the normalized quantities of permeated (R)- and (S)-2-BuOH versus permeation time through the chiral membrane. In the pervaporation process, the (R)-isomer preferentially permeated through the chiral membrane in high selectivity ( $\alpha^R = 9.24$ ) and enantiomeric excess (ee = 80.5%).

#### 4.7. Light Refraction

Macroscopically processable polymers with high RI values are promising candidate materials for an array of practical

**Table 3. Refractive Indices ( $n_D$ ), Abbé Numbers ( $\nu_D$ ), Revised Abbé Numbers ( $\nu'$ ), and Optical Dispersions ( $D'$ ) of Acetylenic Polymer Films<sup>a</sup>**

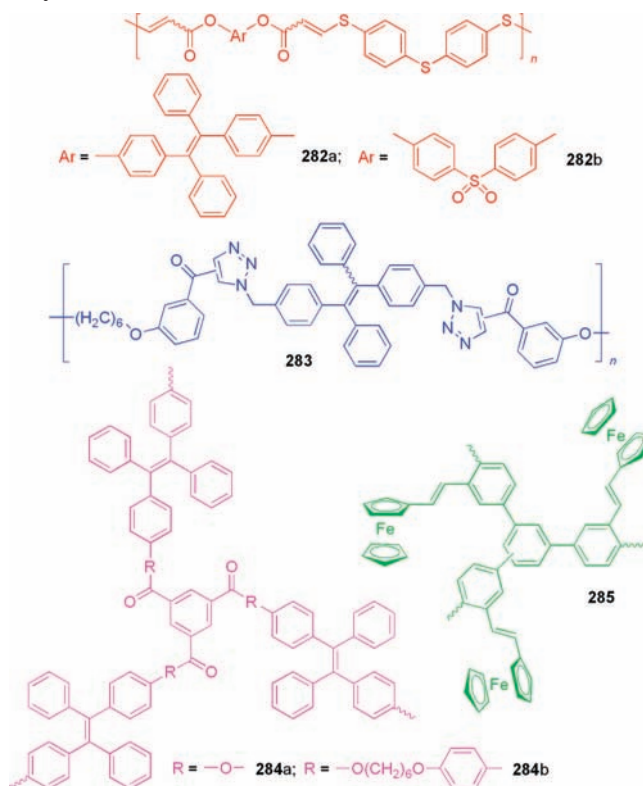
no.	polymer	$n_D$	$\Delta n_D^b$	$\nu_D$	$\nu'$	$D'$
linear polymer						
1	<b>85</b>	1.6963		22.8	69.6	0.0144
2	<b>85(Co)<sup>c</sup></b>	2.0699	+0.3736	18.6	80.0	0.0125
3	<b>282a</b>	1.7075		18.4	70.4	0.0142
4	<b>282a(Co)<sup>c</sup></b>	1.7834	+0.0759	13.6	50.7	0.0197
5	<b>282b</b>	1.7178		26.3	539.0	0.0019
6	<b>282b(Co)<sup>c</sup></b>	1.9076	+0.1898	156.5	643.0	0.0016
7	<b>283</b>	1.6543		17.6	164.0	0.0061
hyperbranched polymer						
8	<b>285</b>	1.7506		75.8	400.5	0.0025
9	<b>285(Co)<sup>c</sup></b>	1.6858	-0.0648	163.3	680.8	0.0015
10	<b>107a</b>	1.6620		15.4	121.4	0.0080
11	<b>107a(UV)<sup>d</sup></b>	1.5826	-0.0794	120.4	2897.5	0.0003
12	<b>134<sup>e</sup></b>	1.8183		6.3	57.0	0.0175
13	<b>134(UV)<sup>d</sup></b>	1.7820	-0.0363	7.5	34.9	0.0287
14	<b>195</b>	1.6213		258.9	1030.7	0.0010
15	<b>196</b>	1.7097		23.7	286.7	0.0035
16	<b>107b</b>	1.6127		68.1	1214.2	0.0008
17	<b>284a</b>	1.6512		14.4	206.7	0.0048
18	<b>284b</b>	1.6886		21.7	392.9	0.0025

<sup>a</sup> RI ( $n_D$ ) value at Fraunhofer D line (589.3 nm); (revised) Abbé numbers ( $\nu_D$  and  $\nu'$ ) and optical dispersion ( $D'$ ) defined by eqs 14–16; chemical structures of **282**–**285** shown in Chart 12. <sup>b</sup> Change in RI:  $\Delta n_D = n_{D,2} - n_{D,1}$ . For example, change in  $n_D$  after cobalt complexation of **85**:  $\Delta n_D = n_{D,85(\text{Co})} - n_{D,85}$  (cf., nos. 1 and 2); change in  $n_D$  after UV irradiation of **107a**:  $\Delta n_D = n_{D,107a(\text{UV})} - n_{D,107a}$  (cf., nos. 10 and 11). <sup>c</sup> Complex with  $\text{Co}_2(\text{CO})_8$ . <sup>d</sup> UV photolysis product. <sup>e</sup> Cobalt complex of **124d** [or **124d(Co)**].

applications in optoelectronic devices, including optical waveguides, memories, and holographic image recording systems. The RI values for most of conventional polymers lie in between  $\sim 1.40$  and  $\sim 1.65$ , with the majority located in a very narrow range of  $\sim 1.5$ – $1.6$ : for example,  $n_D = 1.491$  for poly(methyl methacrylate) (PMMA),  $n_D = 1.581$  for polycarbonate, and  $n_D = 1.590$  for PS.<sup>538</sup> Very few polymers exhibit RI values higher than 1.70. The low refractivities of the existing polymers have greatly limited the scope of their photonic applications and largely retarded the progress in the development of organic photonic systems.

Theory predicts that macromolecules containing groups or units with high polarizabilities and small molecular volumes may show high light refractivities.<sup>539–542</sup> From the structural point of view, the functionalized acetylenic polymers have the potential to display high RI values, because their monomer repeat units contain many components that fulfill the theoretical requirements: electronically mobile aromatic rings, slim triple-bonded rods, highly polarizable heteroatoms or groups, heavy atoms, metallic elements, etc. Indeed, many linear and hyperbranched acetylenic polymers developed by Tang's group show RI values ( $\sim 1.61$ – $2.07$ ) much higher than those of the conventional polymers (Table 3 and Chart 12).<sup>541</sup> Among the acetylenic polymers, those containing heteroatoms and metal elements such as sulfur, cobalt, and iron exhibit refractivities higher than 1.7. Particularly noteworthy are the extremely high RI values of **85(Co)** ( $n_D \approx 2.07$ ), **282b(Co)** ( $n_D \approx 1.91$ ), and **134** ( $n_D \approx 1.82$ ), thanks to the existence of the metallic species in these polymers. Remarkably, **196** and **284b** display high refractivities (RI  $\approx 1.7$ ; Table 3, nos. 15 and 18), although they are pure organic polymers containing neither heteroatoms nor metal elements.

In the advanced optoelectronic systems, the light refractivities of the optical materials should ideally undergo large

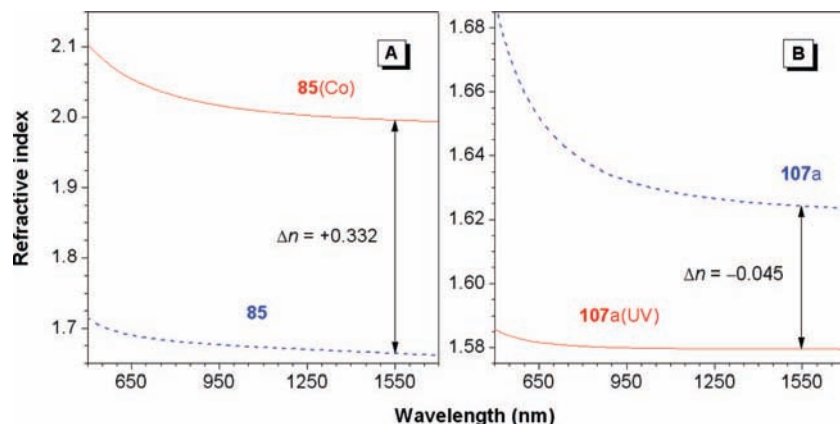
**Chart 12. Examples of Highly Refractive Acetylenic Polymers**

changes when internally modulated or externally perturbed because the photonic functions are often realized by the differences in the RI values of the components in the devices.<sup>550–554</sup> There has been limited room to manipulate the refractivity of conventional condensation and vinyl polymers because of the limited structural tunability of their electronically saturated backbones. For this reason, acetylenic polymers with electronically conjugated backbones are promising materials because they are composed of unsaturated structural units with mobile electrons that can be modulated by molecular engineering or external stimuli. With this in mind, Tang's group worked on the development of RI-tunable acetylenic polymer systems.

Metal complexation or metallization proves to be an effective way to tune the light refractivity of the polymers. While the RI value of **85**, a sulfur-containing linear polymer, is already high ( $\sim 1.7$ ), it can be further boosted to a spectacularly high RI value of  $\sim 2.1$  through cobalt complexation (cf., Table 3, nos. 1 and 2). The light refractivity of the polymer is tuned by the metallization by a stunningly large scale of  $\sim 0.37$  at Fraunhofer D line ( $\Delta n_D$ ). Even at 1550 nm, a telecommunication-important wavelength, the  $\Delta n$  value is still as large as  $\sim 0.33$  (Figure 38A). The refractivities of other sulfur-containing linear polymers such as the series of **282** are also increased by the metallization. However, the RI value of **285**, an iron-containing hyperbranched polymer, is decreased after the metallization (cf., Table 3, nos. 8 and 9). This indicates that the metallization process can be used to positively or negatively modulate the refractivity of an acetylenic polymer, depending on the involved complexation mechanism.

Not only metallization but also photolysis can modulate light refractivities of the acetylenic polymers. Thus, when a thin film of a silicon-containing hyperbranched polymer **107a** is exposed to a UV light via a copper-negative mask, without





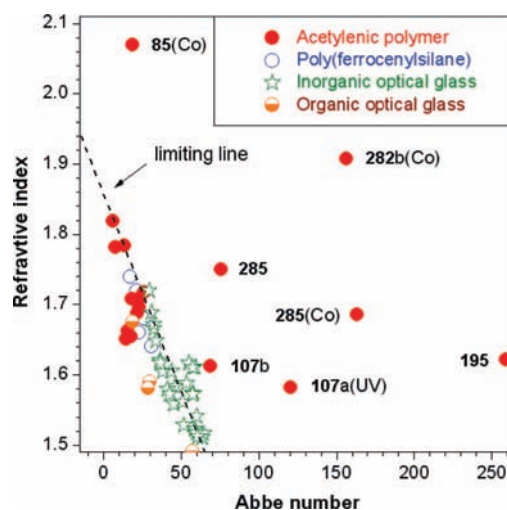
**Figure 38.** Tuning refractive indices of thin films of (A) **85** and (B) **107a** by (A) metallization and (B) photolysis processes. Panels A and B are reproduced with permissions from refs 541 and 545. Copyright 2007 The Royal Society of Chemistry and 2009 American Chemical Society, respectively.

going through a development step, a two-dimensional photopattern is generated. The wavelength-dependent RI spectra of the unexposed and exposed regions of the polymer film are shown in Figure 38B. While **107a** shows high RI values in the wavelength region of 500–1700 nm, its refractivity is decreased dramatically upon UV irradiation, due to the large structural changes caused by the photolysis of the organosilicon polymer. The  $\Delta n$  values at 589.3 and 1550 nm are as large as about  $-0.079$  (Table 3, no. 11) and  $-0.045$  (Figure 38B), respectively. It is worth noting that the RI spectrum of the photolysis product is pretty flat, although its parent form shows large variations with wavelengths. In other words, the UV irradiation can tune not only light refractivity but also chromatic aberration. Similarly, photoirradiation of the film of **134**, a cobalt-metalized form of **124d**, results in the formation of a two-dimensional photopattern, thanks to the large decrease in its RI value induced by the UV photolysis (cf., Table 3, nos. 12 and 13).<sup>45,541</sup>

For an optical material to be useful for technological applications, its chromatic aberration, namely, the variation of its RI value with wavelength, should be small. For a conventional optical material working in the visible spectral region, its chromatic aberration is adversely associated with the Abbé number ( $\nu_D$ ) or constringence defined by the following equation,

$$\nu_D = \frac{n_D - 1}{n_F - n_C} \quad (14)$$

where  $n_D$ ,  $n_F$ , and  $n_C$  are the RI values at 589.3, 486.1, and 656.3 nm, known as Fraunhofer D, F, and C lines, respectively.<sup>539</sup> Generally, an optical material with a high light refractivity exhibits a low Abbé number and vice versa.<sup>539,543</sup> EDF-3 (an extra dense flint), for example, shows a high RI value but a low Abbé number ( $n_D = 1.7200$ ,  $\nu_D = 29.3$ ), whereas the opposite is true for BSC-1, a borosilicate crown ( $n_D = 1.5110$ ,  $\nu_D = 63.5$ ).<sup>539</sup> Organic glasses behave similarly to the inorganic glasses. Poly(vinylcarbazole) (PVK), for example, exhibits a high light refractivity ( $n_D = 1.675$ ) but a low Abbé number ( $\nu_D = 19$ ); in contrast, poly(tetrafluoroethylene) shows a very low RI value (1.345) but a rather high  $\nu_D$  value (83).<sup>544</sup> This general trend is reflected by the “limiting line” in the  $n_D$ – $\nu_D$  plots of these inorganic and organic optical glasses, as marked by the dashed line in Figure 39. Manners and co-workers have developed a series

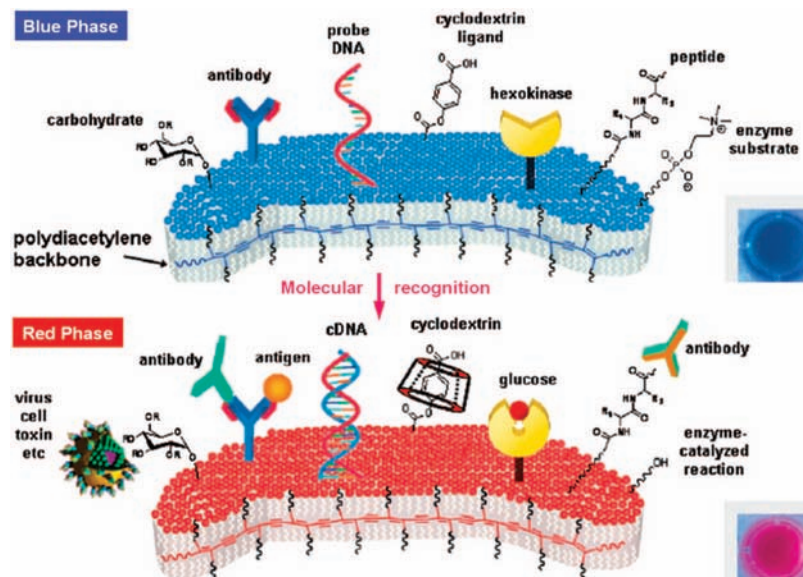


**Figure 39.** Plots of Abbé number ( $\nu_D$ ) versus refractive indices ( $n_D$ ) for acetylenic polymers with linear and hyperbranched structures. Also plotted in the figure for comparison are the data for some linear poly(ferrocenylsilane)s (ref 546), inorganic optical glasses (ref 539), and organic optical glasses (PMMA, PS, PVK, etc.; refs 538 and 540). The data for most of the optical glasses are scattered in the vicinity of the “limiting line” marked by the dashed line.

of highly refractive ferrocene-containing organometallic polymers named poly(ferrocenylsilane)s.<sup>546,547</sup> Although the RI values of these polymers are indeed higher than those of the common organic glasses, their Abbé numbers are lower, as manifested by the fact that their  $n_D$ – $\nu_D$  plots still follow the limiting line. Clearly, development of processable optical materials with both high RI and  $\nu_D$  values is a challenging job.

As can be seen from Figure 39, the linear and hyperbranched acetylenic polymers synthesized by Tang’s group all show high refractivities. Although the  $n_D$ – $\nu_D$  plots for some of the acetylenic polymers still follow the trend line as the common optical materials do, several of the acetylenic polymers clearly deviate from the limiting line. Among the trend-following polymers, **134**, **134(UV)**, and **282a(Co)** show  $n_D$  values in the immediate neighborhood of 1.8. Among the trend-breaking polymers, **85(Co)** displays an extremely high refractivity, while **195** shows an exceptionally high Abbé number. It is remarkable that **282b(Co)**, **285**, and **285(Co)** give both high RI values and Abbé numbers.<sup>541,545</sup>

To evaluate the potential of an optical material for real-world applications, it is proposed to use a revised version



**Figure 40.** Surface ligands and their interactions with target molecules in colorimetric PDA sensors. Reproduced with permission from ref 264. Copyright 2008 American Chemical Society.

of Abbé number ( $\nu'$ ), in which the RI values at the nonabsorbing wavelengths of 1064, 1319, and 1550 nm are used. The first two wavelengths are chosen in view of the practical interest of commercial laser wavelengths, while the last one is the wavelength for telecommunication.<sup>548,549</sup>

$$\nu' = \frac{n_{1319} - 1}{n_{1064} - n_{1550}} \quad (15)$$

where  $n_{1319}$ ,  $n_{1064}$ , and  $n_{1550}$  are the RI values at 1319, 1064, and 1550 nm, respectively. The optical dispersion ( $D'$ ) in the long wavelength region is the reciprocal of the revised Abbé number:

$$D' = \frac{1}{\nu'} \quad (16)$$

Chromatic aberrations of the acetylenic polymers listed in Table 3 are determined using these equations. Most of the polymers show  $\nu'$  values higher than 200. While **195** is a pure organic polymer, it shows a  $\nu'$  value as high as  $\sim 1031$  (Table 3, no. 14). Polymer **107b** contains multiple silicon atoms in its repeat unit and exhibits an even higher  $\nu'$  value ( $\sim 1214$ ). The most astonishing is the  $\nu'$  value ( $\sim 2898$ ) of **107a(UV)**. The  $D'$  value of this polymer is thus unusually low, being practically nil (0.0003). In other words, there is little or no optical dispersion in many of these polymer films. This further demonstrates the great potential of the acetylenic polymers as optical materials for photonic applications.

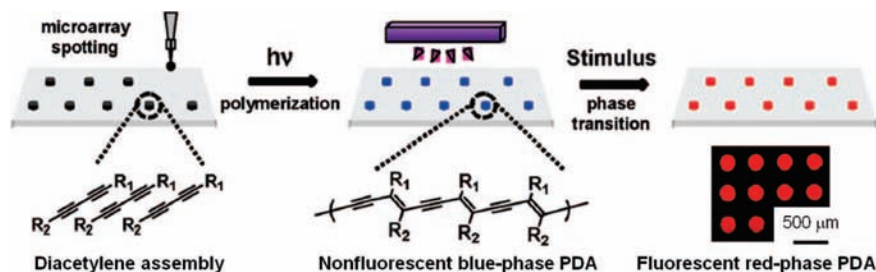
#### 4.8. Thermal Chromism

Among the acetylenic polymers, PDAs are well-known for their “colorful” chromatisms. Extensive studies on PDAs in both solid (crystal, gel, and film) and liquid (sol and solution) states have been conducted in the past few decades. Normally, the PDAs generated by the topopolymerization are blue colored. The polymers can undergo a chromatic change from blue to red in response to heat (thermochromism), solvent (solvatochromism), ion (ionochromism), pH (acidichromism), biological reagent (biochromism), mechanical stress (mechanochromism), ligand–receptor interac-

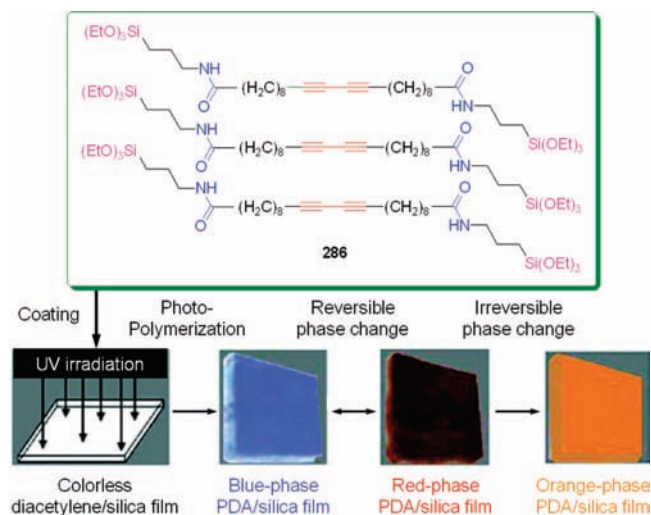
tion (affinochromism), etc.<sup>158,260,263–265</sup> It has been widely accepted that the color transition is caused by a reduction in the effective conjugation length due to the chain distortions imposed by the variation in the enyne backbone conformation. The distortions can be induced by the fluctuations within the side-chain layers activated by external stimuli. This excellent attribute of colorimetric transduction has fostered a wide variety of applications for PDAs in chemo- and biosensing systems.

Wegner,<sup>148</sup> Ringsdorf<sup>253</sup> and Charych<sup>555</sup> have done pioneer work in the area of PDA research. The PDA-based biosensory systems developed to date have been recently summarized by Kim as shown in Figure 40.<sup>264</sup> The PDA films and vesicles functionalized by carbohydrate, antibody, DNA, cyclodextrin, hexokinase, peptide, and enzyme have been found to undergo colorimetric transitions upon interactions with specific targets. Whereas the blue-phase PDAs are nonfluorescent, their red-phase counterparts luminesce upon photoexcitation. Utilizing this unique property, Kim et al. generated patterned arrays of PDA images for the construction of chip-sensor systems. A diacetylene vesicle solution was applied to a surface-modified glass substrate using a standard array spotter (Figure 41). The arrayed diacetylene monomers coated on glass substrate were topopolymerized by UV irradiation, and thermal treatment of the resultant blue-phase PDA arrays furnished the red light-emitting fluorescent patterns.<sup>264,556</sup>

In addition to the sensory systems discussed above, PDAs can also be nanohybridized with inorganic components to afford nanocomposite materials. Lu and co-workers have reported the synthesis of robust PDA/silica nanocomposite films with tunable mesostructure and reversible chromatic transition using a simple sol–gel assembling process.<sup>557</sup> Starting from a series of pre-designed diacetylenic organosilanes of general formula of  $(\text{RO})_3\text{Si}-\text{R}'-\text{Si}(\text{OR})_3$  (**286**) with OR and R' being hydrolyzable alkoxy group and polymerizable diacetylenic unit, respectively, the researchers prepared amphiphilic diacetylenic silicates through alkoxy silane hydrolysis reactions (Figure 42). The collective noncovalent interactions directed the assembly during the coating process, resulting in the formation of nanocomposite film with ordered mesostructure. Subsequent topopolymerization of the di-



**Figure 41.** Schematic representation and fluorescence image of the microarrayed PDA film generated by using a conventional microarray spotter. Reproduced with permission from ref 264. Copyright 2008 American Chemical Society.



**Figure 42.** Photographs of the **286**/silica nanohybrid films showing different colors generated by the thermochromic processes. Reproduced with permission from ref 557. Copyright 2005 American Chemical Society.

acetylene units initiated by the UV irradiation produced the robust blue-phase PDA/silica nanocomposite film.

The PDA/silica nanocomposite undergoes reversible chromatic blue  $\leftrightarrow$  red transitions below 113 °C (Figure 42). Further heating the film to 150 °C, however, results in an irreversible chromatic transition to an orange phase. Almost all the successful colorimetric reversibilities reported so far have been based on the enhanced hydrogen bonding between the head groups of the side chains. Lu's PDA assembly here, however, is produced by the covalent bond formation via hydrolysis and condensation reactions of the alkoxy silane groups, though hydrogen bonding has also played a constructive role in this assembling system. The complete thermochromatic reversibility below 113 °C suggests that the stable covalent interactions between the PDA side chains and the inorganic silica networks help restore the original chain conformations upon removal of the thermal perturbation.

Although hydrogen-bonding unit has been a desired structural motif for directing the ordered stacking in the solid state, insoluble PDAs have often formed, as a result of the strong intermolecular interactions. Many functional PDA-based materials have thus been fabricated in the form of crystals, gels, mono- and multilayer membranes that cannot be further processed after the in situ topopolymerization. Matsumoto and co-workers have recently synthesized some hydrogen bond-free PDAs that are soluble in common organic solvents.<sup>558,559</sup> For example, although PDA **287** is highly crystalline and insoluble in organic solvents right after the solid-state polymerization, it can be readily converted into partially crystalline and soluble polymer by a refluxing dissolution and reprecipitation process.

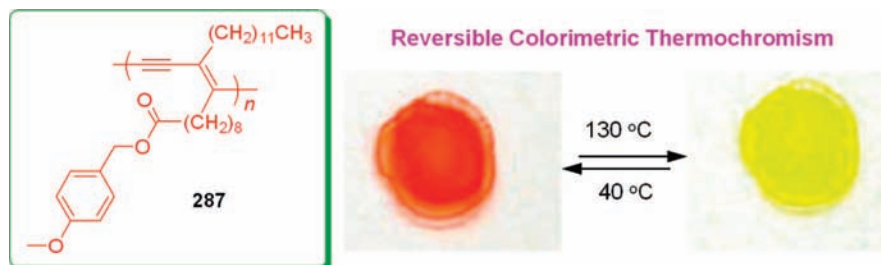
Polymer **287** shows reversible thermochromism in both solid and solution states. Figure 43 shows the reversible colorimetric change of the solid film of **287** prepared by casting its chloroform solution on a glass plate.<sup>559</sup> At 40 °C, it shows a red color, while at 130 °C, the color changes to yellow. This color change is different from the blue-to-red transition observed in most of the traditional PDA systems (vide supra). This red-to-yellow color change is reversible in the temperature range of 40–130 °C, as proved by its reversible light absorption spectra. Matsumoto and co-workers have interpreted this color change as follows: the alkyl side chain of PDA **287** takes a *trans*-zigzag conformation at room temperature, resulting in the aligned polymer main chains with a high effective conjugation length, while at high temperature, the conformation of the alkyl chains is changed to a random structure in the melt state, which has perturbed and shortened the effective conjugation length of the PDA backbone.

In the THF solution, the apparent colors of **287** are red and yellow at –10 and 50 °C, respectively (Figure 44A).<sup>559</sup> Figure 44B shows the fluorescence spectra of the yellow and red solutions. The red solution is evidently more emissive than the yellow one. Through a careful study using NMR and DLS techniques, Matsumoto's group has concluded that aggregates are formed in the solution when its temperature is decreased. At low temperature, the aggregated PDA chains are organized, showing a red-shift in the absorption spectrum. The more efficient emission from the red solution is attributed to the suppression of intramolecular vibrational and rotational motions in the PDA aggregates. Because the intramolecular motions bring about fast nonradiative relaxations, the conformational rigidification in **287** caused by the aggregate formation leads to the enhanced light emission.

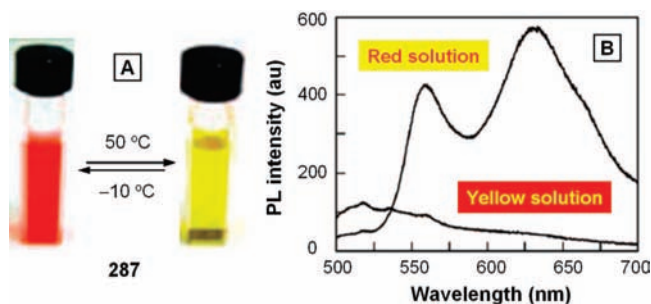
#### 4.9. Patterning and Imaging

Photosensitive polymers have been widely used as photoresist materials in many high-tech processes, such as photolithography and photoengraving. Polymer photoresists are classified into two categories, positive and negative: in the former case, the exposed region is rendered soluble because the polymer is photodegraded, while in the latter case, the exposed region becomes insoluble because the polymer is photocross-linked. If a processable polymer is both photosensitive and light-emitting, it will be an excellent candidate material for the fabrication of luminescent patterns by photolithography processes. The generation of fluorescent patterns is important for the constructions photonic and electronic devices and biological sensing and probing systems, e.g., LCD, OLED, and medicinal diagnostic biochip.<sup>560,561</sup>

Tang and co-workers have found that some LEPAs are photoresponsive and can be used to generate light-emitting



**Figure 43.** Thermochromism of **287** in the solid state. Reproduced with permission from ref 559. Copyright 2008 American Chemical Society.



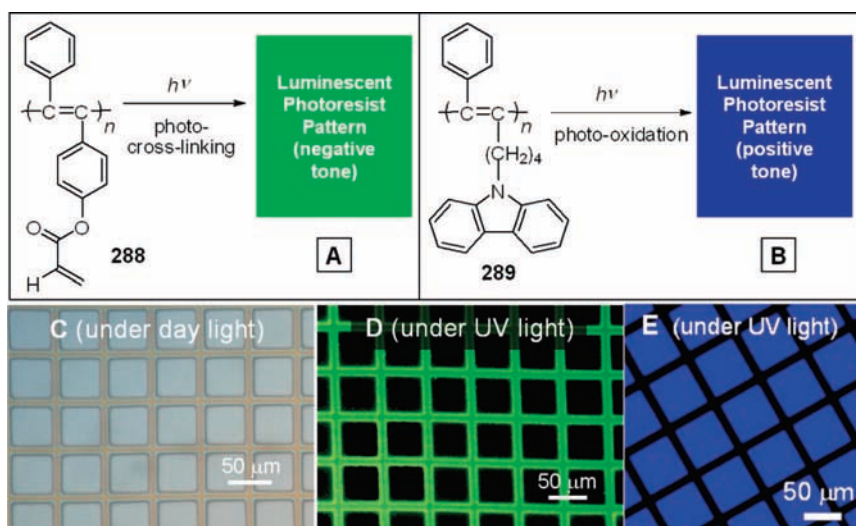
**Figure 44.** Changes in (A) solution color and (B) fluorescence spectrum of **287** in THF by thermal perturbation. Reproduced with permission from ref 559. Copyright 2008 American Chemical Society.

patterns.<sup>487,562–564</sup> For example, UV irradiation readily initiates photopolymerization of acrylic pendants in **288** (Figure 45A), and development of the exposed polymer films gives well-defined photoresist patterns (Figure 45C).<sup>487</sup> The patterned lines glow under UV illumination because the poly(diphenylacetylene) skeleton of **288** emits intense green light (Figure 45D). Whereas disubstituted PAs are resistant to thermolysis, some of them can undergo photooxidation, which quenches their light emissions. Utilizing this property, Tang's group has succeeded in the generation of two-dimensional fluorescence images. For example, UV irradiation of a thin film of **289** in air through a mask quenches the luminescence of the exposed region (black lines), while the unexposed area remains highly emissive (Figure 45E).<sup>564</sup> A PL image is thus directly drawn without going through the development procedure.

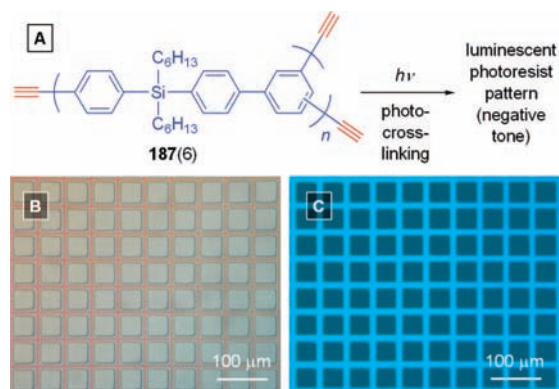
Since hyperbranched polymer **187(6)** is emissive in the solid state and possesses many cross-linkable triple bonds in their peripheries, Tang et al. used it to create fluorescent patterns.<sup>353</sup> The polymer can form uniform, tough films by spin-coating its solution onto silicon wafers. Exposure of the film to UV irradiation through a negative copper photomask causes the exposed region to undergo a cross-linking reaction, while the unexposed region is removed by a development process. This furnishes a photoresist pattern with sharp edges (Figure 46). As can be seen from Figure 46C, the photocross-linked pattern emits a strong blue light under UV illumination.

The *hb*-PTAs prepared by click polymerizations are soluble, film-forming, and luminescent. Since the polymers contain many azido, ethynyl, and triazolyl functional groups, they are expected to be photosusceptible.<sup>71</sup> Indeed, when a thin film of *hb-r*-PTA prepared by thermal polymerization of **97(4)** with **123d** is irradiated with a UV light through a photomask, the exposed region is rendered cross-linked and insoluble. Development of the film gives a three-dimensional negative photoresist pattern (Figure 47A). The high quality of the pattern (sharp line edges, uniform film thickness, etc.) is clearly seen under the normal laboratory lighting, although the photoresist process is yet to be optimized. The photo-pattern is fluorescent: the patterned lines emit white light upon illumination with a UV lamp (Figure 47B).

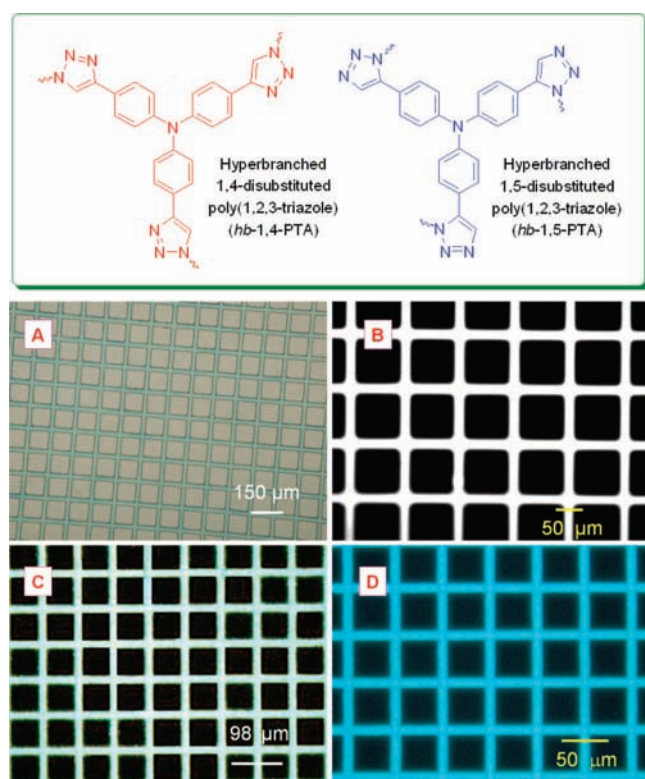
Fluorescent patterns can also be generated by the UV photolyses of the regioregular *hb*-PTAs.<sup>71</sup> The colors of the emissions from their patterns are, however, different. The light emitted from the pattern generated from the photolysis of *hb*-1,4-PTA is yellow in color, whereas that from *hb*-1,5-



**Figure 45.** (A) Photocross-linking of **288** and (B) photo-oxidation of **289**. Formation of (C and D) three-dimensional negative and (E) two-dimensional positive photoresist images. Photographs in panels C/D and E are reproduced with permission from refs 487 and 105. Copyright 2007 and 2005 American Chemical Society, respectively.



**Figure 46.** (A) Photocross-linking of **187(6)**. Three-dimensional negative photoresist pattern generated by photolysis of **187(6)**; photographs taken under (B) normal lighting and (C) UV illumination. Reproduced with permission from ref 353. Copyright 2007 American Chemical Society.



**Figure 47.** Luminescent photoresist patterns generated by photocross-linking of (A and B) *hb-r*-PTA, (C) *hb-1,4*-PTA, and (D) *hb-1,5*-PTA prepared by thermally activated and Cu- and Ru-mediated click polymerizations of **97(4)** with **123d**. Photographs were taken under (A) normal lighting and (B–D) UV illumination. Reproduced with permission from ref 71. Copyright 2008 American Chemical Society.

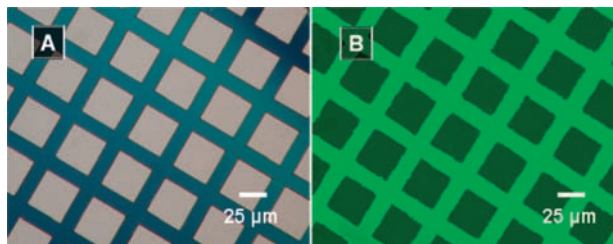
PTA is blue when observed by the naked eyes (although the colors in panels C and D of Figure 47 are somewhat distorted by the photographing process). The emission color of *hb-1,4*-PTA is redder than that of *hb-1,5*-PTA, which is understandable, because the former is more conjugated and aggregated than the latter.<sup>71</sup> This also explains why *hb-r*-PTA emits a white light: the regiorandom polymer contains a roughly equal amount of 1,4- and 1,5-isomeric units and the mixing of the complementary yellow and blue colors of the lights emitted from the two units results in the light emission of a white color. It is noteworthy that all the PTAs have the exact same chemical formula but emit lights of

different colors because of the difference in their regioregularities. In other words, their emission colors are readily modulated by simply changing their regiostructures. The cross-linking mechanism is shown in Scheme 57.<sup>71,565</sup> The UV irradiation cleaves the azide bond and generates a nitrene intermediate. When two nitrene species in different *hb*-PTA molecules are coupled together through the formation of an azo bond, a cross-linked product is resulted. The azo bonds may be photolyzed by further irradiation to yield methylene radicals, whose combination affords a stable cross-linking product.

The diyne units in the *hb*-PDYs are chemically reactive and readily undergo photoinduced cross-linking reactions. Tang's group has generated negative patterns after developing the UV-irradiated thin films of *hb*-PDYs.<sup>113</sup> For example, the optical pattern generated by the UV photolysis of *hb*-PDY **124d** emits very intense green light when observed under a fluorescence microscope (Figure 48B). This is impressive, taking into account that many "normal"  $\pi$ -conjugated polymers show weak emissions in the solid state due to the quenching effect caused by the strong  $\pi$ - $\pi$  stacking interactions between their chromophores. The nonplanar conformation of the TPA unit in **124d** may have hampered the close packing of the chromophores, thereby enabling the polymer film to be highly emissive.

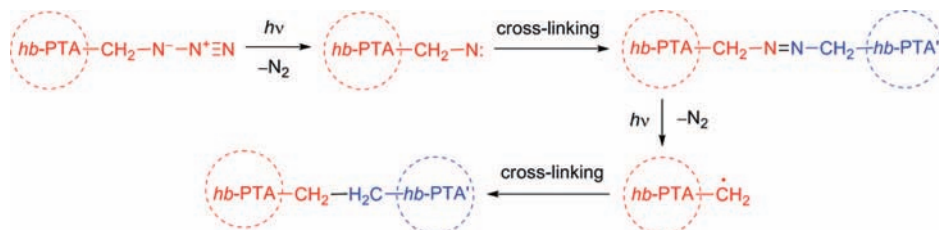
Tang's group has also used photosusceptible PA-perovskite nanohybrid films to generate luminescent patterns. When a thin film of nanohybrid **241** is irradiated through a photo-mask, the exposed regions become weakly fluorescent, giving a two-dimensional fluorescence image (Figure 49).<sup>169</sup> It should be noted that the pattern is created by a one-step irradiation process without going through a development step. In the conventional photolithographic process, the wet or dry development step uses solvent or plasma as developing reagent that can sometimes cause serious damage or deformation to the patterns generated in the photoirradiation step. The formation of the fluorescent pattern by the development-free process is therefore of technological implication and may find practical applications in such systems as optical display and information storage.

Benzophenone has been introduced into biological and synthetic polymers to serve as a photocross-linking agent due to its high photosusceptibility. Noting that *hb*-PAAs contain numerous aryloxy units, Tang's group investigated their photocross-linking behaviors.<sup>344</sup> When a thin film of **290** on a glass plate is exposed to a handheld UV lamp at room temperature, it is readily cross-linked. The cross-linking reaction may have proceeded via a well-established radical mechanism: the carbonyl groups abstract hydrogen atoms from the benzyl units to generate benzyl radicals, whose coupling leads to cross-linking and hence gel formation. Figure 50A shows the effect of radiation dose on the gel formation of **290** after it has been exposed to a weak UV light with a power of  $\sim 1$  mW/cm<sup>2</sup>. Although the photoreaction conditions have not been optimized, **290** already gives a much higher sensitivity ( $D_{0.5} = 50$  mJ/cm<sup>2</sup>) than those of commercial poly(amic ester)-based photoresists ( $D_{0.5} = 650$ – $700$  mJ/cm<sup>2</sup>). Well-resolved patterns with line widths of  $\sim 1.0$   $\mu$ m are readily formed when a film of **290** is exposed to a UV dose of  $\sim 1$  J/cm<sup>2</sup>. Patterns with submicrometer resolutions (line width down to 500 nm) are achieved, as demonstrated by the example given in Figure 50D. Evidently, **290** is an excellent photoresist material.



**Figure 48.** (A) Optical and (B) fluorescent micrographs of the patterns generated from photolysis of *hb*-PDY **124d**. Reproduced with permission from ref 113. Copyright 2007 Elsevier.

**Scheme 57. Photo-Cross-Linking Mechanism for *hb*-PTA**



Tang and co-workers have also worked on the fabrication of magnetic patterns from the acetylenic polymers. The ferrocene-containing *hb*-PAAs synthesized by Tang's group are photosusceptible and can be used to create magnetic patterns.<sup>113,566</sup> Using **293** as a model polymer, Tang and co-workers have developed a two-step process for generating the magnetic patterns. In the first step, microstructured optical patterns are created by developing a thin film of **293** in 1,2-dichloroethane, after the polymer film has been exposed to a UV irradiation through a photomask (Figure 51). In the second step, the patterned organometallic gels are transformed to magnetic ceramics by pyrolyzing the microgrids at a high temperature (1000 °C) under nitrogen. As can be seen from Figure 51C, the photoresist pattern has been successfully converted into a ceramic pattern comprised of fine iron nanoparticles with excellent shape retention. The iron-containing ceramics have been found to show unique soft ferromagnetism.

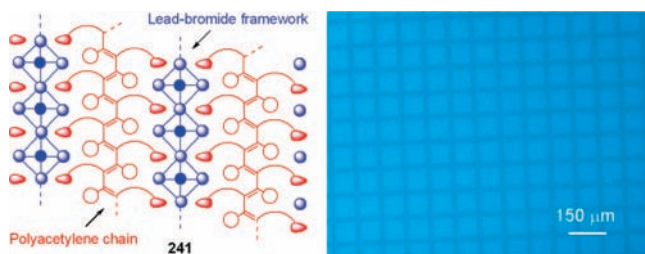
In addition to the optical and magnetic patterns, photonic patterns based on RI differences have also been fabricated by Tang and co-workers, an example of which is shown in Figure 52.<sup>541</sup> The as-prepared solution of organocobalt complex **134** or **124d**(Co) (cf., Scheme 31) can be readily spin-coated onto a glass or silicon wafer to give a homogeneous, yellowish brown-colored, thin solid film. Photoirradiation of the solid film of the metallized polymer through a photomask causes the cobalt carbonyl complex to decompose. The film is readily photobleached, affording a faithful copy of the two-dimensional pattern of the photo-

mask without going through any development processes.<sup>541</sup> The magnified image given in Figure 52B clearly reveals the sharp edges of the photopattern. As discussed in the light refraction part above, the exposed and unexposed regions of the film exhibit different RI values, with the latter being higher than the former. The pattern is thus generated by a pure photonic effect of the polymer complex, thanks to the ready tunability of its light refractivity by photoirradiation.

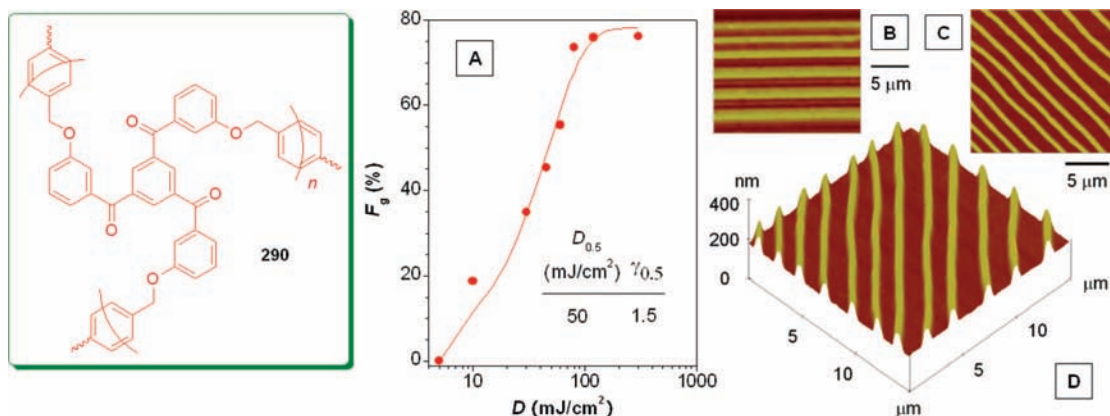
#### 4.10. Ceramization and Magnetization

Acetylenic polymers carrying pendants of stable radicals have been investigated as potential “organic magnets”, but their magnetic susceptibilities are generally very low, even when the polymers are cooled to cryogenic temperatures.<sup>26,60,106,567–570</sup> An alternative approach is to utilize acetylenic polymers as precursors for magnetic materials of nonoxide ceramics. Intensive research has been devoted to the development of preceramic polymers because the excellent processability of organic polymers can help overcome the processing disadvantage of inorganic ceramics.<sup>571–573</sup> In comparison to conventional vinyl polymers, acetylenic polymers have higher carbon contents. It is also easier to incorporate metallic species into acetylenic polymers: for example, the multiple diyne triple bonds in the *hb*-PDYs can form complexes with various transition metals. In addition, the carbon-rich *hb*-PDYs are readily curable at moderate temperatures and efficiently pyrolyzable or carbonizable at high temperatures in high yields. All these attributes make acetylenic polymers excellent candidate precursors to functional, especially magnetic, ceramic materials.

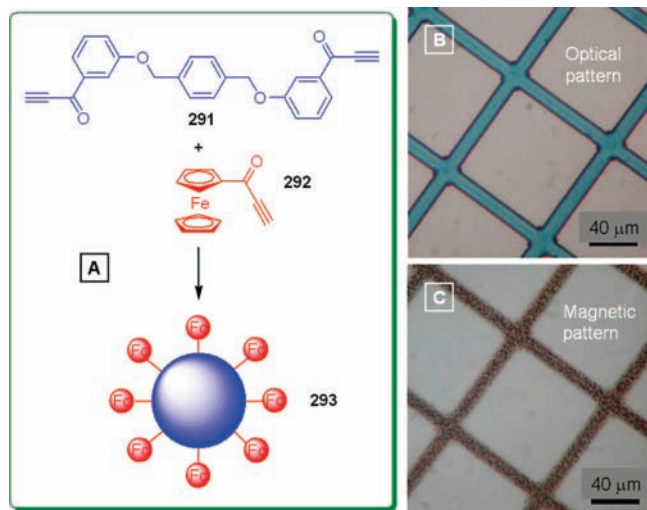
Tang and co-workers have studied the ceramization of the hyperbranched polymers synthesized from acetylenic monomers and the magnetization of the resultant ceramics. Figure 53 shows the ceramization of *hb*-PDY–cobalt complex **134** and magnetization of its ceramic **294**.<sup>45</sup> The pyrolysis of **134** at 1000 °C for 1 h under dry nitrogen furnishes ceramic product in ~65% yield. The ceramic is magnetizable and can be readily attracted to a bar magnet. As can be seen from Figure 53B, with an increase in the strength of externally applied magnetic field, the magnetization of **294** swiftly increases and eventually levels off at a saturation magnetization ( $M_s$ ) of ~118 emu/g, which is much higher



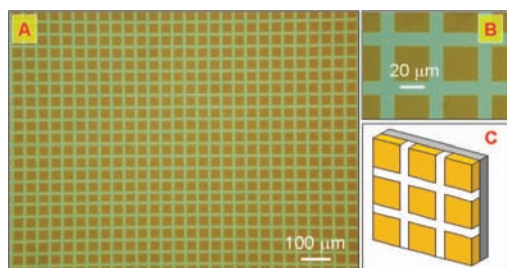
**Figure 49.** Two-dimensional luminescent pattern generated by irradiating a thin film of PA–perovskite nanohybrid **241** with a UV beam through a copper-negative photomask. Reproduced with permission from ref 169. Copyright 2006 American Chemical Society.



**Figure 50.** (A) Plots of gel fractions ( $F_g$ ) of the thin solid films of **290** versus exposure doses ( $D$ ). (B–D) AFM images of micro- and nanoscale patterns obtained from the thin films of **290** exposed to  $\sim 1 \text{ J/cm}^2$  of UV irradiation ( $\lambda = 365 \text{ nm}$ ). Reproduced with permission from ref 344. Copyright 2005 American Chemical Society.



**Figure 51.** (A) Preparation of hyperbranched polymer **293** and optical micrographs of the patterns of **293** fabricated by photolithography (B) before and (C) after pyrolysis at  $1000 \text{ }^\circ\text{C}$  for 1 h under nitrogen. Reproduced with permission from ref 113. Copyright 2007 Elsevier.



**Figure 52.** (A) Optical micrograph of a two-dimensional photonic pattern generated by UV irradiation of organometallic polymer complex **134** through a copper-negative photomask. (B) Image with a high magnification and (C) model of the photonic pattern. In panel C, the brown and white colors denote the unexposed and exposed areas, respectively. Reproduced with permission from ref 541. Copyright 2007 The Royal Society of Chemistry.

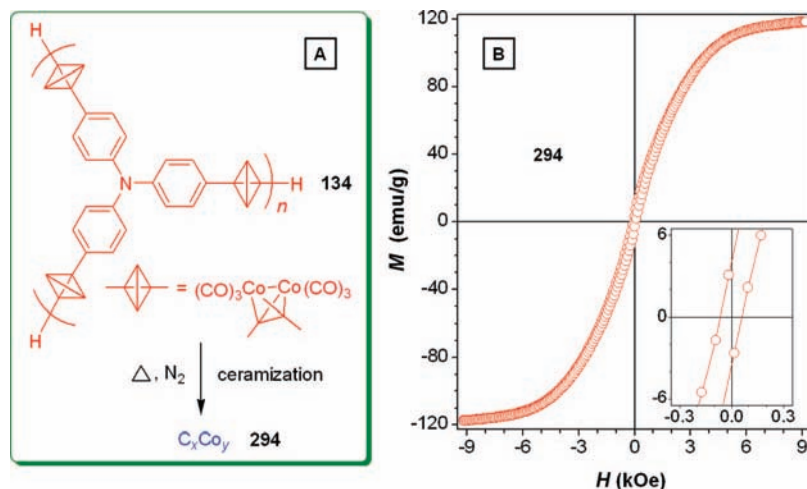
than that of the magnet ( $\gamma\text{-Fe}_2\text{O}_3$ ) used in our daily life ( $M_s = 74 \text{ emu/g}$ ).<sup>574–576</sup> The high  $M_s$  value of **294**, along with its XRD, X-ray photoelectron spectroscopy (XPS), and scanning electron microscopy (SEM) data, indicates that the cobalt nanocrystallites in the ceramic are well-wrapped by carbonaceous species, which have prevented the cobalt particles from being oxidized during and after the pyrolysis and ceramization processes. Polymer **134** is an excellent precursor

to magnetoceramic because its three-dimensional cage structure has enabled the retention of the pyrolyzed species and the steady growth of the magnetic crystallites.<sup>577,578</sup> The hysteresis loop of magnetoceramic **294** is very small, with a coercivity ( $H_c$ ) value of  $0.058 \text{ kOe}$ . The high magnetizability and low coercivity of **294** make it an outstanding soft ferromagnetic material.

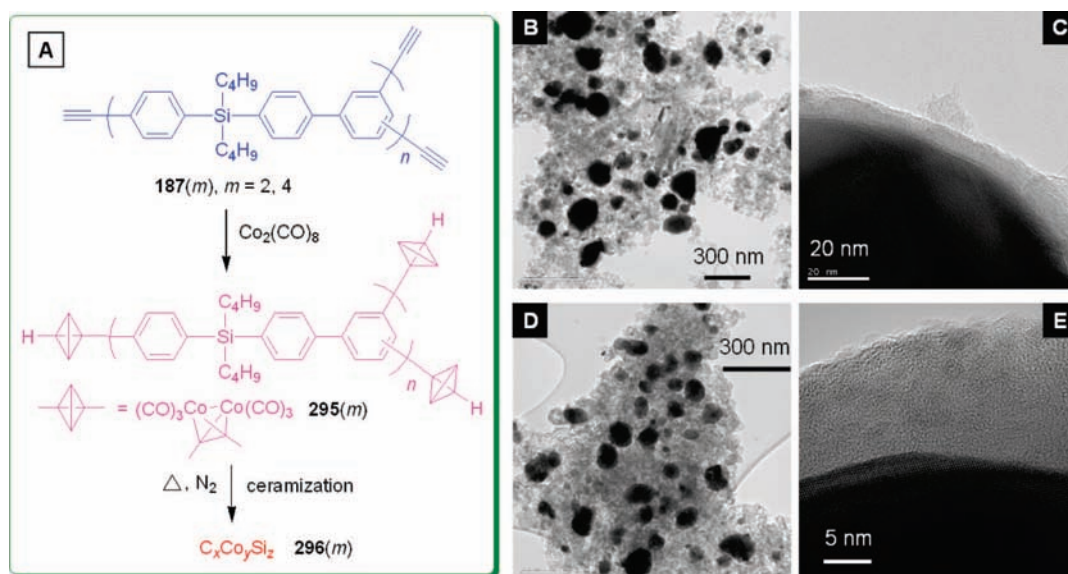
Spectroscopic analyses reveal that hyperbranched poly(arylenesilane)s **187(m)** contain acetylene triple bonds in their peripheries, which provide reactive sites for the polymers to coordinate with transition metals. In other words, **187(m)** should be promising candidate precursors to magnetic ceramic materials. Indeed, the polymers can be readily metallized to give metal complexes **295** (Figure 54). Pyrolyzation of the organometallic polymers at  $1200 \text{ }^\circ\text{C}$  under dry nitrogen produced ceramic products **296** in good yields.<sup>579</sup> The morphologies of the ceramics are characterized by SEM and TEM techniques. As can be seen from the TEM images of the ceramics given in panels B–E of Figure 54, the metallic nanoparticles are wrapped by carbonaceous coats and dispersed in carbonaceous matrices.

Powder XRD patterns (Figure 55A) assisted by XPS and energy-dispersion X-ray (EDX) analyses indicate that the nanoparticles comprise Co and  $\text{Co}_2\text{Si}$  nanocrystallites covered by carbonaceous species. Figure 55B shows the magnetization curves of ceramics **296(m)** at room temperature. It is known that Co is ferromagnetic but its oxides ( $\text{Co}_3\text{O}_4$  and  $\text{CoO}$ ) and silicide ( $\text{Co}_2\text{Si}$ ) are paramagnetic. Ceramic **296(4)** shows an  $M_s$  value of  $\sim 50 \text{ emu/g}$ , in agreement with its high content of ferromagnetic Co nanocrystallites (Figure 55A).<sup>579</sup> The carbonaceous shells may have well wrapped the Co crystallites and prevented them from being oxidized during and after the pyrolysis process. On the other hand, **296(2)** contains a larger amount of paramagnetic  $\text{Co}_2\text{Si}$  and a smaller amount of ferromagnetic Co and, thus, shows a lower  $M_s$  value ( $2.3 \text{ emu/g}$ ). The hysteresis loops of the magnetoceramics are small. The  $H_c$  values of **296(2)** and **296(4)** are  $0.14$  and  $0.30 \text{ kOe}$ , respectively, implying that they are soft magnetic materials.

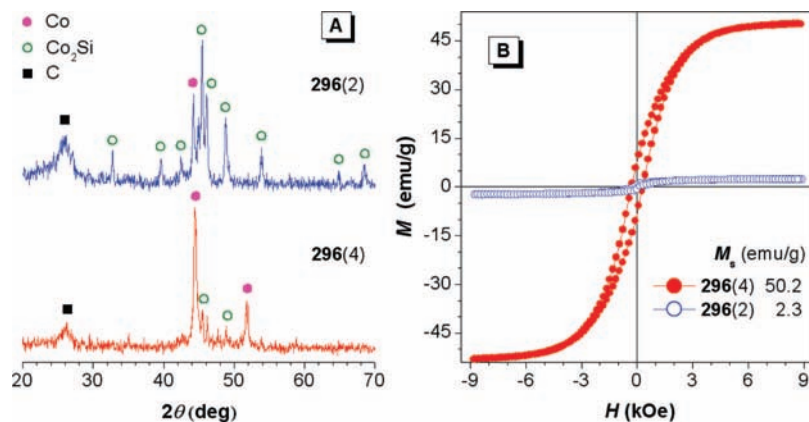
In the two magnetoceramic systems discussed above, the polymers are externally metallized through their complexations with transition-metal compounds. Tang and co-workers have also used internally metallized hyperbranched polymers as magnetoceramic precursors. Hyperbranched polymer **297**, for example, is an organometallic polymer, whose repeat unit or branch contains iron complex (ferrocene). Pyrolysis of



**Figure 53.** (A) Schematic representation of ceramization process and (B) plot of magnetization ( $M$ ) versus applied magnetic field ( $H$ ) at 300 K for magnetoceramic **294**. Inset in panel B: enlarged portions of the  $M$ – $H$  plot in the low-strength region of the applied magnetic field. Reproduced with permission from ref 45. Copyright 2004 American Chemical Society.



**Figure 54.** (A) Schematic representation of ceramization process. TEM images of magnetic ceramics of (B and C) **296(2)** and (D and E) **296(4)**. Reproduced with permission from ref 579. Copyright 2009 Springer.

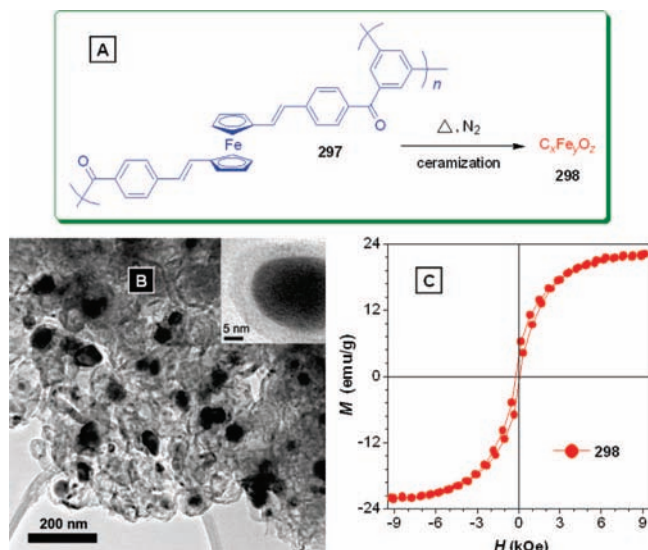


**Figure 55.** (A) XRD patterns and (B)  $M$ – $H$  plots for magnetoceramics **296(m)** at 298 K. Reproduced with permission from ref 579. Copyright 2009 Springer.

**297** under dry nitrogen readily transforms it into magnetic ceramic **298** (Figure 56A).<sup>566,580</sup> Composition analyses by XPS, EDX, and XRD indicate that the iron species in **298** exists mainly in the forms of  $\gamma$ - $\text{Fe}_2\text{O}_3$  and Fe. The latter does not segregate on the surface but rather forms in the bulk

inside the carbeneous matrix. The graphitization of amorphous carbon catalyzed by transition metals at high temperatures has been well-documented in the literature. It involves the formation of an intermediate compound of metal carbide, which then recrystallizes as metal crystals and graphite.





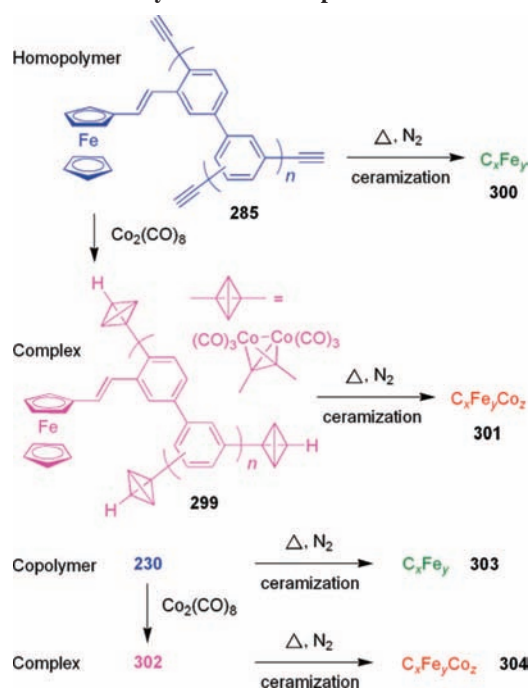
**Figure 56.** (A) Schematic representation of ceramization process for polymer **297** to ceramic **298**. (B) TEM images and (C) magnetization plot for ceramic **298** at 300 K. Inset in panel B: enlarged TEM image.

Indeed, the  $\alpha$ -Fe nanoparticles in the ceramic matrix catalyze the graphite crystallization during the pyrolytic process of **297**. An intense peak associated with the (002) reflection of graphite at  $2\theta = 26.4^\circ$  in the XRD patterns is observed. A relatively small amount of  $Fe_3C$  is also found in **298** as an intermediate of the crystallization, suggesting that the process of graphitization has not been completed.

The structure of the nanocrystallites in the ceramic was studied by high-resolution TEM. Figure 56B manifests that the iron-rich nanocrystallites are embedded in the abundant graphite matrix. Most of the Fe particles take irregular round shapes with sizes in the range of  $\sim 15$ – $25$  nm. From the enlarged image of one Fe nanoparticle shown in the inset of Figure 56B, the graphite can be identified with a lattice spacing of  $3.4 \text{ \AA}$ . The graphite ribbon appears to encapsulate the  $\alpha$ -Fe particles as a shell, which has functioned as a protective coating to prevent the nanoparticles from being oxidized. This observation further proves the proposed graphite formation catalyzed by the  $\alpha$ -Fe particles. The magnetization behavior of the ceramic is shown in Figure 56C. At 300 K, **298** exhibits an  $M_s$  value of  $\sim 22$  emu/g. This  $M_s$  value is relatively low, in comparison to that of the bulk  $\alpha$ -Fe ( $M_s$  up to  $\sim 222$  emu/g). This is understandable, because the iron content in the ceramic is relatively low, as can be estimated from the molecular formula of the precursor polymer **297**.

If a hyperbranched polymer is internally iron-rich and can meanwhile externally take up cobalt atoms through metal complexation, it will potentially furnish ceramic materials with very high magnetizability. Tang and co-workers explored this possibility.<sup>354</sup> As shown in Scheme 58, hyperbranched homopolymer **285** and copolymer **230** (cf., Scheme 48) are inherently iron-rich. Their complexations with  $Co_2(CO)_8$  yield organometallic complexes **299** and **302** containing both Fe and Co atoms. Pyrolyses of complexes **299** and **302** are expected to afford magnetoceramics **301** and **304** with  $M_s$  values higher than those of the ceramics **300** and **303** prepared from polymers **285** and **230**, respectively. As anticipated, the  $M_s$  values of magnetoceramics **301** and **304** from complexes **299** and **302** are 2.6- and 3.3-fold higher than those of **300** and **303** from parent polymers **285**

### Scheme 58. Ceramization of Metal-Containing Hyperbranched Polymers and Complexes

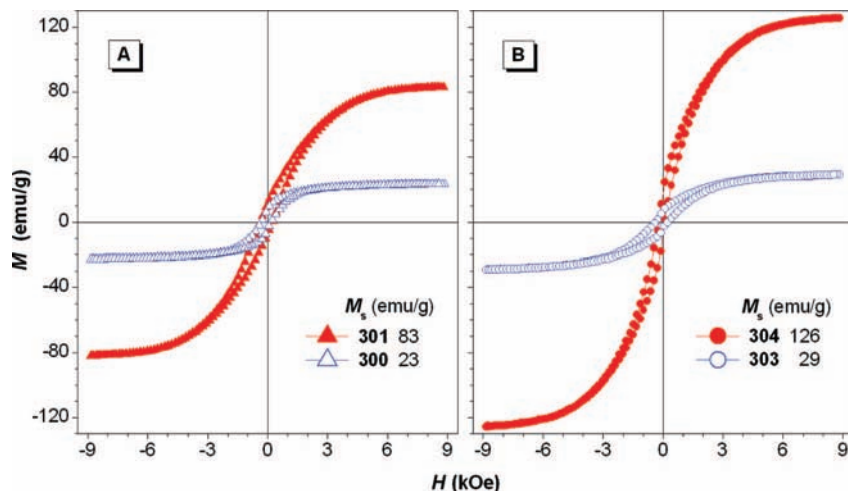


and **230**, respectively (Figure 57).<sup>354,545</sup> The  $M_s$  value of **303** is higher than that of **300** because the former contains more iron than the latter, as can be derived from the molecular formulas of their precursors **230** and **285**, respectively. This effect is amplified in the cases of ceramics **304** and **301**. It is remarkable that **304** shows an  $M_s$  value as high as 126 emu/g.

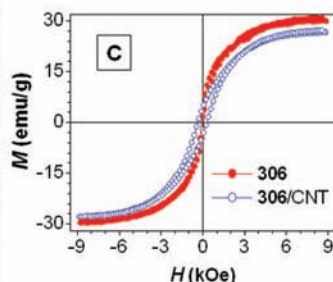
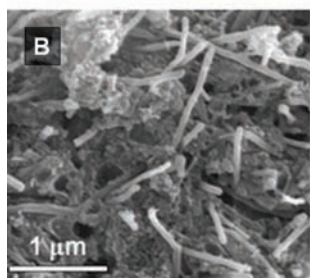
Ferrocene-containing PA **305** can efficiently wrap MWNTs to give processable **305**/CNT nanohybrid. Since **305** is a precursor to magnetic ceramics and CNT possesses excellent electrical conductivity, the ceramization product of **305**/CNT nanohybrid may be both magnetically susceptible and electrically conductive, which may find applications in giant magnetoresistance and spintronics systems.<sup>575</sup> Tang and co-workers have pyrolyzed polymer **305** and hybrid **305**/CNT under argon at  $1000^\circ\text{C}$  and obtained magnetoceramics **306** and **306**/CNT, respectively.<sup>431</sup> In the pyrolysis of the hybrid, magnetic ceramic is formed in the bulk matrix, with the CNTs well-dispersed within it (Figure 58B). This in turn confirms the uniform dispersion of the CNTs in the matrix of parent polymer **305**. The  $M_s$  values of ceramics **306** and **306**/CNT are 29.9 and 26.9 emu/g, respectively (Figure 58C). The  $M_s$  value of the **306**/CNT hybrid is among the best results reported so far for the magnetic nanocomposites obtained by attaching magnetic nanoparticles to CNTs.

### 4.11. Microfabrication and Nanomechanics

Advances in nanotechnology have led to the expansion of scope and techniques of microfabrication. Polymers have been widely used in the nanotechnology development. Acetylenic polymers have been found useful in several unique nanofabrication systems. For example, substituted PAs have been used to prepare separation membranes with molecular voids that show gas permeability superior to those of the most permeable conventional polymer membranes prepared from silicon rubbers.<sup>581</sup> The PAs with very bulky substituents are fabricated into membranes by a traditional casting technique, in which the evaporation of solvent



**Figure 57.**  $M$ – $H$  plots for magnetoceramics (A) **300** and **301** and (B) **303** and **304** at 300 K. Panels A and B are reproduced with permission from refs 354 and 545. Copyright 2007 and 2009 American Chemical Society, respectively.

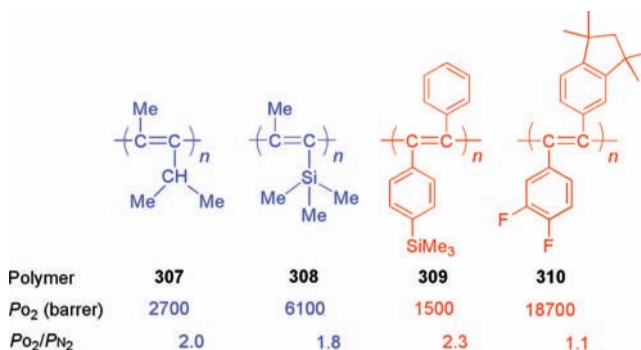


**Figure 58.** (A) Schematic representation of ceramization process. (B) SEM images and (C)  $M$ – $H$  plot for hybrid magnetoceramic **306**/CNT at 298 K. Reproduced with permission from ref 431. Copyright 2008 American Chemical Society.

molecules generates molecular-scale voids within the polymer membranes due to the very long relaxation time of the rigid PA chains. Mixed gas molecules pass through the membranes through entry into and exit out of the molecular voids with different retention times, thereby leading to gas separation in high permeation rates. This remarkable feature is attributed to the large free volumes in the polymer membranes originating from the stiff polyene backbone, bulky pendant groups, and low cohesive energy structure of the substituted PAs.

Some examples of substituted PAs with high gas permeabilities are shown in Chart 13. The oxygen permeability coefficient ( $PO_2$ ) of **307** is 2700 barrers and its separation factor of oxygen against nitrogen ( $PO_2/PN_2$ ) is 2.0. When the isopropyl pendant in **307** is replaced by a bulkier trimethylsilyl group, the resultant poly(1-trimethylsilyl-1-propyne) (**308**) exhibits an even higher  $PO_2$  value, although its  $PO_2/PN_2$  value is decreased. The discovery of this very high oxygen permeability (6100 barrers) for **308** by the research group of Higashimura and Masuda in 1983<sup>582</sup> has

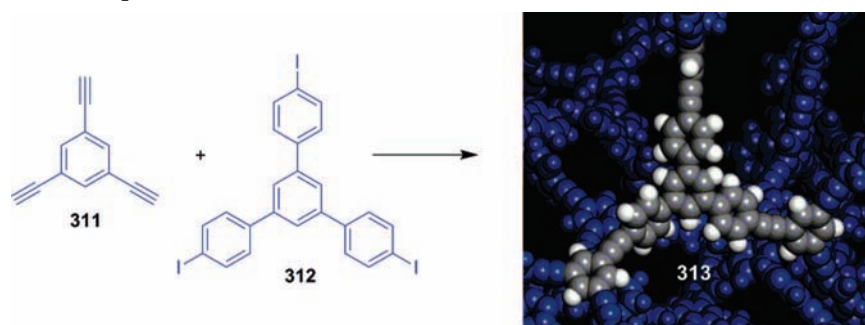
**Chart 13.** Examples of Oxygen Permeability ( $PO_2$ ) and Selectivity ( $PO_2/PN_2$ ) of PA Membranes



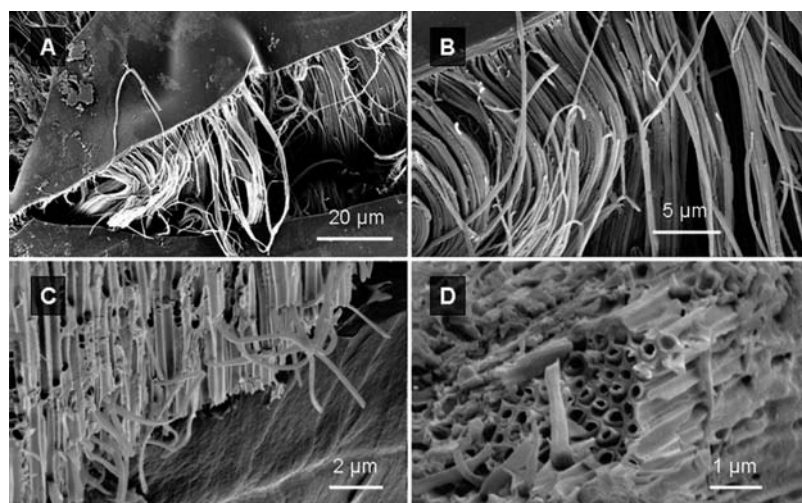
triggered a surge of interest in the design and syntheses of substituted PAs with bulky substituent groups in an effort to develop even more permeable polymers. Poly(diphenylacetylene) derivatives with bulky spherical substituents, e.g., poly[1-phenyl-2-(4-trimethylsilylphenyl)acetylene] (**309**), are another group of substituted PAs that show excellent gas permeabilities, in addition to high thermal stabilities. Recently, Masuda's group has succeeded in the synthesis of an indan-containing poly(diphenylacetylene) derivative (**310**) with a huge  $PO_2$  value (18700 barrers).<sup>583</sup> This polymer is the most oxygen-permeable polymer among all existing polymers.

Cooper et al. have fabricated a series of rigid, three-dimensional, microporous PAE networks by using Sonogashira–Hagihara coupling reactions. The molecular voids in the PAE networks are readily created and rigidly held by the connection of stiff aromatic rings in the three-dimensional space. Polymer **313** prepared from the polycondensing of arylacetylene **311** with aryltriiodide **312** enjoys a large apparent Brunauer–Emmett–Teller surface area of 1018  $m^2/g$  and a high hydrogen gas uptake of 155  $cm^3/g$  ( $\sim 1.4$  wt %) at 77.3 K (Scheme 59).<sup>584</sup> This network polymer is chemically and thermally very stable and retains its microporosity structure under various conditions. It thus has the potential to be used as a gas-storage medium.

In the two examples discussed above, the fine microstructures are generated at the molecular level. Nanostructured materials have also been fabricated from acetylenic polymers. For example, Sun, Tang, and co-workers have created three-dimensional polymer nanostructures by carrying out in situ

Scheme 59. Fabrication of Microporous PAE Networks<sup>a</sup>

<sup>a</sup> Reproduced with permission from ref 584. Copyright 2008 American Chemical Society

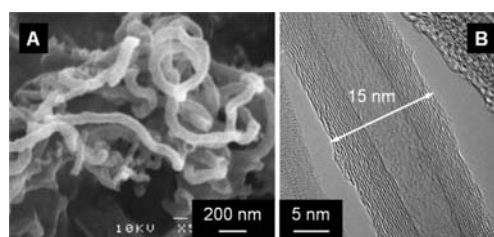


**Figure 59.** SEM micrographs of the nanotubes of *hb*-PAA **194** prepared inside an AAO template with a pore size of  $\sim 250$  nm. Magnification is sequentially increased from panel A to panel D to reveal the fine details of the nanotube structure. Reproduced with permission from ref 113. Copyright 2007 Elsevier.

diyne polymerizations in the presence of an anodic aluminum oxide (AAO) template.<sup>113</sup> The nanostructured polymers are released by breakage or dissolution of the AAO template in aqueous sodium hydroxide solutions. Typical examples of the SEM images of *hb*-PAA **194** (cf., Scheme 43) are shown in Figure 59. The nanostructured polymers adopt the shapes and sizes of the pores of the template and form micrometer-long nanotubes, as can be clearly seen from the image given in Figure 59D.

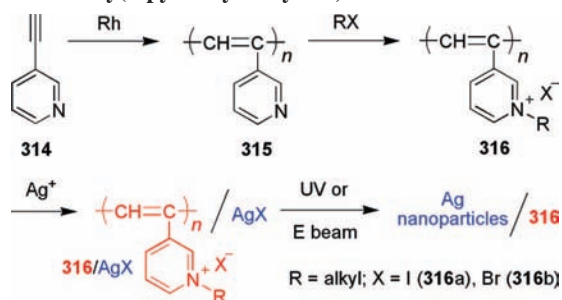
Metallic species such as iron, nickel, and cobalt are known to catalyze the growth of CNTs in the chemical vapor deposition (CVD) processes. Because of the ready thermal curability of *hb*-PDYs, spin-coated thin film of organometallic polymer **124d**(Co) is envisioned to prevent the metallic nanoclusters from agglomerating in the CVD process and, hence, to provide nanoscopic catalyst seeds for the CNT growth. This proves to be the case. Tang and co-workers have grown uniform bundles of MWNTs by a CVD process at 700 °C with acetylene gas as the carbon source.<sup>541</sup> The diameters and lengths of the CNTs are alterable by varying the surface activation and growth time. Thanks to the hyperbranched carbon-rich backbone structure and the thus-achieved suppression to the agglomeration of the metallic catalyst seeds, the diameters of the CNTs are small in size ( $\sim 15$  nm) and uniform in size distribution (Figure 60).

Metal-polymer nanocomposites have the potential to combine the existing characteristic properties of their components as well as to generate new properties arising



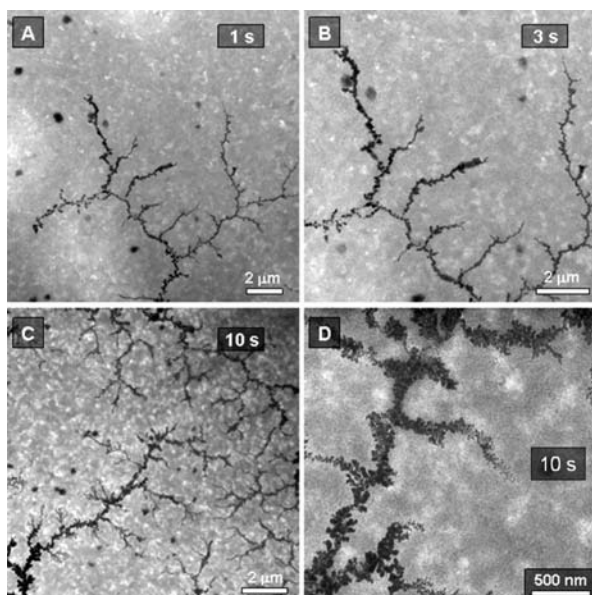
**Figure 60.** (A) SEM and (B) TEM microphotographs of the CNTs prepared by a CVD process at 700 °C on the silicon wafers spin-coated with thin films of organometallic polymer **134**. Reproduced with permission from ref 541. Copyright 2007 The Royal Society of Chemistry.

from the molecular interactions between the two components. Silver-polymer nanocomposites have attracted much attention due to their broad application in catalysis, electronics, optics, photonics, and even biology (biocide). In situ fabrication of silver-polymer nanocomposites is a preferred approach because it can help suppress the detrimental aggregation of the nanoparticles. Nonconjugated polyelectrolytes have usually been used as polymer matrices, in which silver cationic precursors are dispersed and then subjected to controlled chemical or photochemical reduction. In contrast, conjugated polyelectrolytes have been much less explored as polymer matrices. Recently, Sun, Tang, and co-workers have used conjugated PA-based polyelectrolyte **316**, which is derived from the ionization of poly(3-pyridinylacetylene) **315**, as a matrix to host

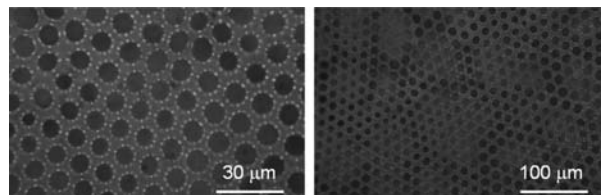
**Scheme 60. Fabrication of Silver Nanoparticles in the Matrix of Poly(3-pyridinylacetylene) Salt**


silver nanoparticles with the aim of achieving controlled fabrication of silver nanoparticles by external stimuli (Scheme 60). The formation of the silver nanoparticles is triggered by the flux of incident UV light or electron beam. Figure 61 shows the TEM images of AgI/316a nanocomposite after exposure to electron beams for the specific periods of time. It can be seen that the amount of silver nanoparticles is greatly increased with lengthening the irradiation time, eventually leading to an interconnected silver network in the conjugated polymer matrix. Such a nanodimensional network structure is expected to endow the nanocomposite with high and anisotropic electrical conductivity.

Besides the structures at the nanometer levels, “big” structures of micrometer scale have also been fabricated from the acetylenic polymers by macroscopic processing techniques. For example, the self-assembling of *hb*-PDY 124d by a simple breath-figure process furnishes nicely ordered, micrometer-sized structures.<sup>113,585</sup> Figure 62 shows the photographs of the patterned structures of 124d fabricated by Tang and co-workers by blowing a stream of moist air over its CS<sub>2</sub> solutions. Hexagonally ordered hollow bubble arrays with an average void size of  $\sim 10 \mu\text{m}$  are obtained over a large area.<sup>113</sup> The honeycomb patterns obtained from the breath-figure process are light-emitting when photoexcited by UV light and can thus potentially be used as the active layers in the fabrication of advanced optical and photonic devices.



**Figure 61.** (A–C) TEM images of AgI/316a after exposure to electron beams for specific periods of time. (D) Magnified image of panel C.



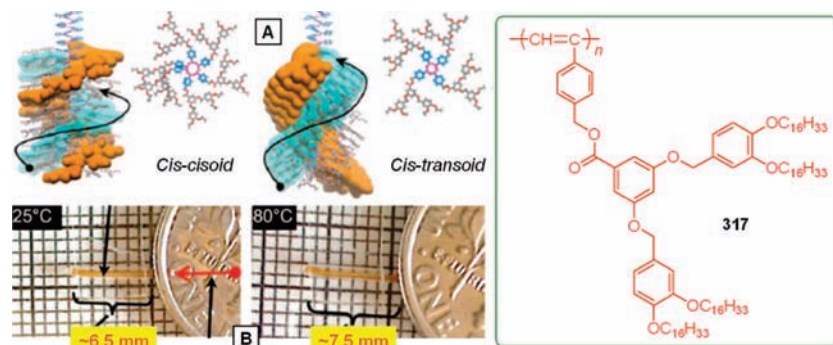
**Figure 62.** Optical micrographs of breath figures of *hb*-PDY 124d obtained by blow-drying its CS<sub>2</sub> solutions in a stream of moist air. Reproduced with permission from ref 113. Copyright 2007 Elsevier.

Inspired by the nanomechanical functions of natural systems, many research groups are working on the development of artificial molecular nanomachines, e.g., molecular muscles<sup>586</sup> and nanomotors,<sup>587</sup> in the expectation that the work done by microscopic events can be translated into macroscopic outputs. The self-organizable dendronized PPA derivatives developed by Percec and co-workers offer a suitable architecture for the construction of molecular nanomachines capable of expressing their motions in the large length scale. The polyene backbone of the dendronized helical *cis*-PPA derivative 317 undergoes the reversible macroscopic extension and contraction resulting from the thermally reversible *cisoidal*-to-*transoidal* conformational isomerization.<sup>588</sup> As shown in Figure 63, the conformation of the backbone of 317 changes from *cis-cisoidal* to *cis-transoidal* when the temperature is increased from 25 to 80 °C. This microscopic change in the polymer conformation brings about an expansion in the polyene backbone. Macroscopically, the oriented fiber of 317 is capable of conducting a mechanical work by displacing a dime up to 250 times its mass. This example demonstrates that a single macromolecule can function as a nanomechanical actuator.

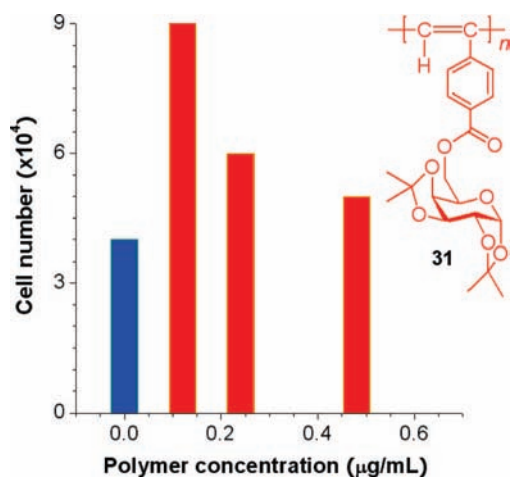
## 4.12. Biological Activity

Decorating the PA backbones with the pendants of naturally occurring building blocks may impart biocompatibility to the  $\pi$ -conjugated polymers. The wrapping of the unnatural polymer chains by the natural molecular coats may result in the “naturalization” of the synthetic polymers, thereby generating cytophilic molecular wires. Tang and co-workers have systematically investigated the cytotoxicity of a series of PPA derivatives bearing pendant groups of natural origin (amino acids, sugars, nucleosides, etc.) and found them all biocompatible. The bioactivity data for a sugar-containing PPA derivative (31) is plotted in Figure 64.<sup>208</sup> The HeLa cells were subcultured onto the microtiter plates, into which a THF solution of 31 was added a few hours after the cells had been seeded. The cells were stained with trypan blue and counted with a hemocytometer. As can be seen from Figure 64, in the presence of a small amount of polymer 31, the cells grow faster. At a polymer concentration of 0.12  $\mu\text{g/mL}$ , the cell population is 20-fold higher than that of the control where the polymer concentration is zero, although the cell growth returns to normal when the polymer concentration is increased. This indicates that the polymer is cytophilic and can stimulate the growth of the living cells at a low polymer feed.<sup>208</sup>

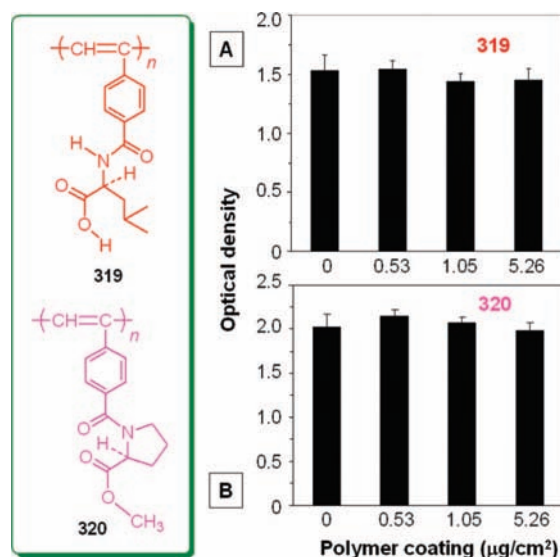
Figure 65 shows the biocompatibility data of a PPA derivative decorated by *L*-alanine pendants (318).<sup>66</sup> The HeLa cells were subcultured onto the microtiter plates precoated with polymer 318, and the adhesion and growth of the living cells were monitored on an optical microscope. After incubation for one day, the cells were found to adhere to, and grow



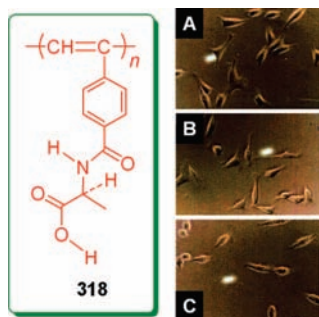
**Figure 63.** (A) Self-organizable dendronized helical chains of PPA derivative **317** with *cis-cisoid* and *cis-transoid* conformations. (B) Images showing the expansion and contraction of the oriented fibers of **317** at macroscopic scale by the lift of a dime on the inclined plane. Reproduced with permission from ref 588. Copyright 2008 American Chemical Society.



**Figure 64.** Growth of living HeLa cells in the incubation media containing polymer **31** with different concentrations. Reproduced with permission from ref 208. Copyright 2007 American Chemical Society.



**Figure 66.** Growth of HeLa cells on the microtiter plates precoated with polymers (A) **319** and (B) **320** after three-days incubation.



**Figure 65.** HeLa cell adhesion to the microtiter plates precoated with different amounts of **318** (μg/cm<sup>2</sup>): (A) 0 (control), (B) 15.8, and (C) 22.2. Cell incubation time: 1 day. Reproduced with permission from ref 66. Copyright 2008 American Chemical Society.

on, the plates as they did in the control experiment, in which the plates without the polymer coatings were used. The polymer exhibited no toxicity to the cells; that is to say, it was biocompatible. Even when the polymer coating density was increased to as high as  $\sim 22$  mg/cm<sup>2</sup>, no dead cells were found throughout the experiment, demonstrative of excellent cytocompatibility of the polymer. Similar results were obtained for the PPA derivatives carrying other amino acid pendants, such as **319** and **320** (Figure 66). This proves that the incorporation of the naturally occurring building blocks into the PA structure is a versatile strategy for conferring biocompatibility on the conjugated polymers.

## 5. Summary and Perspective

In this review, we have given a broad overview of the polymer chemistry based on carbon–carbon triple bonds and the structures and properties of the acetylenic polymers, including the development of new polymerization techniques for polymer syntheses, understanding of multilevel structures of the acetylenic polymers, and exploration of their advanced functional properties. Although the acetylenic polymer research has been started much later than the studies of vinyl polymers, remarkable progress has been made in this area in the past few decades. As a result, acetylenic molecules have been developed into a group of versatile monomers with multifaceted reactivities and rich polymerization behaviors, and acetylenic polymers have emerged as a new family of advanced materials with novel structures and unique functionalities.

We now understand that the triple-bonded acetylenic molecules are all-around players with multiple talents, which can function as unsaturated and multifunctional monomers to undergo various linear and nonlinear polymerization processes, including metathesis, coupling, addition, and cyclization reactions. The utilization of rich chemistry of the acetylenic monomers has enabled the design and synthesis of a great diversity of acetylenic macromolecules with desired structures, under the condition that monomer structures and catalyst systems are judiciously matched.

The repeat units of the acetylenic polymers can be composed of olefinic double bonds with geometric isomerisms, isolated or interconnected triple bonds, chiral centers with stereoisomerisms, heteroatoms with polarity variations, heterocyclics with regioisomerisms, aromatic rings with varying substitution numbers and positions, etc. The topological structures of the polymers can be linear (one-dimensional) or nonlinear (three-dimensional), mainly determined by the selections of the monomeric building blocks (monoynes, diynes, triynes, etc.) and the choices of the construction strategies or synthetic routes ( $A_2 + B_2$ ,  $AB_2$ ,  $A_2$ ,  $A_2 + B_3$ ,  $A_3$ , etc.). It is worth pointing out that the newly developed polymerization technique using the sole  $A_2$ -type diyne monomers offers a facile tool for the design and synthesis of new hyperbranched polymers. In addition to the efforts devoted to the creation of acetylenic polymers with diverse primary structures, the studies of their secondary and higher-order structures have resulted in the generation of polymers with miscellaneous conformations (e.g., helical chains) and morphologies (e.g., nanofibers) and the development of methods and processes to modulate the hierarchical structures of the polymers internally and externally.

The structural tunability by the internal perturbations (e.g., monomer structure design) and external stimuli (temperature, solvent, pH, UV irradiation, electrical field, etc.) have enabled the researchers to develop a large variety of acetylenic polymers with an array of advanced functional properties, such as electrical conductivity, photoconductivity, liquid crystallinity, photo- or electroluminescence, optical nonlinearity, helical chirality, molecular recognition, light refractivity, thermal chromatism, photonic patternability, soft magnetism, nanomechanical actuation, and biological activity. Some of these unique properties are derived from their inherent unsaturated electronic structures and are thus very difficult to access by the conventional electronically saturated polymers. These special functionalities make the acetylenic polymers promising candidate materials for practical applications as solid-state light emitters, fluorescence sensors, chiral probes, optical power limiters, luminescent photoreists, magnetic coating, nanostructured catalysts, cytophilic tissue-engineering scaffolds, and so forth.

Although the study of acetylenic polymers is still a relatively young area of research, many examples have already manifested the remarkable advantages of the acetylenic polymers over their counterparts of conventional polymers and demonstrated their great potentials in advancing polymer chemistry to new territories and generating new specialty materials with advanced functionalities. It is envisioned that the field of acetylenic polymer research will expand buoyantly. The advances in the acetylene chemistry in the recent decades have brought about many new triple-bond reactions, some of which may be utilized or further developed into new polymerization techniques for the syntheses of new acetylenic polymers. During the process of developing new polymerization techniques and synthesizing new acetylenic polymers, new models, mechanisms, concepts, and theories will be proposed and verified, new phenomena, properties, and functions will be discovered, and new structure–reactivity–property relationships will be established. Looking into the future of the research area, we see a vista of limitless promise. New species of acetylenic polymers with unusual structures may be created, which may show functionalities well beyond our imagination.

## 6. Acknowledgments

This work was partly supported by the Research Grants Council of Hong Kong (603509, 603008, 601608, 602707, 602706, CUHK2/CRF/08, and HKU2/05C), the National Natural Science Foundation of China (20634020), and the Ministry of Science & Technology of China (2009CB623605). B.Z.T. thanks the support from the Cao Guangbiao Foundation of Zhejiang University.

## 7. References

- (1) Hiemenz, P. C.; Lodge, T. P. *Polymer Chemistry*; CRC Press: Boca Raton, FL, 2007.
- (2) Simon, E. *Ann. Chim. Phys.* **1839**, *31*, 265.
- (3) Saunders, K. J. *Organic Polymer Chemistry: An Introduction to Organic Chemistry of Adhesives, Paints, Plastics, and Rubbers*; Chaman and Hall: London, 1973.
- (4) Staudinger, H. *Ber. Dtsch. Chem. Ges.* **1920**, *53*, 1073.
- (5) Carothers, W. H. *Chem. Rev.* **1931**, *8*, 353.
- (6) Carraher, C. E. *Seymour/Carraher's Polymer Chemistry*; CRC Press: Boca Raton, FL, 2008.
- (7) Braunecker, W. A.; Matyjaszewski, K. *Prog. Polym. Sci.* **2008**, *33*, 165.
- (8) Yoon, Y.; Ho, R. M.; Li, F. M.; Leland, M. E.; Park, J. Y.; Cheng, S. Z. D.; Percec, V.; Chu, P. W. *Prog. Polym. Sci.* **1997**, *22*, 765.
- (9) Natta, G.; Mazzanti, G.; Corradini, P. *Atti, Accad. Naz. Lincei, Rend. Classe Sci. Fis. Mat. Nat.* **1958**, *25*, 3.
- (10) *Modern Acetylene Chemistry*; Stang, P. J., Diederich, F., Ed.; VCH: Weinheim, Germany, 1995.
- (11) Brandsma, L. *Preparative Acetylenic Chemistry*, 2nd ed.; Elsevier: Amsterdam, The Netherlands, 1988.
- (12) *The Chemistry of Triple-Bonded Functional Groups*; Patai, S., Rappoport, Z., Ed.; Wiley: New York, 1983.
- (13) Shirakawa, H.; Louis, E. J.; MacDiarmid, A. G.; Chiang, C. K.; Heeger, A. J. *J. Chem. Soc., Chem. Commun.* **1977**, 578.
- (14) Shirakawa, H. *Angew. Chem., Int. Ed.* **2001**, *40*, 2575.
- (15) MacDiarmid, A. G. *Angew. Chem., Int. Ed.* **2001**, *40*, 2581.
- (16) Heeger, A. J. *Angew. Chem., Int. Ed.* **2001**, *40*, 2591.
- (17) Simionescu, C.; Dumitres, S.; Percec, V. *Makromol. Chem.* **1971**, *150*, 95.
- (18) Masuda, T.; Hasegawa, K. I.; Higashimura, T. *Macromolecules* **1974**, *7*, 728.
- (19) Schermer, W.; Wegner, G. *Makromol. Chem.* **1974**, *175*, 667.
- (20) Kang, E. T.; Ehrlich, P.; Bhatt, A.; Anderson, W. *Macromolecules* **1984**, *17*, 1020.
- (21) Tang, B. Z.; Kotera, N. *Macromolecules* **1989**, *22*, 4388.
- (22) Masuda, T.; Hamano, T.; Tsuchihara, K.; Higashimura, T. *Macromolecules* **1990**, *23*, 1374.
- (23) Xu, Z.; Kahr, M.; Walker, K. L.; Wilkins, C. L.; Moore, J. S. *J. Am. Chem. Soc.* **1994**, *116*, 4537.
- (24) Kishimoto, Y.; Eckerle, P.; Miyatake, T.; Ikariya, T.; Noyori, R. *J. Am. Chem. Soc.* **1994**, *116*, 12131.
- (25) Lee, H.-J.; Gal, Y.-S.; Lee, W.-C.; Oh, J.-M.; Jin, S.-H.; Choi, S.-K. *Macromolecules* **1995**, *28*, 1208.
- (26) Nishide, H.; Kaneko, T.; Nii, T.; Katoh, K.; Tsuchida, E.; Lahti, P. M. *J. Am. Chem. Soc.* **1996**, *118*, 9695.
- (27) Yashima, E.; Matsushima, T.; Okamoto, Y. *J. Am. Chem. Soc.* **1997**, *119*, 6345.
- (28) Francke, V.; Mangel, T.; Mullen, K. *Macromolecules* **1998**, *31*, 2447.
- (29) Akaqgi, K.; Piao, G.; Kaneko, S.; Sakamaki, K.; Shirakawa, H.; Kyotani, M. *Science* **1998**, *282*, 1683.
- (30) Aoki, T.; Kobayashi, Y.; Kaneko, T.; Oikawa, E.; Yamamura, Y.; Fujita, Y.; Teraguchi, M.; Nomura, R.; Masuda, T. *Macromolecules* **1999**, *32*, 79.
- (31) Koltzenburg, S.; Stelzer, F.; Nyuken, O. *Makromol. Chem. Phys.* **1999**, *200*, 821.
- (32) Brizius, G.; Pschirer, N. G.; Steffen, W.; Stitzer, K.; zur Loye, H. C.; Bunz, U. H. F. *J. Am. Chem. Soc.* **2000**, *122*, 12435.
- (33) Tang, B. Z.; Chen, H.; Lam, W. Y.; Wang, M. *Chem. Mater.* **2000**, *12*, 213.
- (34) Liu, Y.; Mills, R. C.; Boncella, J. M.; Schanze, K. S. *Langmuir* **2001**, *17*, 7452.
- (35) Lu, Y. F.; Yang, Y.; Sellinger, A.; Lu, M. C.; Huang, J. M.; Fan, H. Y.; Haddad, R.; Lopez, G.; Burns, A. R.; Sasaki, D. Y.; Shelnut, J.; Brinker, C. J. *Nature* **2001**, *410*, 913.
- (36) Li, B. S.; Cheuk, K. K. L.; Salhi, F.; Lam, J. W. Y.; Cha, J. A. K.; Xiao, X.; Bai, C.; Tang, B. Z. *Nano Lett.* **2001**, *1*, 323.
- (37) Gao, G. Z.; Sanda, F.; Masuda, T. *Macromolecules* **2003**, *36*, 3932.
- (38) Schermer, O. A.; Rutenberg, I. M.; Grubbs, R. H. *J. Am. Chem. Soc.* **2003**, *125*, 8515.

- (39) Cheng, Y. J.; Liang, H.; Luh, T. Y. *Macromolecules* **2003**, *36*, 5912.
- (40) Li, B. S.; Cheuk, K. K. L.; Ling, L.; Chen, J.; Xiao, X.; Bai, C.; Tang, B. Z. *Macromolecules* **2003**, *36*, 77.
- (41) Li, B. S.; Chen, J.; Zhu, C. F.; Leung, K. K. L.; Wan, L.; Bai, C.; Tang, B. Z. *Langmuir* **2004**, *20*, 2515.
- (42) Wu, P.; Feldman, A. K.; Nugent, A. K.; Hawker, C. J.; Scheel, A.; Voit, B.; Pyun, J.; Frechet, J. M. J.; Sharpless, K. B.; Fokin, V. V. *Angew. Chem., Int. Ed.* **2004**, *43*, 3928.
- (43) Scheel, A. J.; Komber, H.; Voit, B. I. *Macromol. Rapid Commun.* **2004**, *25*, 1175.
- (44) Smet, M.; Metten, K.; Dehaen, W. *Collect. Czech. Chem. Commun.* **2004**, *69*, 1097.
- (45) Häussler, M.; Zheng, R.; Lam, J. W. Y.; Tong, H.; Dong, H.; Tang, B. Z. *J. Phys. Chem. B* **2004**, *108*, 10645.
- (46) Díaz, D. D.; Punna, S.; Holzer, P.; McPherson, A. K.; Sharpless, K. B.; Fokin, V. V.; Finn, M. G. *J. Polym. Sci., Part A: Polym. Chem.* **2004**, *42*, 4392.
- (47) Malkoch, M.; Thibault, R. J.; Drockenmüller, E.; Messerschmidt, M.; Voit, B.; Russell, T. P.; Hawker, C. J. *J. Am. Chem. Soc.* **2005**, *127*, 14942.
- (48) van Steenis, D. J. V. C.; David, O. R. P.; van Strijdonck, G. P. F.; van Maarseveen, J. H.; Reek, J. N. H. *Chem. Commun.* **2005**, 4333.
- (49) Ye, C.; Xu, G.; Yu, Z.; Lam, J. W. Y.; Jang, J.; Peng, H.; Tu, Y.; Liu, Z.; Jeong, K. U.; Cheng, S. Z. D.; Chen, E. Q.; Tang, B. Z. *J. Am. Chem. Soc.* **2005**, *127*, 7668.
- (50) Wosnick, J. H.; Mello, C. M.; Swager, T. M. *J. Am. Chem. Soc.* **2005**, *127*, 3400.
- (51) Liu, Y.; Wang, N.; Li, Y.; Liu, H.; Li, Y.; Xiao, J.; Xu, X.; Huang, C.; Cui, S.; Zhu, D. *Macromolecules* **2005**, *38*, 4880.
- (52) Percec, V.; Aqad, E.; Peterca, M.; Rudick, J. G.; Lemon, L.; Ronda, J. C.; De, B. B.; Heiney, P. A.; Meijer, E. W. *J. Am. Chem. Soc.* **2006**, *128*, 16365.
- (53) Li, Z.; Li, Q.; Qin, A.; Dong, Y.; Lam, J. W. Y.; Dong, Y.; Ye, C.; Qin, J.; Tang, B. Z. *J. Polym. Sci., Part A: Polym. Chem.* **2006**, *44*, 5672.
- (54) Yin, S.; Xu, H.; Su, X.; Li, G.; Song, Y.; Lam, J.; Tang, B. Z. *J. Polym. Sci., Part A: Polym. Chem.* **2006**, *44*, 2346.
- (55) Knapton, D.; Rowan, S. J.; Weder, C. *Macromolecules* **2006**, *39*, 651.
- (56) Fukushima, T.; Takachi, K.; Tsuchihara, K. *Macromolecules* **2006**, *39*, 3103.
- (57) Mayershofer, M. G.; Nuyken, O.; Buchmeiser, M. R. *Macromolecules* **2006**, *39*, 2452.
- (58) Zhao, X.; Pinto, M. R.; Hardison, L. M.; Mwaura, J.; Müller, J.; Jiang, H.; Witker, D.; Kleiman, V. D.; Reynolds, J. R.; Schanze, K. S. *Macromolecules* **2006**, *39*, 6355.
- (59) Bakbak, S.; Leech, P. J.; Carson, B. E.; Saxena, S.; King, W. P.; Bunz, U. H. F. *Macromolecules* **2006**, *39*, 6793.
- (60) Murata, H.; Miyajima, D.; Nishide, H. *Macromolecules* **2006**, *39*, 6331.
- (61) Nakahashi, A.; Fujita, M.; Miyoshi, E.; Umeyama, T.; Naka, K.; Chujo, Y. *J. Polym. Sci., Part A: Polym. Chem.* **2007**, *45*, 3580.
- (62) Otsuka, I.; Hongo, T.; Nakade, H.; Narumi, A.; Sakai, R.; Satoh, T.; Kaga, H.; Kakuchi, T. *Macromolecules* **2007**, *40*, 8930.
- (63) Qin, A.; Jim, C. K. W.; Lu, W.; Lam, J. W. Y.; Häussler, M.; Dong, Y.; Sung, H. H. Y.; Williams, I. D.; Wong, G. K. L.; Tang, B. Z. *Macromolecules* **2007**, *40*, 2308.
- (64) Scriban, C.; Schrock, R. R.; Muller, P. *Organometallics* **2008**, *27*, 6202.
- (65) Matsumi, N.; Chujo, Y. *Polym. J.* **2008**, *40*, 77.
- (66) Cheuk, K. K. L.; Li, B. S.; Lam, J. W. Y.; Xie, Y.; Tang, B. Z. *Macromolecules* **2008**, *41*, 5997.
- (67) Wong, W.-Y.; Zhou, G.-J.; He, Z.; Cheung, K.-Y.; Ng, A. M.-C.; Djurisic, A. B.; Chan, W.-K. *Macromol. Chem. Phys.* **2008**, *209*, 1319.
- (68) Kwak, G.; Jin, S.-H.; Park, J.-W.; Gal, Y.-S. *Macromol. Chem. Phys.* **2008**, *209*, 1769.
- (69) Karim, M. A.; Cho, Y.-Y.; Park, J. S.; Ryu, T. I.; Lee, M. J.; Song, M.; Jin, S.-H.; Lee, J. W.; Gal, Y.-S. *Macromol. Chem. Phys.* **2008**, *209*, 1967.
- (70) Yoon, J.; Kim, J.-M. *Macromol. Chem. Phys.* **2008**, *209*, 2194.
- (71) Qin, A.; Lam, J. W. Y.; Jim, C. K. W.; Zhang, L.; Yan, J.; Häussler, M.; Liu, J.; Dong, Y.; Liang, D.; Chen, E.; Jia, G.; Tang, B. Z. *Macromolecules* **2008**, *41*, 3808.
- (72) Xie, J.; Hu, L.; Shi, W.; Deng, X.; Cao, Z.; Shen, Q. *Polym. Int.* **2008**, *57*, 965.
- (73) Yeh, M. Y.; Luh, T. Y. *Chem. Asian J.* **2008**, *3*, 1620.
- (74) Kwak, G.; Lee, W.-E.; Jeong, H.; Sakaguchi, T.; Fujiki, M. *Macromolecules* **2009**, *42*, 20.
- (75) Deng, J.; Chen, B.; Luo, X.; Yang, W. *Macromolecules* **2009**, *42*, 933.
- (76) Kumar, P. S.; Wurst, K.; Buchmeiser, M. R. *J. Am. Chem. Soc.* **2009**, *131*, 387.
- (77) Tang, Y.; Zhou, Z.; Ogawa, K.; Lopez, G. P.; Schanze, K. S.; Whitten, D. G. *Langmuir* **2009**, *25*, 21.
- (78) Dei, S.; Matsumoto, A. *Macromol. Chem. Phys.* **2009**, *210*, 11.
- (79) Kaneko, T.; Horie, T.; Matsumoto, S.; Teraguchi, M.; Aoki, T. *Macromol. Chem. Phys.* **2009**, *210*, 22.
- (80) Yang, S.-H.; Huang, C.-H.; Chen, C.-H.; Hsu, C.-S. *Macromol. Chem. Phys.* **2009**, *210*, 37.
- (81) Qin, A.; Tang, L.; Lam, J. W. Y.; Jim, C. K. W.; Yu, Y.; Zhao, H.; Sun, J. Z.; Tang, B. Z. *Adv. Funct. Mater.* **2009**, *19*, 1891.
- (82) Qin, A.; Lam, J. W. Y.; Tang, L.; Jim, C. K. W.; Zhao, H.; Sun, J. Z.; Tang, B. Z. *Macromolecules* **2009**, *42*, 1421.
- (83) Kokado, K.; Chujo, Y. *Macromolecules* **2009**, *42*, 1418.
- (84) Zhou, D.; Chen, Y.; Chen, L.; Zhou, W.; He, X. *Macromolecules* **2009**, *42*, 1454.
- (85) Chen, J. W.; Cao, Y. *Macromol. Rapid Commun.* **2007**, *28*, 1714.
- (86) Voit, B. *J. Polym. Sci., Part A: Polym. Chem.* **2005**, *43*, 2679.
- (87) Tomalia, D. A. *Prog. Polym. Sci.* **2005**, *30*, 294.
- (88) Yates, C. R.; Hayes, W. *Eur. Polym. J.* **2004**, *40*, 1257.
- (89) Gao, C.; Yan, D. *Prog. Polym. Sci.* **2004**, *29*, 183.
- (90) Hecht, S. *J. Polym. Sci., Part A: Polym. Chem.* **2003**, *41*, 1047.
- (91) Kim, Y. H. *J. Polym. Sci., Part A: Polym. Chem.* **1998**, *36*, 1685.
- (92) Simionescu, C. I.; Percec, V. *Prog. Polym. Sci.* **1982**, *8*, 133.
- (93) Choi, S. K.; Gal, Y. S.; Jin, S. H.; Kim, H. K. *Chem. Rev.* **2000**, *100*, 1645.
- (94) Bunz, U. H. F. *Chem. Rev.* **2000**, *100*, 1605.
- (95) Watson, M. D.; Fechtenkotter, A.; Mullen, K. *Chem. Rev.* **2001**, *101*, 1267.
- (96) Hill, D. J.; Mio, M. J.; Prince, R. B.; Hughes, T. S.; Moore, J. S. *Chem. Rev.* **2001**, *101*, 3893.
- (97) Tang, B. Z. *Polym. News* **2001**, *26*, 262.
- (98) Cheuk, K. L.; Li, B. S.; Tang, B. Z. *Curr. Trends Polym. Sci.* **2002**, *7*, 41.
- (99) Lam, J. W. Y.; Tang, B. Z. *J. Polym. Sci., Part A: Polym. Chem.* **2003**, *41*, 2607.
- (100) Zhao, D. H.; Moore, J. S. *Chem. Commun.* **2003**, 807.
- (101) Yamamoto, T. *Synlett* **2003**, 425.
- (102) Mayershofer, M. G.; Nuyken, O. *J. Polym. Sci., Part A: Polym. Chem.* **2005**, *43*, 5723.
- (103) Wong, W. Y. *J. Inorg. Organomet. Polym. Mater.* **2005**, *15*, 197.
- (104) Nielsen, M. B.; Diederich, F. *Chem. Rev.* **2005**, *105*, 1837.
- (105) Lam, J. W. Y.; Tang, B. Z. *Acc. Chem. Res.* **2005**, *38*, 745.
- (106) Iwasaki, T.; Nishide, H. *Curr. Org. Chem.* **2005**, *9*, 1665.
- (107) Furstner, A.; Davies, P. W. *Chem. Commun.* **2005**, 2307.
- (108) Voskerician, G.; Weder, C. *Adv. Polym. Sci.* **2005**, *177*, 209.
- (109) Luh, T. Y.; Cheng, Y. J. *Chem. Commun.* **2006**, 4669.
- (110) Rudick, J. G.; Percec, V. *New J. Chem.* **2007**, *31*, 1083.
- (111) Masuda, T. *J. Polym. Sci., Part A: Polym. Chem.* **2007**, *45*, 165.
- (112) Häussler, M.; Tang, B. Z. *Adv. Polym. Sci.* **2007**, *209*, 1.
- (113) Häussler, M.; Qin, A.; Tang, B. Z. *Polymer* **2007**, *48*, 6181.
- (114) Li, C.; Li, Y. *Macromol. Chem. Phys.* **2008**, *209*, 1541.
- (115) Swager, T. M. *Acc. Chem. Res.* **2008**, *41*, 1181.
- (116) Rudick, J. G.; Percec, V. *Acc. Chem. Res.* **2008**, *41*, 1641.
- (117) Yashima, E.; Maeda, K.; Furusho, Y. *Acc. Chem. Res.* **2008**, *41*, 1166.
- (118) Tang, B. Z. *Macromol. Chem. Phys.* **2008**, *209*, 1303.
- (119) Sanchez, J. C.; Troglor, W. C. *Macromol. Chem. Phys.* **2008**, *209*, 1528.
- (120) Akagi, K.; Mori, T. *Chem. Rec.* **2008**, *8*, 395.
- (121) Kivala, M.; Diederich, F. *Acc. Chem. Res.* **2009**, *42*, 235.
- (122) Grimsdale, A. C.; Chan, K. L.; Martin, R. E.; Jokisz, P. G.; Holmes, A. B. *Chem. Rev.* **2009**, *109*, 897.
- (123) Little, W. A. *J. Polym. Sci., Part C: Polym. Symp.* **1967**, *17*, 3.
- (124) Wiley, R. H.; Lee, J. Y. *Macromol. Sci., Chem.* **1970**, *4*, 203.
- (125) Ehrlich, P.; Kern, R. J.; Pierron, E. D.; Provder, T. *J. Polym. Sci., Part B: Polym. Lett.* **1967**, *5*, 911.
- (126) Simionescu, C. I.; Dumitrescu, S. *Plaste Kautsch.* **1968**, *15*, 84.
- (127) Ito, T.; Shirakawa, H.; Ikeda, S. *J. Polym. Sci., Part A: Polym. Chem.* **1974**, *12*, 11.
- (128) Chiang, C. K.; Fincher, C. R.; Park, Y. W.; Heeger, A. J.; Shirakawa, H.; Louis, E. J.; Gau, S. C.; MacDiarmid, A. G. *Phys. Rev. Lett.* **1977**, *39*, 1098.
- (129) Berlin, A. A.; Cerkašin, M. I. *Vysokomol. Soedin.* **1971**, *13*, 2298.
- (130) Simionescu, C.; Dumitrescu, S.; Percec, V. *Polym. J.* **1976**, *8*, 139.
- (131) Simionescu, C.; Dumitrescu, S.; Percec, V. *Polym. J.* **1976**, *8*, 313.
- (132) Dumitrescu, S.; Percec, V.; Simionescu, C. I. *J. Polym. Sci., Part A: Polym. Chem.* **1977**, *15*, 2893.
- (133) Simionescu, C. I.; Percec, V.; Dumitrescu, S. *J. Polym. Sci., Part A: Polym. Chem.* **1977**, *15*, 2497.
- (134) Kern, R. J. *J. Polym. Sci., Part A: Polym. Chem.* **1969**, *7*, 621.
- (135) Holob, G.; Errlich, P.; Allendoerfer, R. D. *Macromolecules* **1972**, *5*, 569.
- (136) Masuda, T.; Higashimura, T. *Acc. Chem. Res.* **1984**, *17*, 51.
- (137) Masuda, T.; Yamamoto, K.; Higashimura, T. *Polymer* **1982**, *23*, 1663.

- (138) Masuda, T.; Kuwane, Y.; Higashimura, T. *J. Polym. Sci., Part A: Polym. Chem.* **1982**, *20*, 1043.
- (139) Masuda, T.; Yamagata, M.; Higashimura, T. *Macromolecules* **1984**, *17*, 126.
- (140) Xu, K.; Peng, H.; Lam, J. W. Y.; Poon, T. W. H.; Dong, Y.; Xu, H.; Sun, Q.; Cheuk, K. K. L.; Salhi, F.; Lee, P. P. S.; Tang, B. Z. *Macromolecules* **2000**, *33*, 6918.
- (141) Masuda, T.; Sasaki, N.; Higashimura, T. *Macromolecules* **1975**, *8*, 717.
- (142) Katz, T. J.; Lee, S. J. *J. Am. Chem. Soc.* **1980**, *102*, 423.
- (143) Katz, T. J.; Hacker, S. M.; Kendrick, R. D.; Yannoni, C. S. *J. Am. Chem. Soc.* **1985**, *107*, 2182.
- (144) Wallace, K. C.; Liu, A. H.; Davis, W. M.; Schrock, R. R. *Organometallics* **1989**, *8*, 644.
- (145) Schrock, R. R.; Luo, S. F.; Zanetti, N. C.; Fox, H. H. *Organometallics* **1994**, *13*, 3396.
- (146) Schrock, R. R.; Luo, S.; Lee, J. C., Jr.; Zanetti, N. C.; Davis, W. M. *J. Am. Chem. Soc.* **1996**, *118*, 3883.
- (147) Kern, R. J. *J. Polym. Sci., Part A: Polym. Chem.* **1969**, *7*, 621.
- (148) Furlani, A.; Napoletano, C.; Russo, M. V. *J. Polym. Sci., Part A: Polym. Chem.* **1989**, *27*, 75.
- (149) Yang, W.; Tabata, M.; Kobayashi, S.; Yokota, K.; Shimizu, A. *Polym. J.* **1991**, *23*, 1135.
- (150) Kanki, K.; Misumi, Y.; Masuda, T. *Macromolecules* **1999**, *32*, 2384.
- (151) Kishimoto, Y.; Itou, M.; Miyatake, T.; Ikariya, T.; Noyori, R. *Macromolecules* **1995**, *28*, 6662.
- (152) Tang, B. Z.; Poon, W. H.; Leung, S. M.; Leung, W. H.; Peng, H. *Macromolecules* **1997**, *30*, 2209.
- (153) Masuda, T.; Mouri, T.; Higashimura, T. *Bull. Chem. Soc. Jpn.* **1980**, *53*, 1152.
- (154) Cotton, F. A.; Hall, W. T.; Cann, K. J.; Karol, F. J. *Macromolecules* **1981**, *14*, 233.
- (155) Masuda, T.; Takahashi, T.; Higashimura, T. *Macromolecules* **1985**, *18*, 311.
- (156) Niki, A.; Masuda, T.; Higashimura, T. *J. Polym. Sci., Part A: Polym. Chem.* **1987**, *25*, 1553.
- (157) Tang, B. Z.; Kong, X.; Wan, X.; Feng, X. D. *Macromolecules* **1997**, *30*, 5620.
- (158) Sanda, F.; Yukawa, Y.; Masuda, T. *Polymer* **2004**, *45*, 849.
- (159) Maeda, K.; Goto, H.; Yashima, E. *Macromolecules* **2001**, *34*, 1160.
- (160) Saito, M. A.; Maeda, K.; Onouchi, H.; Yashima, E. *Macromolecules* **2000**, *33*, 4616.
- (161) Yuan, W. Z.; Tang, L.; Zhao, H.; Jin, J. K.; Sun, J. Z.; Qin, A. J.; Xu, H. P.; Liu, J. H.; Yang, F.; Zheng, Q.; Chen, E. Q.; Tang, B. Z. *Macromolecules* **2009**, *42*, 52.
- (162) Tang, B. Z.; Kong, X.; Wan, X.; Feng, X.-D.; Kwok, H. S. *Macromolecules* **1998**, *31*, 2419.
- (163) Kong, X.; Lam, J. W. Y.; Tang, B. Z. *Macromolecules* **1999**, *32*, 1722.
- (164) Lam, W.; Dong, Y.; Cheuk, K. L.; Luo, J.; Kwok, H.; Tang, B. Z. *Macromolecules* **2002**, *35*, 1229.
- (165) Lam, W. Y.; Dong, Y.; Tang, B. Z. *Macromolecules* **2002**, *35*, 8288.
- (166) Yuan, W.; Sun, J. Z.; Dong, Y.; Häussler, M.; Yang, F.; Xu, H. P.; Qin, A.; Lam, J. W. Y.; Zheng, Q.; Tang, B. Z. *Macromolecules* **2006**, *39*, 8011.
- (167) Yuan, W. Z.; Zhao, H.; Xu, H. P.; Sun, J. Z.; Lam, J. W. Y.; Mao, Y.; Jin, J. K.; Zhang, S.; Zheng, Q.; Tang, B. Z. *Acta Polym. Sin.* **2007**, *10*, 901.
- (168) Hua, J.; Li, Z.; Lam, J. W. Y.; Xu, H.; Sun, J.; Dong, Y.; Dong, Y.; Qin, A.; Yuan, W.; Chen, H.; Wang, M.; Tang, B. Z. *Macromolecules* **2005**, *38*, 8127.
- (169) Xu, H.; Sun, J.; Qin, A.; Hua, J.; Li, Z.; Dong, Y.; Xu, H.; Yuan, W.; Ma, Y.; Wang, M.; Tang, B. Z. *J. Phys. Chem. B* **2006**, *110*, 21701.
- (170) Xu, H.; Xie, B.-Y.; Yuan, W.; Sun, J.-Z.; Yang, F.; Dong, Y.; Qin, A.; Zhang, S.; Wang, M.; Tang, B. Z. *Chem. Commun.* **2007**, 1322.
- (171) Xu, H.; Jin, J. K.; Mao, Y.; Sun, J. Z.; Yang, F.; Yuan, W.; Dong, Y. Q.; Wang, M.; Tang, B. Z. *Macromolecules* **2008**, *41*, 3874.
- (172) Yin, S.; Xu, H.; Shi, W.; Gao, Y.; Song, Y.; Lam, J. W. Y.; Tang, B. Z. *Polymer* **2005**, *46*, 7670.
- (173) Moad, G.; Rizzardo, E.; Thang, S. H. *Acc. Chem. Res.* **2008**, *41*, 1133.
- (174) Goethals, E. J.; Du Prez, F. *Prog. Polym. Sci.* **2007**, *32*, 220.
- (175) Domski, G. J.; Rose, J. M.; Coates, G. W.; Bolig, A. D.; Brookhart, M. *Prog. Polym. Sci.* **2007**, *32*, 30.
- (176) Bielawski, C. W.; Grubbs, R. H. *Prog. Polym. Sci.* **2007**, *1*.
- (177) Fournier, D.; Hoogenboom, R.; Schubert, U. S. *Chem. Soc. Rev.* **2007**, *36*, 1369.
- (178) Tsarevsky, N. V.; Matyjaszewski, K. *Chem. Rev.* **2007**, *107*, 2270.
- (179) Smid, J.; Van Beylen, M.; Hogen-Esch, T. E. *Prog. Polym. Sci.* **2006**, *31*, 1041.
- (180) Kamigaito, M.; Ando, T.; Sawamoto, M. *Chem. Rev.* **2001**, *101*, 3689.
- (181) Asandei, A. D.; Percec, V. *J. Polym. Sci., Part A: Polym. Chem.* **2001**, *39*, 3392.
- (182) Mayershofner, M. G.; Nuyken, O. *J. Polym. Sci., Part A: Polym. Chem.* **2005**, *43*, 5723.
- (183) Masuda, T.; Yoshimura, T.; Fujimori, J.; Higashimura, T. *J. Chem. Soc., Chem. Commun.* **1987**, 1805.
- (184) Kunzler, J.; Percec, V. *Polym. Prepr.* **1988**, *29*, 80.
- (185) Yoshimura, T.; Masuda, T.; Higashimura, T. *Macromolecules* **1988**, *21*, 1899.
- (186) Masuda, T.; Yoshimura, T.; Higashimura, T. *Macromolecules* **1989**, *22*, 3804.
- (187) Kunzler, J.; Percec, V. *J. Polym. Sci., Part A: Polym. Chem.* **1990**, *28*, 1221.
- (188) Kunzler, J.; Percec, V. *J. Polym. Bull.* **1992**, *29*, 335.
- (189) Masuda, T.; Mishima, K.; Fujimori, J.; Nishida, M.; Muramatsu, H.; Higashimura, T. *Macromolecules* **1992**, *25*, 1401.
- (190) Hayano, S.; Masuda, T. *Macromolecules* **1998**, *31*, 3170.
- (191) Hayano, S.; Masuda, T. *Macromolecules* **1999**, *32*, 7344.
- (192) Kaneshiro, H.; Hayano, S.; Masuda, T. *Macromol. Chem. Phys.* **1999**, *200*, 113.
- (193) Kubo, H.; Hayano, S.; Misumi, Y.; Masuda, T. *Macromol. Chem. Phys.* **2002**, *203*, 279.
- (194) Kishimoto, Y.; Miyatake, T.; Ikariya, T.; Noyori, R. *Macromolecules* **1996**, *29*, 5054.
- (195) Kishimoto, Y.; Eckerle, P.; Miyatake, T.; Kainosho, M.; Ono, A.; Ikariya, T.; Noyori, R. *J. Am. Chem. Soc.* **1999**, *121*, 12035.
- (196) Misumi, Y.; Masuda, T. *Macromolecules* **1998**, *31*, 7572.
- (197) Miyake, M.; Misumi, Y.; Masuda, T. *Macromolecules* **2000**, *33*, 6636.
- (198) Saeed, I.; Shiotaki, M.; Masuda, T. *Macromolecules* **2006**, *39*, 8567.
- (199) Tong, H.; Lam, J. W. Y.; Häussler, M.; Tang, B. Z. *Polym. Prepr.* **2004**, *45*, 835.
- (200) Hua, J. L.; Lam, J. W. Y.; Li, Z.; Qin, A. J.; Sun, J. Z.; Dong, Y. Q.; Dong, Y. P.; Tang, B. Z. *J. Polym. Sci., Part A: Polym. Chem.* **2006**, *44*, 3538.
- (201) Li, Z.; Dong, Y. Q.; Häussler, M.; Lam, J. W. Y.; Dong, Y. P.; Wu, L. J.; Wong, K. S.; Tang, B. Z. *J. Phys. Chem. B* **2006**, *110*, 2302.
- (202) Li, Z.; Dong, Y. Q.; Qin, A. J.; Lam, J. W. Y.; Dong, Y. P.; Yuan, W. Z.; Sun, J. Z.; Hua, J. L.; Wong, K. S.; Tang, B. Z. *Macromolecules* **2006**, *39*, 467.
- (203) Li, Z.; Li, Q. Q.; Qin, A. J.; Dong, Y. Q.; Lam, J. W. Y.; Dong, Y.; Ye, C.; Qiin, J.; Tang, B. Z. *J. Polym. Sci., Part A: Polym. Chem.* **2006**, *44*, 5672.
- (204) Zeng, Q.; Li, Z.; Li, Z.; Ye, C.; Qin, J.; Tang, B. Z. *Macromolecules* **2007**, *40*, 5634.
- (205) Zeng, Q.; Cai, P.; Li, Z.; Qin, J. G.; Tang, B. Z. *Chem. Commun.* **2008**, 1094.
- (206) Zeng, Q.; Lam, J. W. Y.; Jim, C. K. W.; Qin, A. J.; Qin, J. G.; Li, Z.; Tang, B. Z. *J. Polym. Sci., Part A: Polym. Chem.* **2008**, *46*, 8070.
- (207) Zeng, Q.; Zhang, L. Y.; Li, Z.; Qin, J. G.; Tang, B. Z. *Polymer* **2009**, *50*, 434.
- (208) Cheuk, K. K. L.; Lam, J. W. Y.; Li, B. S.; Xie, Y.; Tang, B. Z. *Macromolecules* **2007**, *40*, 2633.
- (209) Buchmeiser, M. R. *Adv. Polym. Sci.* **2005**, *176*, 89.
- (210) Fox, H. H.; Schrock, R. R. *Organometallics* **1992**, *11*, 2763.
- (211) Fox, H. H.; Wolf, M. O.; Odell, R.; Lin, B. L.; Schrock, R. R.; Wrighton, M. S. *J. Am. Chem. Soc.* **1994**, *116*, 2827.
- (212) Schattenmann, F. J.; Schrock, R. R. *Macromolecules* **1996**, *29*, 8990.
- (213) Schattenmann, F. J.; Schrock, R. R.; Davis, W. M. *J. Am. Chem. Soc.* **1996**, *118*, 3295.
- (214) Anders, U.; Nuyken, O.; Wurst, K.; Buchmeiser, M. R. *Angew. Chem., Int. Ed.* **2002**, *114*, 4226.
- (215) Anders, U.; Nuyken, O.; Wurst, K.; Buchmeiser, M. R. *Macromolecules* **2002**, *35*, 9029.
- (216) Kumar, P. S.; Wurst, K.; Buchmeiser, M. R. *J. Am. Chem. Soc.* **2009**, *131*, 387.
- (217) Law, C. C. W.; Lam, J. W. Y.; Dong, Y. P.; Tong, H.; Tang, B. Z. *Macromolecules* **2005**, *38*, 660.
- (218) Schrock, R. R.; Clark, D. N.; Sancho, J.; Wengrovius, J. H.; Rocklage, S. M.; Pedersen, S. F. *Organometallics* **1982**, *1*, 1645.
- (219) Listemann, M. L.; Schrock, R. R. *Organometallics* **1985**, *4*, 74.
- (220) Krouse, S. A.; Schrock, R. R. *Macromolecules* **1989**, *22*, 2569.
- (221) Zhang, X. P.; Bazan, G. C. *Macromolecules* **1994**, *27*, 4627.
- (222) Weiss, K.; Michel, A.; Auth, E. M.; Bunz, U. H. F.; Mangel, T.; Müllen, K. *Angew. Chem., Int. Ed.* **1997**, *36*, 506.
- (223) Bunz, U. H. F. *Acc. Chem. Res.* **2001**, *34*, 998.
- (224) Hay, A. S. *J. Polym. Sci., Part A: Polym. Chem.* **1998**, *36*, 505.
- (225) Hay, A. S. *J. Org. Chem.* **1960**, *25*, 637.
- (226) Newkirk, A. E.; McDonald, R. S.; Hay, A. S. *J. Polym. Sci., Part A: Polym. Chem.* **1964**, *2*, 2217.
- (227) Hay, A. S.; Bolon, D. A.; Leimer, K. R. *J. Polym. Sci., Part A: Polym. Chem.* **1970**, *8*, 1022.
- (228) Hay, A. S.; Bolon, D. A.; Leimer, K.; Clark, R. F. *J. Polym. Sci., Part B: Polym. Phys.* **1970**, *8*, 97.



- (229) Diederich, F. *Chem. Commun.* **2001**, 219.
- (230) Diederich, F. *Nature* **1994**, 369, 199.
- (231) Anthony, J.; Boudon, C.; Diederich, F.; Gisselbrecht, J. P.; Gramlich, V.; Gross, M.; Hobi, M.; Seiler, P. *Angew. Chem., Int. Ed.* **1994**, 33, 763.
- (232) Sonogashira, K.; Tohda, Y.; Hagihara, N. *Tetrahedron Lett.* **1975**, 16, 4467.
- (233) Yang, J. S.; Swager, T. M. *J. Am. Chem. Soc.* **1998**, 120, 11864.
- (234) Kim, J.; McQuade, D. T.; McHugh, S. K.; Swager, T. M. *Angew. Chem., Int. Ed.* **2000**, 39, 3868.
- (235) Kumaraswamy, S.; Bergstedt, T.; Shi, X. B.; Rininsland, F.; Kushon, S.; Xia, W. S.; Ley, K.; Achyuthan, K.; McBranch, D.; Whitten, D. *Proc. Natl. Acad. Sci. U.S.A.* **2004**, 101, 7511.
- (236) Tan, C.; Pinto, M. R.; Kose, M. E.; Ghiviriga, I.; Schanze, K. S. *Adv. Mater.* **2004**, 16, 1208.
- (237) Jiang, H.; Zhao, X.; Schanze, K. S. *Langmuir* **2006**, 22, 5541.
- (238) Kim, I. B.; Wilson, J. N.; Bunz, U. H. F. *Chem. Commun.* **2005**, 1273.
- (239) Wong, W. Y. *Dalton Trans.* **2007**, 4495.
- (240) Tyler McQuade, D.; Pullen, A. E.; Swager, T. M. *Chem. Rev.* **2000**, 100, 2537.
- (241) Thomas III, S. W.; Joly, G. D.; Swager, T. M. *Chem. Rev.* **2007**, 107, 1339.
- (242) Mangel, T.; Eberhardt, A.; Scherf, U.; Bunz, U. H. F.; Müllen, K. *Macromol. Rapid Commun.* **1995**, 16, 571.
- (243) Weder, C.; Sarwa, C.; Montali, A.; Bastiaansen, G.; Smith, P. *Science* **1998**, 279, 835.
- (244) Montali, A.; Bastiaansen, G.; Smith, P.; Weder, C. *Nature* **1998**, 392, 261.
- (245) Pinto, M. R.; Schanze, K. S. *Proc. Natl. Acad. Sci. U.S.A.* **2004**, 101, 7505.
- (246) Rininsland, F.; Xia, W. S.; Wittenburg, S.; Shi, X. B.; Stankewicz, C.; Achyuthan, K.; McBranch, D.; Whitten, D. *Proc. Natl. Acad. Sci. U.S.A.* **2004**, 101, 15295.
- (247) Fan, Q.-L.; Zhou, Y.; Lu, X.-M.; Hou, X.-Y.; Huang, W. *Macromolecules* **2005**, 38, 2927.
- (248) Wegner, G. *Z. Naturforsch., Teil B.* **1969**, 24, 824.
- (249) Wegner, G. *Makromol. Chem.* **1972**, 154, 35.
- (250) Tieke, B.; Lieser, G.; Wegner, G. *J. Polym. Sci., Part A: Polym. Chem.* **1979**, 17, 1631.
- (251) Wegner, G. *Mol. Cryst. Liq. Cryst.* **1979**, 52, 535.
- (252) Day, D.; Ringsdorf, H. *J. Polym. Sci., Part B: Polym. Phys.* **1978**, 16, 205.
- (253) Bader, H.; Ringsdorf, H.; Skura, J. *Angew. Chem., Int. Ed.* **1981**, 20, 91.
- (254) Lauher, J. W.; Fowler, F. W.; Goroff, N. S. *Acc. Chem. Res.* **2008**, 41, 1215.
- (255) Baughman, R. H. *J. Polym. Sci., Part B: Polym. Phys.* **1974**, 12, 1511.
- (256) Sun, A.; Lauher, J. W.; Goroff, N. S. *Science* **2006**, 312, 1030.
- (257) Fowler, F. W.; Lauher, J. W. *J. Phys. Org. Chem.* **2000**, 13, 850.
- (258) Mueller, A.; O'Brien, D. F. *Chem. Rev.* **2002**, 102, 727.
- (259) Zhou, W.; Li, Y.; Zhu, D. *Chem. Asian J.* **2007**, 2, 222.
- (260) Okada, S.; Peng, S.; Spevak, W.; Charych, D. *Acc. Chem. Res.* **1998**, 31, 229.
- (261) Korshak, V. V.; Medvedeva, T. V.; Ovchinnikov, A. A.; Spektor, V. N. *Nature* **1987**, 326, 370.
- (262) Shutt, J. D.; Rickert, S. E. *Langmuir* **1987**, 3, 460.
- (263) Chu, B.; Xu, R. L. *Acc. Chem. Res.* **1991**, 24, 384.
- (264) Ahn, D. J.; Kim, J. M. *Acc. Chem. Res.* **2008**, 41, 805.
- (265) Carpick, R. W.; Sasaki, D. Y.; Marcus, M. S.; Eriksson, M. A.; Burns, A. R. *J. Phys.: Condens. Matter* **2004**, 16, 679.
- (266) Xiao, Y.; Wong, R. A.; Son, D. Y. *Macromolecules* **2000**, 33, 7232.
- (267) Kwak, G.; Masuda, T. *Macromol. Rapid Commun.* **2002**, 23, 68.
- (268) Guo, A.; Fry, B. E.; Neckers, D. C. *Chem. Mater.* **1998**, 10, 531.
- (269) Pang, Y.; Ijadi-Maghsoodi, S.; Barton, T. J. *Macromolecules* **1993**, 26, 5671.
- (270) Sanchez, J. C.; DiPasquale, A. G.; Rheingold, A. L.; Trogler, W. C. *Chem. Mater.* **2007**, 19, 6459.
- (271) Tamao, K.; Uchida, M.; Izumizawa, T.; Kenji, F.; Yamaguchi, S. *J. Am. Chem. Soc.* **1996**, 118, 11974.
- (272) Speier, J. L.; Webster, J. A.; Barnes, G. H. *J. Am. Chem. Soc.* **1957**, 79, 974.
- (273) Son, D. Y.; Bucca, D.; Keller, T. M. *Tetrahedron Lett.* **1996**, 37, 1579.
- (274) Korshak, V. V.; Sladkov, A. M.; Luneva, L. K. *Izv. Akad. Nauk SSSR. Otd. Khim. Nauk* **1962**, 2251.
- (275) Kim, D. S.; Shim, S. C. *J. Polym. Sci., Part A: Polym. Chem.* **1999**, 37, 2263.
- (276) Sanchez, J. C.; Urbas, S. A.; Toal, S. J.; DiPasquale, A. G.; Rheingold, A. L.; Trogler, W. C. *Macromolecules* **2008**, 41, 1237.
- (277) Kim, D. S.; Shim, S. C. *J. Polym. Sci., Part A: Polym. Chem.* **1999**, 37, 2933.
- (278) Chen, R. M.; Chien, K. M.; Wong, K. T.; Jin, B. Y.; Luh, T. Y.; Hsu, J. H.; Fann, W. S. *J. Am. Chem. Soc.* **1997**, 119, 11321.
- (279) Mori, A.; Takahisa, E.; Kajiro, H.; Nishihara, Y.; Hiyama, T. *Macromolecules* **2000**, 33, 1115.
- (280) Sumiya, K.-I.; Kwak, G.; Sanda, F.; Masuda, T. *J. Polym. Sci., Part A: Polym. Chem.* **2004**, 42, 2774.
- (281) Corriu, R. J.-P.; Deforth, T.; Douglas, W. E.; Guerrero, G.; Siebert, W. S. *Chem. Commun.* **1998**, 963.
- (282) Matsumi, N.; Naka, K.; Chujo, Y. *J. Am. Chem. Soc.* **1998**, 120, 5112.
- (283) Truce, W. E.; Simms, J. A. *J. Am. Chem. Soc.* **1956**, 78, 2756.
- (284) McDonald, J. W.; Corbin, J. L.; Newton, W. E. *Inorg. Chem.* **1976**, 15, 9.
- (285) Nuniyasu, H.; Ogawa, A.; Sato, K. I.; Ryu, I.; Kambe, N.; Sonoda, N. *J. Am. Chem. Soc.* **1992**, 114, 5902.
- (286) Han, L.-B.; Zhang, C.; Yazawa, H.; Shimada, S. *J. Am. Chem. Soc.* **2004**, 126, 5080.
- (287) Cao, C. S.; Fraser, L. R.; Love, J. A. *J. Am. Chem. Soc.* **2005**, 127, 17614.
- (288) Shoai, S.; Bichler, P.; Kang, B.; Buckley, H.; Love, J. A. *Organometallics* **2007**, 26, 5778.
- (289) Ogawa, A.; Ikeda, T.; Kimura, K.; Hirao, T. *J. Am. Chem. Soc.* **1999**, 121, 5108.
- (290) Jim, C. K. W.; Qin, A.; Yuen, M. M. F.; Lam, J. W. Y.; Tang, B. Z. *Polym. Prepr.* **2009**, 50 (2), in press.
- (291) Oglaruso, M. A.; Becker, E. I. *J. Org. Chem.* **1965**, 30, 3354.
- (292) Ried, W.; Freitag, D. *Angew. Chem., Int. Ed.* **1968**, 7, 835.
- (293) Berresheim, A. J.; Müller, M.; Müllen, K. *Chem. Rev.* **1999**, 99, 1747.
- (294) Noren, G. K.; Stille, J. K. *Macromol. Rev.* **1971**, 5, 385.
- (295) Mukamal, H.; Harris, F. W.; Stille, J. K. *J. Polym. Sci., Part A: Polym. Chem.* **1967**, 1, 2721.
- (296) Huisgen, R. In *1,3-Dipolar Cycloaddition Chemistry*; Padwa, A., Ed.; Wiley: New York, 1984; p 1176.
- (297) Kolb, H. C.; Finn, M. G.; Sharpless, K. B. *Angew. Chem., Int. Ed.* **2001**, 40, 2004.
- (298) Rostovtsev, V. V.; Green, L. G.; Fokin, V. V.; Sharpless, K. B. *Angew. Chem., Int. Ed.* **2002**, 41, 2596.
- (299) Tornøe, C. W.; Christensen, C.; Meldal, M. *J. Org. Chem.* **2002**, 67, 3057.
- (300) Angell, Y. L.; Burgess, K. *Chem. Soc. Rev.* **2007**, 36, 1674.
- (301) Moses, J. E.; Moorhouse, A. D. *Chem. Soc. Rev.* **2007**, 36, 1249.
- (302) Bock, V. D.; Hiemstra, H.; van Maarseveen, J. H. *Eur. J. Org. Chem.* **2006**, 51.
- (303) Wang, Q.; Chittaboina, S.; Barnhill, H. N. *Lett. Org. Chem.* **2005**, 2, 136.
- (304) O'Reilly, R. K.; Joralemon, M. J.; Wooley, K. L.; Hawker, C. J. *Chem. Mater.* **2005**, 17, 5976.
- (305) Boldt, G. E.; Dickerson, T. J.; Janda, K. D. *Drug Disc. Today* **2006**, 11, 143.
- (306) Sohma, Y.; Kiso, Y. *ChemBioChem* **2006**, 7, 1549.
- (307) Braunschweig, A. B.; Dichtel, W. R.; Miljanic, O. S.; Olson, M. A.; Spruell, J. M.; Khan, S. I.; Heath, J. R.; Stoddart, J. F. *Chem. Asian J.* **2007**, 2, 634.
- (308) Fournier, D.; Hoogenboom, R.; Schubert, U. S. *Chem. Soc. Rev.* **2007**, 36, 1369.
- (309) Lutz, J. F. *Angew. Chem., Int. Ed.* **2007**, 46, 1018.
- (310) Voit, B. *New J. Chem.* **2007**, 31, 1139.
- (311) Binder, W. H.; Sachsenhofer, R. *Macromol. Rapid Commun.* **2007**, 28, 15.
- (312) Williams, C. K. *Chem. Soc. Rev.* **2007**, 36, 1573.
- (313) Golas, P. L.; Matyjaszewski, K. *QSAR Comb. Sci.* **2007**, 26, 1116.
- (314) Spain, S. G.; Gibson, M. I.; Cameron, N. R. *J. Polym. Sci., Part A: Polym. Chem.* **2007**, 45, 2059.
- (315) Barner, L.; Davis, T. P.; Stenzel, M. H.; Barner-Kowollik, C. *Macromol. Rapid Commun.* **2007**, 28, 539.
- (316) Yagci, Y.; Tasdelen, M. A. *Prog. Polym. Sci.* **2006**, 31, 1133.
- (317) Goodall, G. W.; Hayes, W. *Chem. Soc. Rev.* **2006**, 35, 280.
- (318) Hawker, C. J.; Wooley, K. L. *Science* **2005**, 309, 1200.
- (319) Wu, P.; Feldman, A. K.; Nugent, A. K.; Hawker, C. J.; Scheel, A.; Voit, B.; Pyun, J.; Fréchet, J. M. J.; Sharpless, K. B.; Fokin, V. V. *Angew. Chem., Int. Ed.* **2004**, 43, 3928.
- (320) Bharathi, P.; Moore, J. S. *Macromolecules* **2000**, 33, 3212.
- (321) Kim, C.; Chang, Y.; Kim, J. S. *Macromolecules* **1996**, 29, 6353.
- (322) Fomina, L.; Salcedo, R. *Polymer* **1996**, 37, 1723.
- (323) Dong, Y. Q.; Li, Z.; Lam, J. W. Y.; Dong, Y. P.; Feng, X. D.; Tang, B. Z. *Chin. J. Polym. Sci.* **2005**, 23, 665.
- (324) Li, Z.; Qin, A. J.; Lam, J. W. Y.; Dong, Y. P.; Dong, Y. Q.; Ye, C.; Williams, I. D.; Tang, B. Z. *Macromolecules* **2006**, 39, 1436.
- (325) Morgenroth, F.; Müllen, K. *Tetrahedron* **1997**, 53, 15349.
- (326) Li, Z.; Yu, G.; Hu, P.; Ye, C.; Liu, Y.; Qin, J.; Li, Z. *Macromolecules* **2009**, 42, 1589.
- (327) Korshak, V. V.; Sergeev, V. A.; Shitikov, V. K.; Volpin, M. E.; Kolomnikov, I. S. *Dokl. Akad. Nauk. SSSR* **1971**, 201, 112.

- (328) Tang, B. Z.; Xu, K.; Sun, Q.; Lee, P. P. S.; Peng, H.; Salhi, F.; Dong, Y. *ACS Symp. Ser.* **2000**, *760*, 146.
- (329) Lam, J. W. Y.; Luo, J.; Peng, H.; Xie, Z.; Xu, K.; Dong, Y.; Cheng, L.; Qiu, C.; Kwork, H. S.; Tang, B. Z. *Chin. J. Polym. Sci.* **2001**, *19*, 585.
- (330) Häussler, M.; Lam, J. W. Y.; Zheng, Y.; Peng, H.; Luo, J.; Chen, J.; Law, C. C. W.; Tang, B. Z. *C. R. Chim.* **2003**, *196*, 289.
- (331) Lam, J. W. Y.; Chen, J.; Law, C. C. W.; Peng, H.; Xie, Z.; Cheuk, K. K. L.; Kwork, H. S.; Tang, B. Z. *Macromol. Symp.* **2003**, *196*, 289.
- (332) Häussler, M.; Dong, H. C.; Lam, J. W. Y.; Zheng, R. H.; Qin, A. J.; Tang, B. Z. *Chin. J. Polym. Sci.* **2005**, *23*, 567.
- (333) Xu, K. T.; Tang, B. Z. *Chin. J. Polym. Sci.* **1999**, *17*, 397.
- (334) Xu, K.; Peng, H.; Sun, Q.; Dong, Y.; Salhi, F.; Luo, J.; Chen, J.; Huang, Y.; Zhang, D.; Xu, Z.; Tang, B. Z. *Macromolecules* **2002**, *35*, 5821.
- (335) Chen, J.; Peng, H.; Law, C. C. W.; Dong, Y.; Lam, J. W. Y.; Williams, I. D.; Tang, B. Z. *Macromolecules* **2003**, *36*, 4319.
- (336) Lam, J. W. Y.; Chen, J.; Law, C. C. W.; Peng, H.; Xie, Z.; Cheuk, K. K. L.; Kwok, H. S.; Tang, B. Z. *Macromol. Symp.* **2003**, *196*, 289.
- (337) Peng, H.; Luo, J.; Cheng, L.; Lam, J. W. Y.; Xu, K.; Dong, Y.; Zhang, D.; Huang, Y.; Xu, Z.; Tang, B. Z. *Opt. Mater.* **2003**, *21*, 315.
- (338) Xie, Z.; Peng, H.; Lam, J. W. Y.; Chen, J.; Zheng, Y.; Qiu, C.; Kwok, H. S.; Tang, B. Z. *Macromol. Symp.* **2003**, *195*, 179.
- (339) Häussler, M.; Chen, J.; Lam, J. W. Y.; Tang, B. Z. *J. Nonlinear Opt. Phys. Mater.* **2004**, *13*, 335.
- (340) Law, C. C. W.; Chen, J.; Lam, J. W. Y.; Peng, H.; Tang, B. Z. *J. Inorg. Organomet. Polym. Mater.* **2004**, *14*, 39.
- (341) Peng, H.; Dong, H. C.; Dong, Y. P.; Jia, D. M.; Tang, B. Z. *Chin. J. Polym. Sci.* **2004**, *22*, 501.
- (342) Peng, H.; Dong, Y. P.; Jia, D. M.; Tang, B. Z. *Chin. Sci. Bull.* **2004**, *49*, 2637.
- (343) Zheng, R.; Dong, H.; Peng, H.; Lam, J. W. Y.; Tang, B. Z. *Macromolecules* **2004**, *37*, 5196.
- (344) Dong, H.; Zheng, R.; Lam, J. W. Y.; Häussler, M.; Qin, A.; Tang, B. Z. *Macromolecules* **2005**, *38*, 6382.
- (345) Peng, H.; Lam, J. W. Y.; Tang, B. Z. *Polymer* **2005**, *46*, 5746.
- (346) Peng, H.; Lam, J. W. Y.; Tang, B. Z. *Macromol. Rapid Commun.* **2005**, *26*, 673.
- (347) Peng, H.; Zheng, R. H.; Dong, H. C.; Jia, D. M.; Tang, B. Z. *Chin. J. Polym. Sci.* **2005**, *23*, 1.
- (348) Li, Z.; Lam, J. W. Y.; Dong, Y.; Dong, Y.; Sung, H. H. Y.; Williams, I. D.; Tang, B. Z. *Macromolecules* **2006**, *39*, 6458.
- (349) Häussler, M.; Liu, J.; Lam, J. W. Y.; Anjun, Q. I. N.; Zheng, R.; Tang, B. Z. *J. Polym. Sci., Part A: Polym. Chem.* **2007**, *45*, 4249.
- (350) Häussler, M.; Liu, J.; Zheng, R.; Lam, J. W. Y.; Qin, A.; Tang, B. Z. *Macromolecules* **2007**, *40*, 1914.
- (351) Qin, A.; Lam, J. W. Y.; Dong, H.; Lu, W.; Jim, C. K. W.; Dong, Y.; Häussler, M.; Sung, H. H. Y.; Williams, I. D.; Wong, G. K. L.; Tang, B. Z. *Macromolecules* **2007**, *40*, 4879.
- (352) Shi, J.; Tong, B.; Zhao, W.; Shen, J.; Zhi, J.; Dong, Y.; Häussler, M.; Lam, J. W. Y.; Tang, B. Z. *Macromolecules* **2007**, *40*, 5612.
- (353) Liu, J.; Zheng, R.; Tang, Y.; Häussler, M.; Lam, J. W. Y.; Qin, A.; Ye, M.; Hong, Y.; Gao, P.; Tang, B. Z. *Macromolecules* **2007**, *40*, 7473.
- (354) Shi, J. B.; Tong, B.; Li, Z.; Shen, J. B.; Zhao, W.; Fu, H. H.; Zhi, J.; Dong, Y. P.; Häussler, M.; Lam, J. W. Y.; Tang, B. Z. *Macromolecules* **2007**, *40*, 8195.
- (355) Jim, C. K. W.; Qin, A.; Lam, J. W. Y.; Häussler, M.; Liu, J.; Yuen, M. M. F.; Kim, J. K.; Ng, K. M.; Tang, B. Z. *Macromolecules* **2009**, *42*, 4099.
- (356) Zhang, L.; Chen, X. G.; Xue, P.; Sun, H. H. Y.; Williams, I. D.; Sharpless, K. B.; Fokin, V. V.; Jia, G. C. *J. Am. Chem. Soc.* **2005**, *127*, 15998.
- (357) Simionescu, C.; Dumitrescu, S.; Percec, V. *J. Polym. Sci., Part C: Polym. Symp.* **1978**, *209*.
- (358) Simionescu, C. I.; Percec, V. *J. Polym. Sci., Part C: Polym. Lett.* **1979**, *17*, 421.
- (359) Simionescu, C. I.; Percec, V. *J. Polym. Sci., Part A: Polym. Chem.* **1980**, *18*, 147.
- (360) Percec, V.; Rudick, J. G.; Nombel, P.; Buchowicz, W. *J. Polym. Sci., Part A: Polym. Chem.* **2002**, *40*, 3212.
- (361) Percec, V.; Rudick, J. G. *Macromolecules* **2005**, *38*, 7241.
- (362) Percec, V.; Rudick, J. G.; Aqad, E. *Macromolecules* **2005**, *38*, 7205.
- (363) Gibson, H. W.; Bailey, F. C.; Epstein, A. J.; Rommelmann, H.; Kaplan, S.; Harbour, J.; Yang, X. Q.; Tanner, D. B.; Pochan, J. M. *J. Am. Chem. Soc.* **1983**, *105*, 4417.
- (364) Krause, J. O.; Wang, D.; Anders, U.; Weberskirch, R.; Zarka, M. T.; Nuyken, O.; Jäger, C.; Haarer, D.; Buchmeiser, M. R. *Macromol. Symp.* **2004**, *217*, 179.
- (365) Simionescu, C. I.; Percec, V. *J. Polym. Sci., Part C: Polym. Symp.* **1980**, *43*.
- (366) Tabata, M.; Takamura, H.; Yokota, K.; Nozaki, Y.; Hoshina, T.; Minakawa, H.; Kodaira, K. *Macromolecules* **1994**, *27*, 6234.
- (367) Tabata, M.; Tanaka, Y.; Sadahiro, Y.; Sone, T.; Yokota, K.; Miura, I. *Macromolecules* **1997**, *30*, 5200.
- (368) Sun, J. Z.; Chen, H. Z.; Xu, R. S.; Wang, M.; Lam, J. W. Y.; Tang, B. Z. *Chem. Commun.* **2002**, 1222.
- (369) Nakamura, M.; Tabata, M.; Sone, T.; Mawatari, Y.; Miyasaka, A. *Macromolecules* **2002**, *35*, 2000.
- (370) Lee, P. P. S.; Lam, J. W. Y.; Bensheng, L. I.; Poon, T. W. H.; Tang, B. Z. *Polym. Prepr.* **1999**, *40*, 659.
- (371) Lam, J. W. Y.; Ngai, L. Y.; Poon, T. W. H.; Lin, Z.; Tang, B. Z. *Polym. Prepr.* **2000**, *41*, 289.
- (372) Ciardelli, F.; Benedetti, E.; Pieroni, O. *Macromol. Chem.* **1967**, *103*, 1.
- (373) Pieroni, O.; Matera, F.; Ciardelli, F. *Tetrahedron Lett.* **1972**, 597.
- (374) Ciardelli, F.; Lanzillo, S.; Pieroni, O. *Macromolecules* **1974**, *7*, 174.
- (375) Moore, J. S.; Gorman, C. B.; Grubbs, R. H. *J. Am. Chem. Soc.* **1991**, *113*, 1704.
- (376) Cheuk, K. K. L.; Lam, J. W. Y.; Chen, J. W.; Lai, L. M.; Tang, B. Z. *Macromolecules* **2003**, *36*, 5947.
- (377) Li, B. S.; Cheuk, K. K. L.; Ling, L. S.; Chen, J. W.; Xiao, X. D.; Bai, C. L.; Tang, B. Z. *Macromolecules* **2003**, *36*, 77.
- (378) Li, B. S.; Cheuk, K. K. L.; Yang, D. L.; Lam, J. W. Y.; Wan, L. J.; Bai, C. L.; Tang, B. Z. *Macromolecules* **2003**, *36*, 5447.
- (379) Li, B. S.; Kang, S. Z.; Cheuk, K. K. L.; Wan, L. J.; Ling, L. S.; Bai, C. L.; Tang, B. Z. *Langmuir* **2004**, *20*, 7598.
- (380) Lai, L. M.; Lam, J. W. Y.; Cheuk, K. K. L.; Sung, H. H. Y.; Williams, I. D.; Tang, B. Z. *J. Polym. Sci., Part A: Polym. Chem.* **2005**, *43*, 3701.
- (381) Lai, L. M.; Lam, J. W. Y.; Qin, A. J.; Dong, Y. Q.; Tang, B. Z. *J. Phys. Chem. B* **2006**, *110*, 11128.
- (382) Lai, L. M.; Lam, J. W. Y.; Tang, B. Z. *J. Polym. Sci., Part A: Polym. Chem.* **2006**, *44*, 2117.
- (383) Lam, J. W. Y.; Cheuk, K. K. L.; Li, B. S.; Xie, Y.; Tang, B. Z. *Chin. J. Polym. Sci.* **2007**, *25*, 119.
- (384) Liu, J. H.; Yan, J. J.; Chen, E. Q.; Lam, J. W. Y.; Dong, Y. P.; Liang, D. H.; Tang, B. Z. *Polymer* **2008**, *49*, 3366.
- (385) Aoki, T.; Kokai, M.; Shinohara, K.; Oikawa, E. *Chem. Lett.* **1993**, 2009.
- (386) Yashima, E.; Huang, S. L.; Matsushima, T.; Okamoto, Y. *Macromolecules* **1995**, *28*, 4184.
- (387) Yashima, E.; Maeda, Y.; Okamoto, Y. *J. Am. Chem. Soc.* **1998**, *120*, 8895.
- (388) Kwak, G.; Masuda, T. *Macromolecules* **2000**, *33*, 6633.
- (389) Lai, L. M.; Lam, J. W. Y.; Tang, B. Z. *J. Polym. Sci., Part A: Polym. Chem.* **2006**, *44*, 6190.
- (390) Sun, Q.; Tang, B. Z. *Polym. Prepr.* **1999**, *40* (1), 558.
- (391) Sun, Q.; Tang, B. Z. *Polym. Prepr.* **1999**, *40* (1), 560.
- (392) Nakako, H.; Nomura, R.; Tabata, M.; Masuda, T. *Macromolecules* **1999**, *32*, 2861.
- (393) Nakako, H.; Mayahara, Y.; Nomura, R.; Tabata, M.; Masuda, T. *Macromolecules* **2000**, *33*, 3978.
- (394) Nomura, R.; Fukushima, Y.; Nakako, H.; Masuda, T. *J. Am. Chem. Soc.* **2000**, *122*, 8830.
- (395) Lam, J. W. Y.; Dong, Y. P.; Cheuk, K. K. L.; Tang, B. Z. *Macromolecules* **2003**, *36*, 7927.
- (396) Lam, J. W. Y.; Dong, Y. P.; Cheuk, K. K. L.; Law, C. C. W.; Lai, L. M.; Tang, B. Z. *Macromolecules* **2004**, *37*, 6695.
- (397) Aoki, T.; Kobayashi, Y.; Kaneko, T.; Oikawa, E.; Yamamura, Y.; Fujita, Y.; Teraguchi, M.; Nomura, R.; Masuda, T. *Macromolecules* **1999**, *32*, 79.
- (398) Aoki, T.; Shinohara, K.; Kaneko, T.; Oikawa, E. *Macromolecules* **1996**, *29*, 4192.
- (399) Percec, V.; Rudick, J. G.; Peterca, M.; Staley, S. R.; Wagner, M.; Obata, M.; Mitchell, C. M.; Cho, W. D.; Balagurusamy, V. S. K.; Lowe, J. N.; Glodde, M.; Weichold, O.; Chung, K. J.; Ghionni, N.; Magonov, S. N.; Heiney, P. A. *Chem.—Eur. J.* **2006**, *12*, 5731.
- (400) Percec, V.; Aqad, E.; Peterca, M.; Rudick, J. G.; Lemon, L.; Ronda, J. C.; De, B. B.; Heiney, P. A.; Meijer, E. W. *J. Am. Chem. Soc.* **2006**, *128*, 16365.
- (401) Percec, V.; Rudick, J. G.; Peterca, M.; Wagner, M.; Obata, M.; Mitchell, C. M.; Cho, W. D.; Balagurusamy, V. S. K.; Heiney, P. A. *J. Am. Chem. Soc.* **2005**, *127*, 15257.
- (402) Cheuk, K. K. L.; Lam, J. W. Y.; Lai, L. M.; Dong, Y.; Tang, B. Z. *Macromolecules* **2003**, *36*, 9752.
- (403) Akagi, K.; Piao, G.; Kaneko, S.; Sakamaki, K.; Shirakawa, H.; Kyotani, M. *Science* **1998**, *282*, 1683.
- (404) Aoki, T.; Kaneko, T.; Maruyama, N.; Sumi, A.; Takahashi, M.; Sato, T.; Teraguchi, M. *J. Am. Chem. Soc.* **2003**, *125*, 6346.
- (405) Yashima, E.; Maeda, K.; Okamoto, Y. *Nature* **1999**, *399*, 449.
- (406) Yashima, E.; Maeda, K. *Macromolecules* **2008**, *41*, 3.
- (407) Prince, R. B.; Saven, J. G.; Wolynes, P. G.; Moore, J. S. *J. Am. Chem. Soc.* **1999**, *121*, 3114.

- (408) Cheuk, K. K. L.; Li, B. S.; Tang, B. Z. In *Encyclopedia of Nanoscience and Nanotechnology*; Nalwa, H. S., Ed.; American Scientific Publishers: Valencia, CA, 2004; Vol. 8, pp 703–713.
- (409) Sakurai, S. I.; Ohsawa, S.; Nagai, K.; Okoshi, K.; Kumaki, J.; Yashima, E. *Angew. Chem., Int. Ed.* **2007**, *46*, 7605.
- (410) Percec, V.; Rudick, J. G.; Wagner, M.; Obata, M.; Mitchell, C. M.; Cho, W. D.; Magonov, S. N. *Macromolecules* **2006**, *39*, 7342.
- (411) Kyotani, M.; Matsushita, S.; Nagai, T.; Matsui, Y.; Shimomura, M.; Kaito, A.; Akagi, K. *J. Am. Chem. Soc.* **2008**, *130*, 10880.
- (412) Maeda, T.; Furusho, Y.; Sakurai, S. I.; Kumaki, J.; Okoshi, K.; Yashima, E. *J. Am. Chem. Soc.* **2008**, *130*, 7938.
- (413) Lu, Y. F.; Yang, Y.; Sellinger, A.; Lu, M. C.; Huang, J. M.; Fan, H. Y.; Haddad, R.; Lopez, G.; Burns, A. R.; Sasaki, D. Y.; Shelnutt, J.; Brinker, C. J. *Nature* **2001**, *410*, 913.
- (414) Yang, Y.; Lu, Y. F.; Lu, M. C.; Huang, J. M.; Haddad, R.; Xomeritakis, G.; Liu, N. G.; Malanoski, A. P.; Sturmayer, D.; Fan, H. Y.; Sasaki, D. Y.; Assink, R. A.; Shelnutt, J. A.; van Swol, F.; Lopez, G. P.; Burns, A. R.; Brinker, C. J. *J. Am. Chem. Soc.* **2003**, *125*, 1269.
- (415) Himo, F.; Lovell, T.; Hilgraf, R.; Rostovtsev, V. V.; Noodleman, L.; Sharpless, K. B.; Fokin, V. V. *J. Am. Chem. Soc.* **2005**, *127*, 210.
- (416) Boren, B. C.; Narayan, S.; Rasmussen, L. K.; Zhang, L.; Zhao, H. T.; Lin, Z. Y.; Jia, G. C.; Fokin, V. V. *J. Am. Chem. Soc.* **2008**, *130*, 8923.
- (417) Voit, B. *J. Polym. Sci., Part A: Polym. Chem.* **2000**, *38*, 2505.
- (418) Hawker, C. J.; Lee, R.; Fréchet, J. M. J. *J. Am. Chem. Soc.* **1991**, *113*, 4583.
- (419) Xu, K. T.; Peng, H.; Tang, B. Z. *Polym. Prepr.* **2001**, *42* (1), 555.
- (420) Peng, H.; Xu, K. T.; Luo, J. D.; Tang, B. Z. *Polym. Prepr.* **2001**, *42* (1), 560.
- (421) Tang, B. Z.; Chen, H. Z.; Xu, R. S.; Lam, J. W. Y.; Cheuk, K. K. L.; Wong, H. N. C.; Wang, M. *Chem. Mater.* **2000**, *12*, 213.
- (422) Kang, E. T.; Ehrlich, P.; Bhatt, A. P.; Anderson, W. A. *Appl. Phys. Lett.* **1982**, *41*, 1136.
- (423) Kang, E. T.; Ehrlich, P.; Bhatt, A. P.; Anderson, W. A. *Macromolecules* **1984**, *17*, 1020.
- (424) Zhao, J.; Yang, M.; Shen, Z. *Polym. J.* **1991**, *23*, 963.
- (425) Zhou, S.; Hong, H.; He, Y.; Yang, D.; Jin, X.; Qian, R. *Polymer* **1992**, *33*, 2189.
- (426) Kang, E. T.; Neoh, K. G.; Masuda, T.; Higashimura, T.; Yamamoto, M. *Polymer* **1989**, *30*, 1328.
- (427) Vohlidal, J.; Sedlacek, J.; Pacovska, M.; Lavastre, O.; Dixneuf, P. H.; Balcar, H.; Pfeyler, J. *Polymer* **1997**, *38*, 3359.
- (428) Zhao, H.; Yuan, W. Z.; Tang, L.; Sun, J. Z.; Xu, H. P.; Qin, A. J.; Mao, Y.; Jin, J. K.; Tang, B. Z. *Macromolecules* **2008**, *41*, 8566.
- (429) Tang, B. Z.; Xu, H. *Macromolecules* **1999**, *32*, 2569.
- (430) Yuan, W. Z.; Mao, Y.; Zhao, H.; Sun, J. Z.; Xu, H. P.; Jin, J. K.; Zheng, Q.; Tang, B. Z. *Macromolecules* **2008**, *41*, 701.
- (431) Yuan, W. Z.; Sun, J. Z.; Liu, J. Z.; Dong, Y.; Li, Z.; Xu, H. P.; Qin, A.; Häussler, M.; Jin, J. K.; Zheng, Q.; Tang, B. Z. *J. Phys. Chem. B* **2008**, *112*, 8896.
- (432) Yuan, W. Z.; Lam, J. W. Y.; Shen, X. Y.; Sun, J. Z.; Mahtab, F.; Zheng, Q.; Tang, B. Z. *Macromolecules* **2009**, *42*, 2523.
- (433) Pugh, C.; Percec, V. *Mol. Cryst. Liq. Cryst.* **1990**, *178*, 193.
- (434) Oh, S. Y.; Akagi, K.; Shirakawa, H.; Araya, K. *Macromolecules* **1993**, *26*, 6203.
- (435) Akagi, K.; Shirakawa, H. *Macromol. Symp.* **1996**, *104*, 137.
- (436) Goto, H.; Akagi, K.; Shirakawa, H. *Synth. Met.* **1997**, *84*, 373.
- (437) Koltzenburg, S.; Wolff, D.; Stelzer, F.; Springer, J.; Nuyken, O. *Macromolecules* **1998**, *31*, 9166.
- (438) Koltzenburg, S.; Ungerank, M.; Stelzer, F.; Nuyken, O. *Macromol. Chem. Phys.* **1999**, *200*, 814.
- (439) Koltzenburg, S.; Stelzer, F.; Nuyken, O. *Macromol. Chem. Phys.* **1999**, *200*, 821.
- (440) Gal, Y. S.; Lee, W. C.; Kim, S. H.; Lee, S. S.; Jwa, S. T.; Park, S. H. *J. Macromol. Sci.: Pure Appl. Chem.* **1999**, *A36*, 429.
- (441) Ting, C.-H.; Hsu, C.-S. *J. Polym. Res.* **2001**, *8*, 159.
- (442) Ting, C.-H.; Chen, J.-T.; Hsu, C.-S. *Macromolecules* **2002**, *35*, 1180.
- (443) Schenning, A. P. H. J.; Franssen, M.; Meijer, E. W. *Macromol. Rapid Commun.* **2002**, *23*, 266.
- (444) Stagnaro, P.; Conzatti, L.; Costa, G.; Gallot, B.; Tavani, C.; Valenti, B. *Macromol. Chem. Phys.* **2003**, *204*, 714.
- (445) Goto, H.; Dai, X. M.; Ueoka, T.; Akagi, K. *Macromolecules* **2004**, *37*, 4783.
- (446) Okoshi, K.; Sakajiri, K.; Kumaki, J.; Yashima, E. *Macromolecules* **2005**, *38*, 4061.
- (447) Kang, S. W.; Jin, S. H.; Chien, L. C.; Sprunt, S. *Adv. Funct. Mater.* **2004**, *14*, 329.
- (448) Chen, L.; Chen, Y.; Zha, D.; Yang, Y. *J. Polym. Sci., Part A: Polym. Chem.* **2006**, *44*, 2499.
- (449) Qu, J.; Suzuki, Y.; Shiotsuki, M.; Sanda, F.; Masuda, T. *Macromol. Chem. Phys.* **2007**, *208*, 1992.
- (450) Zhou, D.; Chen, Y.; Chen, L.; Zhou, W.; He, X. *Macromolecules* **2009**, *42*, 1454.
- (451) Kong, X. X.; Tang, B. Z. *Chem. Mater.* **1998**, *10*, 3352.
- (452) Kong, X. X.; Wan, X. H.; Kwok, H. S.; Feng, X. D.; Tang, B. Z. *Chin. J. Polym. Sci.* **1998**, *16*, 185.
- (453) Tang, B. Z.; Kong, X. X. *Chin. J. Polym. Sci.* **1999**, *17*, 289.
- (454) Huang, Y.; Bu, L. J.; Bu, L. W.; Zhang, D. Z.; Su, C. W.; Xu, Z. D.; Lam, W. Y.; Tang, B. Z.; Mays, J. W. *Polym. Bull.* **2000**, *44*, 539.
- (455) Lam, J. W. Y.; Kong, X.; Dong, Y.; Cheuk, K.; Xu, K.; Tang, B. Z. *Macromolecules* **2000**, *33*, 5027.
- (456) Geng, J.; Zhao, X.; Zhou, E.; Li, G.; Lam, J. W. Y.; Tang, B. Z. *Mol. Cryst. Liq. Cryst.* **2002**, *399*, 17.
- (457) Lam, J. W. Y.; Dong, Y.; Luo, J.; Cheuk, K. K. L.; Xie, Z.; Tang, B. Z. *Thin Solid Films* **2002**, *417*, 143.
- (458) Geng, J.; Zhao, X.; Zhou, E.; Li, G.; Lam, J. W. Y.; Tang, B. Z. *Polymer* **2003**, *44*, 8095.
- (459) Geng, J.; Zhao, X.; Zhou, E.; Li, G.; Lam, J. W. Y.; Tang, B. Z. *Mol. Cryst. Liq. Cryst.* **2003**, *399*, 17.
- (460) Lam, J. W. Y.; Law, C. K.; Dong, Y.; Wang, J.; Ge, W.; Tang, B. Z. *Opt. Mater.* **2003**, *21*, 321.
- (461) Dong, Y.; Lam, J. W. Y.; Peng, H.; Cheuk, K. K. L.; Kwok, H. S.; Tang, B. Z. *Macromolecules* **2004**, *37*, 6408.
- (462) Geng, J.; Geng, F.; Wang, J.; Zhu, B.; Gao, L. I.; Zhou, E.; Lam, J. W. Y.; Tang, B. Z. *Liq. Cryst.* **2004**, *31*, 271.
- (463) Geng, J.; Wang, S.; Ling, W.; Li, G.; Zhou, E.; Lam, J. W. Y.; Tang, B. Z. *Liq. Cryst.* **2004**, *31*, 71.
- (464) Geng, J.; Zhou, E.; Li, G.; Lam, J. W. Y.; Tang, B. Z. *J. Polym. Sci., Part B: Polym. Phys.* **2004**, *42*, 1333.
- (465) Ye, C.; Xu, G.; Yu, Z. Q.; Lam, J. W. Y.; Jang, J. H.; Peng, H. L.; Tu, Y. F.; Liu, Z. F.; Jeong, K. U.; Cheng, S. Z. D.; Chen, E. Q.; Tang, B. Z. *J. Am. Chem. Soc.* **2005**, *127*, 7668.
- (466) Xing, C.; Lam, J. W. Y.; Zhao, K.; Tang, B. Z. *J. Polym. Sci., Part A: Polym. Chem.* **2008**, *46*, 2960.
- (467) Nagai, K.; Sakajiri, K.; Maeda, K.; Okoshi, K.; Sato, T.; Yashima, E. *Macromolecules* **2006**, *39*, 5371.
- (468) Kwak, G.; Minakuchi, M.; Sakaguchi, T.; Masuda, T.; Fujiki, M. *Chem. Mater.* **2007**, *19*, 3654.
- (469) Masuda, T.; Tang, B. Z.; Tanaka, T.; Higashimura, T. *Macromolecules* **1986**, *19*, 1459.
- (470) Masuda, T.; Iguchi, Y.; Tang, B. Z.; Higashimura, T. *Polymer* **1988**, *29*, 2041.
- (471) Green, M. M.; Cheon, K. S.; Yang, S. Y.; Park, J. W.; Swansburg, S.; Liu, W. H. *Acc. Chem. Res.* **2001**, *34*, 672.
- (472) Gu, H.; Nakamura, Y.; Sato, T.; Teramoto, A.; Geen, M. M.; Jha, S. K.; Andreola, C.; Reidy, M. P. *Macromolecules* **1998**, *31*, 6362.
- (473) Huang, Y. M.; Ge, W. K.; Lam, J. W. Y.; Tang, B. Z. *Appl. Phys. Lett.* **1999**, *75*, 4094.
- (474) Huang, Y. M.; Lam, J. W. Y.; Cheuk, K. K. L.; Ge, W. K.; Tang, B. Z. *Macromolecules* **1999**, *32*, 5976.
- (475) Lee, C. W.; Wong, K. S.; Lam, W. Y.; Tang, B. Z. *Chem. Phys. Lett.* **1999**, *307*, 67.
- (476) Wong, K. S.; Lee, C. W.; Tang, B. Z. *Synth. Met.* **1999**, *101*, 505.
- (477) Huang, Y. M.; Lam, J. W. Y.; Cheuk, K. K. L.; Ge, W.; Tang, B. Z. *Thin Solid Films* **2000**, *363*, 146.
- (478) Lee, P. P. S.; Geng, Y.; Kwok, H. S.; Tang, B. Z. *Thin Solid Films* **2000**, *363*, 149.
- (479) Xu, H. Y.; Guang, S. Y.; Zhang, S. Y.; Tong, B. Y.; Tang, B. Z. *Acta Polym. Sin.* **2001**, 186.
- (480) Huang, M. Y. M.; Law, C. K.; Ge, W.; Lam, J. W. Y.; Tang, B. Z. *J. Lumin.* **2002**, *99*, 161.
- (481) Xie, Z.; Lam, J. W. Y.; Dong, Y.; Qiu, C.; Kwok, H. S.; Tang, B. Z. *Opt. Mater.* **2003**, *21*, 231.
- (482) Chen, J.; Xie, Z.; Lam, J. W. Y.; Law, C. C. W.; Tang, B. Z. *Macromolecules* **2003**, *36*, 1108.
- (483) Huang, Y. M.; Song, Y.; Huang, C.; Zhou, X. P.; Ouyang, Y. D.; Ge, W.; Lam, J. W. Y.; Tang, B. Z. *J. Lumin.* **2005**, *114*, 241.
- (484) Chen, J.; Kwok, H. S.; Tang, B. Z. *J. Polym. Sci., Part A: Polym. Chem.* **2006**, *44*, 2487.
- (485) Lam, J. W. Y.; Dong, Y.; Kwok, H. S.; Tang, B. Z. *Macromolecules* **2006**, *39*, 6997.
- (486) Law, C. C. W.; Lam, J. W. Y.; Qin, A.; Dong, Y.; Kwok, H. S.; Tang, B. Z. *Polymer* **2006**, *47*, 6642.
- (487) Yuan, W. Z.; Qin, A.; Lam, J. W. Y.; Sun, J. Z.; Dong, Y.; Häussler, M.; Liu, J.; Xu, H. P.; Zheng, Q.; Tang, B. Z. *Macromolecules* **2007**, *40*, 3159.
- (488) Lam, J. W. Y.; Qin, A.; Dong, Y.; Hong, Y.; Jim, C. K. W.; Liu, J.; Dong, Y.; Kwok, H. S.; Tang, B. Z. *J. Phys. Chem. B* **2008**, *112*, 11227.
- (489) Qin, A. J.; Jim, C. K. W.; Tang, Y. H.; Lam, J. W. Y.; Liu, J. Z.; Mahtab, F.; Gao, P.; Tang, B. Z. *J. Phys. Chem. B* **2008**, *112*, 9281.
- (490) Sanda, F.; Nakai, T.; Kobayashi, N.; Masuda, T. *Macromolecules* **2004**, *37*, 2703.

- (491) Huang, C. H.; Lee, C. W.; Hsu, C.-S.; Renaud, C.; Nguyen, T. P. *Thin Solid Films* **2007**, *515*, 7671.
- (492) Cheng, Y. J.; Luh, T. Y. *Chem.—Eur. J.* **2004**, *10*, 5361.
- (493) Luo, J. D.; Xie, Z. L.; Lam, J. W. Y.; Cheng, L.; Chen, H. Y.; Qiu, C. F.; Kwok, H. S.; Zhan, X. W.; Liu, Y. Q.; Zhu, D. B.; Tang, B. Z. *Chem. Commun.* **2001**, 1740.
- (494) Chen, J. W.; Law, C. C. W.; Lam, J. W. Y.; Dong, Y. P.; Lo, S. M. F.; Williams, I. D.; Zhu, D. B.; Tang, B. Z. *Chem. Mater.* **2003**, *15*, 1535.
- (495) Hong, Y.; Lam, J. W. Y.; Tang, B. Z. *Chem. Commun.* **2009**, 4332 and references cited therein.
- (496) Yu, G.; Yin, S.; Liu, Y.; Chen, J.; Xu, X.; Sun, X.; Ma, D.; Zhan, X.; Peng, Q.; Shuai, Z.; Tang, B. Z.; Zhu, D.; Fang, W.; Luo, Y. *J. Am. Chem. Soc.* **2005**, *127*, 6335.
- (497) Tang, B. Z. *Macromol. Chem. Phys.* **2009**, *210*, 900.
- (498) Chen, H. Y.; Lam, W. Y.; Luo, J. D.; Ho, Y. L.; Tang, B. Z.; Zhu, D. B.; Wong, M.; Kwok, H. S. *Appl. Phys. Lett.* **2002**, *81*, 574.
- (499) Liu, C.; Yang, W.; Mo, Y.; Cao, Y.; Chen, J.; Tang, B. Z. *Synth. Met.* **2003**, *135–136*, 187.
- (500) Liu, J.; Lam, J. W. Y.; Tang, B. Z. *J. Inorg. Organomet. Polym. Mater.* **2009**, *19*, 249.
- (501) Li, Z.; Dong, Y. Q.; Lam, J. W. Y.; Sun, J.; Qin, A.; Häußler, M.; Dong, Y. P.; Sung, H. H. Y.; Williams, I. D.; Kwok, H. S.; Tang, B. Z. *Adv. Funct. Mater.* **2009**, *19*, 905.
- (502) Tong, H.; Hong, Y.; Dong, Y.; Häußler, M.; Lam, J. W. Y.; Li, Z.; Guo, Z.; Guo, Z.; Tang, B. Z. *Chem. Commun.* **2006**, 3705.
- (503) Dong, Y. Q.; Lam, J. W. Y.; Qin, A. J.; Liu, J. Z.; Li, Z.; Tang, B. Z. *Appl. Phys. Lett.* **2007**, *91*, 011111–1.
- (504) Tong, H.; Hong, Y.; Dong, Y.; Häußler, M.; Li, Z.; Lam, J. W. Y.; Dong, Y.; Sung, H. H. Y.; Williams, I. D.; Tang, B. Z. *J. Phys. Chem. B* **2007**, *111*, 11817.
- (505) Hong, Y.; Häußler, M.; Lam, J. W. Y.; Li, Z.; Sin, K. K.; Dong, Y. Q.; Tong, H.; Liu, J.; Qin, A.; Renneberg, R.; Tang, B. Z. *Chem.—Eur. J.* **2008**, *14*, 6428.
- (506) Tada, K.; Hidayat, R.; Hirohata, M.; Teraguchi, M.; Masuda, T.; Yoshino, K. *Jpn. J. Appl. Phys.* **1996**, *35*, L1138.
- (507) Sun, R.; Zheng, Q.; Zhang, X.; Masuda, T.; Kobayashi, T. *Jpn. J. Appl. Phys.* **1999**, *38*, 2017.
- (508) Wong, W. Y.; Wang, X. Z.; He, Z.; Djurii, A. B.; Yip, C. T.; Cheung, K. Y.; Wang, H.; Mak, C. S. K.; Chan, W. K. *Nat. Mater.* **2007**, *6*, 521.
- (509) Wong, W. Y.; Wang, X. Z.; He, Z.; Chan, K. K.; Djurii, A. B.; Cheung, K. Y.; Yip, C. T.; Ng, A. M. C.; Yan, Y. X.; Mak, C. S. K.; Chan, W. K. *J. Am. Chem. Soc.* **2007**, *129*, 14372.
- (510) Kim, I. B.; Erdogan, B.; Wilson, J. N.; Bunz, U. H. F. *Chem.—Eur. J.* **2004**, *10*, 6247.
- (511) Dong, Y. Q.; Lam, J. W. Y.; Qin, A.; Li, Z.; Liu, J.; Sun, J.; Dong, Y. P.; Tang, B. Z. *Chem. Phys. Lett.* **2007**, *446*, 124.
- (512) Li, Z.; Dong, Y. Q.; Mi, B.; Tang, Y. H.; Häußler, M.; Tong, H.; Dong, Y. P.; Lam, J. W. Y.; Ren, Y.; Sung, H. H. Y.; Wong, K. S.; Gao, P.; Williams, I. D.; Kwok, H. S.; Tang, B. Z. *J. Phys. Chem. B* **2005**, *109*, 10061.
- (513) Lee, M.; Katz, H. E.; Erben, C.; Gill, D. M.; Gopalan, P.; Heber, J. D.; McGee, D. J. *Science* **2002**, *298*, 1401.
- (514) Shi, Y.; Zhang, C.; Zhang, H.; Bechtel, J. H.; Dalton, L. R.; Robinson, B. H.; Steier, W. H. *Science* **2000**, *288*, 119.
- (515) Burland, D. M.; Miller, R. D.; Walsh, C. A. *Chem. Rev.* **1994**, *94*, 31.
- (516) Ma, H.; Jen, A. K. Y. *Adv. Mater.* **2001**, *13*, 1201.
- (517) Moerner, W. E.; Jepsen, A. G.; Thompson, C. L. *Annu. Rev. Mater. Sci.* **1997**, *32*, 585.
- (518) Barclay, G. G.; Ober, C. K. *Prog. Polym. Sci.* **1993**, *18*, 899.
- (519) Tutt, L. W.; Kost, A. *Nature* **1992**, *356*, 225.
- (520) Kuebler, S. M.; Denning, R. G.; Anderson, H. L. *J. Am. Chem. Soc.* **2000**, *122*, 339.
- (521) Wang, X.; Wu, J. C.; Xu, H. Y.; Wang, P.; Tang, B. Z. *J. Polym. Sci., Part A: Polym. Chem.* **2008**, *46*, 2072.
- (522) Yin, S. C.; Xu, H. Y.; Su, X. Y.; Wu, L.; Song, Y. L.; Tang, B. Z. *Dyes Pigment.* **2007**, *75*, 675.
- (523) Yin, S. C.; Xu, H. Y.; Li, G.; Su, X. Y.; Gao, Y. C.; Song, Y. F.; Tang, B. Z. *Chin. J. Polym. Sci.* **2006**, *24*, 221.
- (524) Xu, H. Y.; Yin, S. C.; Zhu, W. J.; Song, Y. L.; Tang, B. Z. *Polymer* **2006**, *47*, 6986.
- (525) Yin, S. C.; Xu, H. Y.; Su, X. Y.; Li, G.; Song, Y. L.; Lam, J.; Tang, B. Z. *J. Polym. Sci., Part A: Polym. Chem.* **2006**, *44*, 2346.
- (526) Yin, S. C.; Xu, H. Y.; Su, X. Y.; Gao, Y. C.; Song, Y. L.; Jacky, W. Y. L.; Tang, B. Z.; Shi, W. F. *Polymer* **2005**, *46*, 10592.
- (527) Nomura, R.; Karim, S. M. A.; Kajii, H.; Hidayat, R.; Yoshino, K.; Masuda, T. *Macromolecules* **2000**, *33*, 4313.
- (528) Xu, H. Y.; Guang, S. Y.; Tang, B. Z. *Chin. Chem. Lett.* **2000**, *11*, 21.
- (529) Tang, B. Z.; Xu, H.; Lam, J. W. Y.; Lee, P. P. S.; Xu, K.; Sun, Q.; Cheuk, K. K. L. *Chem. Mater.* **2000**, *12*, 1446.
- (530) Xu, H.; Tang, B. Z. *Pure Appl. Chem.* **1999**, *36*, 1197.
- (531) Xu, H. Y.; Tang, B. Z. *Chin. J. Polym. Sci.* **1999**, *17*, 391.
- (532) Higashimura, T.; Tang, B. Z.; Masuda, T.; Yamaoka, H.; Matsuyama, T. *Polym. J.* **1985**, *17*, 393.
- (533) Masuda, T.; Tang, B. Z.; Higashimura, T.; Yamaoka, H. *Macromolecules* **1985**, *18*, 2369.
- (534) Peng, H.; Cheng, L.; Luo, J. D.; Xu, K. T.; Sun, Q. H.; Dong, Y. P.; Salhi, F.; Lee, P. P. S.; Chen, J. W.; Tang, B. Z. *Macromolecules* **2002**, *35*, 5349.
- (535) Yashima, E.; Matsushima, T.; Okamoto, Y. *J. Am. Chem. Soc.* **1997**, *119*, 6345.
- (536) Prince, R. B.; Barnes, S. A.; Moore, J. S. *J. Am. Chem. Soc.* **2000**, *122*, 2758.
- (537) Teraguchi, M.; Suzuki, J.; Kaneko, T.; Aoki, T.; Masuda, T. *Macromolecules* **2003**, *36*, 9694.
- (538) Seferis, J. C. In *Polymer Handbook*, 3rd ed.; Brandrup, J., Immergut, E. H., Eds.; Wiley: New York, 1989; pp VI/451–VI/461.
- (539) Hecht, E. *Optics*, 4th ed.; Addison Wesley: San Francisco, CA, 2002.
- (540) Okutsu, R.; Suzuki, Y.; Ando, S.; Ueda, M. *Macromolecules* **2008**, *41*, 6165.
- (541) Häußler, M.; Lam, J. W. Y.; Qin, A.; Tse, K. K. C.; Li, M. K. S.; Liu, J.; Jim, C. K. W.; Gao, P.; Tang, B. Z. *Chem. Commun.* **2007**, 2584.
- (542) Olshavsky, M.; Allcock, H. R. *Macromolecules* **1997**, *30*, 4179.
- (543) Dislich, H. *Angew. Chem., Int. Ed.* **1979**, *18*, 49.
- (544) Simmrock, H. U.; Marthy, A.; Dominguez, L.; Meyer, W. H.; Wegener, G. *Angew. Chem., Int. Ed.* **1989**, *28*, 1122.
- (545) Shi, J.; Jim, C. K. W.; Liu, J.; Lam, J. W. Y.; Dong, Y.; Tang, B. Z. *Polym. Prepr.* **2009**, *50* (2), in press.
- (546) Paquet, C.; Cyr, P. W.; Kumacheva, E.; Manners, I. *Chem. Commun.* **2004**, 234.
- (547) Foucher, D. A.; Tang, B. Z.; Manners, I. *J. Am. Chem. Soc.* **1992**, *114*, 6246.
- (548) Yang, C. J.; Jenekhe, S. A. *Chem. Mater.* **1994**, *6*, 196.
- (549) Kim, D. Y.; Sundheimer, M.; Otomo, A.; Stegman, G. I.; Winfried, H. G. H.; Mohlhaupt, G. R. *Appl. Phys. Lett.* **1993**, *63*, 290.
- (550) Ho, P. K. H.; Thomas, S.; Friend, R. H.; Tessler, N. *Science* **1999**, *285*, 233.
- (551) Kudo, H.; Yamamoto, M.; Nishikubo, T. *Macromolecules* **2006**, *39*, 1759.
- (552) Höfler, T.; Weinberger, M.; Kern, W.; Rentenberger, S.; Pogantsch, A. *Adv. Funct. Mater.* **2006**, *16*, 2369.
- (553) Bertarelli, C.; Bianco, A.; D'Amore, F.; Gallazzi, M. C.; Zerbi, G. *Adv. Funct. Mater.* **2004**, *14*, 357.
- (554) Lin, Q.; Yang, B.; Li, J.; Meng, X.; Shen, J. *Polymer* **2000**, *41*, 8305.
- (555) Charych, D. H.; Nagy, J. O.; Spevak, W.; Bednarski, M. D. *Science* **1993**, *261*, 585.
- (556) Kim, J. M.; Lee, Y. B.; Yang, D. H.; Lee, J. S.; Lee, G. S.; Ahn, D. J. *J. Am. Chem. Soc.* **2005**, *127*, 17580.
- (557) Peng, H. S.; Tang, J.; Pang, J. B.; Chen, D. Y.; Yang, L.; Ashbaugh, H. S.; Brinker, C. J.; Yang, Z. Z.; Lu, Y. F. *J. Am. Chem. Soc.* **2005**, *127*, 12782.
- (558) Dei, S.; Shimogaki, T.; Matsumoto, A. *Macromolecules* **2008**, *41*, 6055.
- (559) Dei, S.; Matsumoto, A.; Matsumoto, A. *Macromolecules* **2008**, *41*, 2467.
- (560) Campbell, L.; Sharp, D. N.; Harrison, M. T.; Denning, R. G.; Turberfield, A. J. *Nature* **2000**, *404*, 53.
- (561) Kim, J. M. *Macromol. Rapid Commun.* **2007**, *28*, 1191.
- (562) Hua, J. L.; Lam, J. W. Y.; Dong, H. C.; Wu, L. J.; Wong, K. S.; Tang, B. Z. *Polymer* **2006**, *47*, 18.
- (563) Lam, J. W. Y.; Qin, A. J.; Dong, Y. P.; Lai, L. M.; Häußler, M.; Dong, Y. Q.; Tang, B. Z. *J. Phys. Chem. B* **2006**, *110*, 21613.
- (564) Lam, J. W. Y.; Häußler, M.; Tang, B. Z. *Mol. Cryst. Liq. Cryst.* **2004**, *415*, 43.
- (565) Singh, P. N. D.; Mandel, S. M.; Sankaranarayanan, J.; Muthukrishnan, S.; Chang, M.; Robinson, R. M.; Lahti, P. M.; Ault, B. S.; Gudmundsdottir, A. D. *J. Am. Chem. Soc.* **2007**, *129*, 16263.
- (566) Dong, H.; Qin, A.; Jim, C. K. W.; Lam, J. W. Y.; Häußler, M.; Tang, B. Z. *J. Inorg. Organomet. Polym. Mater.* **2008**, *18*, 201.
- (567) Nishide, H. *Adv. Mater.* **1995**, *7*, 937.
- (568) Nishide, H.; Kaneko, T.; Igarashi, M.; Tsuchida, E.; Yoshioka, N.; Lahti, P. M. *Macromolecules* **1994**, *27*, 3082.
- (569) Nishide, H.; Kaneko, T.; Yoshioka, N.; Akiyama, H.; Igarashi, M.; Tsuchida, E. *Macromolecules* **1993**, *26*, 4567.
- (570) Yoshioka, N.; Nishide, H.; Kaneko, T.; Yoshiki, H.; Tsuchida, E. *Macromolecules* **1992**, *25*, 3838.
- (571) Tang, B. Z.; Petersen, R.; Foucher, D. A.; Lough, A.; Coombs, N.; Sodhi, R.; Manners, I. *J. Chem. Soc., Chem. Commun.* **1993**, *6*, 523.
- (572) Petersen, R.; Foucher, D. A.; Tang, B. Z.; Lough, A.; Raju, N. P.; Greedan, J. E.; Manners, I. *Chem. Mater.* **1995**, *7*, 2045.
- (573) Nguyen, P.; Gomez-Elipse, P.; Manners, I. *Chem. Rev.* **1999**, *99*, 1515.

- (574) Tang, B. Z.; Geng, Y.; Lam, J. W. Y.; Li, B.; Jing, X.; Wang, X.; Wang, F.; Pakhomov, A. B.; Zhang, X. X. *Chem. Mater.* **1999**, *11*, 1581.
- (575) Tang, B. Z. *CHEMTECH* **1999**, *29*, 7.
- (576) Tang, B. Z.; Geng, Y.; Sun, Q.; Zhang, X.; Jing, X. *Pure Appl. Chem.* **2000**, *72*, 157.
- (577) Sun, Q.; Xu, K.; Peng, H.; Zheng, R.; Häussler, M.; Tang, B. Z. *Macromolecules* **2003**, *36*, 2309.
- (578) Sun, Q.; Lam, J. W. Y.; Xu, K.; Xu, H.; Cha, J. A. P.; Wong, P. C. L.; Wen, G.; Zhang, X.; Jing, X.; Wang, F.; Tang, B. Z. *Chem. Mater.* **2000**, *12*, 2617.
- (579) Liu, J. Z.; Lam, J. W. Y.; Häussler, M.; Qin, A. J. *Inorg. Organomet. Polym. Mater.* **2009**, *19*, 133.
- (580) Dong, H. C. Synthesis of Hyperbranched Polyarylenes and Poly(aroylarylene)s by Polycyclotrimerization of Alkynes and Their Applications as Photoresist and Precursors for Magnetic Ceramics. M. Phil. Thesis, HKUST, June 2005.
- (581) Nagai, K.; Masuda, T.; Nakagawa, T.; Freeman, B. D.; Pinnau, Z. *Prog. Polym. Sci.* **2001**, *26*, 721.
- (582) Masuda, T.; Isobe, E.; Higashimura, T.; Takada, K. *J. Am. Chem. Soc.* **1983**, *105*, 7473.
- (583) Hu, Y.; Shiotsuki, M.; Sanda, F.; Freeman, B. D.; Masuda, T. *Macromolecules* **2008**, *41*, 8525.
- (584) Jiang, J. X.; Su, F.; Trewin, A.; Wood, C. D.; Niu, H.; Jones, J. T. A.; Khimyak, Y. Z.; Cooper, A. I. *J. Am. Chem. Soc.* **2008**, *130*, 7710.
- (585) Salhi, F.; Cheuk, K. K. L.; Sun, Q.; Lam, J. W. Y.; Cha, J. A. K.; Li, G.; Li, B.; Luo, J.; Chen, J.; Tang, B. Z. *J. Nanosci. Nanotech.* **2001**, *1*, 137.
- (586) Liu, Y.; Flood, A. H.; Bonvallet, P. A.; Vignon, S. A.; Northrop, B. H.; Tseng, H.-R.; Jeppesen, J. O.; Huang, T. J.; Brough, B.; Baller, M.; Magonov, S.; Solares, S. D.; Goddard, W. A.; Ho, C.-M.; Stoddart, J. F. *J. Am. Chem. Soc.* **2005**, *127*, 9745.
- (587) Vicario, J.; Katsonis, N.; Ramon, B. S.; Bastiaansen, C. W. M.; Broer, D. J.; Feringa, B. L. *Nature* **2006**, *440*, 163.
- (588) Percec, V.; Rudick, J. G.; Peterca, M.; Heiney, P. A. *J. Am. Chem. Soc.* **2008**, *130*, 7503.

CR900149D